Non-Abelian Anyons and Topological Quantum Computation

Chetan Nayak[1,2], Steven H. Simon[3], Ady Stern[4], Michael Freedman[1], Sankar Das Sarma[5],

[1]*Microsoft Station Q, University of California, Santa Barbara, CA 93108*
[2]*Department of Physics and Astronomy, University of California, Los Angeles, CA 90095-1547*
[3]*Alcatel-Lucent, Bell Labs, 600 Mountain Avenue, Murray Hill, New Jersey 07974*
[4]*Department of Condensed Matter Physics, Weizmann Institute of Science, Rehovot 76100, Israel*
[5]*Department of Physics, University of Maryland, College Park, MD 20742*

Topological quantum computation has recently emerged as one of the most exciting approaches to constructing a fault-tolerant quantum computer. The proposal relies on the existence of topological states of matter whose quasiparticle excitations are neither bosons nor fermions, but are particles known as *Non-Abelian anyons*, meaning that they obey *non-Abelian braiding statistics*. Quantum information is stored in states with multiple quasiparticles, which have a topological degeneracy. The unitary gate operations which are necessary for quantum computation are carried out by braiding quasiparticles, and then measuring the multi-quasiparticle states. The fault-tolerance of a topological quantum computer arises from the non-local encoding of the states of the quasiparticles, which makes them immune to errors caused by local perturbations. To date, the only such topological states thought to have been found in nature are fractional quantum Hall states, most prominently the $\nu = 5/2$ state, although several other prospective candidates have been proposed in systems as disparate as ultra-cold atoms in optical lattices and thin film superconductors. In this review article, we describe current research in this field, focusing on the general theoretical concepts of non-Abelian statistics as it relates to topological quantum computation, on understanding non-Abelian quantum Hall states, on proposed experiments to detect non-Abelian anyons, and on proposed architectures for a topological quantum computer. We address both the mathematical underpinnings of topological quantum computation and the physics of the subject using the $\nu = 5/2$ fractional quantum Hall state as the archetype of a non-Abelian topological state enabling fault-tolerant quantum computation.

Contents

I. INTRODUCTION

In recent years, physicists' understanding of the quantum properties of matter has undergone a major revolution precipitated by surprising experimental discoveries and profound theoretical revelations. Landmarks include the discoveries of the fractional quantum Hall effect and high-temperature superconductivity and the advent of topological quantum field theories. At the same time, new potential applications for quantum matter burst on the scene, punctuated by the discoveries of Shor's factorization algorithm and quantum error correction protocols. Remarkably, there has been a convergence between these developments. Nowhere is this more dramatic than in topological quantum computation, which seeks to exploit the emergent properties of many-particle systems to encode and manipulate quantum information in a manner which is resistant to error.

It is rare for a new scientific paradigm, with its attendant concepts and mathematical formalism, to develop in parallel with potential applications, with all of their detailed technical issues. However, the physics of topological phases of matter

is not only evolving alongside topological quantum computation but is even informed by it. Therefore, this review must necessarily be rather sweeping in scope, simply to introduce the concepts of non-Abelian anyons and topological quantum computation, their inter-connections, and how they may be realized in physical systems, particularly in several fractional quantum Hall states. (For a popular account, see Collins, 2006; for a slightly more technical one, see Das Sarma et al., 2006a.) This exposition will take us on a tour extending from knot theory and topological quantum field theory to conformal field theory and the quantum Hall effect to quantum computation and all the way to the physics of gallium arsenide devices.

The body of this paper is composed of three parts, Sections II, III, and IV. Section II is rather general, avoids technical details, and aims to introduce concepts at a qualitative level. Section II should be of interest, and should be accessible, to all readers. In Section III we describe the theory of topological phases in more detail. In Section IV, we describe how a topological phase can be used as a platform for fault-tolerant quantum computation. The second and third parts are probably of more interest to theorists, experienced researchers, and those who hope to conduct research in this field.

Section II.A.1 begins by discussing the concept of braiding statistics in $2+1$-dimensions. We define the idea of a non-Abelian anyon, a particle exhibiting non-Abelian braiding statistics. Section II.A.2 discusses how non-Abelian anyons can arise in a many-particle system. We then review the basic ideas of quantum computation, and the problems of errors and decoherence in section II.B.1. Those familiar with quantum computation may be able to skip much of this section. We explain in section II.B.2 how non-Abelian statistics naturally leads to the idea of topological quantum computation, and explain why it is a good approach to error-free quantum computation. In section II.C, we briefly describe the non-Abelian quantum Hall systems which are the most likely arena for observing non-Abelian anyons (and, hence, for producing a topological quantum computer). Section II.C.1 gives a very basic review of quantum Hall physics. Experts in quantum Hall physics may be able to skip much of this section. Section II.C.2 introduces non-Abelian quantum Hall states. This section also explains the importance (and summarizes the results) of numerical work in this field for determining which quantum Hall states are (or might be) non-Abelian. Section II.C.3 describes some of the proposed interference experiments which may be able to distinguish Abelian from non-Abelian quantum Hall states. Section II.C.4 shows how qubits and elementary gates can be realized in a quantum Hall device. Section II.C.5 discusses some of the engineering issues associated with the physical systems where quantum Hall physics is observed. In section II.D we discuss some of the other, non-quantum-Hall systems where it has been proposed that non-Abelian anyons (and hence topological quantum computation) might occur.

Sections III and IV are still written to be accessible to the broadest possible audiences, but they should be expected to be somewhat harder going than Section II. Section III introduces the theory of topological phases in detail. Topological quantum computation can only become a reality if some physical system 'condenses' into a non-Abelian topological phase. In Section III, we describe the universal low-energy, long-distance physics of such phases. We also discuss how they can be experimentally detected in the quantum Hall regime, and when they might occur in other physical systems. Our focus is on a sequence of universality classes of non-Abelian topological phases, associated with $\mathrm{SU}(2)_k$ Chern-Simons theory which we describe in section III.A. The first interesting member of this sequence, $k = 2$, is realized in chiral p-wave superconductors and in the leading theoretical model for the $\nu = 5/2$ fractional quantum Hall state. Section III.B shows how this universality class can be understood with conventional BCS theory. In section III.C, we describe how the topological properties of the entire sequence of universality classes (of which $k = 2$ is a special case) can be understood using Witten's celebrated connection between Chern-Simons theory and the Jones polynomial of knot theory. In section III.D, we describe an alternate formalism for understanding the topological properties of Chern-Simons theory, namely through conformal field theory. The discussion revolves around the application of this formalism to fractional quantum Hall states and explains how non-Abelian quantum Hall wavefunctions can be constructed with conformal field theory. Appendix A gives a highly-condensed introduction to conformal field theory. In Section III.E, we discuss the gapless edge excitations which necessarily accompany chiral (i.e. parity, P and time-reversal T-violating) topological phases. These excitations are useful for interferometry experiments, as we discuss in Section III.F. Finally, in Section III.G, we discuss topological phases which do not violate parity and time-reversal symmetries. These phases emerge in models of electrons, spins, or bosons on lattices which could describe transition metal oxides, Josephson junction arrays, or ultra-cold atoms in optical lattices.

In Section IV, we discuss how quasiparticles in topological phases can be used for quantum computation. We first discuss the case of $\mathrm{SU}(2)_2$, which is the leading candidate for the $\nu = 5/2$ fractional quantum Hall state. We show in Section IV.A how qubits and gates can be manipulated in a gated GaAs device supporting this quantum Hall state. We discuss why quasiparticle braiding alone is not sufficient for universal quantum computation and how this limitation of the $\nu = 5/2$ state can be circumvented. Section IV.B discusses in detail how topological computations can be performed in the simplest non-Abelian theory that is capable of universal topological quantum computation, the so-called "Fibonacci-Anyon" theory. In IV.C, we show that the $\mathrm{SU}(2)_k$ theories support universal topological quantum computation for all integers k except $k = 1, 2, 4$. In IV.D, we discuss the physical processes which will cause errors in a topological quantum computer.

Finally, we briefly conclude in section V. We discuss questions for the immediate future, primarily centered on the $\nu = 5/2$ and $\nu = 12/5$ fractional quantum Hall states. We also discuss a broader set of question relating to non-Abelian topological phases and fault-tolerant quantum computation.

II. BASIC CONCEPTS

A. Non-Abelian Anyons

1. Non-Abelian Braiding Statistics

Quantum statistics is one of the basic pillars of the quantum mechanical view of the world. It is the property which distinguishes fermions from bosons: the wave function that describes a system of many identical particles should satisfy the proper symmetry under the interchange of any two particles. In 3 spatial dimension and one time dimension ($3+1$ D) there are only two possible symmetries — the wave function of bosons is symmetric under exchange while that of fermions is anti-symmetric. One cannot overemphasize, of course, the importance of the symmetry of the wavefunction, which is the root of the Pauli principle, superfluidity, the metallic state, Bose-Einstein condensation, and a long list of other phenomena.

The limitation to one of two possible types of quantum symmetry originates from the observation that a process in which two particles are adiabatically interchanged twice is equivalent to a process in which one of the particles is adiabatically taken around the other. Since, in three dimensions, wrapping one particle all the way around another is topologically equivalent to a process in which none of the particles move at all, the wave function should be left unchanged by two such interchanges of particles. The only two possibilities are for the wavefunction to change by a $\pm$ sign under a single interchange, corresponding to the cases of bosons and fermions, respectively.

We can recast this in path integral language. Suppose we consider all possible trajectories in $3+1$ dimensions which take N particles from initial positions R_1, R_2, ..., R_N at time t_i to final positions R_1, R_2, ..., R_N at time t_f. If the particles are distinguishable, then there are no topologically non-trivial trajectories, i.e. all trajectories can be continuously deformed into the trajectory in which the particles do not move at all (straight lines in the time direction). If the particles are indistinguishable, then the different trajectories fall into topological classes corresponding to the elements of the permutation group S_N, with each element of the group specifying how the initial positions are permuted to obtain the final positions. To define the quantum evolution of such a system, we must specify how the permutation group acts on the states of the system. Fermions and bosons correspond to the only two one-dimensional irreducible representations of the permutation group of N identical particles.[1]

Two-dimensional systems are qualitatively different from three (and higher dimensions) in this respect. A particle loop that encircles another particle in two dimensions cannot be deformed to a point without cutting through the other particle. Consequently, the notion of a winding of one particle around another in two dimensions is well-defined. Then, when two particles are interchanged twice in a clockwise manner, their trajectory involves a non-trivial winding, and the system does not necessarily come back to the same state. This topological difference between two and three dimensions, first realized by Leinaas and Myrheim, 1977 and by Wilczek, 1982a, leads to a profound difference in the possible quantum mechanical properties, at least as a matter of principle, for quantum systems when particles are confined to $2+1$ D (see also Goldin et al., 1981 and Wu, 1984). (As an aside, we mention that in $1+1$ D, quantum statistics is not well-defined since particle interchange is impossible without one particle going through another, and bosons with hard-core repulsion are equivalent to fermions.)

Suppose that we have two identical particles in two dimensions. Then when one particle is exchanged in a counter-clockwise manner with the other, the wavefunction can change by an arbitrary phase,

$$\psi(\mathbf{r_1}, \mathbf{r_2}) \rightarrow e^{i\theta}\psi(\mathbf{r_1}, \mathbf{r_2}) \tag{1}$$

The phase need not be merely a $\pm$ sign because a second counter-clockwise exchange need not lead back to the initial state but can result in a non-trivial phase:

$$\psi(\mathbf{r_1}, \mathbf{r_2}) \rightarrow e^{2i\theta}\psi(\mathbf{r_1}, \mathbf{r_2}) \tag{2}$$

The special cases $\theta = 0, \pi$ correspond to bosons and fermions, respectively. Particles with other values of the 'statistical angle' θ are called *anyons* (Wilczek, 1990). We will often refer to such particles as anyons with statistics θ.

Let us now consider the general case of N particles, where a more complex structure arises. The topological classes of trajectories which take these particles from initial positions R_1, R_2, ..., R_N at time t_i to final positions R_1, R_2, ..., R_N at time t_f are in one-to-one correspondence with the elements of the braid group $\mathcal{B}_N$. An element of the braid group can be visualized by thinking of trajectories of particles as world-lines (or strands) in 2+1 dimensional space-time originating at initial positions and terminating at final positions, as shown in Figure 1. The time direction will be represented vertically on the page, with the initial time at the bottom and the final time at the top. An element of the N-particle braid group is an equivalence class of such trajectories up to smooth deformations. To represent an element of a class, we will draw the trajectories on paper with the initial and final points ordered along lines at the initial and final times. When drawing the trajectories, we must be careful to distinguish when one strand passes over or under another, corresponding to a clockwise or counter-clockwise exchange. We also require that any intermediate time slice must intersect N strands. Strands cannot 'double back', which would amount to particle creation/annihilation at intermediate stages. We do not allow this because we assume that the particle number is known. (We will consider particle creation/annihilation later in this paper when we discuss field theories of anyons and, from a mathematical perspective, when we discuss the idea of a "category" in section IV below.) Then, the multiplication of two elements of the braid group is simply the successive execution

[1] Higher dimensional representations of the permutation group, known as 'parastatistics', can always be decomposed into fermions or bosons with an additional quantum number attached to each particle (Doplicher et al., 1971, 1974).

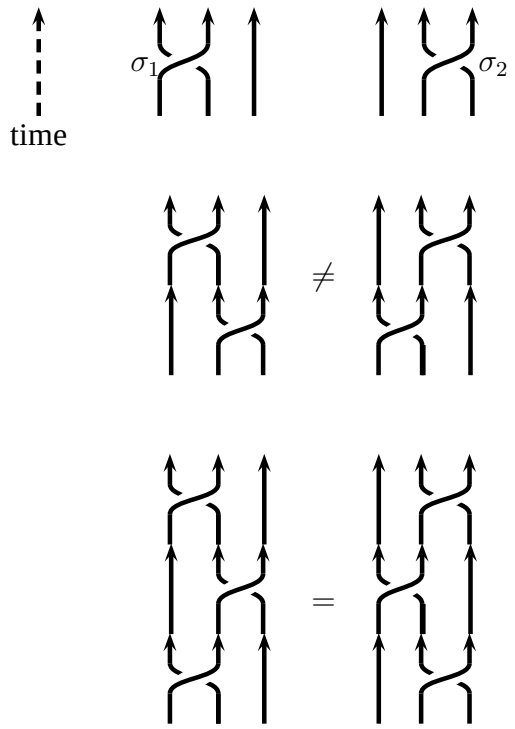

FIG. 1 **Top:** The two elementary braid operations σ_1 and σ_2 on three particles. **Middle:** Here we show $\sigma_2\sigma_1 \neq \sigma_1\sigma_2$, hence the braid group is Non-Abelian. **Bottom:** The braid relation (Eq. 3) $\sigma_i\sigma_{i+1}\sigma_i = \sigma_{i+1}\sigma_i\sigma_{i+1}$.

of the corresponding trajectories, i.e. the vertical stacking of the two drawings. (As may be seen from the figure, the order in which they are multiplied is important because the group is non-Abelian, meaning that multiplication is not commutative.)

The braid group can be represented algebraically in terms of generators σ_i, with $1 \leq i \leq N-1$. We choose an arbitrary ordering of the particles $1, 2, \ldots, N$.[2] σ_i is a counter-clockwise exchange of the i^{th} and $(i+1)^{\text{th}}$ particles. σ_i^{-1} is, therefore, a clockwise exchange of the i^{th} and $(i+1)^{\text{th}}$ particles. The σ_is satisfy the defining relations (see Fig. 1),

$$\begin{aligned} \sigma_i\sigma_j &= \sigma_j\sigma_i \quad \text{for } |i-j| \geq 2 \\ \sigma_i\sigma_{i+1}\sigma_i &= \sigma_{i+1}\sigma_i\,\sigma_{i+1} \quad \text{for } 1 \leq i \leq n-1 \end{aligned} \tag{3}$$

The only difference from the permutation group S_N is that $\sigma_i^2 \neq 1$, but this makes an enormous difference. While the permutation group is finite, the number of elements in the group $|S_N| = N!$, the braid group is infinite, even for just two particles. Furthermore, there are non-trivial topological classes of trajectories even when the particles are distinguishable, e.g. in the two-particle case those trajectories in which one particle winds around the other an integer number of times. These topological classes correspond to the elements of the 'pure' braid group, which is the subgroup of the braid group containing only elements which bring each particle back to its own initial position, not the initial position of one of the other particles. The richness of the braid group is the key fact enabling quantum computation through quasiparticle braiding.

To define the quantum evolution of a system, we must now specify how the braid group acts on the states of the system. The simplest possibilities are one-dimensional representations of the braid group. In these cases, the wavefunction acquires a phase θ when one particle is taken around another, analogous to Eqs. 1, 2. The special cases $\theta = 0, \pi$ are bosons and fermions, respectively, while particles with other values of θ are *anyons* (Wilczek, 1990). These are straightforward many-particle generalizations of the two-particle case considered above. An arbitrary element of the braid group is represented by the factor $e^{im\theta}$ where m is the total number of times that one particle winds around another in a counter-clockwise manner (minus the number of times that a particle winds around another in a clockwise manner). These representations are Abelian since the order of braiding operations in unimportant. However, they can still have a quite rich structure since there can be n_s different particle species with parameters θ_{ab}, where $a, b = 1, 2, \ldots, n_s$, specifying the phases resulting from braiding a particle of type a around a particle of type b. Since distinguishable particles can braid non-trivially, i.e. θ_{ab} can be non-zero for $a \neq b$ as well as for $a = b$, anyonic 'statistics' is, perhaps, better understood as a kind of topological interaction between particles.

We now turn to non-Abelian braiding statistics, which are associated with higher-dimensional representations of the braid group. Higher-dimensional representations can occur when there is a degenerate set of g states with particles at fixed positions R_1, R_2, ..., R_n. Let us define an orthonormal basis ψ_α, $\alpha = 1, 2, \ldots, g$ of these degenerate states. Then an element of the braid group – say σ_1, which exchanges particles 1 and 2 – is represented by a $g \times g$ unitary matrix $\rho(\sigma_1)$ acting on these states.

$$\psi_\alpha \rightarrow [\rho(\sigma_1)]_{\alpha\beta}\,\psi_\beta \tag{4}$$

On the other hand, exchanging particles 2 and 3 leads to:

$$\psi_\alpha \rightarrow [\rho(\sigma_2)]_{\alpha\beta}\,\psi_\beta \tag{5}$$

Both $\rho(\sigma_1)$ and $\rho(\sigma_2)$ are $g \times g$ dimensional unitary matrices, which define unitary transformation within the subspace of degenerate ground states. If $\rho(\sigma_1)$ and $\rho(\sigma_1)$ do not commute, $[\rho(\sigma_1)]_{\alpha\beta}[\rho(\sigma_2)]_{\beta\gamma} \neq [\rho(\sigma_2)]_{\alpha\beta}[\rho(\sigma_1)]_{\beta\gamma}$, the particles obey *non-Abelian braiding statistics*. Unless they commute for any interchange of particles, in which case the particles' braiding statistics is Abelian, braiding quasiparticles will cause non-trivial rotations within the degenerate many-quasiparticle Hilbert space. Furthermore, it will essentially be true at low energies that the *only* way to make non-trivial unitary operations on this degenerate space is by braiding quasiparticles around each other. This statement is equivalent to a

[2] Choosing a different ordering would amount to a relabeling of the elements of the braid group, as given by conjugation by the braid which transforms one ordering into the other.

statement that no local perturbation can have nonzero matrix elements within this degenerate space.

A system with anyonic particles must generally have multiple types of anyons. For instance, in a system with Abelian anyons with statistics θ, a bound state of two such particles has statistics 4θ. Even if no such stable bound state exists, we may wish to bring two anyons close together while all other particles are much further away. Then the two anyons can be approximated as a single particle whose quantum numbers are obtained by combining the quantum numbers, including the topological quantum numbers, of the two particles. As a result, a complete description of the system must also include these 'higher' particle species. For instance, if there are $\theta = \pi/m$ anyons in system, then there are also $\theta = 4\pi/m, 9\pi/m, \ldots, (m-1)^2\pi/m$. Since the statistics parameter is only well-defined up to 2π, $\theta = (m-1)^2\pi/m = -\pi/m$ for m even and $\pi - \pi/m$ for m odd. The formation of a different type of anyon by bringing together two anyons is called *fusion*. When a statistics π/m particle is fused with a statistics $-\pi/m$ particle, the result has statistics $\theta = 0$. It is convenient to call this the 'trivial' particle. As far as topological properties are concerned, such a boson is just as good as the absence of any particle, so the 'trivial' particle is also sometimes simply called the 'vacuum'. We will often denote the trivial particle by $\mathbf{1}$.

With Abelian anyons which are made by forming successively larger composites of π/m particles, the *fusion rule* is: $\frac{n^2\pi}{m} \times \frac{k^2\pi}{m} = \frac{(n+k)^2\pi}{m}$. (We will use $a \times b$ to denote a fused with b.) However, for non-Abelian anyons, the situation is more complicated. As with ordinary quantum numbers, there might not be a unique way of combining topological quantum numbers (e.g. two spin-$1/2$ particles could combine to form either a spin-0 or a spin-1 particle). The different possibilities are called the different *fusion channels*. This is usually denoted by

$$\phi_a \times \phi_b = \sum_c N_{ab}^c \phi_c \tag{6}$$

which represents the fact that when a particle of species a fuses with one of species b, the result can be a particle of species c if $N_{ab}^c \neq 0$. For Abelian anyons, the fusion multiplicities $N_{ab}^c = 1$ for only one value of c and $N_{ab}^{c'} = 0$ for all $c' \neq c$. For particles of type k with statistics $\theta_k = \pi k^2/m$, i.e. $N_{kk'}^{k''} = \delta_{k+k',k''}$. For non-Abelian anyons, there is at least one a, b such that there are multiple fusion channels c with $N_{ab}^c \neq 0$. In the examples which we will be considering in this paper, $N_{ab}^c = 0$ or 1, but there are theories for which $N_{ab}^c > 1$ for some a, b, c. In this case, a and b can fuse to form c in $N_{ab}^c > 1$ different distinct ways. We will use $\bar{a}$ to denote the antiparticle of particle species a. When a and $\bar{a}$ fuse, they can always fuse to 1 in precisely one way, i.e. $N_{a\bar{a}}^1 = 1$; in the non-Abelian case, they may or may not be able to fuse to other particle types as well.

The different fusion channels are one way of accounting for the different degenerate multi-particle states. Let us see how this works in one simple model of non-Abelian anyons which we discuss in more detail in section III. As we discuss in section III, this model is associated with 'Ising anyons' (which are so-named for reasons which will become clear in sections III.D and III.E), $SU(2)_2$, and chiral p-superconductors. There are slight differences between these three theories, relating to Abelian phases, but these are unimportant for the present discussion. This model has three different types of anyons, which can be variously called $1, \sigma, \psi$ or $0, \frac{1}{2}, 1$. (Unfortunately, the notation is a little confusing because the trivial particle is called '**1**' in the first model but '0' in the second, however, we will avoid confusion by using bold-faced **1** to denote the trivial particle.) The fusion rules for such anyons are

$$\begin{aligned} \sigma \times \sigma &= \mathbf{1} + \psi, \quad \sigma \times \psi = \sigma, \quad \psi \times \psi = \mathbf{1}, \\ \mathbf{1} \times x &= x \quad \text{for} \quad x = \mathbf{1}, \sigma, \psi \end{aligned} \tag{7}$$

(Translating these rules into the notation of $SU(2)_2$, we see that these fusion rules are very similar to the decomposition rules for tensor products of irreducible SU(2) representations, but differ in the important respect that 1 is the maximum spin so that $\frac{1}{2} \times \frac{1}{2} = 0 + 1$, as in the SU(2) case, but $\frac{1}{2} \times 1 = \frac{1}{2}$ and $1 \times 1 = 0$.) Note that there are two different fusion channels for two σs. As a result, if there are four σs which fuse together to give $\mathbf{1}$, there is a two-dimensional space of such states. If we divided the four σs into two pairs, by grouping particles $1, 2$ and $3, 4$, then a basis for the two-dimensional space is given by the state in which $1, 3$ fuse to $\mathbf{1}$ or $1, 3$ fuse to ψ ($2, 4$ must fuse to the same particle type as $1, 3$ do in order that all four particles fuse to $\mathbf{1}$). We can call these states Ψ_1 and Ψ_ψ; they are a basis for the four-quasiparticle Hilbert space with total topological charge $\mathbf{1}$. (Similarly, if they all fused to give ψ, there would be another two-dimensional degenerate space; one basis is given by the state in which the first pair fuses to $\mathbf{1}$ while the second fuses to ψ and the state in which the opposite occurs.)

Of course, our division of the four σs into two pairs was arbitrary. We could have divided them differently, say, into the pairs $1, 3$ and $2, 4$. We would thereby obtain two different basis states, $\tilde{\Psi}_1$ and $\tilde{\Psi}_\psi$, in which both pairs fuse to $\mathbf{1}$ or to ψ, respectively. This is just a different basis in the same two-dimensional space. The matrix parametrizing this basis change (see also Appendix A) is called the F-matrix: $\tilde{\Psi}_a = F_{ab}\Psi_b$, where $a, b = 1, \psi$. There should really be 6 indices on F if we include indices to specify the 4 particle types: $\left[F_l^{ijk}\right]_{ab}$, but we have dropped these other indices since $i = j = k = l = \sigma$ in our case. The F-matrices are sometimes called $6j$ symbols since they are analogous to the corresponding quantities for SU(2) representations. Recall that in SU(2), there are multiple states in which spins $\mathbf{j}_1, \mathbf{j}_2, \mathbf{j}_3$ couple to form a total spin $\mathbf{J}$. For instance, $\mathbf{j}_1$ and $\mathbf{j}_2$ can add to form $\mathbf{j}_{12}$, which can then add with $\mathbf{j}_3$ to give $\mathbf{J}$. The eigenstates of $(\mathbf{j}_{12})^2$ form a basis of the different states with fixed $\mathbf{j}_1$, $\mathbf{j}_2$, $\mathbf{j}_3$, and $\mathbf{J}$. Alternatively, $\mathbf{j}_2$ and $\mathbf{j}_3$ can add to form $\mathbf{j}_{23}$, which can then add with $\mathbf{j}_1$ to give $\mathbf{J}$. The eigenstates of $(\mathbf{j}_{23})^2$ form a different basis. The $6j$ symbol gives the basis change between the two. The F-matrix of a system of anyons plays the same role when particles of topological charges i, j, k fuse to total topological charge l. If i and j fuse to a, which then fuses with k to give topological charge l, the different allowed a define a basis. If j and k fuse to b and then fuse with i to

give topological charge l, this defines another basis, and the F-matrix is the unitary transformation between the two bases. States with more than 4 quasiparticles can be understood by successively fusing additional particles, in a manner described in Section III.A. The F-matrix can be applied to any set of 4 consecutively fused particles.

The different states in this degenerate multi-anyon state space transform into each other under braiding. However, two particles cannot change their fusion channel simply by braiding with each other since their total topological charge can be measured along a far distant loop enclosing the two particles. They must braid with a third particle in order to change their fusion channel. Consequently, when two particles fuse in a particular channel (rather than a linear superposition of channels), the effect of taking one particle around the other is just multiplication by a phase. This phase resulting from a counter-clockwise exchange of particles of types a and b which fuse to a particle of type c is called R_c^{ab}. In the Ising anyon case, as we will derive in section III and Appendix A.1, $R_1^{\sigma\sigma} = e^{-\pi i/8}$, $R_\psi^{\sigma\sigma} = e^{3\pi i/8}$, $R_1^{\psi\psi} = -1$, $R_\sigma^{\sigma\psi} = i$. For an example of how this works, suppose that we create a pair of σ quasiparticles out of the vacuum. They will necessarily fuse to $\mathbf{1}$. If we take one around another, the state will change by a phase $e^{-\pi i/8}$. If we take a third σ quasiparticle and take it around one, but not both, of the first two, then the first two will now fuse to ψ, as we will show in Sec. III. If we now take one of the first two around the other, the state will change by a phase $e^{3\pi i/8}$.

In order to fully specify the braiding statistics of a system of anyons, it is necessary to specify (1) the particle species, (2) the fusion rules N_{ab}^c, (3) the F-matrices, and (4) the R-matrices. In section IV, we will introduce the other sets of parameters, namely the topological spins Θ_a and the S-matrix, which, together with the parameters 1-4 above fully characterize the topological properties of a system of anyons. Some readers may be familiar with the incarnation of these mathematical structures in conformal field theory (CFT), where they occur for reasons which we explain in section III.D; we briefly review these properties in the CFT context in Appendix A.

Quasiparticles obeying non-Abelian braiding statistics or, simply non-Abelian anyons, were first considered in the context of conformal field theory by Moore and Seiberg, 1988, 1989 and in the context of Chern-Simons theory by Witten, 1989. They were discussed in the context of discrete gauge theories and linked to the representation theory of *quantum groups* by Bais, 1980; Bais et al., 1992, 1993a,b. They were discussed in a more general context by Fredenhagen et al., 1989 and Fröhlich and Gabbiani, 1990. The properties of non-Abelian quasiparticles make them appealing for use in a quantum computer. But before discussing this, we will briefly review how they could occur in nature and then the basic ideas behind quantum computation.

2. Emergent Anyons

The preceding considerations show that exotic braiding statistics is a theoretical possibility in $2+1$-D, but they do not tell us when and where they might occur in nature. Electrons, protons, atoms, and photons, are all either fermions or bosons even when they are confined to move in a two-dimensional plane. However, if a system of many electrons (or bosons, atoms, etc.) confined to a two-dimensional plane has excitations which are localized disturbances of its quantum-mechanical ground state, known as *quasiparticles*, then these quasiparticles can be anyons. When a system has anyonic quasiparticle excitations above its ground state, it is in a *topological phase of matter*. (A more precise definition of a topological phase of matter will be given in Section III.)

Let us see how anyons might arise as an emergent property of a many-particle system. For the sake of concreteness, consider the ground state of a $2+1$ dimensional system of of electrons, whose coordinates are $(r_1, \ldots, r_n)$. We assume that the ground state is separated from the excited states by an energy gap (i.e, it is incompressible), as is the situation in fractional quantum Hall states in 2D electron systems. The lowest energy electrically-charged excitations are known as quasiparticles or quasiholes, depending on the sign of their electric charge. (The term "quasiparticle" is also sometimes used in a generic sense to mean both quasiparticle and quasihole as in the previous paragraph). These quasiparticles are local disturbances to the wavefunction of the electrons corresponding to a quantized amount of total charge.

We now introduce into the system's Hamiltonian a scalar potential composed of many local "traps", each sufficient to capture exactly one quasiparticle. These traps may be created by impurities, by very small gates, or by the potential created by tips of scanning microscopes. The quasiparticle's charge screens the potential introduced by the trap and the "quasiparticle-tip" combination cannot be observed by local measurements from far away. Let us denote the positions of these traps to be $(R_1, \ldots, R_k)$, and assume that these positions are well spaced from each other compared to the microscopic length scales. A state with quasiparticles at these positions can be viewed as an excited state of the Hamiltonian of the system without the trap potential or, alternatively, as the ground state in the presence of the trap potential. When we refer to the ground state(s) of the system, we will often be referring to multi-quasiparticle states in the latter context. The quasiparticles' coordinates $(R_1, \ldots, R_k)$ are parameters both in the Hamiltonian and in the resulting ground state wavefunction for the electrons.

We are concerned here with the effect of taking these quasiparticles around each other. We imagine making the quasiparticles coordinates $\mathbf{R} = (R_1, \ldots, R_k)$ adiabatically time-dependent. In particular, we consider a trajectory in which the final configuration of quasiparticles is just a permutation of the initial configuration (i.e. at the end, the positions of the quasiparticles are identical to the intial positions, but some quasiparticles may have interchanged positions with others.) If the ground state wave function is single-valued with respect to $(R_1, .., R_k)$, *and if there is only one ground state for any given set of R_i's*, then the final ground state to which the system returns to after the winding is identical to the initial one, up to a phase. Part of this phase is simply the dynamical phase which depends on the energy of the quasiparticle state and

the length of time for the process. In the adiabatic limit, it is $\int dtE(\vec{R}(t))$. There is also a a geometric phase which does not depend on how long the process takes. This Berry phase is (Berry, 1984),

$$\alpha = i \oint d\mathbf{R} \cdot \langle \psi(\mathbf{R}) | \nabla_{\vec{R}} | \psi(\mathbf{R}) \rangle \tag{8}$$

where $|\psi(\mathbf{R})\rangle$ is the ground state with the quasiparticles at positions $\mathbf{R}$, and where the integral is taken along the trajectory $\mathbf{R}(t)$. It is manifestly dependent only on the trajectory taken by the particles and not on how long it takes to move along this trajectory.

The phase α has a piece that depends on the geometry of the path traversed (typically proportional to the area enclosed by all of the loops), and a piece θ that depends only on the topology of the loops created. If $\theta \neq 0$, then the quasiparticles excitations of the system are anyons. In particular, if we consider the case where only two quasiparticles are interchanged clockwise (without wrapping around any other quasiparticles), θ is the statistical angle of the quasiparticles.

There were two key conditions to our above discussion of the Berry phase. The single valuedness of the wave function is a technical issue. The non-degeneracy of the ground state, however, is an important physical condition. In fact, most of this paper deals with the situation in which this condition does not hold. We will generally be considering systems in which, once the positions $(R_1, .., R_k)$ of the quasiparticles are fixed, there remain multiple degenerate ground states (i.e. ground states in the presence of a potential which captures quasiparticles at positions $(R_1, .., R_k)$), which are distinguished by a set of internal quantum numbers. For reasons that will become clear later, we will refer to these quantum numbers as "topological".

When the ground state is degenerate, the effect of a closed trajectory of the R_i's is not necessarily *just* a phase factor. The system starts and ends in ground states, but the initial and final ground states may be different members of this degenerate space. The constraint imposed by adiabaticity in this case is that the adiabatic evolution of the state of the system is confined to the subspace of ground states. Thus, it may be expressed as a unitary transformation within this subspace. The inner product in (8) must be generalized to a matrix of such inner products:

$$\mathbf{m}_{ab} = \langle \psi_a(\mathbf{R}) | \vec{\nabla}_{\mathbf{R}} | \psi_b(\mathbf{R}) \rangle \tag{9}$$

where $|\psi_a(\mathbf{R})\rangle$, $a = 1, 2, \ldots, g$ are the g degenerate ground states. Since these matrices at different points $\vec{R}$ do not commute, we must path-order the integral in order to compute the transformation rule for the state, $\psi_a \rightarrow M_{ab}\, \psi_b$ where

$$\begin{aligned} M_{ab} &= \mathcal{P} \exp\left(i \oint d\mathbf{R} \cdot \mathbf{m} \right) \\ &= \sum_{n=0}^{\infty} i^n \int_0^{2\pi} ds_1 \int_0^{s_1} ds_2 \ldots \int_0^{s_{n-1}} ds_n \Big[\dot{\mathbf{R}}(s_1) \cdot \mathbf{m}_{aa_1}(\mathbf{R}(s_1)) \ldots \\ &\qquad \dot{\mathbf{R}}(s_n) \cdot \mathbf{m}_{a_n b}(\mathbf{R}(s_n)) \Big] \end{aligned} \tag{10}$$

Where $\mathbf{R}(s)$, $s \in [0, 2\pi]$ is the closed trajectory of the particles and the path-ordering symbol $\mathcal{P}$ is defined by the second equality. Again, the matrix M_{ab} may be the product of topological and non-topological parts. In a system in which quasiparticles obey non-Abelian braiding statistics, the non-topological part will be Abelian, that is, proportional to the unit matrix. Only the topological part will be non-Abelian.

The requirements for quasiparticles to follow non-Abelian statistics are then, first, that the N-quasiparticle ground state is degenerate. In general, the degeneracy will not be exact, but it should vanish exponentially as the quasiparticle separations are increased. Second, that adiabatic interchange of quasiparticles applies a unitary transformation on the ground state, whose non-Abelian part is determined only by the topology of the braid, while its non-topological part is Abelian. If the particles are not infinitely far apart, and the degeneracy is only approximate, then the adiabatic interchange must be done faster than the inverse of the energy splitting (Thouless and Gefen, 1991) between states in the nearly-degenerate subspace (but, of course, still much slower than the energy gap between this subspace and the excited states). Third, the only way to make unitary operations on the degenerate ground state space, so long as the particles are kept far apart, is by braiding. The simplest (albeit uninteresting) example of degenerate ground states may arise if each of the quasiparticles carried a spin $1/2$ with a vanishing g–factor. If that were the case, the system would satisfy the first requirement. Spin orbit coupling may conceivably lead to the second requirement being satisfied. Satisfying the third one, however, is much harder, and requires the subtle structure that we describe below.

The degeneracy of N-quasiparticle ground states is conditioned on the quasiparticles being well separated from one another. When quasiparticles are allowed to approach one another too closely, the degeneracy is lifted. In other words, when non-Abelian anyonic quasiparticles are close together, their different fusion channels are split in energy. This dependence is analogous to the way the energy of a system of spins depends on their internal quantum numbers when the spins are close together and their coupling becomes significant. The splitting between different fusion channels is a means for a measurement of the internal quantum state, a measurement that is of importance in the context of quantum computation.

B. Topological Quantum Computation

1. Basics of Quantum Computation

As the components of computers become smaller and smaller, we are approaching the limit in which quantum effects become important. One might ask whether this is a problem or an opportunity. The founders of the field of quantum computation (Manin, 1980, Feynman, 1982, 1986, Deutsch, 1985, and most dramatically, Shor, 1994) answered in favor of the latter. They showed that a computer which operates coherently on quantum states has potentially much greater power than a classical computer (Nielsen and Chuang, 2000).

The problem which Feynman had in mind for a quantum

computer was the simulation of a quantum system (Feynman, 1982). He showed that certain many-body quantum Hamiltonians could be simulated *exponentially faster* on a quantum computer than they could be on a classical computer. This is an extremely important potential application of a quantum computer since it would enable us to understand the properties of complex materials, e.g. solve high-temperature superconductivity. Digital simulations of large scale quantum many-body Hamiltonians are essentially hopeless on classical computers because of the exponentially-large size of the Hilbert space. A quantum computer, using the physical resource of an exponentially-large Hilbert space, may also enable progress in the solution of lattice gauge theory and quantum chromodynamics, thus shedding light on strongly-interacting nuclear forces.

In 1994 Peter Shor found an application of a quantum computer which generated widespread interest not just inside but also outside of the physics community (Shor, 1994). He invented an algorithm by which a quantum computer could find the prime factors of an m digit number in a length of time $\sim\ m^2 \log m \log\log m$. This is much faster than the fastest known algorithm for a classical computer, which takes $\sim \exp(m^{1/3})$ time. Since many encryption schemes depend on the difficulty of finding the solution to problems similar to finding the prime factors of a large number, there is an obvious application of a quantum computer which is of great basic and applied interest.

The computation model set forth by these pioneers of quantum computing (and refined in DiVincenzo, 2000), is based on three steps: initialization, unitary evolution and measurement. We assume that we have a system at our disposal with Hilbert space $\mathcal{H}$. We further assume that we can initialize the system in some known state $|\psi_0\rangle$. We unitarily evolve the system until it is in some final state $U(t)|\psi_0\rangle$. This evolution will occur according to some Hamiltonian $H(t)$ such that $dU/dt = iH(t)\,U(t)/\hbar$. We require that we have enough control over this Hamiltonian so that $U(t)$ can be made to be any unitary transformation that we desire. Finally, we need to measure the state of the system at the end of this evolution. Such a process is called *quantum computation* (Nielsen and Chuang, 2000). The Hamiltonian $H(t)$ is the software program to be run. The initial state is the input to the calculation, and the final measurement is the output.

The need for versatility, i.e., for one computer to efficiently solve many different problems, requires the construction of the computer out of smaller pieces that can be manipulated and reconfigured individually. Typically the fundamental piece is taken to be a quantum two state system known as a "qubit" which is the quantum analog of a bit. (Of course, one could equally well take general "dits", for which the fundamental unit is some d-state system with d not too large). While a classical bit, i.e., a classical two-state system, can be either "zero" or "one" at any given time, a qubit can be in one of the infinitely many superpositions $a|0\rangle + b|1\rangle$. For n qubits, the state becomes a vector in a 2^n–dimensional Hilbert space, in which the different qubits are generally entangled with one another.

The quantum phenomenon of superposition allows a system to traverse many trajectories in parallel, and determine its state by their coherent sum. In some sense this coherent sum amounts to a massive quantum parallelism. It should not, however, be confused with classical parallel computing, where many computers are run in parallel, and no coherent sum takes place.

The biggest obstacle to building a practical quantum computer is posed by errors, which would invariably happen during any computation, quantum or classical. For any computation to be successful one must devise practical schemes for error correction which can be effectively implemented (and which must be sufficiently fault-tolerant). Errors are typically corrected in classical computers through redundancies, i.e., by keeping multiple copies of information and checking against these copies.

With a quantum computer, however, the situation is more complex. If we measure a quantum state during an intermediate stage of a calculation to see if an error has occurred, we collapse the wave function and thus destroy quantum superpositions and ruin the calculation. Furthermore, errors need not be merely a discrete flip of $|0\rangle$ to $|1\rangle$, but can be continuous: the state $a|0\rangle + b|1\rangle$ may drift, due to an error, to the state $\rightarrow a|0\rangle + be^{i\theta}|1\rangle$ with arbitrary θ.

Remarkably, in spite of these difficulties, error correction is possible for quantum computers (Calderbank and Shor, 1996; Gottesman, 1998; Preskill, 2004; Shor, 1995; Steane, 1996a). One can represent information redundantly so that errors can be identified without measuring the information. For instance, if we use three spins to represent each qubit, $|0\rangle \rightarrow |000\rangle$, $|1\rangle \rightarrow |111\rangle$, and the spin-flip rate is low, then we can identify errors by checking whether all three spins are the same (here, we represent an up spin by 0 and a down spin by 1). Suppose that our spins are in in the state $\alpha|000\rangle + \beta|111\rangle$. If the first spin has flipped erroneously, then our spins are in the state $\alpha|100\rangle + \beta|011\rangle$. We can detect this error by checking whether the first spin is the same as the other two; this does not require us to measure the state of the qubit. ("We measure the errors, rather than the information." (Preskill, 2004)) If the first spin is different from the other two, then we just need to flip it. We repeat this process with the second and third spins. So long as we can be sure that two spins have not erroneously flipped (i.e. so long as the basic spin-flip rate is low), this procedure will correct spin-flip errors. A more elaborate encoding is necessary in order to correct phase errors, but the key observation is that a phase error in the σ_z basis is a bit flip error in the σ_x basis.

However, the error correction process may itself be a little noisy. More errors could then occur during error correction, and the whole procedure will fail unless the basic error rate is very small. Estimates of the threshold error rate above which error correction is impossible depend on the particular error correction scheme, but fall in the range $10^{-4} - 10^{-6}$ (see, e.g. Aharonov and Ben-Or, 1997; Knill et al., 1998). This means that we must be able to perform $10^4 - 10^6$ operations perfectly before an error occurs. This is an extremely stringent constraint and it is presently unclear if local qubit-based quantum computation can ever be made fault-tolerant through quantum error correction protocols.

Random errors are caused by the interaction between the quantum computer and the environment. As a result of this interaction, the quantum computer, which is initially in a pure superposition state, becomes entangled with its environment. This can cause errors as follows. Suppose that the quantum computer is in the state $|0\rangle$ and the environment is in the state $|E_0\rangle$ so that their combined state is $|0\rangle|E_0\rangle$. The interaction between the computer and the environment could cause this state to evolve to $\alpha|0\rangle|E_0\rangle + \beta|1\rangle|E_1\rangle$, where $|E_1\rangle$ is another state of the environment (not necessarily orthogonal to $|E_0\rangle$). The computer undergoes a transition to the state $|1\rangle$ with probability $|\beta|^2$. Furthermore, the computer and the environment are now entangled, so the reduced density matrix for the computer alone describes a mixed state, e.g. $\rho = \mathrm{diag}(|\alpha|^2, |\beta|^2)$ if $\langle E_0|E_1\rangle = 0$. Since we cannot measure the state of the environment accurately, information is lost, as reflected in the evolution of the density matrix of the computer from a pure state to a mixed one. In other words, the environment has caused *decoherence*. Decoherence can destroy quantum information even if the state of the computer does not undergo a transition. Although whether or not a transition occurs is basis-dependent (a bit flip in the σ_z basis is a phase flip in the σ_x basis), it is a useful distinction because many systems have a preferred basis, for instance the ground state $|0\rangle$ and excited state $|1\rangle$ of an ion in a trap. Suppose the state $|0\rangle$ evolves as above, but with $\alpha = 1$, $\beta = 0$ so that no transition occurs, while the state $|1\rangle|E_0\rangle$ evolves to $|1\rangle|E_1'\rangle$ with $\langle E_1'|E_1\rangle = 0$. Then an initial pure state $(a|0\rangle + b|1\rangle)|E_0\rangle$ evolves to a mixed state with density matrix $\rho = \mathrm{diag}(|a|^2, |b|^2)$. The correlations in which our quantum information resides is now transferred to correlation between the quantum computer and the environment. The quantum state of a system invariably loses coherence in this way over a characteristic time scale T_{coh}. It was universally assumed until the advent of quantum error correction (Shor, 1995; Steane, 1996a) that quantum computation is intrinsically impossible since decoherence-induced quantum errors simply cannot be corrected in any real physical system. However, when error-correcting codes are used, the entanglement is transferred from the quantum computer to ancillary qubits so that the quantum information remains pure while the entropy is in the ancillary qubits.

Of course, even if the coupling to the environment were completely eliminated, so that there were no random errors, there could still be systematic errors. These are unitary errors which occur while we process quantum information. For instance, we may wish to rotate a qubit by 90 degrees but might inadvertently rotate it by 90.01 degrees.

From a practical standpoint, it is often useful to divide errors into two categories: (i) errors that occur when a qubit is being processed (i.e., when computations are being performed on that qubit) and (ii) errors that occur when a qubit is simply storing quantum information and is not being processed (i.e., when it is acting as a quantum memory). From a fundamental standpoint, this is a bit of a false dichotomy, since one can think of quantum information storage (or quantum memory) as being a computer that applies the identity operation over and over to the qubit (i.e., leaves it unchanged). Nonetheless, the problems faced in the two categories might be quite different. For quantum information processing, unitary errors, such as rotating a qubit by 90.01 degrees instead of 90, are an issue of how precisely one can manipulate the system. On the other hand, when a qubit is simply storing information, one is likely to be more concerned about errors caused by interactions with the environment. This is instead an issue of how well isolated one can make the system. As we will see below, a topological quantum computer is protected from problems in both of these categories.

2. Fault-Tolerance from Non-Abelian Anyons

Topological quantum computation is a scheme for using a system whose excitations satisfy non-Abelian braiding statistics to perform quantum computation in a way that is naturally immune to errors. The Hilbert space $\mathcal{H}$ used for quantum computation is the subspace of the total Hilbert space of the system comprised of the degenerate ground states with a fixed number of quasiparticles at fixed positions. Operations within this subspace are carried out by braiding quasiparticles. As we discussed above, the subspace of degenerate ground states is separated from the rest of the spectrum by an energy gap. Hence, if the temperature is much lower than the gap and the system is weakly perturbed using frequencies much smaller than the gap, the system evolves only within the ground state subspace. Furthermore, that evolution is severely constrained, since it is essentially the case (with exceptions which we will discuss) that *the only way the system can undergo a nontrivial unitary evolution - that is, an evolution that takes it from one ground state to another - is by having its quasiparticles braided*. The reason for this exceptional stability is that any local perturbation (such as the electron-phonon interaction and the hyperfine electron-nuclear interaction, two major causes for decoherence in non-topological solid state spin-based quantum computers (Witzel and Das Sarma, 2006)) has no nontrivial matrix elements within the ground state subspace. Thus, the system is rather immune from decoherence (Kitaev, 2003). Unitary errors are also unlikely since the unitary transformations associated with braiding quasiparticles are sensitive only to the topology of the quasiparticle trajectories, and not to their geometry or dynamics.

A model in which non-Abelian quasiparticles are utilized for quantum computation starts with the construction of qubits. In sharp contrast to most realizations of a quantum computer, a qubit here is a non-local entity, being comprised of several well-separated quasiparticles, with the two states of the qubit being two different values for the internal quantum numbers of this set of quasiparticles. In the simplest non-Abelian quantum Hall state, which has Landau-level filling factor $\nu = 5/2$, two quasiparticles can be put together to form a qubit (see Sections II.C.4 and IV.A). Unfortunately, as we will discuss below in Sections IV.A and IV.C, this system turns out to be incapable of universal topological quantum computation using only braiding operations; some unprotected operations are necessary in order to perform universal quantum computation. The simplest system that is capa-

ble of universal topological quantum computation is discussed in Section IV.B, and utilizes three quasiparticles to form one qubit.

As mentioned above, to perform a quantum computation, one must be able to initialize the state of qubits at the beginning, perform arbitrary controlled unitary operations on the state, and then measure the state of qubits at the end. We now address each of these in turn.

Initialization may be performed by preparing the quasiparticles in a specific way. For example, if a quasiparticle-anti-quasiparticle pair is created by "pulling" it apart from the vacuum (e.g. pair creation from the vacuum by an electric field), the pair will begin in an initial state with the pair necessarily having conjugate quantum numbers (i.e., the "total" quantum number of the pair remains the same as that of the vacuum). This gives us a known initial state to start with. It is also possible to use measurement and unitary evolution (both to be discussed below) as an initialization scheme — if one can measure the quantum numbers of some quasiparticles, one can then perform a controlled unitary operation to put them into any desired initial state.

Once the system is initialized, controlled unitary operations are then performed by physically dragging quasiparticles around one another in some specified way. When quasiparticles belonging to different qubits braid, the state of the qubits changes. Since the resulting unitary evolution depends only on the topology of the braid that is formed and not on the details of how it is done, it is insensitive to wiggles in the path, resulting, e.g., from the quasiparticles being scattered by phonons or photons. Determining which braid corresponds to which computation is a complicated but eminently solvable task, which will be discussed in more depth in section IV.B.3.

Once the unitary evolution is completed, there are two ways to measure the state of the qubits. The first relies on the fact that the degeneracy of multi-quasiparticle states is split when quasiparticles are brought close together (within some microscopic length scale). When two quasiparticles are brought close together, for instance, a measurement of this energy (or a measurement of the force between two quasiparticles) measures the the topological charge of the pair. A second way to measure the topological charge of a group of quasiparticles is by carrying out an Aharanov-Bohm type interference experiment. We take a "beam" of test quasiparticles, send it through a beamsplitter, send one partial wave to the right of the group to be measured and another partial wave to the left of the group and then re-interfere the two waves (see Figure 2 and the surrounding discussion). Since the two different beams make different braids around the test group, they will experience different unitary evolution depending on the topological quantum numbers of the test group. Thus, the re-interference of these two beams will reflect the topological quantum number of the group of quasiparticles enclosed.

This concludes a rough description of the way a topological quantum computation is to be performed. While the unitary transformation associated with a braid depends only on the topology of the braid, one may be concerned that errors could occur if one does not return the quasiparticles to precisely the correct position at the end of the braiding. This apparent problem, however, is evaded by the nature of the computations, which correspond to closed world lines that have no loose ends: when the computation involves creation and annihilation of a quasiparticle quasi-hole pair, the world-line is a closed curve in space-time. If the measurement occurs by bringing two particles together to measure their quantum charge, it does not matter where precisely they are brought together. Alternatively, when the measurement involves an interference experiment, the interfering particle must close a loop. In other words, a computation corresponds to a set of *links* rather than open braids, and the initialization and measurement techniques *necessarily* involve bringing quasiparticles together in some way, closing up the trajectories and making the full process from initialization to measurement completely topological.

Due to its special characteristics, then, topological quantum computation intrinsically guarantees fault-tolerance, at the level of "hardware", without "software"-based error correction schemes that are so essential for non-topological quantum computers. This immunity to errors results from the stability of the ground state subspace with respect to external local perturbations. In non-topological quantum computers, the qubits are local, and the operations on them are local, leading to a sensitivity to errors induced by local perturbations. In a topological quantum computer the qubits are non-local, and the operations — quasiparticle braiding — are non-local, leading to an immunity to local perturbations.

Such immunity to local perturbation gives topolgical quantum memories exceptional protection from errors due to the interaction with the environment. However, it is crucial to note that topological quantum computers are also exceptionally immune to unitary errors due to imprecise gate operation. Unlike other types of quantum computers, the operations that can be performed on a topological quantum computer (braids) naturally take a discrete set of values. As discussed above, when one makes a 90 degree rotation of a spin-based qubit, for example, it is possible that one will mistakenly rotate by 90.01 degrees thus introducing a small error. In contrast, braids are discrete: either a particle is taken around another, or it is not. There is no way to make a small error by having slight imprecision in the way the quasiparticles are moved. (Taking a particle only part of the way around another particle rather than all of the way does not introduce errors so long as the topological class of the link formed by the particle trajectories – as described above – is unchanged.)

Given the exceptional stability of the ground states, and their insensitivity to local perturbations that do not involve excitations to excited states, one may ask then which physical processes do cause errors in such a topological quantum computer. Due to the topological stability of the unitary transformations associated with braids, the only error processes that we must be concerned about are processes that might cause us to form the wrong link, and hence the wrong computation. Certainly, one must keep careful track of the positions of *all* of the quasiparticles in the system during the computation and assure that one makes the correct braid to do the correct computation. This includes not just the "intended" quasiparticles which we need to manipulate for our quantum compu-

tation, but also any "unintended" quasiparticle which might be lurking in our system without our knowledge. Two possible sources of these unintended quasiparticles are thermally excited quasiparticle-quasihole pairs, and randomly localized quasiparticles trapped by disorder (e.g. impurities, surface roughness, etc.). In a typical thermal fluctuation, for example, a quasiparticle-quasihole pair is thermally created from the vacuum, braids with existing intended quasiparticles, and then gets annihilated. Typically, such a pair has opposite electrical charges, so its constituents will be attracted back to each other and annihilate. However, entropy or temperature may lead the quasiparticle and quasihole to split fully apart and wander relatively freely through part of the system before coming back together and annihilating. This type of process may change the state of the qubits encoded in the intended quasiparticles, and hence disrupt the computation. Fortunately, as we will see in Section IV.B below there is a whole class of such processes that do not in fact cause error. This class includes all of the most likely such thermal processes to occur: including when a pair is created, encircles a single already existing quasiparticle and then re-annihilates, or when a pair is created and one of the pair annihilates an already existing quasiparticle. For errors to be caused, the excited pair must braid at least two intended quasiparticles. Nonetheless, the possibility of thermally-excited quasiparticles wandering through the system creating unintended braids and thereby causing error is a serious one. For this reason, topological quantum computation must be performed at temperatures well below the energy gap for quasiparticle-quasihole creation so that these errors will be exponentially suppressed.

Similarly, localized quasiparticles that are induced by disorder (e.g. randomly-distributed impurities, surface roughness, etc.) are another serious obstacle to overcome, since they enlarge the dimension of the subspace of degenerate ground states in a way that is hard to control. In particular, these unaccounted-for quasiparticles may couple by tunneling to their intended counterparts, thereby introducing dynamics to what is supposed to be a topology-controlled system, and possibly ruining the quantum computation. We further note that, in quantum Hall systems (as we will discuss in the next section), slight deviations in density or magentic field will also create unintented quasiparticles that must be carefully avoided.

Finally, we also note that while non-Abelian quasiparticles are natural candidates for the realization of topological qubits, not every system where quasiparticles satisfy non-Abelian statistics is suitable for quantum computation. For this suitability it is essential that the set of unitary transformations induced by braiding quasiparticles is rich enough to allow for all operations needed for computation. The necessary and sufficient conditions for universal topological quantum computation are discussed in Section IV.C.

C. Non-Abelian Quantum Hall States

A necessary condition for topological quantum computation using non-Abelian anyons is the existence of a physical system where non-Abelian anyons can be found, manipulated (e.g. braided), and conveniently read out. Several theoretical models and proposals for systems having these properties have been introduced in recent years (Fendley and Fradkin, 2005; Freedman et al., 2005a; Kitaev, 2006; Levin and Wen, 2005b), and in section II.D below we will mention some of these possibilities briefly. Despite the theoretical work in these directions, the only real physical system where there is even indirect experimental evidence that non-Abelian anyons exist are quantum Hall systems in two-dimensional (2D) electron gases (2DEGs) in high magnetic fields. Consequently, we will devote a considerable part of our discussion to putative non-Abelian quantum Hall systems which are also of great interest in their own right.

1. Rapid Review of Quantum Hall Physics

A comprehensive review of the quantum Hall effect is well beyond the scope of this article and can be found in the literature (Das Sarma and Pinczuk, 1997; Prange and Girvin, 1990). This effect, realized for two dimensional electronic systems in a strong magnetic field, is characterized by a gap between the ground state and the excited states (incompressibility); a vanishing longitudinal resistivity $\rho_{xx} = 0$, which implies a dissipationless flow of current; and the quantization of the Hall resistivity precisely to values of $\rho_{xy} = \frac{1}{\nu}\frac{h}{e^2}$, with ν being an integer (the integer quantum Hall effect), or a fraction (the fractional quantum Hall effect). These values of the two resistivities imply a vanishing longitudinal conductivity $\sigma_{xx} = 0$ and a quantized Hall conductivity $\sigma_{xy} = \nu\frac{e^2}{h}$.

To understand the quantized Hall effect, we begin by ignoring electron-electron Coulomb interactions, then the energy eigenstates of the single-electron Hamiltonian in a magnetic field, $H_0 = \frac{1}{2m}\left(\mathbf{p}_i - \frac{e}{c}\mathbf{A}(\mathbf{x}_i)\right)^2$ break up into an equally-spaced set of degenerate levels called Landau levels. In symmetric gauge, $\mathbf{A}(\mathbf{x}) = \frac{1}{2}\mathbf{B}\times\mathbf{x}$, a basis of single particle wavefunctions in the lowest Landau level (LLL) is given by $\varphi_m(z) = z^m \exp(-|z|^2/(4{\ell_0}^2))$, where $z = x + iy$. If the electrons are confined to a disk of area A pierced by magnetic flux $B\cdot A$, then there are $N_\Phi = BA/\Phi_0 = BAe/hc$ states in the lowest Landau level (and in each higher Landau level), where B is the magnetic field; h, c, and e are, respectively, Planck's constant, the speed of light, and the electron charge; and $\Phi_0 = hc/e$ is the flux quantum. In the absence of disorder, these single-particle states are all precisely degenerate. When the chemical potential lies between the ν^{th} and $(\nu+1)^{\text{th}}$ Landau levels, the Hall conductance takes the quantized value $\sigma_{xy} = \nu\frac{e^2}{h}$ while $\sigma_{xx} = 0$. The two-dimensional electron density, n, is related to ν via the formula $n = \nu eB/(hc)$. In the presence of a periodic potential and/or disorder (e.g. impurities), the Landau levels broaden into bands. However, except at the center of a band, all states are localized when disorder is present (see Das Sarma and Pinczuk, 1997; Prange and Girvin, 1990 and refs. therein). When the chemical potential lies in the region of localized states between the centers of the ν^{th} and $(\nu+1)^{\text{th}}$ Landau bands, the Hall conductance again takes the quantized value $\sigma_{xy} = \nu\frac{e^2}{h}$ while $\sigma_{xx} = 0$. The

density will be near but not necessarily equal to $\nu eB/(hc)$. This is known as the Integer quantum Hall effect (since ν is an integer).

The neglect of Coulomb interactions is justified when an integer number of Landau levels is filled, so long as the energy splitting between Landau levels, $\hbar\omega_c = \frac{\hbar eB}{mc}$ is much larger than the scale of the Coulomb energy, $\frac{e^2}{\ell_0}$, where $\ell_0 = \sqrt{hc/eB}$ is the magnetic length. When the electron density is such that a Landau level is only partially filled, Coulomb interactions may be important.

In the absence of disorder, a partially-filled Landau level has a very highly degenerate set of multi-particle states. This degeneracy is broken by electron-electron interactions. For instance, when the number of electrons is $N = N_\Phi/3$, i.e. $\nu = 1/3$, the ground state is non-degenerate and there is a gap to all excitations. When the electrons interact through Coulomb repulsion, the Laughlin state

$$\Psi = \prod_{i>j} (z_i - z_j)^3 \; e^{-\sum_i |z_i|^2/4{\ell_0}^2} \tag{11}$$

is an approximation to the ground state (and is the exact ground state for a repulsive ultra-short-ranged model interaction, see for instance the article by Haldane in Prange and Girvin, 1990). Such ground states survive even in the presence of disorder if it is sufficiently weak compared to the gap to excited states. More delicate states with smaller excitation gaps are, therefore, only seen in extremely clean devices, as described in subsection II.C.5. However, some disorder is necessary to pin the charged quasiparticle excitations which are created if the density or magnetic field are slightly varied. When these excitations are localized, they do not contribute to the Hall conductance and a plateau is observed.

Quasiparticle excitations above fractional quantum Hall ground states, such as the $\nu = 1/3$ Laughlin state (11), are emergent anyons in the sense described in section II.A.2. An explicit calculation of the Berry phase, along the lines of Eq. 8 shows that quasiparticle excitations above the $\nu = 1/k$ Laughlin states have charge e/k and statistical angle $\theta = \pi/k$ (Arovas et al., 1984). The charge is obtained from the non-topological part of the Berry phase which is proportional to the flux enclosed by a particle's trajectory times the quasiparticle charge. This is in agreement with a general argument that such quasiparticles must have fractional charge (Laughlin, 1983). The result for the statistics of the quasiparticles follows from the topological part of the Berry phase; it is in agreement with strong theoretical arguments which suggest that fractionally charged excitations are necessarily Abelian anyons (see Wilczek, 1990 and refs. therein). Definitive experimental evidence for the existence of fractionally charged excitations at $\nu = 1/3$ has been accumulating in the last few years (De Picciotto et al., 1997; Goldman and Su, 1995; Saminadayar et al., 1997). The observation of fractional statistics is much more subtle. First steps in that direction have been recently reported (Camino et al., 2005) but are still debated (Godfrey et al., 2007; Rosenow and Halperin, 2007).

The Laughlin states, with $\nu = 1/k$, are the best understood fractional quantum Hall states, both theoretically and experimentally. To explain more complicated observed fractions, with ν not of the form $\nu = 1/k$, Haldane and Halperin (Haldane, 1983; Halperin, 1984; Prange and Girvin, 1990) used a hierarchical construction in which quasiparticles of a principle $\nu = 1/k$ state can then themselves condense into a quantized state. In this way, quantized Hall states can be constructed for any odd-denominator fraction ν – but only for odd-denominator fractions. These states all have quasiparticles with fractional charge and Abelian fractional statistics. Later, it was noticed by Jain (Heinonen, 1998; Jain, 1989) that the most prominent fractional quantum Hall states are of the form $\nu = p/(2p+1)$, which can be explained by noting that a system of electrons in a high magnetic field can be approximated by a system of auxiliary fermions, called 'composite fermions' , in a lower magnetic field. If the the electrons are at $\nu = p/(2p+1)$, then the lower magnetic field seen by the 'composite fermions' is such that they fill an integer number of Landau levels $\nu' = p$. (See Halperin et al., 1993; López and Fradkin, 1991 for a field-theoretic implementations.) Since the latter state has a gap, one can hope that the approximation is valid. The composite fermion picture of fractional quantum Hall states has proven to be qualitatively and semi-quantitatively correct in the LLL (Murthy and Shankar, 2003).

Systems with filling fraction $\nu > 1$, can be mapped to $\nu' \leq 1$ by keeping the fractional part of ν and using an appropriately modified Coulomb interaction to account for the difference between cyclotron orbits in the LLL and those in higher Landau levels (Prange and Girvin, 1990). This involves the assumption that the inter-Landau level coupling is negligibly small. We note that this may not be a particularly good assumption for higher Landau levels, where the composite fermion picture less successful.

Our confidence in the picture described above for the $\nu = 1/k$ Laughlin states and the hierarchy of odd-denominator states which descend from them derives largely from numerical studies. Experimentally, most of what is known about quantum Hall states comes from transport experiments — measurements of the conductance (or resistance) tensor. While such measurements make it reasonably clear when a quantum Hall plateau exists at a given filling fraction, the nature of the plateau (i.e., the details of the low-energy theory) is extremely hard to discern. Because of this difficulty, numerical studies of small systems (exact diagonalizations and Monte Carlo) have played a very prominent role in providing further insight. Indeed, even Laughlin's original work (Laughlin, 1983) on the $\nu = 1/3$ state relied heavily on accompanying numerical work. The approach taken was the following. One assumed that the splitting between Landau levels is the largest energy in the problem. The Hamiltonian is projected into the lowest Landau level, where, for a finite number of electrons and a fixed magnetic flux, the Hilbert space is finite-dimensional. Typically, the system is given periodic boundary conditions (i.e. is on a torus) or else is placed on a sphere; occasionally, one works on the disk, e.g. to study edge excitations. The Hamiltonian is then a finite-sized matrix which can be diagonalized by a computer so long as the number of electrons is not too large. Originally, Laughlin examined only 3 electrons, but modern computers can handle

sometimes as many as 18 electrons. The resulting ground state wavefunction can be compared to a proposed trial wavefunction. Throughout the history of the field, this approach has proven to be extremely powerful in identifying the nature of experimentally-observed quantum Hall states when the system in question is deep within a quantum Hall phase, so that the associated correlation length is short and the basic physics is already apparent in small systems.

There are several serious challenges in using such numerical work to interpret experiments. First of all, there is always the challenge of extrapolating finite-size results to the thermodynamic limit. Secondly, simple overlaps between a proposed trial state and an exact ground state may not be sufficiently informative. For example, it is possible that an exact ground state will be adiabatically connected to a particular trial state, i.e., the two wavefunctions represent the same phase of matter, but the overlaps may not be very high. For this reason, it is necessary to also examine quantum numbers and symmetries of the ground state, as well as the response of the ground state to various perturbations, particularly the response to changes in boundary conditions and in the flux.

Another difficulty is the choice of Hamiltonian to diagonalize. One may think that the Hamiltonian for a quantum Hall system is just that of 2D electrons in a magnetic field interacting via Coulomb forces. However, the small but finite width (perpendicular to the plane of the system) of the quantum well slightly alters the effective interaction between electrons. Similarly, screening (from any nearby conductors, or from inter-Landau-level virtual excitations), in-plane magnetic fields, and even various types of disorder may alter the Hamiltonian in subtle ways. To make matters worse, one may not even know all the physical parameters (dimensions, doping levels, detailed chemical composition, etc.) of any particular experimental system very accurately. Finally, Landau-level mixing is not small because the energy splitting between Landau levels is not much larger than the other energies in the problem. Thus, it is not even clear that it is correct to truncate the Hilbert space to the finite-dimensional Hilbert space of a single Landau level.

In the case of very robust states, such as the $\nu = 1/3$ state, these subtle effects are unimportant; the ground state is essentially the same irrespective of these small deviations from the idealized Hamiltonian. However, in the case of weaker states, such as those observed between $\nu = 2$ and $\nu = 4$ (some of which we will discuss below), it appears that very small changes in the Hamiltonian can indeed greatly affect the resulting ground state. Therefore, a very valuable approach has been to guess a likely Hamiltonian, and search a space of "nearby" Hamiltonians, slightly varying the parameters of the Hamiltonian, to map out the phase diagram of the system. These phase diagrams suggest the exciting technological possibility that detailed numerics will allow us to engineer samples with just the right small perturbations so as display certain quantum Hall states more clearly (Manfra et al., 2007; Peterson and Das Sarma, 2007).

2. Possible Non-Abelian States

The observation of a quantum Hall state with an even denominator filling fraction (Willett et al., 1987), the $\nu = 5/2$ state, was the first indication that not all fractional quantum Hall states fit the above hierarchy (or equivalently composite fermion) picture. Independently, it was recognized Fubini, 1991; Fubini and Lutken, 1991; Moore and Read, 1991 that conformal field theory gives a way to write a variety of trial wavefunctions for quantum Hall states, as we describe in Section III.D below. Using this approach, the so-called Moore-Read Pfaffian wavefunction was constructed (Moore and Read, 1991):

$$\Psi_{\rm Pf} = {\rm Pf}\left(\frac{1}{z_i - z_j}\right) \prod_{i<j}(z_i - z_j)^m e^{-\sum_i |z_i|^2/4{\ell_0}^2} \quad (12)$$

The Pfaffian is the square root of the determinant of an antisymmetric matrix or, equivalently, the antisymmetrized sum over pairs:

$${\rm Pf}\left(\frac{1}{z_j - z_k}\right) = \mathcal{A}\left(\frac{1}{z_1 - z_2}\frac{1}{z_3 - z_4}\dots\right) \quad (13)$$

For m even, this is an even-denominator quantum Hall state in the lowest Landau level. Moore and Read, 1991 suggested that its quasiparticle excitations would exhibit non-Abelian statistics (Moore and Read, 1991). This wavefunction is the exact ground state of a 3-body repulsive interaction; as we discuss below, it is also an approximate ground state for more realistic interactions. This wavefunction is a representative of a universality class which has remarkable properties which we discuss in detail in this paper. In particular, the quasiparticle excitations above this state realize the second scenario discussed in Eqs. 9, 10 in section II.A.2. There are 2^{n-1} states with $2n$ quasiholes at fixed positions, thereby establishing the degeneracy of multi-quasiparticle states which is required for non-Abelian statistics (Nayak and Wilczek, 1996). Furthermore, these quasihole wavefunctions can also be related to conformal field theory (as we discuss in section III.D), from which it can be deduced that the 2^{n-1}-dimensional vector space of states can be understood as the spinor representation of SO(2n); braiding particles i and j has the action of a $\pi/2$ rotation in the $i-j$ plane in $\mathbb{R}^{2n}$ (Nayak and Wilczek, 1996). In short, these quasiparticles are essentially Ising anyons (with the difference being an additional Abelian component to their statistics). Although these properties were uncovered using specific wavefunctions which are eigenstates of the 3-body interaction for which the Pfaffian wavefunction is the exact ground state, they are representative of an entire universality class. The effective field theory for this universality class is $SU(2)$ Chern-Simons theory at level $k = 2$ together with an additional Abelian Chern-Simons term (Fradkin et al., 2001, 1998). Chern-Simons theory is the archetypal topological quantum field theory (TQFT), and we discuss it extensively in section III. As we describe, Chern-Simons theory is related to the Jones polynomial of knot theory (Witten, 1989); consequently, the current through an interferometer in such a non-Abelian quantum Hall state would give a direct measure

of the Jones polynomial for the link produced by the quasiparticle trajectories (Fradkin et al., 1998)!

One interesting feature of the Pfaffian wavefunction is that it is the quantum Hall analog of a $p + ip$ superconductor: the antisymmetrized product over pairs is the real-space form of the BCS wavefunction (Greiter et al., 1992). Read and Green, 2000 showed that the same topological properties mentioned above are realized by a $p + ip$-wave superconductor, thereby cementing the identification between such a paired state and the Moore-Read state. Ivanov, 2001 computed the braiding matrices by this approach (see also Stern et al., 2004; Stone and Chung, 2006). Consequently, we will often be able to discuss $p + ip$-wave superconductors and superfluids in parallel with the $\nu = 5/2$ quantum Hall state, although the experimental probes are significantly different.

As we discuss below, all of these theoretical developments garnered greater interest when numerical work (Morf, 1998; Rezayi and Haldane, 2000) showed that the ground state of systems of up to 18 electrons in the $N = 1$ Landau level at filling fraction 1/2 is in the universality class of the Moore-Read state. These results revived the conjecture that the lowest Landau level ($N = 0$) of both spins is filled and inert and the electrons in the $N = 1$ Landau level form the analog of the Pfaffian state (Greiter et al., 1992). Consequently, it is the leading candidate for the experimentally-observed $\nu = 5/2$ state.

Read and Rezayi, 1999 constructed a series of non-Abelian quantum Hall states at filling fraction $\nu = N + k/(Mk + 2)$ with M odd, which generalize the Moore-Read state in a way which we discuss in section III. These states are referred to as the Read-Rezayi $\mathbb{Z}_k$ parafermion states for reasons discussed in section III.D. Recently, a quantum Hall state was observed experimentally with $\nu = 12/5$ (Xia et al., 2004). It is suspected (see below) that the $\nu = 12/5$ state may be (the particle hole conjugate of) the $\mathbb{Z}_3$ Read-Rezayi state, although it is also possible that 12/5 belongs to the conventional Abelian hierarchy as the $2/5$ state does. Such an option is not possible at $\nu = 5/2$ as a result of the even denominator.

In summary, it is well-established that if the observed $\nu = 5/2$ state is in the same universality class as the Moore-Read Pfaffian state, then its quasiparticle excitations are non-Abelian anyons. Similarly, if the $\nu = 12/5$ state is in the universality class of the $\mathbb{Z}_3$ Read-Rezayi state, its quasiparticles are non-Abelian anyons. There is no direct experimental evidence that the $\nu = 5/2$ is in this particular universality class, but there is evidence from numerics, as we further discuss below. There is even less evidence in the case of the $\nu = 12/5$ state. In subsections II.C.3 and II.C.4, we will discuss proposed experiments which could directly verify the non-Abelian character of the $\nu = 5/2$ state and will briefly mention their extension to the $\nu = 12/5$ case. Both of these states, as well as others (e.g. Ardonne and Schoutens, 1999; Simon et al., 2007c), were constructed on the basis of very deep connections between conformal field theory, knot theory, and low-dimensional topology (Witten, 1989). Using methods from these different branches of theoretical physics and mathematics, we will explain the structure of the non-Abelian statistics of the $\nu = 5/2$ and $12/5$ states within the context of a large class of non-Abelian topological states. We will see in section III.C that this circle of ideas enables us to use the theory of knots to understand experiments on non-Abelian anyons.

In the paragraphs below, we will discuss numerical results for $\nu = 5/2, 12/5$, and other candidates in greater detail.

(a) 5/2 State: The $\nu = 5/2$ fractional quantum Hall state is a useful case history for how numerics can elucidate experiments. This incompressible state is easily destroyed by the application of an in-plane magnetic field (Eisenstein et al., 1990). At first it was assumed that this implied that the 5/2 state is spin-unpolarized or partially polarized since the in-plane magnetic field presumably couples only to the electron spin. Careful finite-size numerical work changed this perception, leading to our current belief that the 5/2 FQH state is actually in the universality class of the spin-polarized Moore-Read Pfaffian state.

In rather pivotal work (Morf, 1998), it was shown that spin-polarized states at $\nu = 5/2$ have lower energy than spin-unpolarized states. Furthermore, it was shown that varying the Hamiltonian slightly caused a phase transition between a gapped phase that has high overlap with the Moore-Read wavefunction and a compressible phase. The proposal put forth was that the most important effect of the in-plane field was not on the electron spins, but rather was to slightly alter the shape of the electron wavefunction perpendicular to the sample which, in turn, slightly alters the effective electron-electron interaction, pushing the system over a phase boundary and destroying the gapped state. Further experimental work showed that the effect of the in-plane magnetic field is to drive the system across a phase transition from a gapped quantum Hall phase into an anisotropic compressible phase (Lilly et al., 1999a; Pan et al., 1999a). Further numerical work (Rezayi and Haldane, 2000) then mapped out a full phase diagram showing the transition between gapped and compressible phases and showing further that the experimental systems lie exceedingly close to the phase boundary. The correspondence between numerics and experiment has been made more quantitative by comparisons between the energy gap obtained from numerics and the one measured in experiments (Morf and d'Ambrumenil, 2003; Morf et al., 2002). Very recently, this case has been further strengthened by the application of the density-matrix renormalization group method (DMRG) to this problem (Feiguin et al., 2007b).

One issue worth considering is possible competitors to the Moore-Read Pfaffian state. Experiments have already told us that there is a fractional quantum Hall state at $\nu = 5/2$. Therefore, our job is to determine which of the possible states is realized there. Serious alternatives to the Moore-Read Pfaffian state fall into two categories. On the one hand, there is the possibility that the ground state at $\nu = 5/2$ is not fully spin-polarized. If it were completely unpolarized, the so-called $(3, 3, 1)$ state (Das Sarma and Pinczuk, 1997; Halperin, 1983) would be a possibility. However, Morf's numerics (Morf, 1998) and a recent variational Monte Carlo study (Dimov et al., 2007) indicate that an unpolarized state is higher in energy than a fully-polarized state. This can be understood as a consequence of a tendency towards spontaneous ferromag-

netism; however, a partially-polarized alternative (which may be either Abelian or non-Abelian) to the Pfaffian is not ruled out (Dimov et al., 2007). Secondly, even if the ground state at $\nu = 5/2$ is fully spin-polarized, the Pfaffian is not the only possibility. It was very recently noticed that the Pfaffian state is not symmetric under a particle-hole transformation of a single Landau level (which, in this case, is the $N = 1$ Landau level, with the $N = 0$ Landau level filled and assumed inert), even though this is an exact symmetry of the Hamiltonian in the limit that the energy splitting between Landau levels is infinity. Therefore, there is a distinct state, dubbed the anti-Pfaffian (Lee et al., 2007b; Levin et al., 2007), which is an equally good state in this limit. Quasiparticles in this state are also essentially Ising anyons, but they differ from Pfaffian quasiparticles by Abelian statistical phases. In experiments, Landau-level mixing is not small, so one or the other state is lower in energy. On a finite torus, the symmetric combination of the Pfaffian and the anti-Pfaffian will be lower in energy, but as the thermodynamic limit is approached, the anti-symmetric combination will become equal in energy. This is a possible factor which complicates the extrapolation of numerics to the thermodynamic limit. On a finite sphere, particle-hole symmetry is not exact; it relates a system with $2N - 3$ flux quanta with a system with $2N + 1$ flux quanta. Thus, the anti-Pfaffian would not be apparent unless one looked at a different value of the flux. To summarize, the only known alternatives to the Pfaffian state – partially-polarized states and the anti-Pfaffian – have not really been tested by numerics, either because the spin-polarization was assumed to be 0% or 100% (Morf, 1998) or because Landau-level mixing was neglected.

With this caveat in mind, it is instructive to compare the evidence placing the $\nu = 5/2$ FQH state in the Moore-Read Pfaffian universality class with the evidence placing the $\nu = 1/3$ FQH state in the corresponding Laughlin universality class. In the latter case, there have been several spectacular experiments (De Picciotto et al., 1997; Goldman and Su, 1995; Saminadayar et al., 1997) which have observed quasiparticles with electrical charge $e/3$, in agreement with the prediction of the Laughlin universality class. In the case of the $\nu = 5/2$ FQH state, we do not yet have the corresponding measurements of the quasiparticle charge, which should be $e/4$. However, the observation of charge $e/3$, while consistent with the Laughlin universality class, does not uniquely fix the observed state in this class (see, for example, Simon et al., 2007c; Wójs, 2001. Thus, much of our confidence derives from the amazing (99% or better) overlap between the ground state obtained from exact diagonalization for a finite size 2D system with up to 14 electrons and the Laughlin wavefunction. In the case of the $\nu = 5/2$ FQH state, the corresponding overlap (for 18 electrons on the sphere) between the $\nu = 5/2$ ground state and the Moore-Read Pfaffian state is reasonably impressive ($\sim$ 80%). This can be improved by modifying the wavefunction at short distances without leaving the Pfaffian phase (Moller and Simon, 2007). However, on the torus, as we mentioned above, the symmetric combination of the Pfaffian and the anti-Pfaffian is a better candidate wavefunction in a finite-size system than the Pfaffian itself (or the anti-Pfaffian). Indeed, the symmetric combination of the Pfaffian and the anti-Pfaffian has an overlap of 97% for 14 electrons (Rezayi and Haldane, 2000).

To summarize, the overlap is somewhat smaller in the $5/2$ case than in the $1/3$ case when particle-hole symmetry is not accounted for, but only slightly smaller when it is. This is an indication that Landau-level mixing – which will favor either the Pfaffian or the anti-Pfaffian – is an important effect at $\nu = 5/2$, unlike at $\nu = 1/3$. Moreover, Landau-level mixing is likely to be large because the 5/2 FQH state is typically realized at relatively low magnetic fields, making the Landau level separation energy relatively small.

Given that potentially large effects have been neglected, it is not too surprising that the gap obtained by extrapolating numerical results for finite-size systems (Morf and d'Ambrumenil, 2003; Morf et al., 2002) is substantially larger than the experimentally-measured activation gap. Also, the corresponding excitation gap obtained from numerics for the $\nu = 1/3$ state is much larger than the measured activation gap. The discrepancy between the theoretical excitation gap and the measured activation gap is a generic problem of all FQH states, and may be related to poorly understood disorder effects and Landau-level mixing.

Finally, it is important to mention that several very recent (2006-07) numerical works in the literature have raised some questions about the identification of the observed $5/2$ FQH state with the Moore-Read Pfaffian (Toke and Jain, 2006; Toke et al., 2007; Wojs and Quinn, 2006). Considering the absence of a viable alternative (apart from the anti-Pfaffian and partially-polarized states, which were not considered by these authors) it seems unlikely that these doubts will continue to persist, as more thorough numerical work indicates (Moller and Simon, 2007; Peterson and Das Sarma, 2007; Rezayi, 2007).

(b) 12/5 State: While our current understanding of the 5/2 state is relatively good, the situation for the experimentally observed 12/5 state is more murky, although the possibilities are even more exciting, at least from the perspective of topological quantum computation. One (relatively dull) possibility is that the $12/5$ state is essentially the same as the observed $\nu = 2/5$ state, which is Abelian. However, Read and Rezayi, in their initial work on non-Abelian generalizations of the Moore-Read state (Read and Rezayi, 1999) proposed that the 12/5 state might be (the particle-hole conjugate of) their $\mathbb{Z}_3$ parafermion (or $SU(2)$ level 3) state. This is quite an exciting possibility because, unlike the non-Abelian Moore-Read state at 5/2, the $\mathbb{Z}_3$ parafermion state would have braiding statistics that allow universal topological quantum computation.

The initial numerics by Read and Rezayi (Read and Rezayi, 1999) indicated that the 12/5 state is very close to a phase transition between the Abelian hierarchy state and the non-Abelian parafermion state. More recent work by the same authors (Rezayi and Read, 2006) has mapped out a detailed phase diagram showing precisely for what range of parameters a system should be in the non-Abelian phase. It was found that the non-Abelian phase is not very "far" from the results that would be expected from most real experimental systems. This again suggests that (if the system is not already in the non-Abelian phase), we may be able to engineer slight changes in

an experimental sample that would push the system over the phase boundary into the non-Abelian phase.

Experimentally, very little is actually known about the 12/5 state. Indeed, a well quantized plateau has only ever been seen in a single published (Xia et al., 2004) experiment. Furthermore, there is no experimental information about spin polarization (the non-Abelian phase should be polarized whereas the Abelian phase could be either polarized or unpolarized), and it is not at all clear why the 12/5 state has been seen, but its particle-hole conjugate, the 13/5 state, has not (in the limit of infinite Landau level separation, these two states will be identical in energy). Nonetheless, despite the substantial uncertainties, there is a great deal of excitement about the possibility that this state will provide a route to topological quantum computation.

(c) Other Quantum Hall States: The most strongly observed fractional quantum Hall states are the composite fermion states $\nu = p/(2p+1)$, or are simple generalizations of them. There is little debate that these states are likely to be Abelian. However, there are a number of observed exotic states whose origin is not currently agreed upon. An optimist may look at any state of unknown origin and suggest that it is a non-Abelian state. Indeed, non-Abelian proposals (published and unpublished) have been made for a great variety states of uncertain origin including (Jolicoeur, 2007; Scarola et al., 2002; Simon et al., 2007a,c; Wojs et al., 2006) 3/8, 4/11, 8/3, and 7/3. Of course, other more conventional Abelian proposals have been made for each of these states too (Chang and Jain, 2004; Goerbig et al., 2004; López and Fradkin, 2004; Wojs and Quinn, 2002; Wojs et al., 2004). For each of these states, there is a great deal of research left to be done, both theoretical and experimental, before any sort of definitive conclusion is reached.

In this context, it is worthwhile to mention another class of quantum Hall systems where non-Abelian anyons could exist, namely bilayer or multilayer $2D$ systems (Das Sarma and Pinczuk, 1997; Greiter et al., 1991; He et al., 1993, 1991). More work is necessary in investigating the possibility of non-Abelian multilayer quantum Hall states.

3. Interference Experiments

While numerics give useful insight about the topological nature of observed quantum Hall states, experimental measurements will ultimately play the decisive role. So far, rather little has been directly measured experimentally about the topological nature of the $\nu = 5/2$ state and even less is known about other putative non-Abelian quantum Hall states such as $\nu = 12/5$. In particular, there is no direct experimental evidence for the non-Abelian nature of the quasiparticles. The existence of a degenerate, or almost degenerate, subspace of ground states leads to a zero-temperature entropy and heat capacity, but those are very hard to measure experimentally. Furthermore, this degeneracy is just one requirement for non-Abelian statistics to take place. How then does one demonstrate experimentally that fractional quantum Hall states, particularly the $\nu = 5/2$ state, are indeed non-Abelian?

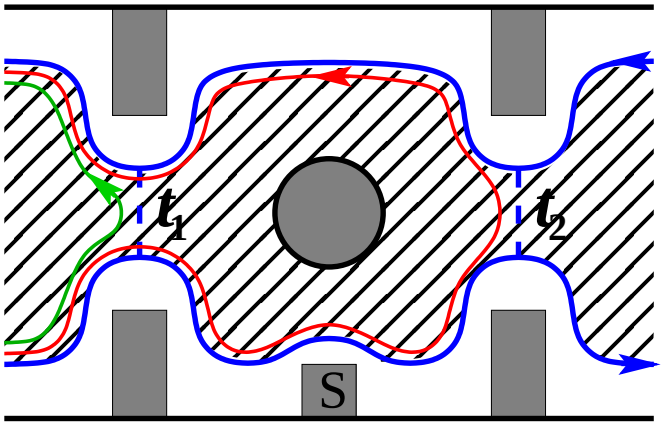

FIG. 2 A quantum Hall analog of a Fabry-Perot interferometer. Quasiparticles can tunnel from one edge to the other at either of two point contacts. To lowest order in the tunneling amplitudes, the backscattering probability, and hence the conductance, is determined by the interference between these two processes. The area in the cell can be varied by means of a side gate S in order to observe an interference pattern.

The fundamental quasiparticles (i.e. the ones with the smallest electrical charge) of the Moore-Read Pfaffian state have charge $e/4$ (Greiter et al., 1992; Moore and Read, 1991). The fractional charge does not uniquely identify the state – the Abelian $(3,3,1)$ state has the same quasiparticle charge – but a different value of the minimal quasiparticle charge at $\nu = 5/2$ would certainly rule out the Pfaffian state. Hence, the first important measurement is the quasiparticle charge, which was done more than 10 years ago in the case of the $\nu = 1/3$ state (De Picciotto et al., 1997; Goldman and Su, 1995; Saminadayar et al., 1997).

If the quasiparticle charge is shown to be $e/4$, then further experiments which probe the braiding statistics of the charge $e/4$ quasiparticles will be necessary to pin down the topological structure of the state. One way to do this is to use a mesoscopic interference device. Consider a Fabry-Perot interferometer, as depicted in Fig. (2). A Hall bar lying parallel to the x–axis is put in a field such that it is at filling fraction $\nu = 5/2$. It is perturbed by two constrictions, as shown in the figure. The two constrictions introduce two amplitudes for inter-edge tunnelling, $t_{1,2}$. To lowest order in $t_{1,2}$, the four-terminal longitudinal conductance of the Hall bar, is:

$$G_L \propto |t_1|^2 + |t_2|^2 + 2\mathrm{Re}\{t_1^* t_2 e^{i\phi}\} \qquad (14)$$

For an integer Landau filling, the relative phase ϕ may be varied either by a variation of the magnetic field or by a variation of the area of the "cell" defined by the two edges and the two constrictions, since that phase is $2\pi\Phi/\Phi_0$, with $\Phi = BA$ being the flux enclosed in the cell, A the area of the cell, and Φ_0 the flux quantum. Thus, when the area of the cell is varied by means of a side gate (labeled S in the figure), the backscattered current should oscillate.

For fractional quantum Hall states, the situation is different (de C. Chamon et al., 1997). In an approximation in which the electronic density is determined by the requirement of charge

neutrality, a variation of the area of the cell varies the flux it encloses and keeps its bulk Landau filling unaltered. In contrast, a variation of the magnetic field changes the filling fraction in the bulk, and consequently introduces quasiparticles in the bulk. Since the statistics of the quasiparticles is fractional, they contribute to the phase ϕ. The back-scattering probability is then determined not only by the two constrictions and the area of the cell they define, but also by the number of localized quasiparticles that the cell encloses. By varying the voltage applied to an anti-dot in the cell (the grey circle in Fig. 2), we can independently vary the number of quasiparticles in the cell. Again, however, as the area of the cell is varied, the back-scattered current oscillates.

For non-Abelian quantum Hall states, the situation is more interesting (Bonderson et al., 2006a,b; Chung and Stone, 2006; Das Sarma et al., 2005; Fradkin et al., 1998; Stern and Halperin, 2006). Consider the case of the Moore-Read Pfaffian state. For clarity, we assume that there are localized $e/4$ quasiparticles only within the cell (either at the anti-dot or elsewhere in the cell). If the current in Fig. (2) comes from the left, the portion of the current that is back-reflected from the left constriction does not encircle any of these quasiparticles, and thus does not interact with them. The part of the current that is back-scattered from the right constriction, on the other hand, does encircle the cell, and therefore applies a unitary transformation on the subspace of degenerate ground states. The final state of the ground state subspace that is coupled to the left back–scattered wave, $|\xi_0\rangle$, is then different from the state coupled to the right partial wave, $\hat{U}|\xi_0\rangle$. Here $\hat{U}$ is the unitary transformation that results from the encircling of the cell by the wave scattered from the right constriction. The interference term in the four-terminal longitudinal conductance, the final term in Eq. 14, is then multiplied by the matrix element $\langle\xi_0|\hat{U}|\xi_0\rangle$:

$$G_L \propto |t_1|^2 + |t_1|^2 + 2\mathrm{Re}\Big\{ t_1^* t_2 e^{i\phi} \langle\xi_0|\hat{U}|\xi_0\rangle \Big\} \qquad (15)$$

In section III, we explain how $\langle\xi_0|\hat{U}|\xi_0\rangle$ can be calculated by several different methods. Here we just give a brief description of the result.

For the Moore-Read Pfaffian state, which is believed to be realized at $\nu = 5/2$, the expectation value $\langle\xi_0|\hat{U}|\xi_0\rangle$ depends first and foremost on the parity of the number of $e/4$ quasiparticles localized in the cell. When that number is odd, the resulting expectation value is zero. When that number is even, the expectation value is non-zero and may assume one of two possible values, that differ by a minus sign. As a consequence, when the number of localized quasiparticles is odd, *no interference pattern is seen*, and the back-scattered current does not oscillate with small variations of the area of the cell. When that number is even, the back-scattered current oscillates as a function of the area of the cell.

A way to understand this striking result is to observe that the localized quasiparticles in the cell can be viewed as being created in pairs from the vacuum. Let us suppose that we want to have N quasiparticles in the cell. If N is odd, then we can create $(N+1)/2$ pairs and take one of the resulting quasiparticles outside of the cell, where it is localized. Fusing all $N+1$ of these particles gives the trivial particle since they were created from the vacuum. Now consider what happens when a current-carrying quasiparticle tunnels at one of the two point contacts. If it tunnels at the second one, it braids around the N quasiparticles in the cell (but not the $N+1^{\text{th}}$, which is outside the cell). This changes the fusion channel of the $N+1$ localized quasiparticles. In the language introduced in subsection II.A.1, each $e/4$ quasiparticle is a σ particle. An odd number N of them can only fuse to σ; fused now with the $N+1^{\text{th}}$, they can either give $\mathbf{1}$ or ψ. Current-carrying quasiparticles, when they braid with the N in the cell, toggle the system between these two possibilities. Since the state of the localized quasiparticles has been changed, such a process cannot interfere with a process in which the current-carrying quasiparticle tunnels at the first junction and does not encircle any of the localized quasiparticles. Therefore, the localized quasiparticles 'measure' which trajectory the current-carrying quasiparticles take(Bonderson et al., 2007; Overbosch and Bais, 2001). If N is even, then we can create $(N+2)/2$ pairs and take two of the resulting quasiparticles outside of the cell. If the N quasiparticles in the cell all fuse to the trivial particle, then this is not necessary, we can just create $N/2$ pairs. However, if they fuse to a neutral fermion ψ, then we will need a pair outside the cell which also fuses to ψ so that the total fuses to $\mathbf{1}$, as it must for pair creation from the vacuum. A current-carrying quasiparticle picks up a phase depending on whether the N quasiparticles in the cell fuse to $\mathbf{1}$ or ψ.

The Fabry-Perot interferometer depicted in Fig. 2 allows also for the interference of waves that are back-reflected several times. For an integer filling factor, in the limit of strong back-scattering at the constrictions, the sinusoidal dependence of the Hall bar's conductance on the area of the cell gives way to a resonance-like dependence: the conductance is zero unless a Coulomb peak develops. For the $\nu = 5/2$ state, again, the parity of the number of localized quasiparticles matters: when it is odd, the Coulomb blockade peaks are equally spaced. When it is even, the spacing between the peaks alternate between two values (Stern and Halperin, 2006).

The Moore-Read Pfaffian state, which is possibly realized at $\nu = 5/2$, is the simplest of the non-Abelian states. The other states are more complex, but also richer. The geometry of the Fabry-Perot interferometer may be analyzed for these states as well. In general, for all non-Abelian states the conductance of the Hall bar depends on the internal state of the quasiparticles localized between the constrictions – i.e. the quasiparticle to which they fuse. However, only for the Moore-Read Pfaffian state is the effect quite so dramatic. For example, for the the $\mathbb{Z}_3$ parafermion state which may be realized at $\nu = 12/5$, when the number of localized quasiparticles is larger than three, the fusion channel of the quasiparticles determines whether the interference is fully visible or suppressed by a factor of $-\varphi^{-2}$ (with φ being the golden ratio $(\sqrt{5}+1)/2$) (Bonderson et al., 2006b; Chung and Stone, 2006). The number of quasiparticles, on the other hand, affects only the phase of the interference pattern. Similar to the case of $\nu = 5/2$ here too the position of Coulomb blockade peaks on the two parameter plane of area and magnetic field reflects the non-Abelian nature of the quasiparticles (Ilan

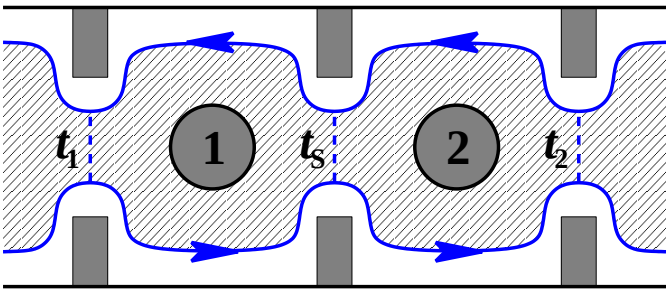

FIG. 3 If a third constriction is added between the other two, the cell is broken into two halves. We suppose that there is one quasiparticle (or any odd number) in each half. These two quasiparticles (labeled 1 and 2) form a qubit which can be read by measuring the conductance of the interferometer if there is no backscattering at the middle constriction. When a single quasiparticle tunnels from one edge to the other at the middle constriction, a σ_x or NOT gate is applied to the qubit.

et al., 2007).

4. A Fractional Quantum Hall Quantum Computer

We now describe how the constricted Hall bar may be utilized as a quantum bit (Das Sarma et al., 2005). To that end, an even number of $e/4$ quasiparticles should be trapped in the cell between the constrictions, and a new, tunable, constriction should be added between the other two so that the cell is broken into two cells with an odd number of quasiparticles in each (See Fig. (3)). One way to tune the number of quasiparticles in each half is to have two antidots in the Hall bar. By tuning the voltage on the antidots, we can change the number of quasiholes on each. Let us assume that we thereby fix the number of quasiparticles in each half of the cell to be odd. For concreteness, let us take this odd number to be one (i.e. let us assume that we are in the idealized situation in which there are no quasiparticles in the bulk, and one quasihole on each antidot). These two quasiholes then form a two-level system, i.e. a qubit. This two-level system can be understood in several ways, which we discuss in detail in section III. In brief, the two states correspond to whether the two σs fuse to $\mathbf{1}$ or ψ or, in the language of chiral p-wave superconductivity, the presence or absence of a neutral ('Majorana') fermion; or, equivalently, as the fusion of two quasiparticles carrying the spin-$1/2$ representation of an SU(2) gauge symmetry in the spin-0 or spin-1 channels.

The interference between the t_1 and t_2 processes depends on the state of the two-level system, so the qubit can be read by a measurement of the four-terminal longitudinal conductance

$$G_L \propto |t_1|^2 + |t_2|^2 \pm 2\mathrm{Re}\{t_1^* t_2 e^{i\phi}\} \tag{16}$$

where the $\pm$ comes from the dependence of $\langle\xi_0|\hat{U}|\xi_0\rangle$ on the state of the qubit, as we discuss in section III.

The purpose of the middle constriction is to allow us to manipulate the qubit. The state may be flipped, i.e. a σ_x or NOT gate can be applied, by the passage of a single quasiparticle from one edge to the other, provided that its trajectory passes in between the two localized quasiparticles. This is a simple example of how braiding causes non-trivial transformations of multi-quasiparticle states of non-Abelian quasiparticles, which we discuss in more detail in section III. If we measure the four-terminal longitudinal conductance G_L before and after applying this NOT gate, we will observe different values according to (16).

For this operation to be a NOT gate, it is important that just a single quasiparticle (or any odd number) tunnel from one edge to the other across the middle constriction. In order to regulate the number of quasiparticles which pass across the constriction, it may be useful to have a small anti-dot in the middle of the constriction with a large charging energy so that only a single quasiparticle can pass through at a time. If we do not have good control over how many quasiparticles tunnel, then it will be essentially random whether an even or odd number of quasiparticles tunnel across; half of the time, a NOT gate will be applied and the backscattering probability (hence the conductance) will change while the other half of the time, the backscattering probability is unchanged. If the constriction is pinched down to such an extreme that the $5/2$ state is disrupted between the quasiparticles, then when it is restored, there will be an equal probability for the qubit to be in either state.

This qubit is topologically protected because its state can only be affected by a charge $e/4$ quasiparticle braiding with it. If a charge $e/4$ quasiparticle winds around one of the antidots, it effects a NOT gate on the qubit. The probability for such an event can be very small because the density of thermally-excited charge $e/4$ quasiparticles is exponentially suppressed at low temperatures, $n_{\mathrm{qp}} \sim e^{-\Delta/(2T)}$. The simplest estimate of the error rate Γ (in units of the gap) is then of activated form:

$$\Gamma/\Delta \sim (T/\Delta)\ e^{-\Delta/(2T)} \tag{17}$$

The most favorable experimental situation (Xia et al., 2004) considered in (Das Sarma et al., 2005) has $\Delta \approx 500$ mK and $T \sim 5$ mK, producing an astronomically low error rate $\sim 10^{-15}$. This should be taken as an overly optimistic estimate. A more definitive answer is surely more complicated since there are multiple gaps which can be relevant in a disordered system. Furthermore, at very low temperatures, we would expect quasiparticle transport to be dominated by variable-range hopping of localized quasiparticles rather than thermal activation. Indeed, the crossover to this behavior may already be apparent (Pan et al., 1999b), in which case, the error suppression will be considerably weaker at the lowest temperatures. Although the error rate, which is determined by the probability for a quasiparticle to wind around the antidot, is not the same as the longitudinal resistance, which is the probability for it to go from one edge of the system to the other, the two are controlled by similar physical processes. A more sophisticated estimate would require a detailed analysis of the quasiparticle transport properties which contribute to the error rate. In addition, this error estimate assumes that all of the trapped (unintended) quasiparticles are kept very far from the quasiparticles which we use for our qubit so that they

cannot exchange topological quantum numbers with our qubit via tunneling. We comment on the issues involved in more detailed error estimates in section IV.D.

The device envisioned above can be generalized to one with many anti-dots and, therefore, many qubits. More complicated gates, such as a CNOT gate can be applied by braiding quasiparticles. It is not clear how to braid quasiparticles localized in the bulk – perhaps by transferring them from one anti-dot to another in a kind of "bucket brigade". This is an important problem for any realization of topological quantum computing. However, as we will discuss in section IV, even if this were solved, there would still be the problem that braiding alone is not sufficient for universal quantum computation in the $\nu = 5/2$ state (assuming that it is the Moore-Read Pfaffian state). One must either use some unprotected operations (just two, in fact) or else use the $\nu = 12/5$, if it turns out to be the $\mathbb{Z}_3$ parafermion non-Abelian state.

5. Physical Systems and Materials Considerations

As seen in the device described in the previous subsection, topological protection in non-Abelian fractional quantum Hall states hinges on the energy gap (Δ) separating the many-body degenerate ground states from the low-lying excited states. This excitation gap also leads to the incompressibility of the quantum Hall state and the quantization of the Hall resistance. Generally speaking, the larger the size of this excitation gap compared to the temperature, the more robust the topological protection, since thermal excitation of stray quasiparticles, which goes as $\exp(-\Delta/(2T))$, would potentially lead to errors.

It must be emphasized that the relevant T here is the temperature of the electrons (or more precisely, the quasiparticles) and not that of the GaAs-AlGaAs lattice surrounding the 2D electron layer. Although the surrounding bath temperature could be lowered to 1 mK or below by using adiabatic demagnetization in dilution refrigerators, the 2D electrons themselves thermally decouple from the bath at low temperatures and it is very difficult to cool the 2D electrons below $T \approx$ 20 mK. It will be a great boost to hopes for topological quantum computation using non-Abelian fractional quantum Hall states if the electron temperature can be lowered to 1 mK or even below, and serious efforts are currently underway in several laboratories with this goal.

Unfortunately, the excitation gaps for the expected non-Abelian fractional quantum Hall states are typically very small (compared, for example, with the $\nu = 1/3$ fractional quantum Hall state). The early measured gap for the 5/2 state was around $\Delta \sim 25$ mK (in 1987) (Willett et al., 1987), but steady improvement in materials quality, as measured by the sample mobility, has considerably enhanced this gap. In the highest mobility samples currently (2007) available, $\Delta \approx 600$ mK (Choi et al., 2007). Indeed, there appears to be a close connection between the excitation gap Δ and the mobility (or the sample quality). Although the details of this connection are not well-understood, it is empirically well-established that enhancing the 2D mobility invariably leads to larger measured excitation gaps. In particular, an empirical relation, $\Delta = \Delta_0 - \Gamma$, where Δ is the measured activation gap and Δ_0 the ideal excitation gap with Γ being the level broadening arising from impurity and disorder scattering, has often been discussed in the literature (see, e.g. Du et al., 1993). Writing the mobility $\mu = e\tau/m$, with τ the zero field Drude scattering time, we can write (an approximation of) the level broadening as $\Gamma = \hbar/(2\tau)$, indicating $\Gamma \sim \mu^{-1}$ in this simple picture, and therefore increasing the mobility should steadily enhance the operational excitation gap, as is found experimentally. It has recently been pointed out (Morf et al., 2002) that by reducing Γ, an FQH gap of 2-3 K may be achievable in the 5/2 FQH state. Much less is currently known about the 12/5 state, but recent numerics (Rezayi and Read, 2006) suggest that the maximal gap in typical samples will be quite a bit lower than for 5/2.

It is also possible to consider designing samples that would inherently have particularly large gaps. First of all, the interaction energy (which sets the overall scale of the gap) is roughly of the $1/r$ Coulomb form, so it scales as the inverse of the interparticle spacing. Doubling the density should therefore increase the gaps by roughly 40%. Although there are efforts underway to increase the density of samples (Willett et al., 2007), there are practical limitations to how high a density one can obtain since, if one tries to over-fill a quantum well with electrons, the electrons will no longer remain strictly two dimensional (i.e., they will start filling higher subbands, or they will not remain in the well at all). Secondly, as discussed in section II.C.2 above, since the non-Abelian states appear generally to be very sensitive to the precise parameters of the Hamiltonian, another possible route to increased excitation gap would be to design the precise form of the inter-electron interaction (which can be modified by well width, screening layers, and particularly spin-orbit coupling (Manfra et al., 2007)) so that the Hamiltonian is at a point in the phase diagram with maximal gap. With all approaches for redesigning samples, however, it is crucial to keep the disorder level low, which is an exceedingly difficult challenge.

Note that a large excitation gap (and correspondingly low temperature) suppresses thermally excited quasiparticles but does not preclude stray localized quasiparticles which could be present even at $T = 0$. As long as their positions are known and fixed, and as long as they are few enough in number to be sufficiently well separated, these quasiparticles would not present a problem, as one could avoid moving other quasiparticles near their positions and one could then tailor algorithms to account for their presence. If the density of stray localized quasiparticles is sufficiently high, however, this would no longer be possible. Fortunately, these stray particles can be minimized in the same way as one of the above discussed solutions to keeping the energy gap large – improve the mobility of the 2D electron sample on which the measurements (i.e. the computation operations) are being carried out. Improvement in the mobility leads to both the enhancement of the excitation gap and the suppression of unwanted quasiparticle localization by disorder.

We should emphasize, however, how extremely high quality the current samples already are. Current "good" sample

mobilities are in the range of $10 - 30 \times 10^6\,\mathrm{cm}^2/(\mathrm{Volt\text{-}sec})$. To give the reader an idea of how impressive this is, we note that under such conditions, at low temperatures, the mean free path for an electron may be a macroscopic length of a tenth of a millimeter or more. (Compare this to, say, copper at room temperature, which has a mean free path of tens of nanometers or less).

Nonetheless, further MBE technique and design improvement may be needed to push low-temperature 2D electron mobilities to $100 \times 10^6\,\mathrm{cm}^2/(\mathrm{Volt\text{-}sec})$ or above for topological quantum computation to be feasible. At lower temperatures, $T < 100$ mK, the phonon scattering is very strongly suppressed (Kawamura and Das Sarma, 1992; Stormer et al., 1990), and therefore, there is essentially no intrinsic limit to how high the 2D electron mobility can be since the extrinsic scattering associated with impurities and disorder can, in principle, be eliminated through materials improvement. In fact, steady materials improvement in modulation-doped 2D GaAs-AlGaAs heterostructures grown by the MBE technique has enhanced the 2D electron mobility from $10^4\,\mathrm{cm}^2/(\mathrm{Volt\text{-}sec})$ in the early 1980's to $30 \times 10^6\,\mathrm{cm}^2/(\mathrm{Volt\text{-}sec})$ in 2004, a three orders of magnitude improvement in materials quality in roughly twenty years. Indeed, the vitality of the entire field of quantum Hall physics is a result of these amazing advances. Another factor of 2-3 improvement in the mobility seems possible (L. Pfeiffer, private communication), and will likely be needed for the successful experimental observation of non-Abelian anyonic statistics and topological quantum computation.

D. Other Proposed Non-Abelian Systems

This review devotes a great deal of attention to the non-Abelian anyonic properties of certain fractional quantum Hall states (e.g. $\nu = 5/2, 12/5$, etc. states) in two-dimensional semiconductor structures, mainly because theoretical and experimental studies of such (possibly) non-Abelian fractional quantized Hall states is a mature subject, dating back to 1986, with many concrete results and ideas, including a recent proposal (Das Sarma et al., 2005) for the construction of qubits and a NOT gate for topological quantum computation (described above in subsection II.C.4 and, in greater detail in section IV). But there are several other systems which are potential candidates for topological quantum computation, and we briefly discuss these systems in this subsection. Indeed, the earliest proposals for fault-tolerant quantum computation with anyons were based on spin systems, not the quantum Hall effect (Kitaev, 2003).

First, we emphasize that the most crucial necessary condition for carrying out topological quantum computation is the existence of appropriate 'topological matter', i.e. a physical system in a topological phase. Such a phase of matter has suitable ground state properties and quasiparticle excitations manifesting non-Abelian statistics. Unfortunately, the necessary and sufficient conditions for the existence of topological ground states are not known even in theoretical models. We note that the topological symmetry of the ground state is an emergent symmetry at low energy, which is not present in the microscopic Hamiltonian of the system. Consequently, given a Hamiltonian, it is very difficult to determine if its ground state is in a topological phase. It is certainly no easier than showing that any other low-energy emergent phenomenon occurs in a particular model. Except for rare exactly solvable models (e.g. Kitaev, 2006, Levin and Wen, 2005b which we describe in section III.G), topological ground states are inferred on the basis of approximations and inspired guesswork. On the other hand, if topological states exist at all, they will be robust (i.e. their topological nature should be fairly insensitive to local perturbations, e.g. electron-phonon interaction or charge fluctuations between traps). For this reason, we believe that if it can be shown that some model Hamiltonian has a topological ground state, then a real material which is described approximately by that model is likely to have a topological ground state as well.

One theoretical model which is known to have a non-Abelian topological ground state is a $p + ip$ wave superconductor (i.e., a superconductor where the order parameter is of $p_x + ip_y$ symmetry). As we describe in section III.B, vortices in a superconductor of $p + ip$ pairing symmetry exhibit non-Abelian braiding statistics. This is really just a reincarnation of the physics of the Pfaffian state (believed to be realized at the $\nu = 5/2$ quantum Hall plateau) in zero magnetic field. Chiral p-wave superconductivity/superfluidity is currently the most transparent route to non-Abelian anyons. As we discuss below, there are multiple physical systems which may host such a reincarnation. The Kitaev honeycomb model (see also section III.G and) (Kitaev, 2006) is a seemingly different model which gives rise to the same physics. In it, spins interact anisotropically in such a way that their Hilbert space can be mapped onto that of a system of Majorana fermions. In various parameter ranges, the ground state is in either an Abelian topological phase, or a non-Abelian one in the same universality class as a $p + ip$ superconductor.

Chiral p-wave superconductors, like quantum Hall states, break parity and time-reversal symmetries, although they do so spontaneously, rather than as a result of a large magnetic field. However, it is also possible to have a topological phase which does not break these symmetries. Soluble theoretical models of spins on a lattice have been constructed which have P, T-invariant topological ground states. A very simple model of this type with an *Abelian* topological ground state, called the 'toric code', was proposed in Kitaev, 2003. Even though it is not sufficient for topological quantum computation because it is Abelian, it is instructive to consider this model because non-Abelian models can be viewed as more complex versions of this model. It describes $s = 1/2$ spins on a lattice interacting through the following Hamiltonian (Kitaev, 2003):

$$H = -J_1 \sum_i A_i - J_2 \sum_p F_p \tag{18}$$

This model can be defined on an arbitrary lattice. The spins are assumed to be on the links of the lattice. $A_i \equiv \prod_{\alpha \in \mathcal{N}(i)} \sigma_z^\alpha$, where $\mathcal{N}(i)$ is the set of spins on links α which touch the vertex i, and $F_p \equiv \prod_{\alpha \in p} \sigma_x^\alpha$, where p is a plaquette and $\alpha \in p$ are the spins on the links comprising

the plaquette. This model is exactly soluble because the A_is and F_ps all commute with each other. For any $J_1, J_2 > 0$, the ground state $|0\rangle$ is given by $A_i|0\rangle = F_p|0\rangle = |0\rangle$ for all i, p. Quasiparticle excitations are sites i at which $A_i|0\rangle = -|0\rangle$ or plaquettes p at which $F_p|0\rangle = -|0\rangle$. A pair of excited sites can be created at i and i' by acting on the ground state with $\prod_{\alpha\in\mathcal{C}} \sigma_x^\alpha$, where the product is over the links in a chain $\mathcal{C}$ on the lattice connecting i and i'. Similarly, a pair of excited plaquettes can be created by acting on the ground state with connected $\prod_{\alpha\in\tilde{\mathcal{C}}} \sigma_z^\alpha$ where the product is over the links crossed by a chain $\tilde{\mathcal{C}}$ on the dual lattice connecting the centers of plaquettes p and p'. Both types of excitations are bosons, but when an excited site is taken around an excited plaquette, the wavefunction acquires a minus sign. Thus, these two types of bosons are *relative semions*.

The toric code model is not very realistic, but it is closely related to some more realistic models such as the quantum dimer model (Chayes et al., 1989; Klein, 1982; Moessner and Sondhi, 2001; Nayak and Shtengel, 2001; Rokhsar and Kivelson, 1988). The degrees of freedom in this model are dimers on the links of a lattice, which represent a spin singlet bond between the two spins on either end of a link. The quantum dimer model was proposed as an effective model for frustrated antiferromagnets, in which the spins do not order, but instead form singlet bonds which resonate among the links of the lattice – the resonating valence bond (RVB) state (Anderson, 1973, 1987; Baskaran et al., 1987; Kivelson et al., 1987) which, in modern language, we would describe as a specific realization of a simple Abelian topological state (Balents et al., 1999, 2000; Moessner and Sondhi, 2001; Senthil and Fisher, 2000, 2001a). While the quantum dimer model on the square lattice does not have a topological phase for any range of parameter values (the RVB state is only the ground state at a critical point), the model on a triangular lattice does have a topological phase (Moessner and Sondhi, 2001).

Levin and Wen, 2005a,b constructed a model which is, in a sense, a non-Abelian generalization of Kitaev's toric code model. It is an exactly soluble model of spins on the links (two on each link) of the honeycomb lattice with three-spin interactions at each vertex and twelve-spin interactions around each plaquette, which we describe in section III.G. This model realizes a non-Abelian phase which supports Fibonacci anyons, which permits universal topological quantum computation (and generalizes straightforwardly to other non-Abelian topological phases). Other models have been constructed (Fendley and Fradkin, 2005; Freedman et al., 2005a) which are not exactly soluble but have only two-body interactions and can be argued to support topological phases in some parameter regime. However, there is still a considerable gulf between models which are soluble or quasi-soluble and models which might be considered realistic for some material.

Models such as the Kitaev and Levin-Wen models are deep within topological phases; there are no other competing states nearby in their phase diagram. However, simple models such as the Heisenberg model or extensions of the Hubbard model are not of this form. The implication is that such models are not deep within a topological phase, and topological phases must compete with other phases, such as broken symmetry phases. In the quantum dimer model (Moessner and Sondhi, 2001; Rokhsar and Kivelson, 1988), for instance, an Abelian topological phase must compete with various crystalline phases which occupy most of the phase diagram. This is presumably one obstacle to finding topological phases in more realistic models, i.e. models which would give an approximate description of some concrete physical system.

There are several physical systems – apart from fractional quantum Hall states – which might be promising hunting grounds for topological phases, including transition metal oxides and ultra-cold atoms in optical traps. The transition metal oxides have the advantage that we already know that they give rise to striking collective phenomena such as high-T_c superconductivity, colossal magnetoresistance, stripes, and thermoelectricity. Unfortunately, their physics is very difficult to unravel both theoretically and experimentally for this very reason: there are often many different competing phenomena in these materials. This is reflected in the models which describe transition metal oxides. They tend to have many closely competing phases, so that different approximate treatments find rather different phase diagrams. There is a second advantage to the transition metal oxides, namely that many sophisticated experimental techniques have been developed to study them, including transport, thermodynamic measurements, photoemission, neutron scattering, X-ray scattering, and NMR. Unfortunately, however, these methods are tailored for detecting broken-symmetry states or for giving a detailed understanding of metallic behavior, not for uncovering a topological phase. Nevertheless, this is such a rich family of materials that it would be surprising if there weren't a topological phase hiding there. (Whether we find it is another matter.) There is one particular material in this family, Sr_2RuO_4, for which there is striking evidence that it is a chiral p-wave superconductor at low temperatures, $T_c \approx 1.5$ K (Kidwingira et al., 2006; Xia et al., 2006). Half-quantum vortices in a thin film of such a superconductor would exhibit non-Abelian braiding statistics (since Sr_2RuO_4 is not spin-polarized, one must use half quantum vortices, not ordinary vortices). However, half quantum vortices are usually not the lowest energy vortices in a chiral p-wave superconductor, and a direct experimental observation of the half vortices themselves would be a substantial milestone on the way to topological quantum computation (Das Sarma et al., 2006b).

The current status of research is as follows. Three-dimensional single-crystals and thin films of Sr_2RuO_4 have been fabricated and studied. The nature of the superconductivity of these samples has been studied by many experimental probes, with the goal of identifying the symmetry of the Cooper-pair. There are many indications that support the identification of the Sr_2RuO_4 as a $p_x + ip_y$ superconductor. First, experiments that probe the spins of the Cooper pair strongly indicate triplet pairing (Mackenzie and Maeno, 2003). Such experiments probe the spin susceptibility through measurements of the NMR Knight shift and of neutron scattering. For singlet spin pairing the susceptibility vanishes at zero temperature, since the spins keep a zero polarization state in order to form Cooper pairs. In contrast, the susceptibility remains finite for triplet pairing, and this is in-

deed the observed behavior. Second, several experiments that probe time reversal symmetry have indicated that it is broken, as expected from a $p \pm ip$ super-conductor. These experiments include muon spin relaxation (Mackenzie and Maeno, 2003) and the polar Kerr effect(Xia et al., 2006). In contrast, magnetic imaging experiments designed to probe the edge currents that are associated with a super-conductor that breaks time reversal symmetry did not find the expected signal (Kirtley et al., 2007). The absence of this signal may be attributed to the existence of domains of $p + ip$ interleaved with those of $p - ip$. Altogether, then, Sr_2RuO_4 is likely to be a three dimensional $p+ip$ super-conductor, that may open the way for a realization of a two-dimensional super-conductor that breaks time reversal symmetry.

The other very promising direction to look for topological phases, ultra-cold atoms in traps, also has several advantages. The Hamiltonian can often be tuned by, for instance, tuning the lasers which define an optical lattice or by tuning through a Feshbach resonance. For instance, there is a specific scheme for realizing the Hubbard model (Jaksch and Zoller, 2005) in this way. At present there are relatively few experimental probes of these systems, as compared with transition metal oxides or even semiconductor devices. However, to look on the bright side, some of the available probes give information that cannot be measured in electronic systems. Furthermore, new probes for cold atoms systems are being developed at a remarkable rate.

There are two different schemes for generating topological phases in ultra-cold atomic gases that seem particularly promising at the current time. The first is the approach of using fast rotating dilute bose gases (Wilkin et al., 1998) to make quantum Hall systems of bosons (Cooper et al., 2001). Here, the rotation plays the role of an effective magnetic field, and the filling fraction is given by the ratio of the number of bosons to the number of vortices caused by rotation. Experimental techniques (Abo-Shaeer et al., 2001; Bretin et al., 2004; Schweikhard et al., 2004) have been developed that can give very large rotation rates and filling fractions can be generated which are as low as $\nu = 500$ (Schweikhard et al., 2004). While this is sufficiently low that all of the bosons are in a single landau level (since there is no Pauli exclusion, nu¿ 1 can still be a lowest Landau level state), it is still predicted to be several orders of magnitude too high to see interesting topological states. Theoretically, the interesting topological states occur for $\nu < 10$ (Cooper et al., 2001). In particular, evidence is very strong that $\nu = 1$, should it be achieved, would be the bosonic analogue of the Moore-Read state, and (slightly less strong) $\nu = 3/2$ and $\nu = 2$ would be the Read-Rezayi states, if the inter-boson interaction is appropriately adjusted (Cooper and Rezayi, 2007; Rezayi et al., 2005). In order to access this regime, either rotation rates will need to be increased substantially, or densities will have to be decreased substantially. While the latter sounds easier, it then results in all of the interaction scales being correspondingly lower, and hence implies that temperature would have to be lower also, which again becomes a challenge. Several other works have proposed using atomic lattice systems where manipulation of parameters of the Hamiltonian induces effective magnetic fields and should also result in quantum hall physics(Mueller, 2004; Popp et al., 2004; Sørensen et al., 2005).

The second route to generating topological phases in cold atoms is the idea of using a gas of ultra-cold fermions with a p-wave Feschbach resonance, which could form a spin-polarized chiral p-wave superfluid (Gurarie et al., 2005). Preliminary studies of such p-wave systems have been made experimentally (Gaebler et al., 2007) and unfortunately, it appears that the decay time of the Feshbach bound states may be so short that thermalization is impossible. Indeed, recent theoretical work (Levinsen et al., 2007) suggests that this may be a generic problem and additional tricks may be necessary if a p-wave superfluid is to be produced in this way.

We note that both the $\nu = 1$ rotating boson system and the chiral p-wave superfluid would be quite closely related to the putative non-Abelian quantum Hall state at $\nu = 5/2$ (as is Sr_2RuO_4). However, there is an important difference between a p-wave superfluid of cold fermions and the $\nu = 5/2$ state. Two-dimensional superconductors, as well as superfluids in any dimension, have a gapless Goldstone mode. Therefore, there is the danger that the motion of vortices may cause the excitation of low-energy modes. Superfluids of cold atoms may, however, be good test grounds for the detection of localized Majorana modes associated with localized vortices, as those are expected to have a clear signature in the absorption spectrum of RF radiation (Tewari et al., 2007b), in the form of a discrete absorption peak whose density and weight are determined by the density of the vortices (Grosfeld et al., 2007). One can also realize, using suitable laser configurations, Kitaev's honeycomb lattice model (Eq. 55) with cold atoms on an optical lattice (Duan et al., 2003). It has recently been shown how to braid anyons in such a model (Zhang et al., 2006).

A major difficulty in finding a topological phase in either a transition metal oxide or an ultra-cold atomic system is that topological phases are hard to detect directly. If the phase breaks parity and time-reversal symmetries, either spontaneously or as a result of an external magnetic field, then there is usually an experimental handle through transport, as in the fractional quantum Hall states or chiral p-wave superconductors. If the state does not break parity and time-reversal, however, there is no 'smoking gun' experiment, short of creating quasiparticles, braiding them, and measuring the outcome.

Any detailed discussion of the physics of these 'alternative' topological systems is well beyond the scope of the current review. We refer the readers to the existing recent literature on these systems for details. In section III (especially III.G), however, we discuss some of the soluble models which support topological phases because many of their mathematical features elucidate the underlying structure of topological phases.

III. TOPOLOGICAL PHASES OF MATTER AND NON-ABELIAN ANYONS

Topological quantum computation is predicated on the existence in nature of topological phases of matter. In this section,

we will discuss the physics of topological phases from several different perspectives, using a variety of theoretical tools. The reader who is interested primarily in the application of topological phases to quantum computation can skim this section briefly and still understand section IV. However, a reader with a background in condensed matter physics and quantum field theory may find it enlightening to read a more detailed account of the theory of topological phases and the emergence of anyons from such phases, with explicit derivations of some of the results mentioned in section II and used in section IV. These readers may find topological phases interesting in and of themselves, apart from possible applications.

Topological phases, the states of matter which support anyons, occur in many-particle physical systems. Therefore, we will be using field theory techniques to study these states. A canonical, but by no means unique, example of a field theory for a topological phase is Chern-Simons theory. We will frequently use this theory to illustrate the general points which we wish to make about topological phases. In section V, we will make a few comments about the problem of classifying topological phases, and how this example, Chern-Simons theory, fits in the general classification. In subsection III.A, we give a more precise definition of a topological phase and connect this definition with the existence of anyons. We also introduce Chern-Simons theory, which we will discuss throughout section III as an example of the general structure which we discuss in subsection III.A. In subsection III.B, we will discuss a topological phase which is superficially rather different but, in fact, will prove to be a special case of Chern-Simons theory. This phase can be analyzed in detail using the formalism of BCS theory. In subsection III.C, we further analyze Chern-Simons theory, giving a more detailed account of its topological properties, especially the braiding of anyons. We describe Witten's work (Witten, 1989) connecting Chern-Simons theory with the knot and link invariants of Jones and Kauffman (Jones, 1985; Kauffman, 1987). We show how the latter can be used to derive the properties of anyons in these topological phases. In section III.D, we describe a complementary approach by which Chern-Simons theory can be understood: through its connection to conformal field theory. We explain how this approach can be particularly fruitful in connection with fractional quantum Hall states. In III.E, we discuss the gapless excitations which must be present at the edge of any chiral topological phase. Their physics is intimately connected with the topological properties of the bulk and, at the same time, is directly probed by transport experiments in quantum Hall devices. In III.F, we apply the knowledge which we have gained about the properties of Chern-Simons theory to the interferometry experiments which we discussed in II.C.3. Finally, in III.G we discuss a related but different class of topological phases which can arise in lattice models and may be relevant to transition metal oxides or 'artificial' solids such as ultra-cold atoms in optical lattices.

A. Topological Phases of Matter

In Section II of this paper, we have used 'topological phase' as essentially being synonymous with any system whose quasiparticle excitations are anyons. However, a precise definition is the following. A system is in a topological phase if, at low temperatures and energies, and long wavelengths, all observable properties (e.g. correlation functions) are invariant under smooth deformations (diffeomorphisms) of the spacetime manifold in which the system lives. Equivalently, all observable properties are independent of the choice of spacetime coordinates, which need not be inertial or rectilinear. (This is the 'passive' sense of a diffeomorphism, while the first statement uses the active sense of a transformation.) By "at low temperatures and energies, and long wavelengths," we mean that diffeomorphism invariance is only violated by terms which vanish as $\sim \max\left(e^{-\Delta/T}, e^{-|x|/\xi}\right)$ for some nonzero energy gap Δ and finite correlation length ξ. Thus, topological phases have, in general, an energy gap separating the ground state(s) from the lowest excited states. Note that an excitation gap, while necessary, is not sufficient to ensure that a system is in a topological phase.

The invariance of all correlation functions under diffeomorphisms means that the only local operator which has non-vanishing correlation functions is the identity. For instance, under an arbitrary change of space-time coordinates $x \to x' = f(x)$, the correlations of a scalar operator $\phi(x)$ must satisfy $\langle 0_i|\phi(x_1)\phi(x_2)\dots\phi(x_n)|0_j\rangle = \langle 0_i|\phi(x_1')\phi(x_2')\dots\phi(x_n')|0_j\rangle$, which implies that $\langle 0_i|\phi(x_1)\phi(x_2)\dots\phi(x_n)|0_j\rangle = 0$ unless $\phi(x) \equiv c$ for some constant c. Here, $|0_i\rangle, |0_j\rangle$ are ground states of the system (which may or may not be different). This property is important because any local perturbation, such as the environment, couples to a local operator. Hence, these local perturbations are proportional to the identity. Consequently, they cannot have non-trivial matrix elements between different ground states. The only way in which they can affect the system is by exciting the system to high-energies, at which diffeomorphism invariance is violated. At low-temperatures, the probability for this is exponentially suppressed.

The preceding definition of a topological phase may be stated more compactly by simply saying that a system is in a topological phase if its low-energy effective field theory is a topological quantum field theory (TQFT), i.e. a field theory whose correlation functions are invariant under diffeomorphisms. Remarkably, topological invariance does not imply trivial low-energy physics.

1. Chern-Simons Theory

Consider the simplest example of a TQFT, Abelian Chern-Simons theory, which is relevant to the Laughlin states at filling fractions of the form $\nu = 1/k$, with k an odd integer. Although there are many ways to understand the Laughlin states, it is useful for us to take the viewpoint of a low-energy effective theory. Since quantum Hall systems are gapped, we should be able to describe the system by a field theory with

very few degrees of freedom. To this end, we consider the action

$$S_{CS} = \frac{k}{4\pi} \int d^2\mathbf{r}\, dt\ \epsilon^{\mu\nu\rho} a_\mu \partial_\nu a_\rho \tag{19}$$

where k is an integer and ϵ is the antisymmetric tensor. Here, a is a U(1) gauge field and indices μ, ν, ρ take the values 0 (for time-direction), 1,2 (space-directions). This action represents the low-energy degrees of freedom of the system, which are purely topological.

The Chern-Simons gauge field a in (19) is an emergent degree of freedom which encodes the low-energy physics of a quantum Hall system. Although in this particular case, it is simply-related to the electronic charge density, we will also be considering systems in which emergent Chern-Simons gauge fields cannot be related in a simple way to the underlying electronic degrees of freedom.

In the presence of an external electromagnetic field and quasiparticles, the action takes the form:

$$S = S_{CS} - \int d^2\mathbf{r}\, dt\ \left(\frac{1}{2\pi} \epsilon^{\mu\nu\rho} A_\mu \partial_\nu a_\rho + j^{\rm qp}_\mu a_\mu \right) \tag{20}$$

where $j^{\rm qp}_\mu$ is the quasiparticle current, $j^{\rm qp}_0 = \rho^{\rm qp}$ is the quasiparticle density, $\mathbf{j}^{\rm qp} = (j^{\rm qp}_1, j^{\rm qp}_2)$ is the quasiparticle spatial current, and A_μ is the external electromagnetic field. We will assume that the quasiparticles are not dynamical, but instead move along some fixed classically-prescribed trajectories which determine $j^{\rm qp}_\mu$. The electrical current is:

$$j_\mu = \partial \mathcal{L} / \partial A_\mu = \frac{1}{2\pi} \epsilon^{\mu\nu\rho} \partial_\nu a_\rho \tag{21}$$

Since the action is quadratic, it is completely solvable, and one can integrate out the field a_μ to obtain the response of the current to the external electromagnetic field. The result of such a calculation is precisely the quantized Hall conductivity $\sigma_{xx} = 0$ and $\sigma_{xy} = \frac{1}{k}\, e^2/h$.

The equation of motion obtained by varying a_0 is the Chern-Simons constraint:

$$\frac{k}{2\pi} \nabla \times \mathbf{a} = j^{\rm qp}_0 + \frac{1}{2\pi} B \tag{22}$$

According to this equation, each quasiparticle has Chern-Simons flux $2\pi/k$ attached to it (the magnetic field is assumed fixed). Consequently, it has electrical charge $1/k$, according to (21). As a result of the Chern-Simons flux, another quasiparticle moving in this Chern-Simons field picks up an Aharonov-Bohm phase. The action associated with taking one quasiparticle around another is, according to Eq. 20, of the form

$$\frac{1}{2} k \int d\mathbf{r}\, dt\, \mathbf{j} \cdot \mathbf{a} = kQ \int_{\mathcal{C}} d\mathbf{r} \cdot \mathbf{a} \tag{23}$$

where Q is the charge of the quasiparticle and the final integral is just the Chern-Simons flux enclosed in the path. (The factor of $1/2$ on the left-hand side is due to the action of the Chern-Simons term itself which, according to the constraint (22) is $-1/2$ times the Aharonov-Bohm phase. This is cancelled by a factor of two coming from the fact that each particle sees the other's flux.) Thus the contribution to a path integral $e^{iS_{CS}}$ just gives an Aharonov-Bohm phase associated with moving a charge around the Chern-Simons flux attached to the other charges. The phases generated in this way give the quasiparticles of this Chern-Simons theory $\theta = \pi/k$ Abelian braiding statistics.[3]

Therefore, an Abelian Chern-Simons term implements Abelian anyonic statistics. In fact, it does nothing else. An Abelian gauge field in $2+1$ dimensions has only one transverse component; the other two components can be eliminated by fixing the gauge. This degree of freedom is fixed by the Chern-Simons constraint (22). Therefore, a Chern-Simons gauge field has no local degrees of freedom and no dynamics.

We now turn to non-Abelian Chern-Simons theory. This TQFT describes non-Abelian anyons. It is analogous to the Abelian Chern-Simons described above, but different methods are needed for its solution, as we describe in this section. The action can be written on an arbitrary manifold $\mathcal{M}$ in the form

$$\begin{aligned} S_{CS}[a] &= \frac{k}{4\pi} \int_{\mathcal{M}} {\rm tr} \left(a \wedge da + \frac{2}{3} a \wedge a \wedge a \right) \\ &= \frac{k}{4\pi} \int_{\mathcal{M}} \epsilon^{\mu\nu\rho} \left(a^{\underline{a}}_\mu \partial_\nu a^{\underline{a}}_\rho + \frac{2}{3}\, f_{\underline{a}\,\underline{b}\,\underline{c}} a^{\underline{a}}_\mu a^{\underline{b}}_\nu a^{\underline{c}}_\rho \right) \end{aligned} \tag{24}$$

In this expression, the gauge field now takes values in the Lie algebra of the group G. $f_{\underline{a}\,\underline{b}\,\underline{c}}$ are the structure constants of the Lie algebra which are simply $\epsilon_{\underline{a}\,\underline{b}\,\underline{c}}$ for the case of SU(2). For the case of SU(2), we thus have a gauge field $a^{\underline{a}}_\mu$, where the underlined indices run from 1 to 3. A matter field transforming in the spin-j representation of the SU(2) gauge group will couple to the combination $a^{\underline{a}}_\mu x_{\underline{a}}$, where $x_{\underline{a}}$ are the three generator matrices of su(2) in the spin-j representation. For gauge group G and coupling constant k (called the 'level'), we will denote such a theory by G_k. In this paper, we will be primarily concerned with SU(2)$_k$ Chern-Simons theory.

To see that Chern-Simons theory is a TQFT, first note that the Chern-Simons action (24) is invariant under all diffeomorphisms of $\mathcal{M}$ to itself, $f : \mathcal{M} \to \mathcal{M}$. The differential form notation in (24) makes this manifest, but it can be checked in coordinate form for $x^\mu \to f^\mu(x)$. Diffeomorphism invariance stems from the absence of the metric tensor in the Chern-Simons action. Written out in component form, as in (24), indices are, instead, contracted with $\epsilon^{\mu\nu\lambda}$.

Before analyzing the physics of this action (24), we will make two observations. First, as a result of the presence of

[3] The Chern-Simons effective action for a hierarchical state is equivalent to the action for the composite fermion state at the same filling fraction (Blok and Wen, 1990; Read, 1990; Wen and Zee, 1992). It is a simple generalization of Eq. 19 which contains several internal gauge fields a^n_μ (with $n = 1, 2, \ldots$), corresponding (in essence) to the action for the different species of particles (either the different levels of the hierarchy, or the different composite fermion Landau levels).

$\epsilon^{\mu\nu\lambda}$, the action changes sign under parity or time-reversal transformations. In this paper, we will concentrate, for the most part, on topological phases which are chiral, i.e. which break parity and time-reversal symmetries. These are the phases which can appear in the fractional quantum Hall effect, where the large magnetic field breaks P, T. However, we shall also discuss non-chiral topological phases in section III.G, especially in connection which topological phases emerging from lattice models.

Secondly, the Chern-Simons action is not quite fully invariant under gauge transformations $a_\mu \rightarrow g a_\mu g^{-1} + g\partial_\mu g^{-1}$, where $g : \mathcal{M} \rightarrow G$ is any function on the manifold taking values in the group G. On a closed manifold, it is only invariant under "small" gauge tranformations. Suppose that the manifold $\mathcal{M}$ is the 3-sphere, S^3. Then, gauge transformations are maps $S^3 \rightarrow G$, which can be classified topologically according to it homotopy $\pi_3(G)$. For any simple compact group G, $\pi_3(G) = \mathbb{Z}$, so gauge transformations can be classified according to their "winding number". Under a gauge transformation with winding m,

$$S_{CS}[a] \rightarrow S_{CS}[a] + 2\pi k m \tag{25}$$

(Deser et al., 1982). While the action is invariant under "small" gauge transformations, which are continuously connected to the identity and have $m = 0$, it is not invariant under "large" gauge transformations ($m \neq 0$). However, it is sufficient for $\exp(iS)$ to be gauge invariant, which will be the case so long as we require that the level k be an integer. The requirement that the level k be an integer is an example of the highly rigid structure of TQFTs. A small perturbation of the microscopic Hamiltonian cannot continuously change the value of k in the effective low energy theory; only a perturbation which is large enough to change k by an integer can do this.

The failure of gauge invariance under large gauge tranformations is also reflected in the properties of Chern-Simons theory on a surface with boundary, where the Chern-Simons action is gauge invariant only up to a surface term. Consequently, there must be gapless degrees of freedom at the edge of the system whose dynamics is dictated by the requirement of gauge invariance of the combined bulk and edge (Wen, 1992), as we discuss in section III.E.

To unravel the physics of Chern-Simons theory, it is useful to specialize to the case in which the spacetime manifold $\mathcal{M}$ can be decomposed into a product of a spatial surface and time, $\mathcal{M} = \Sigma \times \mathbb{R}$. On such a manifold, Chern-Simons theory is a theory of the ground states of a topologically-ordered system on Σ. There are no excited states in Chern-Simons theory because the Hamiltonian vanishes. This is seen most simply in $a_0 = 0$ gauge, where the momentum canonically conjugate to a_1 is $-\frac{k}{4\pi}\, a_2$, and the momentum canonically conjugate to a_2 is $\frac{k}{4\pi}\, a_1$ so that

$$\mathcal{H} = \frac{k}{4\pi} \mathrm{tr}\,(a_2 \partial_0 a_1 - a_1 \partial_0 a_2) - \mathcal{L} = 0 \tag{26}$$

Note that this is a special feature of an action with a Chern-Simons term alone. If the action had both a Chern-Simons and a Yang-Mills term, then the Hamiltonian would not vanish, and the theory would have both ground states and excited states with a finite gap. Since the Yang-Mills term is subleading compared to the Chern-Simons term (i.e. irrelevant in a renormalization group (RG) sense), we can forget about it at energies smaller than the gap and consider the Chern-Simons term alone.

Therefore, when Chern-Simons theory is viewed as an effective field theory, it can only be valid at energies much smaller than the energy gap. As a result, it is unclear, at the moment, whether Chern-Simons theory has anything to say about the properties of quasiparticles – which are excitations above the gap – or, indeed, whether those properties are part of the universal low-energy physics of the system (i.e. are controlled by the infrared RG fixed point). Nevertheless, as we will see momentarily, it does and they are.

Although the Hamiltonian vanishes, the theory is still not trivial because one must solve the constraint which follows by varying a_0. For the sake of concreteness, we will specialize to the case $G =$SU(2). Then the constraint reads:

$$\epsilon_{ij} \partial_i a_j^{\underline{a}} + f^{\underline{a}\,\underline{b}\,\underline{c}} a_1^{\underline{b}} a_2^{\underline{c}} = 0 \tag{27}$$

where $i, j = 1, 2$. The left-hand side of this equation is the field strength of the gauge field $a_i^{\underline{a}}$, where $\underline{a} = 1, 2, 3$ is an su(2) index. Since the field strength must vanish, we can always perform a gauge transformation so that $a_i^{\underline{a}} = 0$ locally. Therefore this theory has no local degrees of freedom. However, for some field configurations satisfying the constraint, there may be a global topological obstruction which prevents us from making the gauge field zero everywhere. Clearly, this can only happen if Σ is topologically non-trivial.

The simplest non-trivial manifold is the annulus, which is topologically equivalent to the sphere with two punctures. Following Elitzur et al., 1989 (see also (Wen and Zee, 1998) for a similar construction on the torus), let us take coordinates (r, ϕ) on the annulus, with $r_1 < r < r_2$, and let t be time. Then we can write $a_\mu = g\partial_\mu g^{-1}$, where

$$g(r, \phi, t) = e^{i\omega(r,\phi,t)}\, e^{i\frac{\phi}{k}\lambda(t)} \tag{28}$$

where $\omega(r, \phi, t)$ and $\lambda(t)$ take values in the Lie algebra su(2) and $\omega(r, \phi, t)$ is a single-valued function of ϕ. The functions ω and λ are the dynamical variables of Chern-Simons theory on the annulus. Substituting (28) into the Chern-Simons action, we see that it now takes the form:

$$S = \frac{1}{2\pi} \int dt\, \mathrm{tr}\,(\lambda \partial_t \Omega) \tag{29}$$

where $\Omega(r, t) = \int_0^{2\pi} d\phi\, (\omega(r_1, \phi, t) - \omega(r_2, \phi, t))$. Therefore, Ω is canonically conjugate to λ. By a gauge transformation, we can always rotate λ and Ω so that they are along the 3 direction in su(2), i.e. $\lambda = \lambda_3 T^3$, $\Omega = \Omega_3 T^3$. Since it is defined through the exponential in (28), Ω_3 takes values in $[0, 2\pi]$. Therefore, its canonical conjugate, λ_3, is quantized to be an integer. From the definition of λ in (28), we see that $\lambda_3 \equiv \lambda_3 + 2k$. However, by a gauge transformation given by a rotation around the 1-axis, we can transform $\lambda \rightarrow -\lambda$. Hence, the independent allowed values of λ are $0, 1, \ldots, k$.

On the two-punctured sphere, if one puncture is of type a, the other puncture must be of type $\bar{a}$. (If the topological charge at one puncture is measured along a loop around the puncture – e.g. by a Wilson loop, see subsection III.C – then the loop can be deformed so that it goes around the other puncture, but in the opposite direction. Therefore, the two punctures necessarily have conjugate topological charges.) For SU(2), $a = \bar{a}$, so both punctures have the same topological charge. Therefore, the restriction to only $k+1$ different possible allowed boundary conditions λ for the two-punctured sphere implies that there are $k+1$ different quasiparticle types in SU(2)$_k$ Chern-Simons theory. As we will describe in later subsections, these allowed quasiparticle types can be identified with the $j = 0, \frac{1}{2}, \ldots, \frac{k}{2}$ representations of the SU(2)$_2$ Kac-Moody algebra.

2. TQFTs and Quasiparticle Properties

We will continue with our analysis of Chern-Simons theory in sections III.C and III.D. Here, we will make some more general observations abut TQFTs and the topological properties of quasiparticles. We turn to the n-punctured sphere, $\Sigma = S^2 \backslash P_1 \cup P_2 \cup \ldots \cup P_n$, i.e. the sphere S^2 with the points $P_1, P_2 \ldots P_n$ deleted, which is equivalent to $n-1$ quasiparticles in the plane (the n^{th} puncture becomes the point at ∞). This will allow us to study the topological properties of quasiparticle excitations purely from ground state properties. To see how braiding emerges in this approach, it is useful to note that diffeomorphisms should have a unitary representation on the ground state Hilbert space (i.e. they should commute with the Hamiltonian). Diffeomorphisms which can be smoothly deformed to the identity should have a trivial action on the Hilbert space of the theory since there are no local degrees of freedom. However, 'large' diffeomorphisms could have a non-trivial unitary representation on the theory's Hilbert space. If we take the quotient of the diffeomorphism group by the set of diffeomorphisms which can be smoothly deformed to the identity, then we obtain the *mapping class group*. On the n-punctured sphere, the braid group $\mathcal{B}_{n-1}$ is a subgroup of the mapping class group.[4] Therefore, if we study Chern-Simons theory on the n-punctured sphere as we did for the 2-punctured sphere above, and determine how the mapping class group acts, we can learn all of the desired information about quasiparticle braiding. We do this by two different methods in subsections III.C and III.D.

One extra transformation in the mapping class group, compared to the braid group, is a 2π rotation of a puncture/particle relative to the rest of the system (a Dehn twist). If we consider particles with a finite extent, rather than point particles, then we must consider the possibility of such rotations. For instance, if the particles are small dipoles, then we can represent their world lines as ribbons. A Dehn twist then corresponds to a twist of the ribbon. Thickening a world line into a ribbon is called a *framing*. A given world line has multiple choices of framing, corresponding to how many times the ribbon twists. A framing is actually essential in Chern-Simons theory because flux is attached to charge through the constraint (22) or (27). By putting the flux and charge at opposite edges of the ribbon, which is a short-distance regularization of the theory, we can associate a well-defined phase to a particle trajectory. Otherwise, we wouldn't know how many times the charge went around the flux.

Any transformation acting on a single particle can only result in a phase; the corresponding phase is called the twist parameter Θ_a. Often, one writes $\Theta_a \equiv e^{2\pi i h_a}$, where h_a is called the *spin* of the particle.[5] (One must, however, be careful to distinguish this from the actual spin of the particle, which determines its transformation properties under the three-dimensional rotation group and must be half-integral.) However, h_a is well-defined even if the system is not rotationally-invariant, so it is usually called the *topological spin* of the particle. For Abelian anyons, it is just the statistics parameter, $\theta = 2\pi i h_a$.

The ground state properties on arbitrary surfaces, including the n-punctured sphere and the torus, can be built up from more primitive vector spaces in the following way. An arbitrary closed surface can be divided into a collection of 3-punctured spheres which are glued together at their boundaries. This is called a 'pants decomposition' because of the topological equivalence of a 3-punctured sphere to a pair of pants. Therefore, the 3-punctured sphere plays a fundamental role in the description of a topological phase. Its Hilbert space is denoted by V_{ab}^c, if a, b, and c are the particle types at the three punctures. If the a and b punctures are fused, a two-punctured sphere will result. From the above analysis, it has a one-dimensional vector space if both punctures have topological charge c and a zero-dimensional vector space otherwise. The dimension of the Hilbert space of the 3-punctured sphere is given by the fusion multiplicity $N_{ab}^c = \dim(V_{ab}^c)$ which appears in the fusion rule, $\phi_a \times \phi_b = \sum_c N_{ab}^c \phi_c$. The Hilbert space on a surface obtained by gluing together 3-punctured spheres is obtained by tensoring together the V's and sum-

[4] The mapping class group is non-trivial solely as a result of the punctures. In particular, any diffeomorphism which moves one or more of the punctures around other punctures cannot be deformed to the identity; conversely, if two diffeomorphisms move the same punctures along trajectories which can be deformed into each other, then the diffeomorphisms themselves can also be deformed into each other. These classes of diffeomorphisms correspond to the braid group which is, in fact, a normal subgroup. If we take the quotient of the mapping class group by the Dehn twists of $n-1$ of the punctures – all except the point at infinity – we would be left with the braid group $\mathcal{B}_{n-1}$.

[5] If a is its own anti-particle, so that two as can fuse to $\mathbf{1}$, then $R_1^{aa} = \pm\Theta_a^*$, where the minus sign is acquired for some particle types a which are not quite their own antiparticles but only up to some transformation which squares to -1. This is analogous to the fact that the fundamental representation of SU(2) is not real but is pseudoreal. Consequently, a spin-$1/2$ particle ψ_μ and antiparticle $\psi^{\mu\dagger}$ can form a singlet, $\psi^{\mu\dagger}\psi_\mu$, but two spin-$1/2$ particles can as well, $\psi_\mu \psi_\nu i(\sigma_y)^{\mu\nu}$, where σ_y is the antisymmetric Pauli matrix. When some quantities are computed, an extra factor of $(i\sigma_y)^2 = -1$ results. This $\pm$ sign is called the Froebenius-Schur indicator. (See, for instance, Bantay, 1997.)

ming over the particle types at the punctures where gluing occurs. For instance, the Hilbert space on the 4-punctured sphere is given by the direct sum $V^e_{abd} = \oplus_c V^c_{ab} V^e_{cd}$; the Hilbert space on the torus is $V_{T^2} = \oplus_a V^a_{1a} V^a_{a1}$. (If one of the particle types is the vacuum, then the corresponding puncture can simply be removed; the 3-punctured sphere is then actually only 2-punctured. Gluing two of them together end to end gives a torus. This is one way of seeing that the degeneracy on the torus is the number of particle types.)

The Hilbert space of the n-punctured sphere with topological charge a at each puncture can be constructed by sewing together a chain of $(n-2)$ 3-punctured spheres. The resulting Hilbert space is: $V^1_{a\ldots a} = \oplus_{b_i} V^{b_1}_{aa} V^{b_2}_{ab_1} \ldots V^a_{ab_{N-3}}$. A simple graphical notation for a set of basis states of this Hilbert space is given by a *fusion chain* (similar to the fusion tree discussed in appendix A):

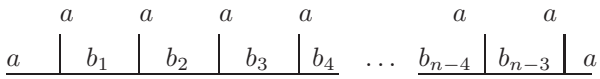

The first two as on the far left fuse to b_1. The next a fuses with b_1 to give b_2. The next a fuses with b_2 to give b_3, and so on. The different basis vectors in this Hilbert space correspond to the different possible allowed b_is. The dimension of this Hilbert space is $N^{b_1}_{aa} N^{b_2}_{ab_1} \ldots N^a_{ab_{N-3}} = (N_a)^{b_1}_a (N_a)^{b_2}_{b_1} \ldots (N_a)^a_{b_{N-3}}$. On the right-hand-side of this equation, we have suggested that the fusion multiplicity N^c_{ab} can be viewed as a matrix $(N_a)^c_b$ associated with quasiparticle species a. Let us denote the largest eigenvalue of the matrix N_a by d_a. Then the Hilbert space of M quasiparticles of type a has dimension $\sim d_a^{M-2}$ for large M. For this reason, d_a is called the *quantum dimension* of an a quasiparticle. It is the asymptotic degeneracy per particle of a collection of a quasiparticle. For Abelian particles, $d_a = 1$ since the multiparticle Hilbert space is one-dimensional (for fixed particle positions). Non-Abelian particles have $d_a > 1$. Note that d_a is not, in general, an integer, which is symptomatic of the non-locality of the Hilbert space: it is *not* the tensor product of d_a-dimensional Hilbert spaces associated locally with each particle.

This non-locality is responsible for the stability of this degenerate ground state Hilbert space. Not only the Yang-Mills term, but all possible gauge-invariant terms which we can add to the action (24) are irrelevant. This means that adding such a term to the action might split the $\sim d_a^{M-2}$-dimensional space of degenerate states in a finite-size system, but the splitting must vanish as the system size and the particle separations go to infinity. In fact, we can make an even stronger statement than that. All ground state matrix elements of gauge-invariant local operators such as the field strength squared, $F^{\underline{a}}_{\mu\nu} F^{\mu\nu\underline{a}}$, vanish identically because of the Chern-Simons constraint. Therefore, the degeneracy is not lifted at all in perturbation theory. It can only be lifted by non-perturbative effects (e.g. instantons/quantum tunneling), which could cause a splitting $\sim e^{-gL}$ where g is inversely proportional to the coefficient of the Yang-Mills term. Therefore, the multi-quasiparticle states are degenerate to within exponential accuracy. At finite-temperatures, one must also consider transitions to excited states, but the contributions of these will be $\sim e^{-\Delta/T}$. Furthermore if we were to add a time dependent (source) term to the action, these properties will remain preserved so long as the frequency of this term remains small compared with the gap.

Aside from the n-punctured spheres, the torus is the most important manifold for considering topological phases. Although not directly relevant to experiments, the torus is very important for numerical simulations since periodic boundary conditions are often the simplest choice. As noted above, the ground state degeneracy on the torus is equal to the number of quasiparticle species. Suppose one can numerically solve a Hamiltonian on the torus. If it has a gap between its ground state(s) and the lowest energy excited states, then its ground state degeneracy is an important topological property of the state – namely the number of of quasiparticle species. A simple physical understanding of this degeneracy can be obtained in the following way. Suppose that we have a system of electrons in a topological phase. If we consider the system on the torus, then the electrons must have periodic boundary conditions around either generator of the torus (i.e. around either handle), but the quasiparticles need not. In the Abelian $\nu = 1/m$ fractional quantum Hall state, for instance, it is possible for a quasiparticle to pick up a phase $e^{2\pi i n/m}$ in going around the meridian of the torus, where n can take any of the values $n = 0, 1, \ldots, m-1$; electrons would still have periodic boundary conditions since they are made up of m quasiparticles. Indeed, all m of these possibilities occur, so the ground state is m-fold degenerate.

Let us make this a little more precise. We introduce operators T_1 and T_2 which create a quasiparticle-quasihole pair, take the quasiparticle around the meridian or longitude, respectively, of the torus and annihilate them again. Then T_1 and T_2 must satisfy:

$$T_2^{-1} T_1^{-1} T_2 T_1 = e^{2\pi i/m} \tag{30}$$

because $T_1^{-1} T_1$ amounts to a contractible quasiparticle-quasihole loop, as does $T_2^{-1} T_2$; by alternating these processes, we cause these loops to be linked. The quasiparticle trajectories in spacetime (which can be visualized as a thickened torus) are equivalent to a simple link between two circles (the Hopf link): the first quasiparticle-quasihole pair is pulled apart along the meridian (T_1); but before they can be brought back together (T_1^{-1}), the second pair is pulled apart along the longitude (T_2). After the first pair is brought back together and annihilated (T_1^{-1}), the second one is, too (T_2^{-1}). In other words, the phase on the right-hand-side of Eq. 30 is simply the phase obtained when one quasiparticle winds around another. This algebra can be represented on a vector space of minimum dimension m. Let us call the states in this vector space $|n\rangle$, $n = 0, 1, \ldots, m-1$. Then

$$\begin{aligned} T_1|n\rangle &= e^{2\pi i n/m}|n\rangle \\ T_2|n\rangle &= |(n+1) \bmod m\rangle \end{aligned} \tag{31}$$

These m states correspond to $n = 0, 1, \ldots, m-1$ quanta of flux threaded through the torus. If we were to cut along a

meridian and open the torus into an annulus, then these states would have flux n threaded through the hole in the annulus and charge n/m at the inner boundary of the annulus (and a compensating charge at the outer boundary). We can instead switch to a basis in which T_2 is diagonal by a discrete Fourier transform. If we write $|\tilde{n}\rangle = \frac{1}{\sqrt{m}} \sum_{n=0}^{m-1} e^{2\pi i n\tilde{n}/m} |n\rangle$, then $|\tilde{n}\rangle$ is an eigenstgate of T_2 with eigenvalue $e^{2\pi i \tilde{n}/m}$. In this basis, T_1 is an off-diagonal operator which changes the boundary conditions of quasiparticles around the longitude of the torus. In non-Abelian states, a more complicated version of the same thing occurs, as we discuss for the case of Ising anyons at the end of section III.B. The different boundary conditions around the meridian correspond to the different possible quasiparticle types which could thread the torus (or, equivalently, could be present at the inner boundary of the annulus if the torus were cut open along a meridian). One can switch to a basis in which the boundary conditions around the longitude are fixed. The desired basis change is analogous to the discrete Fourier transform given above and is given by the 'S-matrix' or 'modular S-matrix' of the theory. Switching the longitude and meridian is one of the generators of the mapping class group of the torus; the S-matrix expresses how it acts on the ground state Hilbert space. The elements of the S-matrix are closely related to quasiparticle braiding. By following a similar construction to the one with T_1, T_2 above, one can see that S_{ab} is equal to the amplitude for creating $a\bar{a}$ and $b\bar{b}$ pairs, braiding a and b, and annihilating again in pairs. This is why, in an Abelian state, the elements of the S-matrix are all phases (up to an overall normalization which ensures unitarity), e.g. $S_{nn'} = \frac{1}{\sqrt{m}} e^{2\pi i n n'/m}$ in the example above. In a non-Abelian state, the different entries in the matrix can have different magnitudes, so the basis change is a little more complicated than a Fourier transform. Entries can even vanish in the non-Abelian case since, after a and b have been braided, a and $\bar{a}$ may no longer fuse to $\mathbf{1}$.

In the case of Ising anyons on the torus (SU(2)$_2$), there are three ground states. One basis is $|\mathbf{1}_m\rangle$, $|\sigma_m\rangle$, $|\psi_m\rangle$, corresponding to the different allowed topological charges which would be measured at the inner boundary of the resulting annulus if the torus were cut open along its meridian. An equally good basis is given by eigenstates of topological charge around the longitude: $|\mathbf{1}_l\rangle$, $|\sigma_l\rangle$, $|\psi_l\rangle$. As we will see in at the end of the next section, the basis change between them is given by

$$S = \begin{pmatrix} \frac{1}{2} & \frac{1}{\sqrt{2}} & \frac{1}{2} \\ \frac{1}{\sqrt{2}} & 0 & -\frac{1}{\sqrt{2}} \\ \frac{1}{2} & -\frac{1}{\sqrt{2}} & \frac{1}{2} \end{pmatrix} \tag{32}$$

The S-matrix not only contains information about braiding, but also about fusion, according to Verlinde's formula (Verlinde, 1988) (for a proof, see Moore and Seiberg, 1988, 1989):

$$N_{ab}^c = \sum_x \frac{S_{ax} S_{bx} S_{\bar{c}x}}{S_{\mathbf{1}x}} \tag{33}$$

Consequently, the quantum dimension of a particle of species a is:

$$d_a = \frac{S_{\mathbf{1}a}}{S_{\mathbf{11}}} \tag{34}$$

The mathematical structure encapsulating these braiding and fusion rules is a *modular tensor category* (Bakalov and Kirillov, 2001; Kassel, 1995; Kitaev, 2006; Turaev, 1994; Walker, 1991). A category is composed of objects and morphisms, which are maps between the objects which preserve their defining structure. The idea is that one can learn more about the objects by understanding the morphisms between them. In our case, the objects are particles with labels (which specify their species) as well as fixed configurations of several particles. The morphisms are particle trajectories, which map a set of labeled partices at some initial time to a set of labeled particles at some final time. A *tensor category* has a tensor product structure for multiplying objects; here, this is simply the fact that one can take two well-separated (and historically well-separated) collections of particles and consider their union to be a new 'tensor-product' collection. Since we consider particles in two dimensions, the trajectories are essentially the elements of the braid group, but they include the additional possibility of twisting. (Allowing twists in the strands of a braid yields a *braided ribbon category*.) We will further allow the trajectories to include the fusion of two particles (so that we now have a *fusion category*). Morphisms can, therefore, be defined by specifying Θ_a, V_{ab}^c, R, and F.

Why is it necessary to invoke category theory simply to specify the topological properties of non-Abelian anyons? Could the braid group not be the highest level of abstraction that we need? The answer is that for a fixed number of particles n, the braid group $\mathcal{B}_n$ completely specifies their topological properties (perhaps with the addition of twists Θ_a to account for the finite size of the particles). However, we need representations of $\mathcal{B}_n$ for all values of n which are compatible with each other and with fusion (of which pair creation and annihilation is simply the special case of fusion to the vacuum). So we really need a more complex – and much more tightly constrained – structure. This is provided by the concept of a modular tensor category. The F and R matrices play particularly important roles. The F matrix can essentially be viewed an associativity relation for fusion: we could first fuse i with j, and then fuse the result with k; or we could fuse i with the result of fusing j with k. The consistency of this property leads to a constraint on the F-matrices called the pentagon equation. (An explicit example of the pentagon equation is worked out in Section IV.B.) Consistency between F and R leads to a constraint called the hexagon equation. Modularity is the condition that the S-matrix be invertible. These self-consistency conditions are sufficiently strong that a solution to them completely defines a topological phase.[6]

An equivalent alternative to studying punctured surfaces is to add non-dynamical charges which are coupled to the Chern-Simons gauge field. Then the right-hand-side of the constraint

[6] Modulo details regarding the central charge c at the edge. $e^{2\pi i c/8}$ can be obtained from the topological spins, but not c itself.

(27) is modified and a non-trivial gauge field configuration is again obtained which is essentially equivalent to that obtained around a puncture. In the following subsections, we will discuss the Hilbert spaces of $SU(2)_k$ Chern-Simons theory, either on the n-punctured sphere or in the presence of non-dynamical sources. These discussions will enable us to compute the braiding and fusion matrices. The non-trivial quasiparticle of $SU(2)_1$ is actually Abelian so we do not discuss this 'trivial' case. The next case, $SU(2)_2$, is non-Abelian and may be relevant to the $\nu = 5/2$ fractional quantum Hall state. It can be understood in several different equivalent ways, which express its underlying free Majorana fermion structure. Quantum computation with Majorana fermions is described in Section IV.A. In the next section, we explain this structure from the perspective of a superconductor with $p+ip$ pairing symmetry. Although this description is very elegant, it cannot be generalized to higher k. Therefore, in the two sections after that, we describe two different approaches to solving $SU(2)_k$ Chern-Simons theory for general k. We recapitulate the case of $SU(2)_2$ in these other languages and also describe the case of $SU(2)_3$. The latter has quasiparticles in its spectrum which are Fibonacci anyons, a particularly beautiful non-Abelian anyonic structure which allows for universal topological quantum computation. It may also underlie the observed $\nu = 12/5$ fractonal quantum Hall state. More details of the Fibonacci theory are given in Sections IV.B.

B. Superconductors with $p + ip$ pairing symmetry

In this section, we will discuss the topological properties of a superconductor with $p + ip$ pairing symmetry following the method introduced by Read and Green (Read and Green, 2000). This is the most elementary way in which a non-Abelian topological state can emerge as the ground state of a many-body system. This non-Abelian topological state has several possible realizations in various two dimensional systems: $p + ip$ superconductors, such as Sr_2RuO_4 (although the non-Abelian quasiparticles are half-quantum vortices in this case (Das Sarma et al., 2006b)); $p + ip$ superfluids of cold atoms in optical traps (Gurarie et al., 2005; Tewari et al., 2007b), and the A-phase (especially the A_1 phase(Leggett, 1975; Volovik, 1994)) of ^{3}He films; and the Moore-Read Pfaffian quantum Hall state (Moore and Read, 1991). The last of these is a quantum Hall incarnation of this state: electrons at filling fraction $\nu = 1/2$ are equivalent to fermions in zero field interacting with an Abelian Chern-Simons gauge field. When the fermions pair and condense in a $p + ip$ superconducting state, the Pfaffian quantum Hall state forms (Greiter et al., 1992). Such a state can occur at $\frac{5}{2} = 2 + \frac{1}{2}$ if the lowest Landau level (of both spins) is filled and inert, and the first excited Landau level is half-filled.

Ordinarily, one makes a distinction between the fermionic quasiparticles (or Bogoliubov-De Gennes quasiparticles) of a superconductor and vortices in a superconductor. This is because, in terms of electron variables, the former are relatively simple while the latter are rather complicated. Furthermore, the energy and length scales associated with the two are very different in the weak-coupling limit. However, fermionic quasiparticles and vortices are really just different types of quasiparticle excitations in a superconductor – i.e. different types of localized disturbances above the ground state. Therefore, we will often refer to them both as simply quasiparticles and use the terms Bogoliubov-de Gennes or fermionic when referring to the former. In a $p + ip$ superconductor, the quasiparticles which exhibit non-Abelian statistics are flux $hc/2e$ vortices.

1. Vortices and Fermion Zero Modes

Let us suppose that we have a system of fully spin-polarized electrons in a superconducting state of $p_x + ip_y$ pairing symmetry. The mean field Hamiltonian for such a superconductor is,

$$H = \int \mathrm{d}\mathbf{r}\, \psi^\dagger(\mathbf{r}) h_0 \psi(\mathbf{r}) \tag{35}$$
$$+ \frac{1}{2}\int \mathrm{d}\mathbf{r}\, \mathrm{d}\mathbf{r}' \left\{ D^*(\mathbf{r},\mathbf{r}')\psi(\mathbf{r}')\psi(\mathbf{r}) + D(\mathbf{r},\mathbf{r}')\psi^\dagger(\mathbf{r})\psi^\dagger(\mathbf{r}') \right\}$$

with single-particle term $h_0 = -\frac{1}{2m}\nabla^2 - \mu$ and complex p-wave pairing function

$$D(\mathbf{r},\mathbf{r}') = \Delta\left(\frac{\mathbf{r}+\mathbf{r}'}{2}\right)(i\partial_{x'} - \partial_{y'})\delta(\mathbf{r}-\mathbf{r}'). \tag{36}$$

The dynamics of Δ is governed by a Landau-Ginzburg-type Hamiltonian and will be briefly discussed later. The quadratic Hamiltonian (36) may be diagonalized by solving the corresponding Bogoliubov-de Gennes equations (BdG) equations,

$$E\begin{pmatrix} u(\mathbf{r}) \\ v(\mathbf{r}) \end{pmatrix} = \tag{37}$$
$$\begin{pmatrix} -\mu(\mathbf{r}) & \frac{i}{2}\{\Delta(\mathbf{r}), \partial_x + i\partial_y\} \\ \frac{i}{2}\{\Delta^*(\mathbf{r}), \partial_x - i\partial_y\} & \mu(\mathbf{r}) \end{pmatrix}\begin{pmatrix} u(\mathbf{r}) \\ v(\mathbf{r}) \end{pmatrix},$$

The Hamiltonian then takes the form:

$$H = E_0 + \sum_E E\,\Gamma_E^\dagger \Gamma_E \tag{38}$$

where $\Gamma_E^\dagger \equiv \int dr \left[u_E(\mathbf{r})\psi(\mathbf{r}) + v_E(\mathbf{r})\psi^\dagger(\mathbf{r})\right]$ is the creation operator formed by the positive energy solutions of the Bogoliubov-de Gennes equations and E_0 is the ground state energy. For the ground state of the Hamiltonian (36) to be degenerate in the presence of several vortices (which are the most interesting quasiparticles in this theory) it is essential that the BdG equations have solutions with eigenvalue zero in this situation.

Before searching for zero eigenvalues of (38) in the presence of vortices, however, we focus on a uniform superconductor, where Δ is a constant. Read and Green (Read and Green, 2000) retain only the potential part of h_0, which for a uniform superconductor is a constant $-\mu$. With this simplification, a BdG eigenstate with momentum k has energy

$$E_k = \sqrt{\mu^2 + \Delta^2|k|^2} \tag{39}$$

The ground state of (36) is the celebrated BCS wave function, written here in an un-normalized form,

$$|\mathrm{g.s.}\rangle = \prod_{\mathbf{k}} \left(1 + \frac{v_{\mathbf{k}}}{u_{\mathbf{k}}} c^\dagger_{\mathbf{k}} c^\dagger_{-\mathbf{k}}\right) |\mathrm{vac}\rangle = e^{\sum_{\mathbf{k}} \frac{v_{\mathbf{k}}}{u_{\mathbf{k}}} c^\dagger_{\mathbf{k}} c^\dagger_{-\mathbf{k}}} |\mathrm{vac}\rangle \tag{40}$$

where

$$\begin{pmatrix} |u_{\mathbf{k}}|^2 \\ |v_{\mathbf{k}}|^2 \end{pmatrix} = \frac{1}{2}\left(1 \mp \frac{\mu}{\sqrt{\mu^2 + |\Delta k|^2}}\right) \tag{41}$$

are the BCS coherence factors. The wave function (40) describes a coherent state of an undetermined number of Cooper pairs, each in an internal state of angular momentum $\ell = -1$. Its projection onto a fixed even number of particles N is carried out by expanding the exponent in (40) to the $(N/2)^{\text{th}}$ order. When written in first quantized language, this wave function describes a properly anti-symmetrized wave function of $N/2$ Cooper-pairs, each in an internal state

$$g(\mathbf{r}) = \sum_{\mathbf{k}} \frac{v_{\mathbf{k}}}{u_{\mathbf{k}}} e^{i\mathbf{k}\mathbf{r}} \tag{42}$$

In first quantized form the multiparticle BCS wavefunction is then of the form of the Pfaffian of an antisymmetric matrix whose $i-j$ element is $g(\mathbf{r}_i - \mathbf{r}_j)$, an antisymmetrized product of pair wavefunctions

$$\begin{aligned} \Psi_{BCS} &= \mathrm{Pf}\left[g(\mathbf{r}_i - \mathbf{r}_j)\right] \\ &= \mathcal{A}\left[g(\mathbf{r}_1 - \mathbf{r}_2) g(\mathbf{r}_3 - \mathbf{r}_4) \ldots g(\mathbf{r}_{N-1} - \mathbf{r}_N)\right] \end{aligned} \tag{43}$$

with $\mathcal{A}$ being an antisymmetrization operator.

The function $g(\mathbf{r})$ depends crucially on the sign of μ, since the small k behavior of $v_{\mathbf{k}}/u_{\mathbf{k}}$ depends on that sign. When $\mu > 0$, we have $g(r) = 1/(x+iy)$ in the long distance limit (Read and Green, 2000). If we assume this form holds for all distances, the Pfaffian wave function obtained is identical to the Moore-Read form discussed below in connection with the Ising model and the $\nu = 5/2$ quantum Hall state in section III.D (see Eqs. **??**). The slow decay of $g(r)$ implies a weak Cooper pairing. (But it does not imply that the state is gapless. One can verify that electron Green functions all decay exponentially for any non-zero μ.) When $\mu < 0$ the function $g(r)$ decays much more rapidly with r, generically in an exponential way, such that the Cooper pairs are strongly bound. Furthermore, there is a topological distinction between the $\mu > 0$ and $\mu < 0$ phases. The distinction, which is discussed in detail in (Read and Green, 2000), implies that, despite the fact that both states are superconducting, the $\mu > 0$ and $\mu < 0$ states must be separated by a phase transition. (In the analogous quantum Hall state, both states are characterized by the same Hall conductivity but are separated by a phase transition, and are distinguished by their thermal Hall conductivities(Read and Green, 2000)) Indeed, from (39) we see that the gap vanishes for a uniform $p+ip$ superconductor with $\mu = 0$. The low-energy BdG eigenstates at this second-order phase transition point form a Dirac cone.

For every solution (u, v) of the BdG equations with energy E, there is a solution (v^*, u^*) of energy $-E$. A solution with $u = v^*$ therefore has energy zero. We will soon be considering situations in which there are multiple zero energy solutions (u_i, u_i^*), $i = 1, 2, \ldots$. If we denote the corresponding operators by γ_i (see eq. 47 below), then they satisfy:

$$\gamma_i^\dagger = \gamma_i \tag{44}$$

Eq. (44) is the definition of a Majorana fermion operator.

Let us now consider the BdG equations in the presence of vortices when the bulk of the superconductor is in the $\mu > 0$ phase. As usual, a vortex is characterized by a point of vanishing Δ, and a 2π-winding of the phase of Δ around that point. In principle we should, then, solve the BdG equations in the presence of such a non-uniform Δ. However, we can, instead, solve them in the presence of a non-uniform μ, which is much simpler. All that we really need is to make the core of the superconductor topologically distinct from the bulk – i.e. a puncture in the superconductivity. Making $\mu < 0$ in the core is just as good as taking Δ to zero, as far as topological properties are concerned. Therefore, we associate the core of the vortex with a region of $\mu < 0$, whereas the bulk is at $\mu > 0$. Thus, there is a $\mu = 0$ line encircling the vortex core. This line is an internal edge of the system. We will consider the dynamics of edge excitations in more detail in section III.E, but here we will be content to show that a zero energy mode is among them.

The simplest situation to consider is that of azymuthal symmetry, with the polar coordinates denoted by r and θ. Imagine the vortex core to be at the origin, so that $\Delta(r,\theta) = |\Delta(r)|e^{i\theta + i\Omega}$. Here Ω is the phase of the order parameter along the $\theta = 0$ line, a phase which will play an important role later in our discussion. Assume that the $\mu = 0$ line is the circle $r = r_0$, and write

$$\mu(r) = \Delta\, h(r), \tag{45}$$

with $h(r)$ large and positive for large r, and $h(r) < 0$ for $r < r_0$; therefore, the electron density will vanish for $r \ll r_0$. Such a potential defines an edge at $r = r_0$. There are low-energy eigenstates of the BdG Hamiltonian which are spatially localized near $r = 0$ and are exponentially decaying for $r \to \infty$:

$$\phi_E^{edge}(r,\theta) = e^{i\ell\theta} e^{-\int_0^r h(r')dr'} \begin{pmatrix} e^{-i\theta/2} \\ e^{i\theta/2} \end{pmatrix}, \tag{46}$$

The spinor on the right-hand-side points in a direction in pseudospin space which is tangent to the $r = r_0$ circle at θ. This wavefunction describes a chiral wave propagating around the edge, with angular momentum ℓ and energy $E = \Delta\ell/r_0$. Since the flux is an odd multiple of $hc/2e$, the Bogoliubov quasiparticle (46) must be anti-periodic as it goes around the vortex. However, the spinor on the right-hand-side of (46) is also anti-periodic. Therefore, the angular momentum ℓ must be an integer, $\ell \in \mathbb{Z}$. Consequently, a flux $hc/2e$ vortex has an $\ell = 0$ solution, with energy $E = 0$. (Conversely, if the flux through the vortex were an even multiple of $hc/2e$, ℓ would be a half-integer, $\ell \in \mathbb{Z} + \frac{1}{2}$, and there would be no zero-mode.) The operator corresponding to this zero mode, which we will

call γ, can be written in the form:

$$\gamma = \frac{1}{\sqrt{2}} \int dr \, \left[F(\mathbf{r})\, e^{-\frac{i}{2}\Omega} \psi(\mathbf{r}) + F^*(\mathbf{r})\, e^{\frac{i}{2}\Omega} \psi^\dagger(\mathbf{r}) \right] \quad (47)$$

Here, $F(\mathbf{r}) = e^{-\int_0^r h(r')dr'} e^{-i\theta/2}$. Since each γ is an equal superposition of electron and hole, it is overall a chargeless, neutral fermion operator

When there are several well separated vortices at positions $\mathbf{R}_i$, the gap function near the i^{th} vortex takes the form $\Delta(\mathbf{r}) = |\Delta(\mathbf{r})| \exp(i\theta_i + i\Omega_i)$, with $\theta_i = \arg(\mathbf{r} - \mathbf{R_i})$ and $\Omega_i = \sum_{j \neq i} \arg((\mathbf{R_j} - \mathbf{R}_i))$. There is then one zero energy solution per vortex. Each zero energy solution γ_i is localized near the core of its vortex at $\mathbf{R_i}$, but the phase Ω_i that replaces Ω in (47) depends on the position of all vortices. Moreover, the dependence of the Majorana operators γ_i on the positions $\mathbf{R_i}$ is not single valued.

While for any $E \neq 0$ the operators $\Gamma_E^\dagger, \Gamma_E$ are conventional fermionic creation and annihilation operators, the γ_i's are not. In particular, for $E \neq 0$ we have $(\Gamma_E^\dagger)^2 = \Gamma_E^2 = 0$, but the zero energy operators follow (with a convenient choice of normalization) $\gamma_i^2 = 1$. The two types of fermion operator share the property of mutual anti-commutation, i.e., the γ's satisfy $\{\gamma_i, \gamma_j\} = 2\delta_{ij}$.

2. Topological Properties of $p + ip$ Superconductors

The existence of the γ_i's implies a degeneracy of the ground state. The counting of the number of degenerate ground states should be done with care. A pair of conventional fermionic creation and annihilation operators span a two dimensional Hilbert space, since their square vanishes. This is not true for a Majorana operator. Thus, to count the degeneracy of the ground state when $2N_0$ vortices are present, we construct "conventional" complex (Dirac) fermionic creation and annihilation operators,

$$\psi_i = (\gamma_i + i\gamma_{N_0+i})/2 \quad (48)$$

$$\psi_i^\dagger = (\gamma_i - i\gamma_{N_0+i})/2 \quad (49)$$

These operators satisfy $\psi_i^2 = \left(\psi_i^\dagger\right)^2 = 0$ and thus span a two-dimensional subspace of degenerate ground states associated with these operators. Over all, then, the system has 2^{N_0} degenerate ground states. If the fermion number is fixed to be even or odd, then the degeneracy is 2^{N_0-1}. Therefore, the quantum dimension of a vortex is $d_{\text{vort}} = \sqrt{2}$ or, in the notation introduced in Sec. II.A.1 for Ising anyons, $d_\sigma = \sqrt{2}$.

For any two vortices i and j, we can associate a two state system. If we work in the basis of $i\gamma_i\gamma_j$ eigenstates, then $i\gamma_i\gamma_j$ acts as σ_z with eigenvalues ± 1, while γ_i and γ_j act as σ_x and σ_y. (However, it is important to keep in mind that Majorana fermions γ_k, γ_l anti-commute with γ_i, γ_j, *unlike* operators associated with different spins, which commute.) The two eigenvalues $i\gamma_i\gamma_j = \mp 1$ are the two fusion channels of two fermions. If we form the Dirac fermion $\psi = (\gamma_i + i\gamma_j)/2$, then the two $i\gamma_i\gamma_j$ eigenstates have $\psi^\dagger\psi = 0, 1$. Therefore, we will call these fusion channels $\mathbf{1}$ and ψ. (One is then tempted to refer to the state for which $\psi^\dagger\psi = 1$ as a "filled fermion", and to the $\psi^\dagger\psi = 0$ state as an empty fermion. Note however that the eigenvalue of $\psi^\dagger\psi$ has no bearing on the occupation of single-particle states.)

Of course, the pairing of vortices to form Dirac fermions is arbitrary. A given pairing defines a basis, but one can transform to a basis associated with another pairing. Consider four vortices with corresponding zero modes γ_1, γ_2, γ_3, γ_4. The F-matrix transforms states from the basis in which $i\gamma_1\gamma_2$ and $i\gamma_3\gamma_4$ are diagonal to the basis in which $i\gamma_1\gamma_4$ and $i\gamma_2\gamma_3$ are diagonal. Since $i\gamma_1\gamma_4$ acts as σ_x on an $i\gamma_1\gamma_2$ eigenstate, the F-matrix is just the basis change from the σ_z basis to the σ_x basis:

$$[F_\sigma^{\sigma\sigma\sigma}] = \frac{1}{\sqrt{2}} \begin{pmatrix} 1 & 1 \\ 1 & -1 \end{pmatrix} \quad (50)$$

We will refer to this type of non-Abelian anyons by the name 'Ising anyons'; they are the model introduced in Section II.A.1. The reason for the name will be explained in Section III.E.

In a compact geometry, there must be an even number of vortices (since a vortex carries half a flux quantum, and the number of flux quanta penetrating a compact surface must be integer). In a non-compact geometry, if the number of vortices is odd, the edge has a zero energy state of its own, as we show in Section III.E.

Now, let us examine what happens to the Majorana operators and to the ground states as vortices move. The positions of the vortices are parameters in the Hamiltonian (36). When they vary adiabatically in time, the operators γ_i vary adiabatically in time. In principle, there are two sources for this variation - the explicit dependence of γ_i on the positions and the Berry phase associated with the motion. The choice of phases taken at (47) is such that the Berry phase vanishes, and the entire time dependence is explicit. The non-single-valuedness of the phases in (47) implies then that a change of 2π in Ω, which takes place when one vortex encircles another, does not leave the state unchanged.

As vortices adiabatically traverse trajectories that start and end in the same set of positions (Ivanov, 2001; Stern et al., 2004), there is a unitary transformation U within the subspace of ground states that takes the initial state $|\psi(t=0)\rangle$ to the final one $|\psi(t=T)\rangle$,

$$|\psi(t=T)\rangle = U|\psi(t=0)\rangle. \quad (51)$$

Correspondingly, the time evolution of the operators γ_i is

$$\gamma_i(t=T) = U\gamma_i(t=0)U^\dagger. \quad (52)$$

By reading the time evolution of γ_i from their explicit form (47) we can determine U up to a phase. Indeed, one expects this Abelian phase to depend not only on the topology of the trajectory but also on its geometry, especially in the analogous quantum Hall case, where there is an Aharonov-Bohm phase accumulated as a result of the charge carried by the quasiparticle.

When vortex i encircles vortex $i+1$, the unitary transformation is simple: both γ_i and γ_{i+1} are multiplied by -1, with

all other operators unchanged. This is a consequence of the fact that when the order parameter changes by a phase factor 2π, fermionic operators change by a phase π. Exchange trajectories, in which some of the vortices trade places, are more complicated, since the phase changes of Ω_k associated with a particular trajectory do not only depend on the winding numbers, but also on the details of the trajectory and on the precise definition of the cut of the function $\arg(\mathbf{r})$ where its value jumps by 2π.

The simplest example is the interchange of two vortices. Inevitably, one of the vortices crosses the branch cut line of the other vortex. We can place the branch cuts so that a counterclockwise exchange of vortices 1 and 2 transforms $c_1 \to c_2$ and $c_2 \to -c_1$ while a clockwise exchange transforms $c_1 \to -c_2$ and $c_2 \to c_1$ (Ivanov, 2001).

This may be summarized by writing the representation matrices for the braid group generators (Ivanov, 2001; Nayak and Wilczek, 1996):

$$\rho(\sigma_i) = e^{i\theta}\, e^{-\frac{\pi}{4}\gamma_i\gamma_{i+1}} \tag{53}$$

where θ is the Abelian part of the transformation. The two eigenvalues $i\gamma_i\gamma_{i+1} = \mp 1$ are the two fusion channels $\mathbf{1}$ and ψ of a pair of vortices. From (53), we see that the R-matrices satisfy $R^{\sigma\sigma}_{\psi} = i\, R^{\sigma\sigma}_{\mathbf{1}}$ (i.e., the phase of taking two σ particles around each other differ by i depending on whether they fuse to ψ or $\mathbf{1}$). It is difficult to obtain the Abelian part of the phase using the methods of this section, but we will derive it by other methods in Sections III.C and III.D. The non-Abelian part of (53), i.e. the second factor on the right-hand-side, is the same as a $\pi/2$ rotation in the spinor representation of SO(2n) (see Nayak and Wilczek, 1996 for details). The fact that braiding only enacts $\pi/2$ rotations is the reason why this type of non-Abelian anyon does not enable universal topological quantum computation, as we discuss further in section IV.

According to (53), if a system starts in a ground state $|\mathrm{gs}_\alpha\rangle$ and vortex j winds around vortex $j+1$, the system's final state is $\gamma_j\gamma_{j+1}\,|\mathrm{gs}_\alpha\rangle$. Writing this out in terms of the original electron operators, we have

$$\left(c_j e^{\frac{i}{2}\Omega_j} + c_j^\dagger e^{-\frac{i}{2}\Omega_j}\right)\left(c_{j+1} e^{\frac{i}{2}\Omega_{j+1}} + c_{j+1}^\dagger e^{-\frac{i}{2}\Omega_{j+1}}\right)|\mathrm{gs}_\alpha\rangle\,, \tag{54}$$

where $c_j^{(\dagger)}$ annihilates a particle in the state $F(r-R_j)$ and $c_{j+1}^{(\dagger)}$ creates a particle in the state $(F(r-R_{j+1}))$ localized very close to the cores of the jth and $(j+1)$th vortex, respectively. Eq. (54) seemingly implies that the motion of the jth vortex around the $(j+1)$th vortex affects the occupations of states very close to the cores of the two vortices. This is in contrast, however, to the derivation leading to Eq. (54), which explicitly assumes that vortices are kept far enough from one another so that tunneling between vortex cores may be disregarded.

This seeming contradiction is analyzed in detail in Stern et al., 2004, where it is shown that the unitary transformation (54) does not affect the occupation of the core states of the $j, j+1$ vortices, because all ground states are composed of superpositions in which the core states have a probability of one-half to be occupied and one-half to be empty. The unitary transformation within the ground state subspace does not change that probability. Rather, they affect phases in the superpositions. Using this point of view it is then possible to show that two ingredients are essential for the non-Abelian statistics of the vortices. The first is the *quantum entanglement* of the occupation of states near the cores of distant vortices. The second ingredient is familiar from (Abelian) fractional statistics: the *geometric phase* accumulated by a vortex traversing a closed loop.

Therefore, we conclude that, for $p-$wave superconductors, the existence of zero-energy intra-vortex modes leads, first, to a multitude of ground states, and, second, to a particle-hole symmetric occupation of the vortex cores in all ground states. When represented in occupation-number basis, a ground state is a superposition which has equal probability for the vortex core being empty or occupied by one fermion. When a vortex traverses a trajectory that encircles another vortex, the phase it accumulates depends again on the number of fluid particles it encircles. Since a fluid particle is, in this case, a Cooper pair, the occupation of a vortex core by a fermion, half a pair, leads to an accumulation of a phase of π relative to the case when the core is empty. And since the ground state is a superposition with equal weights for the two possibilities, the relative phase of π introduced by the encircling might in this case transform the system from one ground state to another.

Now consider the ground state degeneracy of a $p+ip$ superconductor on the torus. Let us define, following Oshikawa et al., 2007 (see also Chung and Stone, 2007), the operators A_1, A_2 which create a pair of Bogoliubov-de Gennes quasiparticles, take one around the meridian or longitude of the torus, respectively, and annihilate them again. We then define B_1, B_2 as operators which create a vortex-antivortex pair, take the vortex around the meridian or longitude of the torus, respectively, and annihilate them. B_1 increases the flux through the hole encircled by the longitude of the torus by one half of a flux quantum while B_2 does the same for the other hole. These operators satisfy the commutation relations $[A_1, A_2] = 0$ and $A_1B_2 = -B_2A_1$, $A_2B_1 = -B_1A_2$. We can construct a multiplet of ground states as follows. Since A_1 and A_2 commute and square to 1, we can label states by their A_1 and A_2 eigenvalues ± 1. Let $|1,1\rangle$ be the state with both eigenvalues equal to 1, i.e. $A_1|1,1\rangle = A_2|1,1\rangle = |1,1\rangle$. Then $B_1|1,1\rangle = |1,-1\rangle$ and $B_2|1,1\rangle = |-1,1\rangle$. Suppose we now try to apply B_2 to $B_1|1,1\rangle = |1,-1\rangle$. This will create a vortex-antivortex pair; the Majorana zero modes, γ_a, γ_b associated with the vortex and anti-vortex will be in the state $|0\rangle$ defined by $(\gamma_a + i\gamma_b)\,|0\rangle = 0$. When the vortex is taken around the longitude of the torus, its Majorana mode will be multiplied by -1: $\gamma_a \to -\gamma_a$. Now, the vortex-antivortex pair will no longer be in the state $|0\rangle$, but will instead be in the state $|1\rangle$ defined by $(\gamma_a - i\gamma_b)\,|1\rangle = 0$. Consequently, the vortex-antivortex pair can no longer annihilate to the vacuum. When they fuse, a fermion is left over. Therefore, $B_2B_1|1,1\rangle$ does not give a new ground state (and, by a similar argument, neither does $B_1B_2|1,1\rangle$). Consequently, a $p+ip$ superconductor has 'only' three ground states on the torus. A basis in which B_1 is diagonal is given by: $(|1,1\rangle \pm |1,-1\rangle)/\sqrt{2}$, with eigenvalue ± 1, and $|-1,1\rangle$, with eigenvalue 0 (since there is zero amplitude for $B_1|-1,1\rangle$ to be in the ground state subspace).

They can be identified with the states $|1_m\rangle$, $|\psi_m\rangle$, and $|\sigma_m\rangle$ in Ising anyon language. Meanwhile, B_2 is diagonal in the basis $(|1,1\rangle \pm |-1,1\rangle)/\sqrt{2}$, $|1,-1\rangle$. By changing from one basis to the other, we find the S-matrix given in the previous subsection follows.

The essential feature of chiral p-wave superconductors is that they have Majorana fermion excitations which have zero energy modes at vortices (and gapless excitations at the edge of the system, see section III.E). The Majorana character is a result of the superconductivity, which mixes particle and hole states; the zero modes and gapless edge excitations result from the chirality. Majorana fermions arise in a completely different way in the Kitaev honeycomb lattice model (Kitaev, 2006):

$$H = -J_x \sum_{x-\text{links}} \sigma_j^x \sigma_j^x - J_y \sum_{y-\text{links}} \sigma_j^y \sigma_j^y - J_z \sum_{z-\text{links}} \sigma_j^x \sigma_j^z \tag{55}$$

where the z-links are the vertical links on the honeycomb lattice, and the x and y links are at angles $\pm\pi/3$ from the vertical. The spins can be represented by Majorana fermions b^x, b^y, b^z, and c, according to $\sigma_j^x = ib_j^x c_j$, $\sigma_j^x = ib_j^y c_j$, $\sigma_j^x = ib_j^z c_j$ so long as the constraint $b_j^x b_j^y b_j^z c_j = 1$ is satisfied. Then, the Hamiltonian is quartic in Majorana fermion operators, but the operators $b_j^x b_k^x$, $b_j^y b_k^y$, $b_j^z b_k^z$ commute with the Hamiltonian. Therefore, we can take their eigenvalues as parameters $u_{jk} = b_j^\alpha b_k^\alpha$, with $\alpha = x, y$, or z appropriate to the jk link. These parameters can be varied to minimize the Hamiltonian, which just describes Majorana fermions hopping on the honeycomb lattice:

$$H = \frac{i}{4} \sum_{jk} t_{jk} c_j c_k \tag{56}$$

where $t_{jk} = 2J_\alpha u_{jk}$ for nearest neighbor j, k and zero otherwise. For different values of the J_αs, the t_{jk}'s take different values. The topological properties of the corresponding c_j bands are encapsulated by their Chern number (Kitaev, 2006). For a certain range of J_αs, a P, T-violating perturbation gives the Majorana fermions a gap in such a way as to support zero modes on vortex-like excitations (plaquettes on which one of the u_{jk}s is reversed in sign). These excitations are identical in topological character to the vortices of a $p+ip$ superconductor discussed above.

C. Chern-Simons Effective Field Theories, the Jones Polynomial, and Non-Abelian Topological Phases

1. Chern-Simons Theory and Link Invariants

In the previous subsection, we have seen an extremely simple and transparent formulation of the quasiparticle braiding properties of a particular non-Abelian topological state which, as we will see later in this section, is equivalent to SU(2)$_2$ Chern-Simons theory. It describes the multi-quasiparticle Hilbert space and the action of braiding operations in terms of free fermions. Most non-Abelian topological states are not so simple, however. In particular, SU(2)$_k$ Chern-Simons theory for $k > 2$ does not have a free fermion or boson description.[7] Therefore, in the next two subsections, we discuss these field theories using more general methods.

Even though its Hamiltonian vanishes and it has no local degrees of freedom, solving Chern-Simons theory is still a non-trivial matter. The reason is that it is difficult in a non-Abelian gauge theory to disentangle the physical topological degrees of freedom from the unphysical local gauge degrees of freedom. There are essentially two approaches. Each has its advantages, and we will describe them both. One is to work entirely with gauge-invariant quantities and derive rules governing them; this is the route which we pursue in this subsection. The second is to pick a gauge and simply calculate within this gauge, which we do in the next subsection (III.D).

Consider SU(2)$_k$ non-Abelian Chern-Simons theory:

$$S_{CS}[a] = \frac{k}{4\pi} \int_{\mathcal{M}} \text{tr}\left(a \wedge da + \frac{2}{3} a \wedge a \wedge a \right) \tag{57}$$

We modify the action by the addition of sources, $j^{\mu \underline{a}}$, according to $\mathcal{L} \to \mathcal{L} + \text{tr}\,(j \cdot a)$. We take the sources to be a set of particles on prescribed classical trajectories. The i^{th} particle carries the spin j_i representation of SU(2). As we saw in subsection III.A, there are only $k+1$ allowed representations; later in this subsection, we will see that if we give a particle a higher spin representation than $j = k/2$, then the amplitude will vanish identically. Therefore, j_i must be in allowed set of $k+1$ possibilities: $0, \frac{1}{2}, \ldots, \frac{k}{2}$. The functional integral in the presence of these sources can be written in terms of Wilson loops, $W_{\gamma_i, j_i}[a]$, which are defined as follows. The holonomy $U_{\gamma,j}[a]$ is an $SU(2)$ matrix associated with a curve γ. It is defined as the path-ordered exponential integral of the gauge field along the path γ:

$$\begin{aligned} U_{\gamma,j}[a] &\equiv \mathcal{P} e^{i \oint_\gamma \mathbf{a}^{\underline{c}} T^{\underline{c}} \cdot d\mathbf{l}} \\ &= \sum_{n=0}^{\infty} i^n \int_0^{2\pi} ds_1 \int_0^{s_1} ds_2 \ldots \int_0^{s_{n-1}} ds_n \Big[\dot{\gamma}(s_1) \cdot \mathbf{a}^{\underline{a}_1}(\gamma(s_1)) T^{\underline{a}_1} \ldots \\ &\qquad \dot{\gamma}(s_n) \cdot \mathbf{a}^{\underline{a}_n}(\gamma(s_n)) T^{\underline{a}_n} \Big] \end{aligned} \tag{58}$$

where $\mathcal{P}$ is the path-ordering symbol. The Lie algebra generators $T^{\underline{a}}$ are taken in the spin j representation. $\vec{\gamma}(s)$, $s \in [0, 2\pi]$ is a parametrization of γ; the holonomy is clearly independent of the parametrization. The Wilson loop is the trace of the holonomy:

$$W_{\gamma,j}[a] = \text{tr}\,(U_{\gamma,j}[a]) \tag{59}$$

Let us consider the simplest case, in which the source is a quasiparticle-quasihole pair of type j which is created out of the ground state, propagated for a period of time, and then

[7] It is an open question whether there is an alternative description of an SU(2)$_k$ topological phase with $k > 2$ in terms of fermions or bosons which is similar to the $p + ip$ chiral superconductor formulation of SU(2)$_2$.

annihilated, returning the system to the ground state. The amplitude for such a process is given by:

$$\langle 0|0\rangle_{\gamma,j} = \int \mathcal{D}a\, e^{iS_{CS}[a]}\, W_{\gamma,j}[a] \tag{60}$$

Here, γ is the spacetime loop formed by the trajectory of the quasiparticle-quasihole pair. The Wilson loop was introduced as an order parameter for confinement in a gauge theory because this amplitude roughly measures the force between the quasiparticle and the quasihole. If they were to interact with a confining force $V(r) \sim r$, then the logarithm of this amplitude would be proportional to the the area of the loop; if they were to have a short-ranged interaction, it would be proportional to the perimeter of the loop. However, Chern-Simons theory is independent of a metric, so the amplitude cannot depend on any length scales. It must simply be a constant. For $j = 1/2$, we will call this constant d. As the notation implies, it is, in fact, the quantum dimension of a $j = 1/2$ particle. As we will see below, d can be determined in terms of the level k, and the quantum dimensions of higher spin particles can be expressed in terms of d.

We can also consider the amplitude for two pairs of quasiparticles to be created out of the ground state, propagated for some time, and then annihilated, returning the system to the ground state:

$$\langle 0|0\rangle_{\gamma_1,j_1;\gamma_2,j_2} = \int \mathcal{D}a\, e^{iS_{CS}[a]}\, W_{\gamma,j}[a]\, W_{\gamma',j'}[a] \tag{61}$$

This amplitude can take different values depending on how γ and γ' are linked as in Fig. 4a vs 4b. If the curves are unlinked the integral must give d^2, but when they are linked the value can be nontrivial. In a similar way, we can formulate the amplitudes for an arbitrary number of sources.

It is useful to think about the history in figure 4a as a two step process: from $t = -\infty$ to $t = 0$ and from $t = 0$ to $t = \infty$. (The two pairs are created at some time $t < 0$ and annihilated at some time $t > 0$.) At $t = 0^-$, the system is in a four-quasiparticle state. (Quasiparticles and quasiholes are topologically equivalent if G =SU(2), so we will use 'quasiparticle' to refer to both.) Let us call this state ψ:

$$\psi[A] = \int_{a(\mathbf{x},0)=A(\mathbf{x})} \mathcal{D}a(\mathbf{x},t)\, W_{\gamma_-,j}[a]\, W_{\gamma'_-,j'}[a] \times e^{\int_{-\infty}^{0} dt \int d^2x\, \mathcal{L}_{\rm CS}} \tag{62}$$

where γ_- and γ'_- are the arcs given by $\gamma(t)$ and $\gamma'(t)$ for $t < 0$. $A(\mathbf{x})$ is the value of the gauge field on the $t = 0$ spatial slice; the wavefunctional $\psi[A]$ assigns an amplitude to every spatial gauge field configuration. For G=SU(2) and $k > 1$, there are actually two different four-quasiparticle states: if particles 1 and 2 fuse to the identity field $j = 0$, then particles 3 and 4 must as well; if particles 1 and 2 fuse to $j = 1$, then particles 3 and 4 must as well. These are the only possibilities. (For $k = 1$, fusion to $j = 1$ is not possible.) Which one the system is in depends on how the trajectories of the four quasiparticles are intertwined. Although quasiparticles 1 and 2 were created as a pair from the vacuum, quasiparticle 2 braided with quasiparticle 3, so 1 and 2 may no longer fuse to the vacuum. In just a moment, we will see an example of a different four-quasiparticle state.

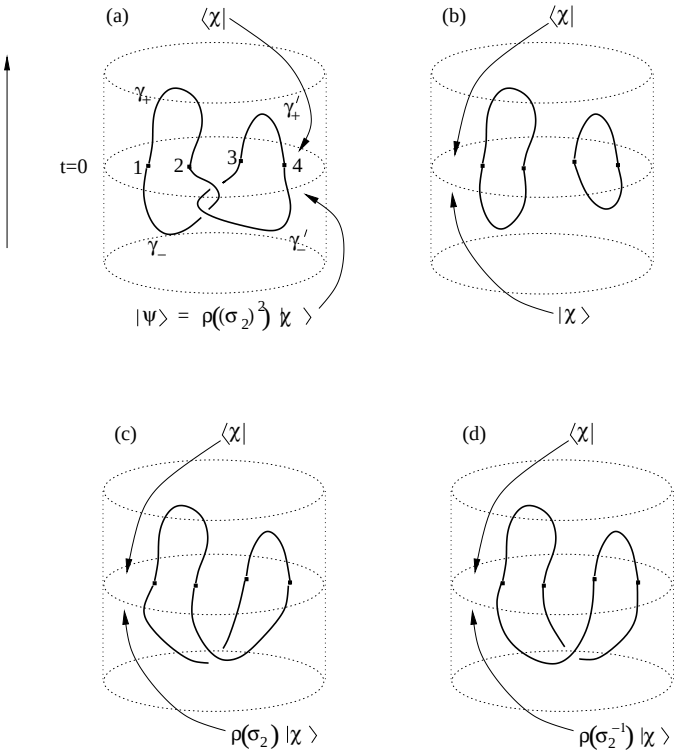

FIG. 4 The functional integrals which give (a) $\langle\chi|\rho(\sigma_2^2)\,|\chi\rangle$ (b) $\langle\chi|\chi\rangle$, (c) $\langle\chi|\rho(\sigma_2)\,|\chi\rangle$, (d) $\langle\chi|\rho(\sigma_2^{-1})\,|\chi\rangle$.

We now interpret the $t = 0$ to $t = \infty$ history as the conjugate of a $t = -\infty$ to $t = 0$ history. In other words, it gives us a four quasiparticle bra rather than a four quasiparticle ket:

$$\chi^*[A] = \int_{a(\mathbf{x},0)=A(\mathbf{x})} \mathcal{D}a(\mathbf{x},t)\, W_{\gamma_+,j}[a]\, W_{\gamma'_+,j'}[a] \times e^{\int_{0}^{\infty} dt \int d^2x\, \mathcal{L}_{\rm CS}} \tag{63}$$

In the state $|\chi\rangle$, quasiparticles 1 and 2 fuse to form the trivial quasiparticle, as do quasiparticles 3 and 4. Then we can interpret the functional integral from $t = -\infty$ to $t = \infty$ as the matrix element between the bra and the ket:

$$\langle\chi|\psi\rangle = \int \mathcal{D}a\, e^{iS_{CS}[a]}\, W_{\gamma_1,j_1}[a]\, W_{\gamma_2,j_2}[a] \tag{64}$$

Now, observe that $|\psi\rangle$ is obtained from $|\chi\rangle$ by taking quasiparticle 2 around quasiparticle 3, i.e. by exchanging quasiparticles 2 and 3 twice, $|\psi\rangle = \rho(\sigma_2^2)\,|\chi\rangle$. Hence,

$$\langle\chi|\rho(\sigma_2^2)\,|\chi\rangle = \int \mathcal{D}a\, e^{iS_{CS}[a]}\, W_{\gamma_1,j_1}[a]\, W_{\gamma_2,j_2}[a] \tag{65}$$

In this way, we can compute the entries of the braiding matrices $\rho(\sigma_i)$ by computing functional integrals such as the one on the right-hand-side of (65). Note that we should normalize the state $|\chi\rangle$ by computing the figure 4b, which gives its matrix element with itself.

Consider, now, the state $\rho(\sigma_2)\,|\chi\rangle$, in which particles 2 and 3 are exchanged just once. It is depicted in figure 4c. Similarly, the state $\rho\big(\sigma_2^{-1}\big)\,|\psi\rangle$ is depicted in figure 4d. From the figure, we see that

$$\langle\chi|\rho(\sigma_2)\,|\chi\rangle \;=\; d \tag{66}$$
$$\langle\chi|\rho\big(\sigma_2^{-1}\big)\,|\chi\rangle \;=\; d \tag{67}$$

since both histories contain just a single unknotted loop. Meanwhile,

$$\langle\chi|\chi\rangle = d^2 \tag{68}$$

Since the four-quasiparticle Hilbert space is two-dimensional, $\rho(\sigma_2)$ has two eigenvalues, λ_1, λ_2, so that

$$\rho(\sigma) - (\lambda_1+\lambda_2) + \lambda_1\lambda_2\rho\big(\sigma^{-1}\big) = 0 \tag{69}$$

Taking the expectation value in the state $|\chi\rangle$, we find:

$$d - (\lambda_1+\lambda_2)\,d^2 + \lambda_1\lambda_2 d = 0 \tag{70}$$

so that

$$d = \frac{1+\lambda_1\lambda_2}{\lambda_1+\lambda_2} \tag{71}$$

Since the braiding matrix is unitary, λ_1 and λ_2 are phases. The overall phase is unimportant for quantum computation, so we really need only a single number. In fact, this number can be obtained from self-consistency conditions (Freedman et al., 2004). However, the details of the computation of λ_1, λ_2 within is technical and requires a careful discussion of framing; the result is (Witten, 1989) that $\lambda_1 = -e^{-3\pi i/2(k+2)}$, $\lambda_2 = e^{\pi i/2(k+2)}$. These eigenvalues are simply $R_0^{\frac{1}{2},\frac{1}{2}} = \lambda_1$, $R_1^{\frac{1}{2},\frac{1}{2}} = \lambda_2$. Consequently,

$$d = 2\,\cos\left(\frac{\pi}{k+2}\right) \tag{72}$$

and

$$q^{-1/2}\rho(\sigma_i) - q^{1/2}\rho\big(\sigma_i^{-1}\big) = q - q^{-1} \tag{73}$$

where $q = -e^{\pi i/(k+2)}$ (see Fig. 18). Since this operator equation applies regardless of the state to which it is applied, we can apply it locally to any given part of a knot diagram to relate the amplitude to the amplitude for topologically simpler processes, as we will see below (Kauffman, 2001). This is an example of a *skein relation*; in this case, it is the skein relation which defines the Jones polynomial. In arriving at this skein relation, we are retracing the connection between Wilson loops in Chern-Simons theory and knot invariants which was made in the remarkable paper (Witten, 1989). In this paper, Witten showed that correlation functions of Wilson loop operators in SU(2)$_k$ Chern-Simons theory are equal to corresponding evaluations of the Jones polynomial, which is a topological invariant of knot theory (Jones, 1985):

$$\int \mathcal{D}a\, W_{\gamma_1,\frac{1}{2}}[a]\ldots W_{\gamma_n,\frac{1}{2}}[a]\, e^{iS_{CS}[a]} = V_L(q) \tag{74}$$

$V_L(q)$ is the Jones polynomial associated with the link $L = \gamma_1\cup\ldots\cup\gamma_n$, evaluated at $q = -e^{\pi i/(k+2)}$ using the skein relation (73). Note that we assume here that all of the quasiparticles transform under the $j=\frac{1}{2}$ representation of $SU(2)$. The other quasiparticle types can be obtained through the fusion of several $j = 1/2$ quasiparticles, as we will discuss below in Section III.C.2.

2. Combinatorial Evaluation of Link Invariants and Quasiparticle Properties

The Jones polynomial (Jones, 1985) $V_L(q)$ is a formal Laurent series in a variable q which is associated to a link $L = \gamma_1\cup\ldots\cup\gamma_n$. It can be computed recursively using (73). We will illustrate how this is done by showing how to use a skein relation to compute a related quantity called the Kauffman bracket $K_L(q)$ (Kauffman, 1987), which differs from the Jones polynomial by a normalization:

$$V_L(q) = \frac{1}{d}\,(-q^{3/2})^{w(L)}\,K_L(q) \tag{75}$$

where $w(L)$ is the writhe of the link. (The Jones polynomial is defined for an oriented link. Given an orientation, each crossing can be assigned a sign ±1; the writhe is the sum over all crossings of these signs.) The link L embedded in three-dimensional space (or, rather, three-dimensional spacetime in our case) is projected onto the plane. This can be done faithfully if we are careful to mark overcrossings and undercrossings. Such a projection is not unique, but the same Kauffman bracket is obtained for all possible $2D$ projections of a knot (we will see an example of this below). An unknotted loop ◯ is given the value $K_{\bigcirc}(q) = d \equiv -q - q^{-1} = 2\cos\pi/(k+2)$. For notational simplicity, when we draw a knot, we actually mean the Kauffman bracket associated to this knot. Hence, we write

$$= d \tag{76}$$

The disjoint union of n unknotted loops is assigned the value d^n.

The Kauffman bracket for any given knot can be obtained recursively by repeated application of the following skein relation which relates it with the Kauffman brackets for two knots both of which have one fewer crossing according to the rule:

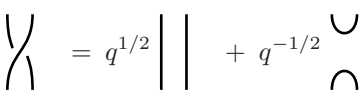

$$= q^{1/2} \quad + \; q^{-1/2} \tag{77}$$

With this rule, we can eliminate all crossings. At this point, we are left with a linear combination of the Kauffman brackets for various disjoint unions of unknotted loops. Adding up these contributions of the form d^m with their appropriate coefficients coming from the recursion relation (77), we obtain the Kauffman bracket for the knot with which we started.

Let us see how this works with a simple example. First, consider the two arcs which cross twice in figure 5. We will

assume that these arcs continue in some arbitrary way and form closed loops. By applying the Kauffman bracket recursion relation in figure 5, we see that these arcs can be replaced by two arcs which do not cross. In Section II.C.3, we will use

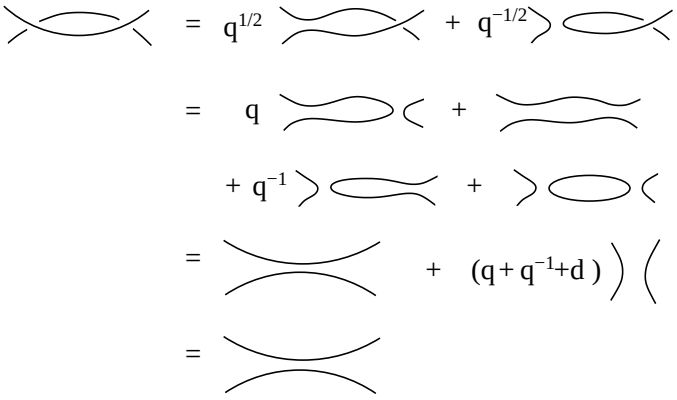

FIG. 5 The Kauffman bracket is invariant under continuous motions of the arcs and, therefore, independent of the particular projection of a link to the plane.

these methods to evaluate some matrix elements relevant to interference experiments.

Now, let us consider the two fusion channels of a pair of quasiparticles in some more detail. When the two quasiparticles fuse to the trivial particle, as 1 and 2 did above, we can depict such a state, which we will call $|0\rangle$, as $\frac{1}{\sqrt{d}}$ times the state yielded by the functional integral (62) with a Wilson line which looks like $\bigcup$ because two quasiparticles which are created as a pair out of the ground state must necessarily fuse to spin 0 if they do not braid with any other particles. (The factor $1/\sqrt{d}$ normalizes the state.) Hence, we can project any two quasiparticles onto the $j = 0$ state by evolving them with a history which looks like:

$$\Pi_0 \;=\; \frac{1}{d} \bigcup\!\!\bigcap \tag{78}$$

On the right-hand-side of this equation, we mean a functional integral between two times t_1 and t_2. The functional integral has two Wilson lines in the manner indicated pictorially. On the left-hand-side, we have suggested that evolving a state through this history can be viewed as acting on it with the projection operator $\Pi_0 = |0\rangle\langle 0|$.

However, the two quasiparticles could instead be in the state $|1\rangle$, in which they fuse to form the $j = 1$ particle. Since these states must be orthogonal, $\langle 0|1\rangle = 0$, we must get identically zero if we follow the history (78) with a history which defines a projection operator Π_1 onto the $j = 1$ state:

$$\Pi_1 \;=\; \Big|\Big| \;-\; \frac{1}{d} \bigcup\!\!\bigcap \tag{79}$$

It is easy to see that if this operator acts on a state which is given by a functional integral which looks like $\bigcup$, the result is zero.

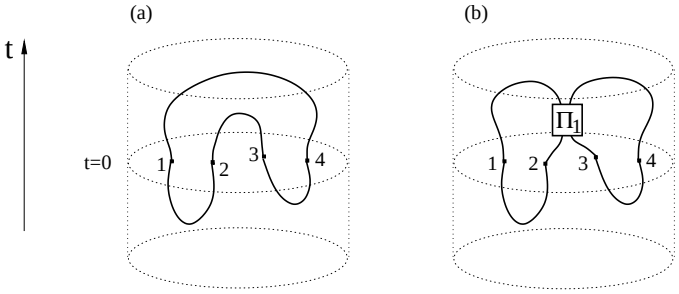

FIG. 6 The elements of the F-matrix can be obtained by computing matrix elements between kets in which 1 and 2 have a definite fusion channel and bras in which 1 and 4 have a definite fusion channel.

The projection operators Π_0 , Π_1, which are called *Jones-Wenzl projection operators*, project a pair of a quasiparticles onto the two natural basis states of their qubit. In other words, we do not need to introduce new types of lines in order to compute the expectation values of Wilson loops carrying $j = 0$ or $j = 1$. We can denote them with pairs of lines projected onto either of these states. Recall that a $j = 1/2$ loop had amplitude d, which was the quantum dimension of a $j = 1/2$ particle. Using the projection operator (79), we see that a $j = 1$ loop has amplitude $d^2 - 1$ (by connecting the top of the line segments to the bottom and evaluating the Kauffman bracket). One can continue in this way to construct projection operators which project m lines onto $j = m/2$. This projection operator must be orthogonal to the $j = 0, 1, 3/2, 2, \ldots, (m-1)/2$ projection operators acting on subsets of the m lines, and this condition is sufficient to construct all of the Jones-Wenzl projection operators recursively. Similarly, the quantum dimensions can be computed through a recursion relation. At level k, we find that quasiparticles with $j > k/2$ have quantum dimensions which vanish identically (e.g. for $k = 1$, $d = 1$ so the quantum dimension of a $j = 1$ particle is $d^2 - 1 = 0$). Consequently, these quasiparticle types do not occur. Only $j = 0, \frac{1}{2}, \ldots, \frac{k}{2}$ occur.

The entries in the F-matrix can be obtained by graphically computing the matrix element between a state in which, for instance, 1 and 2 fuse to the vacuum and 3 and 4 fuse to the vacuum and a state in which 1 and 4 fuse to the vacuum and 2 and 3 fuse to the vacuum, which is depicted in Figure 6a. (The matrix element in this figure must be normalized by the norms of the top and bottom states to obtain the F-matrix elements.) To compute the matrix element between a state in which 1 and 2 fuse to the vacuum and 3 and 4 fuse to the vacuum and a state in which 1 and 4 fuse to $j = 1$ and 2 and 3 fuse to $j = 1$, we must compute the diagram in Figure 6b. For $k = 2$, we find the same F-matrix as was found for Ising anyons in Section III.B.

Let us now briefly consider the ground state properties of the SU(2)$_k$ theory on the torus. As above, we integrate the Chern-Simons Lagrangian over a 3-manifold $\mathcal{M}$ with boundary Σ, i.e. $\mathcal{M} = \Sigma \times (-\infty, 0]$ in order to obtain a $t = 0$ state. The boundary Σ is the spatial slice at $t = 0$. For the torus, $\Sigma = T^2$, we take $\mathcal{M}$ to be the solid torus, $\mathcal{M} = S^1 \times D^2$, where D^2 is the disk. By foliating the solid torus, we ob-

tain earlier spatial slices. If there are no quasiparticles, then there are no Wilson lines terminating at Σ. However, the functional integral can have Wilson loops in the body of the solid torus as in Figure 7a. These correspond to processes in the past, $t < 0$, in which a quasiparticle-quashole pair was created, taken around the meridian of the torus and annihilated. The Wilson loop can be in any of the $k+1$ allowed representations $j = 0, \frac{1}{2}, \ldots, \frac{k}{2}$; in this way, we obtain $k+1$ ground state kets on the torus (we will see momentarily that they are all linearly independent). Wilson loops around the meridian are contractible (Figure 7b), so they can be simply evaluated by taking their Kauffman bracket; they multiply the state by d_j. Evidently, these Wilson loop operators are diagonal in this basis. Bras can be obtained by integrating the Chern-Simons Lagrangian over the 3-manifold $\mathcal{M}' = \Sigma \times [0,\infty) = S^3 \backslash S^1 \times D^2$, i.e. the exterior of the torus. Wilson loops in the exterior torus are now contractible if they are parallel to a longitude but non-trivial if they are around the meridian, as in in Figure 7c. Again, we obtain $k+1$ ground state bras in this way. The matrix elements between these bras and kets (appropriately normalized such that the matrix product of a bra with its conjugate ket is unity) are the entries in the S-matrix, which is precisely the basis change between the longitudinal and meridinal bases. A matrix element can be computed by evaluating the corresponding picture. The ab entry in the S-matrix is given by evaluating the Kauffman bracket of the picture in Figure 7d (and dividing by the normalization of the states). This figure makes the relationship between the S-matrix and braiding clear.

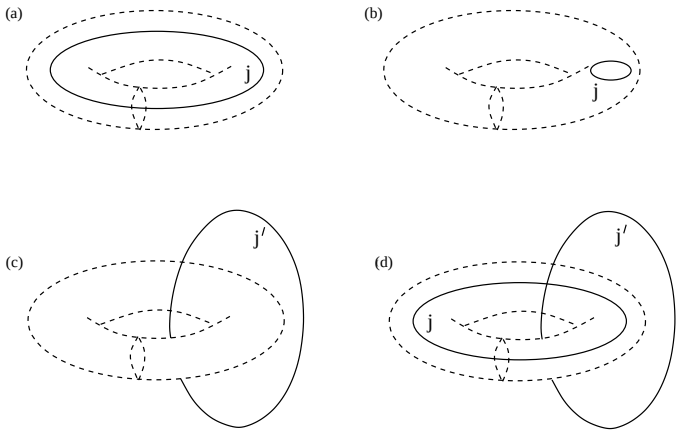

FIG. 7 Different degenerate ground states on the torus are given by performing the functional integral with longitudinal Wilson loops (a) carrying spin $j = 0, \frac{1}{2}, \ldots, \frac{k}{2}$. Meridinal Wilson loops are contractible (b); they do not give new ground states. The corresponding bras are have Wilson lines in the exterior solid torus (c). S-matrix elements are given by evaluating the history obtained by combining a bra and ket with their linked Wilson lines.

Finally, we comment on the difference between $SU(2)_2$ and Ising anyons, which we have previously described as differing only slightly from each other (See also the end of section III.E below). The effective field theory for Ising anyons contains an additional U(1) Chern-Simons gauge field, in addition to an $SU(2)_2$ gauge field (Fradkin et al., 2001, 1998). The consequences of this difference are that $\Theta_\sigma = e^{-\pi i/8}$ while $\Theta_{1/2} = e^{-3\pi i/8}$; $R_1^{\sigma\sigma} = e^{-\pi i/8}$ while $R_0^{\frac{1}{2},\frac{1}{2}} = -e^{-3\pi i/8}$; $R_\psi^{\sigma\sigma} = e^{3\pi i/8}$ while $R_1^{\frac{1}{2},\frac{1}{2}} = e^{\pi i/8}$; $[F_\sigma^{\sigma\sigma\sigma}]_{ab} = -\left[F_{\frac{1}{2}}^{\frac{1}{2},\frac{1}{2},\frac{1}{2}}\right]_{ab}$. The rest of the F-matrices are the same, as are the fusion multiplicities N_{ab}^c and the S-matrix. In other words, the basic structure of the non-Abelian statistics is the same in the two theories, but there are some minor differences in the U(1) phases which result from braiding. Both theories have threefold ground state degeneracy on the torus; the Moore-Read Pfaffian state has ground state degeneracy 6 because of an extra U(1) factor corresponding to the electrical charge degrees of freedom.

Of course, in the $k = 2$ case we have already obtained all of these results by the method of the previous subsection. However, this approach has two advantages: (1) once Witten's result (74) and Kauffman's recursion relation (77) are accepted, braiding matrix elements can be obtained by straightforward high school algebra; (2) the method applies to all levels k, unlike free Majorana fermion methods which apply only to the $k = 2$ case. There is an added bonus, which is that this formalism is closely related to the techniques used to analyze lattice models of topological phases, which we discuss in a later subsection.

D. Chern-Simons Theory, Conformal Field Theory, and Fractional Quantum Hall States

1. The Relation between Chern-Simons Theory and Conformal Field Theory

Now, we consider Chern-Simons theory in a particular gauge, namely holomorphic gauge (to be defined below). The ground state wavefunction(s) of Chern-Simons theory can be obtained by performing the functional integral from the distant past, $t = -\infty$, to time $t = 0$ as in the previous subsection:

$$\psi[A(\mathbf{x})] \;=\; \int_{a(\mathbf{x},0)=A(\mathbf{x})} \mathcal{D}a(\mathbf{x},t)\; e^{\int_{-\infty}^{0} dt \int_\Sigma d^2x\, \mathcal{L}_{\rm CS}} \qquad (80)$$

For the sake of concreteness, let us consider the torus, $\Sigma = T^2$, for which the spacetime manifold is $\mathcal{M} = (-\infty, 0] \times T^2 = S^1 \times D^2$. We assume for simplicity that there are no Wilson loops (either contained within the solid torus or terminating at the boundary). If x and y are coordinates on the torus (the fields will be subject to periodicity requirements), we write $z = x + iy$. We can then change to coordinates z, $\bar{z}$, and, as usual, treat $a_{\bar{z}}^a$ and $a_{\bar{z}}^a$ as independent variables. Then, we take the holomorphic gauge, $a_{\bar{z}}^a = 0$. The field $a_{\bar{z}}^a$ only appears in the action linearly, so the functional integral over $a_{\bar{z}}^a$ may be performed, yielding a δ-function:

$$\int Da\, e^{\frac{k}{4\pi}\int_{D^2\times S^1} \epsilon^{\mu\nu\lambda}\left(a_\mu^a \partial_\nu a_\lambda^a + \frac{2}{3} f_{abc} a_\mu^a a_\nu^b a_\lambda^c\right)} = \int Da_i\, \delta(f_{ij}^a)\, e^{\frac{k}{4\pi}\int_{D^2\times S^1} \epsilon^{ij} a_i^a \partial_{\bar{z}} a_j^a} \qquad (81)$$

where $i, j = t, z$. Here $f_{ij}^a = partial_i a_j^a - partial_j a_i^a + i\epsilon_{\underline{abc}} a_i^a a_j^b$ are the spatial components of the field strength.

There are no other cubic terms in the action once $a_{\bar{z}}$ has been eliminated (as is the case in any such gauge in which one of the components of the gauge field vanishes). The constraint imposed by the δ-function can be solved by taking

$$a_i^a = \partial_i U\, U^{-1} \tag{82}$$

where U is a single-valued function taking values in the Lie group. Substituting this into the right-hand-side of (81), we find that the action which appears in the exponent in the functional integral takes the form

$$\begin{aligned} S &= \frac{k}{4\pi}\int_{D^2\times S^1} \epsilon^{ij}\mathrm{tr}\left(\partial_i U\, U^{-1}\partial_{\bar{z}}\left(\partial_j U\, U^{-1}\right)\right) \\ &= \frac{k}{4\pi}\int_{D^2\times S^1} \epsilon^{ij}\Big[\mathrm{tr}\left(\partial_i U\, U^{-1}\partial_{\bar{z}}\partial_j U\, U^{-1}\right) + \\ &\qquad\qquad \mathrm{tr}\left(\partial_i U\, U^{-1}\partial_j U\, \partial_{\bar{z}} U^{-1}\right)\Big] \\ &= \frac{k}{4\pi}\int_{D^2\times S^1} \epsilon^{ij}\Big[\partial_j\mathrm{tr}\left(\partial_i\, U^{-1}\partial_{\bar{z}} U\right) + \\ &\qquad\qquad \mathrm{tr}\left(\partial_i U\, U^{-1}\partial_j U\, \partial_{\bar{z}} U^{-1}\right)\Big] \\ &= \frac{k}{4\pi}\int_{T^2} \mathrm{tr}\left(\partial_z U^{-1}\partial_{\bar{z}} U\right) + \\ &\frac{k}{12\pi}\int_{D^2\times S^1} \epsilon^{\mu\nu\lambda}\mathrm{tr}\left(\partial_\mu U\, U^{-1}\partial_\nu U\, U^{-1}\,\partial_\lambda U\, U^{-1}\right) \end{aligned} \tag{83}$$

The Jacobian which comes from the δ-function $\delta(f_{ij}^{\overline{a}})$ is cancelled by that associated with the change of integration variable from Da to DU. In the final line, the first term has been integrated by parts while the second term, although it appears to be an integral over the $3D$ manifold, only depends on the boundary values of U (Wess and Zumino, 1971; Witten, 1983). This is the Wess-Zumino-Witten (WZW) action. What we learn from (83) then, is that, in a particular gauge, the ground state wavefunction of $2+1$-D Chern-Simons theory can be viewed as the partition function of a $2+0$-dimensional WZW model.

For positive integer k, the WZW model is a $2D$ conformal field theory which, in the SU(2) case, has Virasoro central charge $c = \bar{c} = \frac{3k}{k+2}$. (For a brief review of some of the basics of conformal field theory, see appendix A and references therein.) However, in computing properties of the Chern-Simons theory from which we have derived it, we will couple only to $a_z = \partial_z U \cdot U^{-1}$; i.e. only to the holomorphic or right-moving sector of the theory. Thus, it is the chiral WZW model which controls the ground state wavefunction(s) of Chern-Simons theory.

If we were to follow the same strategy to calculate the Chern-Simons ground state wavefunction with Wilson lines or punctures present, then we would end up with a correlation function of operators in the chiral WZW model transforming under the corresponding representations of SU(2). (Strictly speaking, it is not a correlation function, but a *conformal block*, which is a chiral building block for a correlation function. While correlation functions are single-valued, conformal blocks have the non-trivial monodromy properties which we need, as is discussed in appendix A.) Therefore, following (Elitzur et al., 1989; Witten, 1989), we have mapped the problem of computing the ground state wavefunction (in $2+0$-dimensions) of Chern-Simons theory, which is a topological theory with a gap, to the problem of computing a correlation function in the chiral WZW model (in $1+1$-dimensions), which is a critical theory. This is a bit peculiar since one theory is gapped while the other is gapless. However, the gapless degrees of freedom of the WZW model for the $t = 0$ spatial slice are pure gauge degrees of freedom for the corresponding Chern-Simons theory. (In the very similar situation of a surface Σ with boundary, however, the corresponding conformally-invariant $1+1$-D theory describes the actual dynamical excitations of the edge of the system, as we discuss in section III.E.) Only the topological properties of the chiral WZW conformal blocks are physically meaningful for us.

More complicated topological states with multiple Chern-Simons fields and, possibly, Higgs fields (Fradkin et al., 2001, 1999, 1998) correspond in a similar way to other chiral rational conformal field theories which are obtained by tensoring or cosetting WZW models. (RCFTs are those CFTs which have a finite number of primary fields – see appendix A for the definition of a primary field – under some extended chiral algebra which envelopes the Virasoro algebra; a Kac-Moody algebra in the WZW case; and, possibly, other symmetry generators.) Consequently, it is possible to use the powerful algebraic techniques of rational conformal field theory to compute the ground state wavefunctions of a large class of topological states of matter. The quasiparticles of the topological state correspond to the primary fields of the chiral RCFT. (It is a matter of convenience whether one computes correlation functions with a primary field or one of its descendants since their topological properties are the same. This is a freedom which can be exploited, as we describe below.)

The conformal blocks of an RCFT have one property which is particularly useful for us, namely they are holomorphic functions of the coordinates. This makes them excellent candidate wavefunctions for quantum Hall states. We identify primary fields with the quasiparticles of the quantum Hall state, and compute the corresponding conformal block. However, there is one important issue which must be resolved: a quantum Hall wavefunction is normally viewed as a wavefunction for electrons (the quasiparticle positions, by contrast, are usually viewed merely as some collective coordinates specifying a given excited state). Where are the electrons in our RCFT? Electrons have trivial braiding properties. When one electron is taken around another, the wavefunction is unchanged, except for a phase change which is an odd integral multiple of 2π. More importantly, when any quasiparticle is taken around an electron, the wavefunction is unchanged apart from a phase change which is an integral multiple of 2π. Therefore, the electron must be a descendant of the identity. In other words, the RCFT must contain a fermionic operator by which we can extend the chiral algebra. This new symmetry generator is essentially the electron creation operator – which is, therefore, a descendant of the identity under its own action. Not all RCFTs have such an operator in their spectrum, so this is a strong constraint on RCFTs which can describe quantum Hall states. If we are interested, instead, in a quantum Hall state of bosons,

as could occur with ultra-cold bosonic atoms in a rotating optical trap (Cooper et al., 2001), then the RCFT must contain a bosonic field by which we can extend the chiral algebra.

An RCFT correlation function of N_e electron operators therefore corresponds to the Chern-Simons ground state wavefunction with N_e topologically-trivial Wilson lines. From a purely topological perspective, such a wavefunction is just as good as a wavefunction with no Wilson lines, so the Wilson lines would seem superfluous. However, if the descendant field which represents the electron operator is chosen cleverly, then the wavefunction with N_e Wilson lines may be a 'good' trial wavefunction for electrons in the quantum Hall regime. Indeed, in some cases, one finds that these trial wavefunctions are the exact quantum Hall ground states of simple model Hamiltonians (Ardonne and Schoutens, 1999; Blok and Wen, 1992; Greiter et al., 1991; Moore and Read, 1991; Read and Rezayi, 1999; Simon et al., 2007a; Wen and Wu, 1994). In the study of the quantum Hall effect, however, a wavefunction is 'good' if it is energetically favorable for a realistic Hamiltonian, which is beyond the scope of the underlying Chern-Simons theory, which itself only knows about braiding properties. It is unexpected good luck that the trial wavefunctions obtained from Chern-Simons theory are often found to be 'good' from this energetic perspective, which is a reflection of how highly constrained quantum Hall wavefunctions are, and how central these braiding properties are to their physics. We emphasize, however, that a wavefunction obtained in this way will *not* be the exact ground state wavefunction for electrons with Coulomb interactions. In some cases it might not even have particularly high overlap with the ground state wavefunction, or have good energetics. The one thing which it does capture is the topological structure of a particular universality class.

2. Quantum Hall Wavefunctions from Conformal Field Theory

Ideally, the logic which would lead us to a particular RCFT would be as follows, as displayed in Fig. 8. One begins with the experimental observation of the quantized Hall effect at some filling fraction ν (shown at the top). We certainly know that the Hamiltonian for the system is simply that of 2D electrons in a magnetic field, and at the bottom, we know the form of the low energy theory should be of Chern-Simons form. One would like to be able to "integrate out" high energy degrees of freedom directly to obtain the low-energy theory. Given the low-energy Chern-Simons effective field theory, one can pass to the associated RCFT, as described above. With the RCFT in hand, one can construct wavefunctions, as we will describe below. Indeed, such a procedure has been explicitly achieved for Abelian quantum Hall states (López and Fradkin, 1991; Zhang et al., 1989). In some special non-Abelian cases, progress in this direction has been made (Wen, 1991b, 1999).

For most non-Abelian theories, however, the situation is not so simple. The RCFT is usually obtained through inspired guesswork (Ardonne and Schoutens, 1999; Blok and Wen, 1992; Cappelli et al., 2001; Moore and Read, 1991; Read and Rezayi, 1999; Simon et al., 2007c). One may try to justify it *ex post facto* by solving for the properties of quasiholes of a system with some unrealistic (e.g. involving 3-body or higher interactions) but soluble Hamiltonian. The degeneracy can be established by counting (Nayak and Wilczek, 1996; Read, 2006; Read and Rezayi, 1996). The braiding matrices can be obtained by numerically computing the Berry integrals for the given wavefunctions (Tserkovnyak and Simon, 2003) or by using their connection to conformal field theory to deduce them (Gurarie and Nayak, 1997; Moore and Read, 1991; Nayak and Wilczek, 1996; Slingerland and Bais, 2001). One can then deduce the Chern-Simons effective field theory of the state either from the quasiparticle properties or from the associated conformal field theory with which both it and the wavefunctions are connected.

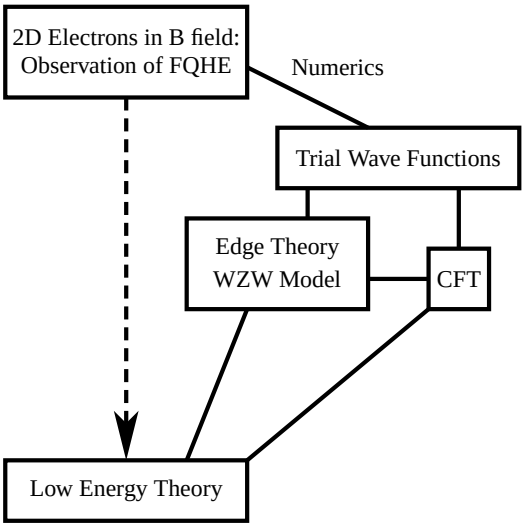

FIG. 8 How one arrives at a low-energy theory of the quantum Hall effect. At the top, one begins with the experimental observation of the quantized Hall effect. At the bottom, we know the low energy theory should be of Chern-Simons form. One would like to be able to "integrate out" high energy degrees of freedom directly to obtain the low energy theory, as shown by the dotted line, but must instead take a more circuitous route, as described in the text.

We now show how such wavefunctions can be constructed through some examples. In appendix A, we review some of the rudiments of conformal field theory.

(a) Wavefunctions from CFTs: Our goal is to construct a LLL FQH wavefunction $\Psi(z_1, \ldots, z_N)$ which describes an electron fluid in a circular droplet centered at the origin. Ψ must be a homogeneous antisymmetric analytic function of the z_is, independent of the $\bar{z}_i$s apart from the Gaussian factor, which we will frequently ignore (see Sec. II.C.1). If we consider the FQHE of bosons, we would need Ψ to instead be symmetric. The filling fraction ν of a FQH wavefunction Ψ is given by $\nu = N/N_\Phi$ where N is the number of electrons and N_Φ is the number of flux quanta penetrating the droplet (Prange and Girvin, 1990). In the LLL, N_Φ is given by the highest power of z occurring in Ψ.

We will also frequently need the fact that in an incompressible state of filling fraction ν, multiplying a wavefuncton by a

factor $\prod_i (z_i - w)^m$ pushes a charge νm away from the point w. This can be understood (Laughlin, 1983) as insertion of m flux quanta at the point w, which, via Faraday's law creates an azimuthal electric field, which, then, via the Hall conductivity transfers charge νm away from the point w.

Our strategy will be to choose a particular chiral RCFT, pick an "electron" field ψ_e in this theory (which, by the reasoning given above, must be a fermionic generator of the extended chiral algebra of the theory), and write a ground state trial wavefunction $\Psi_{\rm gs}$ for N electrons as

$$\Psi_{\rm gs} = \langle\, \psi_e(z_1) \dots \psi_e(z_N) \,\rangle \tag{84}$$

The field ψ_e must be fermionic since the quantum Hall wavefunction on the left-hand-side must be suitable for electrons. Not all RCFTs have such a field in their spectrum, so this requirement constrains our choice. This requirement also ensures that we will obtain a wavefunction which has no branch cuts; in particular, there will only be one conformal block on the right-hand-side of (84). We must do a little more work in choosing ψ_e so that there are no poles either on the right-hand-side of (84). As discussed above, the correlation function on the right-hand-side of (84) is a ground state wavefunction of Chern-Simons theory with N_e trivial topological charges at fixed positions $z_1, z_2, \dots, z_{N_e}$.

Of course, there isn't a unique choice of RCFT, even at a given filling fraction. Therefore, there are different fractional quantum Hall states which can be constructed in this way. Which fractional quantum Hall state is actually observed at a particular ν is determined by comparing the energies of the various possible competing ground states. Having a good wavefunction is, by itself, no guarantee that this wavefunction actually describes the physical system. Only a calculation of its energy gives real evidence that it is better than other possible states.

The reason for introducing this complex machinery simply to construct a wavefunction becomes clearer when we consider quasihole wavefunctions, which are Chern-Simons ground state wavefunctions with N_e trivial topological charges and N_{qh} non-trivial topological charges. In general, there are many possible quasihole operators, corresponding to the different primary fields of the theory, so we must really consider $N_{qh1}, N_{qh2}, \dots N_{qhm}$ numbers of quasiholes if there are m primary fields. Each different primary field corresponds to a different topologically-distinct type of "defect" in the ground state. (As in the case of electrons, we are free to choose a descendant field in place of the corresponding primary field since the two have identical topological properties although the wavefunction generated by a descendant will be different from that generated by its primary.) Let us suppose that we focus attention on a particular type of quasiparticle which, in most cases, will be the quasiparticle of minimal electrical charge. Then we can write a wavefunction with quasiholes at positions $w_1, \dots, w_M$ as

$$\Psi(w_1 \dots w_M) = \langle \psi_{qh}(w_1) \dots \psi_{qh}(w_M)\ \ \psi_e(z_1) \dots \psi_e(z_N) \rangle \tag{85}$$

where ψ_{qh} is the corresponding primary field. Since ψ_{qh} is a primary field and ψ_e is a descendant of the identity, we are guaranteed that ψ_{qh} and ψ_e are local with respect to each other, i.e. taking one field around can only produce a phase which is a multiple of 2π. Consequently, the wavefunction Ψ remains analytic in the electron coordinates z_i even after the fields $\psi_{qh}(w_1) \dots \psi_{qh}(w_M)$ have been inserted into the correlation function.

One important feature of the conformal block on the right-hand-side of (85) is that $\psi_{qh}(w_a)$ and $\psi_e(z_i)$ are on roughly the same footing – they are both fields in some conformal field theory (or, equivalently, they are both fixed sources coupled to the Chern-Simons gauge field). However, when intepreted as a wavefunction on the left-hand-side of (85), the electron coordinates z_i are the variables for which the wavefunction gives a probability amplitude while the quasihole coordinates w_a are merely some parameters in this wavefunction. If we wished to normalize the wavefunction differently, we could multiply by an arbitrary function of the w_as. However, the particular normalization which is given by the right-hand-side of (85) is particularly convenient, as we will see momentarily. Note that since the quasihole positions w_j are merely parameters in the wavefunction, the wavefunction need not be analytic in these coordinates.

(b) Quasiparticle Braiding: The branch cuts in quasihole positions w_a are symptoms of the fact that there may be a vector space of conformal blocks corresponding to the right-hand-side of (85). In such a case, even when the quasihole positions are fixed, there are several possible linearly independent wavefunctions. These multiple degenerate states are necessary for non-Abelian statistics, and they will generically mix when the quasiholes are dragged around each other.

However, there is still a logical gap in the above reasoning. The wavefunctions produced by an RCFT have the correct braiding properties for the corresponding Chern-Simons ground state wavefunction built into them through their explicit monodromy properties. As a result of the branch cuts in the conformal blocks as a function of the w_as, when one quasihole is taken around another, the wavefunction Ψ^α transforms into $M^{\alpha\beta}\Psi^\beta$, where the index $\alpha = 1, 2, \dots, g$ runs over the g different degenerate n-quasihole states. However, when viewed as quantum Hall wavefunctions, their quasiparticle braiding properties are a combination of their explicit monodromy and the Berry matrix which is obtained from:

$$e^{i\gamma_{\alpha\beta}} = \mathcal{P} \exp\left(\oint d\vec{w} \left\langle \Psi^\alpha \middle| \nabla_{\vec{w}} \middle| \Psi^\beta \right\rangle \right) \tag{86}$$

where Ψ^α, $\alpha = 1, 2, \dots, g$ are the g different degenerate n-quasihole states and P is the path ordering symbol. In this equation, the z_is are integrated over in order to compute the inner product, but the w_as are held fixed, except for the one which is taken around some loop.

Strictly speaking, the effect of braiding is to transform a state according to $\Psi^\alpha \to e^{i\gamma_{\alpha\beta}} M^{\beta\gamma} \Psi^\gamma$. By changing the normalization of the wavefunction, we can alter $e^{i\gamma_{\alpha\beta}}$ and $M^{\beta\gamma}$. Only the product of the two matrices on the right-hand-side of this equation is gauge invariant and physically meaningful. When we presume that the braiding properties of this wavefunction are given by those of the corresponding CFT and Chern-Simons theory, we take it to be equal to $M^{\beta\gamma}$ and

ignore $e^{i\gamma_{\alpha\beta}}$. This can only be correct if $\gamma_{\alpha\beta}$ vanishes up to a geometric phase proportional to the area for a wavefunction given by a CFT conformal block. In the case of the Laughlin states, it can be verified that this is indeed correct by repeating the the Arovas, Schrieffer, Wilczek calculation (Arovas et al., 1984) with the Laughlin state normalized according to the quasihole position dependence given by the corresponding CFT (see below) (Blok and Wen, 1992). This calculation rests upon the plasma analogy originally introduced by Laughlin in his seminal work (Laughlin, 1983). For other, more complex states, it is more difficult to compute the Berry matrix. A version of a plasma analogy for the MR Pfaffian state was constructed in Gurarie and Nayak, 1997; one could thereby verify the vanishing of the Berry matrix for a two-quasihole state and, with some further assumptions, for four and higher multiquasihole states. A direct evaluation of the integral in (86) by the Monte-Carlo method (Tserkovnyak and Simon, 2003) established that it vanishes for MR Pfaffian quasiholes. The effect of Landau level mixing on statistics has also been studied (Simon, 2007). Although there has not been a complete proof that the CFT-Chern-Simons braiding rules are identical to those of the wavefunction, when it is interpreted as an electron wavefunction (i.e. there has not been a complete proof that (86) vanishes when the wavefunction is a CFT conformal block), there is compelling evidence for the MR Pfaffian state, and it is almost certainly true for many other states as well. We will, therefore, take it as a given that we can simply read off the braiding properties of the wavefunctions which we construct below.

(c) The Laughlin State: We now consider wavefunctions generated by perhaps the simplest CFT, the chiral boson. We suppose that the chiral boson has compactification radius $\sqrt{m}$, so that $\phi \equiv \phi + 2\pi\sqrt{m}$. The U(1) Kac-Moody algebra and enveloping Virasoro algebra can be extended by the symmetry generator $e^{i\phi\sqrt{m}}$. Since the dimension of this operator is $m/2$, it is fermionic for m odd and bosonic for even m. The primary fields of this extended chiral algebra are of the form $e^{in\phi/\sqrt{m}}$, with $n = 0, 1, \ldots, m-1$. They are all of the fields which are not descendants and are local with respect to $e^{i\phi\sqrt{m}}$ (and to the Kac-Moody and Virasoro generators), as may be seen from the operator product expansion (OPE) (see Appendix A):

$$e^{i\phi(z)\sqrt{m}}\, e^{in\phi(0)/\sqrt{m}} \sim z^n\, e^{i(n+m)\phi(0)/\sqrt{m}} + \ldots \qquad (87)$$

When z is taken around the origin, the right-hand-side is unchanged. It is convenient to normalize the $U(1)$ current as $j = \frac{1}{\sqrt{m}}\partial\phi$; then the primary field $e^{in\phi/\sqrt{m}}$ has charge n/m. We take $\psi_e = e^{i\phi\sqrt{m}}$ as our electron field (which has charge 1) and consider the resulting ground state wavefunction according to Eq. 84. Using Eq. A7 we find

$$\Psi_{\rm gs} = \langle \psi_e(z_1) \ldots \psi_e(z_N) \rangle = \textstyle\prod_{i<j}\ (z_i - z_j)^m \qquad (88)$$

It is now clear why we have chosen this CFT: to have $\Psi_{\rm gs}$ given by correlators of a vertex operator of the form $e^{i\alpha\phi}$ analytic (no branch cuts or poles) we must have $\alpha^2 = m$ a nonnegative integer, and m must be odd to obtain an antisymmetric wavefunction (or even for symmetric). We recognize $\Psi_{\rm gs}$ as the $\nu = 1/m$ Laughlin wavefunction. The astute reader will notice that the correlator in Eq. 88 actually violates the neutrality condition discussed in Appendix A and so it should actually have zero value. One fix for this problem is to insert into the correlator (by hand) a neutralizing vertex operator at infinity $e^{-iN\phi(z=\infty)\sqrt{m}}$ which then makes Eq. 88 valid (up to a contant factor). Another approach is to insert an operator that smears the neutralizing background over the entire system (Moore and Read, 1991). This approach also conveniently results in the neglected Gaussian factors reappearing! We will ignore these neutralizing factors for simplicity. From now on, we will drop the Gaussian factors from quantum Hall wavefunctions, with the understanding that they result from including a smeared neutralizing background.

The quasihole operator must be a primary field; the primary field of minimum charge is $e^{i\phi/\sqrt{m}}$. Using Eq. A7, Eq. 85 yields

$$\Psi(w_1, \ldots, w_M) = \prod_{i<j}^{M} (w_i - w_j)^{1/m} \prod_{i=1}^{N}\prod_{j=1}^{M} (z_i - w_j)\Psi_{\rm gs} \qquad (89)$$

As mentioned above, the factor $\prod_j (z_j - w)$ "pushes" charge away from the position w leaving a hole of charge precisely $Q = +e/m$. The first term on the right of Eq. 89 results from the fusion of quasihole operators with each other, and explicitly shows the fractional statistics of the quasiholes. Adiabatically taking two quasiholes around each other results in a fractional phase of $2\pi/m$. As promised above, this statistical term appears automatically in the wavefunction given by this CFT!

(d) Moore-Read Pfaffian State:

In the Ising CFT (see Appendix A), we might try to use $\psi_e(z) = \psi(z)$ as the electron field (Moore and Read, 1991). The ψ fields can fuse together in pairs to give the identity (since $\psi \times \psi = \mathbf{1}$) so long as there are an even number of fields. However, when we take two ψ fields close to each other, the OPE tells us that

$$\lim_{z_i \to z_j} \psi(z_i)\psi(z_j) \sim \mathbf{1}/(z_i - z_j) \qquad (90)$$

which diverges as $z_i \to z_j$ and is therefore unacceptable as a wavefunction. To remedy this problem, we tensor the Ising CFT with the chiral boson CFT. There is now an operator $\psi\, e^{i\phi\sqrt{m}}$ by which we can extend the chiral algebra. (If m is even, this symmetry generator is fermionic; if m is odd, it is bosonic.) As before, we will take this symmetry generator to be our electron field. The corresponding primary fields are of the form $e^{in\phi/\sqrt{m}}$, $\sigma\, e^{i(2n+1)\phi/2\sqrt{m}}$, and $\psi\, e^{in\phi/\sqrt{m}}$, where $n = 0, 1, \ldots, m-1$. Again, these are determined by the requirement of locality with respect to the generators of the chiral algebra, i.e. that they are single-valued when taken around a symmetry generator, in particular the elecron field $\psi\, e^{i\phi\sqrt{m}}$. For instance,

$$\begin{aligned}\psi(z)\, e^{i\phi(z)\sqrt{m}} \cdot \sigma(0)\, e^{i(2n+1)\phi(0)/2\sqrt{m}} \sim \\ z^{-1/2}\sigma(0)\, z^{n+1/2} e^{i(2(n+m)+1)\phi(0)/\sqrt{m}} + \ldots \\ = z^n \sigma(0)\, e^{i(2(n+m)+1)\phi(0)/\sqrt{m}}\end{aligned} \qquad (91)$$

and similarly for the other primary fields.

Using our new symmetry generator as the electron field, we obtain the ground state wavefunction according to Eq. 84:

$$\Psi_{\rm gs} = \langle \psi(z_1) \dots \psi(z_N) \rangle \ \prod_{i<j} (z_i - z_j)^m = {\rm Pf}\left(\frac{1}{z_i - z_j} \right) \prod_{i<j} (z_i - z_j)^m \quad (92)$$

(See, e.g. Di Francesco et al., 1997 for the calculation of this correlation function.) Again, m odd gives an antisymmetric wavefunction and m even gives a symmetric wavefunction. For $m = 2$ (and even N), Eq. 92 gives precisely the Moore-Read Pfaffian wavefunction (Eq. 43 with $g = 1/z$ and two Jastrow factors attached).

To determine the filling fraction of our newly constructed wavefunction, we need only look at the exponent of the Jastrow factor in Eq. 92. Recall that the filling fraction is determined by the highest power of any z (See III.D.1 above). There are $m(N-1)$ factors of z_1 in the Jastrow factor. The Pfaffian has a factor of z_1 in the denominator, so the highest power of z_1 is $m(N-1)-1$. However, in the thermodynamic limit, the number of factors scales as mN. Thus the filling fraction is $\nu = 1/m$.

We now consider quasihole operators. As in the Laughlin case we might consider the primary fields $\psi_{qh} = e^{in\phi/\sqrt{m}}$. Similar arguments as in the Laughlin case show that the $n = 1$ case generates precisely the Laughlin quasihole of charge $Q = +e/m$. However we have other options for our quasihole which have smaller electrical charge. The primary field $\sigma\, e^{i\phi/2\sqrt{m}}$ has charge $Q = +e/2m$. We then obtain the wavefunction according to Eq. 85

$$\Psi(w_1, \dots, w_M) = \langle \sigma(w_1) \dots \sigma(w_m) \psi(z_1) \dots \psi(z_N) \rangle \times \prod_{i<j}^{M} (w_i - w_j)^{1/2m} \prod_{i=1}^{N} \prod_{j=1}^{M} (z_i - w_j)^{1/2} \prod_{i<j}^{N} (z_i - z_j)^m \quad (93)$$

Using the fusion rules of the σ fields (See Eq. 7, as well as Fig. 22 and Table II in Appendix A), we see that it is impossible to obtain $\mathbf{1}$ from an odd number of σ fields. We conclude that quasiholes ψ_{qh} can only occur in pairs. Let us then consider the simplest case of two quasiholes. If there is an even number of electrons, the ψ fields fuse in pairs to form $\mathbf{1}$, and the remaining two quasiholes must fuse to form $\mathbf{1}$ also. As discussed in Eq. A3 the OPE of the two σ fields will then have a factor of $(w_1 - w_2)^{-1/8}$. In addition, the fusion of the two vertex operators $e^{i\phi/2\sqrt{m}}$ results in the first term in the second line of Eq. 93, $(w_1 - w_2)^{1/(4m)}$. Thus the phase accumulated by taking the two quasiholes around each other is $-2\pi/8 + 2\pi/4m$.

On the other hand, with an odd number of electrons in the system, the ψ's fuse in pairs, but leave one unpaired ψ. The two σ's must then fuse to form a ψ which can then fuse with the unpaired ψ to give the identity. (See Eq. A3). In this case, the OPE of the two σ fields will give a factor of $(w_1 - w_2)^{3/8}$. Thus the phase accumulated by taking the two quasiholes around each other is $6\pi/8 + 2\pi/4m$.

In the language of section III.B above, when there is an even number of electrons in the system, all of these are paired and the fermion orbital shared by the quasiholes is unoccupied. When an odd electron is added, it 'occupies' this orbital, although the fermion orbital is neutral and the electron is charged (we can think of the electrons' charge as being screened by the superfluid).

When there are many quasiholes, they may fuse together in many different ways. Thus, even when the quasihole positions are fixed there are many degenerate ground states, each corresponding to a different conformal block (see appendix A). This degeneracy is precisely what is required for non-Abelian statistics. Braiding the quasiholes around each other produces a rotation within this degenerate space.

Fusing $2m$ σ fields results in 2^{m-1} conformal blocks, as may be seen by examining the Bratteli diagram of Fig. 22 in appendix A. When two quasiholes come together, they may either fuse to form $\mathbf{1}$ or ψ. As above, if they come together to form $\mathbf{1}$ then taking the two quasiholes around each other gives a phase of $-2\pi/8 + 2\pi/4m$. On the other hand, if they fuse to form ψ then taking them around each other gives a phase of $2\pi 3/8 + 2\pi/4m$.

These conclusions can be illustrated explicitly in the cases of two and four quasiholes. For the case of two quasiholes, the correlation function (93) can be evaluated to give (Moore and Read, 1991; Nayak and Wilczek, 1996) (for an even number of electrons):

$$\Psi(w_1, w_2) \ = \ \prod_{j<k} (z_j - z_k)^2 \times {\rm Pf}\left(\frac{(z_j - w_1)(z_k - w_2) + z_j \leftrightarrow z_k}{z_j - z_k} \right) . \quad (94)$$

where $w_{12} = w_1 - w_2$. For simplicity, we specialize to the case $m = 2$; in general, there would be a prefactor $(w_{12})^{\frac{1}{4m} - \frac{1}{8}}$. When the two quasiholes at w_1 and w_2 are brought together at the point w, a single flux quantum Laughlin quasiparticle results, since two σs can only fuse to the identity in this case, as expected from the above arguments:

$$\Psi_{\rm qh}(w) \ = \ \prod_{j<k} (z_j - z_k)^2 \prod_i (z_i - w) \ {\rm Pf}\left(\frac{1}{z_j - z_k} \right) . \quad (95)$$

The situation becomes more interesting when we consider states with 4 quasiholes. The ground state is 2-fold degenerate (see appendix A). If there is an even number of electrons (which fuse to form the identity), we are then concerned with the $\langle \sigma\sigma\sigma\sigma \rangle$ correlator. As discussed in appendix A, two orthogonal conformal blocks can be specified by whether 1 and 2 fuse to form either $\mathbf{1}$ or ψ. The corresponding wavefunctions obtained by evaluating these conformal blocks are (Nayak and Wilczek, 1996):

$$\Psi^{(1,\psi)} = \frac{(w_{13} w_{24})^{\frac{1}{4}}}{(1 \pm \sqrt{x})^{1/2}} \left(\Psi_{(13)(24)} \ \pm \ \sqrt{x} \ \Psi_{(14)(23)} \right) \quad (96)$$

where $x = w_{14} w_{23} / w_{13} w_{24}$. (Note that we have taken a slightly different anharmonic ratio x than in Nayak and

Wilczek, 1996 in order to make (96) more compact than Eqs. (7.17), (7.18) of Nayak and Wilczek, 1996.) In this expression,

$$\Psi_{(13)(24)} = \prod_{j<k}(z_j - z_k)^2 \times \mathrm{Pf}\left(\frac{(z_j-w_1)(z_j-w_3)(z_k-w_2)(z_k-w_4)+(j\leftrightarrow k)}{z_j-z_k}\right) \tag{97}$$

and

$$\Psi_{(14)(23)} = \prod_{j<k}(z_j - z_k)^2 \times \mathrm{Pf}\left(\frac{(z_j-w_1)(z_j-w_4)(z_k-w_2)(z_k-w_3)+(j\leftrightarrow k)}{z_j-z_k}\right) \tag{98}$$

Suppose, now, that the system is in the state $\Psi^{(1)}$. Braiding 1 around 2 or 3 around 4 simply gives a phase (which is $R_1^{\sigma\sigma}$ multiplied by a contribution from the Abelian part of the theory). However, if we take w_2 around w_3, then after the braiding, the system will be in the state $\Psi^{(\psi)}$ as a result of the branch cuts in (96). Now, 1 and 2 will instead fuse together to form ψ, as expected from the general argument in Eq. A6. Thus, the braiding yields a rotation in the degenerate space. The resulting prediction for the behavior under braiding for the Moore-Read Pfaffian state is in agreement with the results obtained in sections III.B and III.C above.

(e) $\mathbb{Z}_3$ Read-Rezayi State (Briefly): We can follow a completely analogous procedure with a CFT which is the tensor product of the $\mathbb{Z}_3$ parafermion CFT with a chiral boson. As before, the electron operator is a product of a chiral vertex operator from the bosonic theory with an operator from the parafermion theory. The simplest choice is $\psi_e = \psi_1 e^{i\alpha\phi}$. We would like this field to be fermionic so that it can be an electron creation operator by which we can extend the chiral algebra (i.e., so that the electron wavefunction has no branch cuts or singularities). (See appendix A for the notation for parafermion fields.) The fusion rules for ψ_1 in the $\mathbb{Z}_3$ parafermion CFT are: $\psi_1 \times \psi_1 \sim \psi_2$ but $\psi_1 \times \psi_1 \times \psi_1 \sim \mathbf{1}$ so that the correlator in Eq. 84 is only nonzero if N is divisible by 3. From the OPE, we obtain $\psi_1(z_1)\psi_1(z_2) \sim (z_1-z_2)^{-2/3}\psi_2$ so in order to have the wavefunction analytic, we must choose $\alpha = \sqrt{m+2/3}$ with $m \geq 0$ an integer (m odd results in an antisymmetric wavefunction and even results in symmetric). The filling fraction in the thermodynamic limit is determined entirely by the vertex operator $e^{i\alpha\phi}$, resulting in $\nu = 1/\alpha^2 = 1/(m+2/3)$.

The ground state wavefunction for $N = 3n$ electrons takes the form:

$$\Psi_{\mathrm{gs}}(z_1,\ldots,z_{3n}) = \prod_{i<j}(z_i-z_j)^m \times \mathcal{S}\left\{\prod_{0\leq r<s<n}\chi_{r,s}(z_{3r+1},\ldots,z_{3r+k},z_{3k+1},\ldots z_{3s+3})\right\} \tag{99}$$

where M must be odd for electrons, $\mathcal{S}$ means the symmetrization over all permutations, and

$$\chi_{r,s} = (z_{3r+1}-z_{3s+1})(z_{3r+1}-z_{3s+2})\times (z_{3r+2}-z_{3s+2})(z_{3r+2}-z_{3s+3})\ldots \times (z_{3r+3}-z_{3s+3})(z_{3r+3}-z_{3s+1}) \tag{100}$$

With the electron operator in hand, we can determine the primary fields of the theory. The primary field of minimum electrical charge is $\psi_{qh} = \sigma_1 e^{i\phi/3\alpha}$ To see that this field is local with respect to ψ_e (i.e., there should be no branch cuts for the electron coordinates z_i), observe that $\sigma_1(w)\psi_1(z) \sim (z-w)^{-1/3}\psi$ and $e^{i\phi/3\alpha}(w)e^{i\alpha\phi}(z) \sim (z-w)^{1/3}$. Constructing the full wavefunction (as in Eq. 85 and analogous to Eq. 93) the fusion of of $e^{i\phi/3\alpha}$ (from ψ_{qh}) with $e^{i\alpha\phi}$ (from ψ_e) again generates a factor of $\prod_i(z_i-w)^{1/3}$. We conclude that the elementary quasihole has charge $Q = +e\nu/3$.

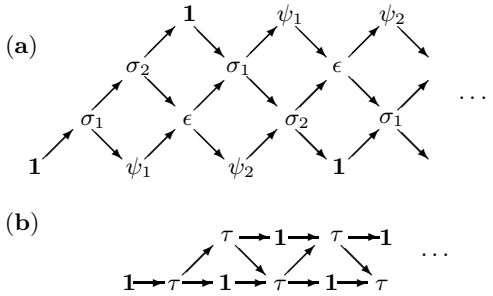

FIG. 9 **(a)** Bratteli diagram for fusion of multiple σ_1 fields in the $\mathbb{Z}_3$ Parafermion CFT. **(b)** Bratteli diagram for Fibonacci anyons.

The general braiding behavior for the $\mathbb{Z}_3$ parafermions has been worked out in Slingerland and Bais, 2001. It is trivial, however, to work out the dimension of the degenerate space by examining the Bratteli diagram Fig. 9a (See the appendix for explanation of this diagram). For example, if the number of electrons is a multiple of 3 then they fuse together to form the identity. Then, for example, with 6 quasiholes one has 5 paths of length 5 ending at **1** (hence a 5 dimensional degenerate space). However, if, for example, the number of electrons is 1 mod 3, then the electrons fuse in threes to form **1** but there is one ψ_1 left over. Thus, the quasiholes must fuse together to form ψ_2 which can fuse with the leftover ψ_1 to form **1**. In this case, for example, with 4 quasiholes there is a 2 dimensional space. It is easy to see that (if the number of electrons is divisible by 3) the number of blocks with n quasiparticles is given by the $n-1^{st}$ Fibonacci number, notated Fib(n-1) defined by $\mathrm{Fib}(1) = \mathrm{Fib}(2) = 1$ and $\mathrm{Fib}(n) = \mathrm{Fib}(n-1) + \mathrm{Fib}(n-2)$ for $n > 2$.

E. Edge Excitations

When a system in a chiral topological phase has a boundary (as it must in any experiment), there must be gapless excitations at the boundary (Halperin, 1982; Wen, 1992). To see this, consider the Chern-Simons action on a manifold $\mathcal{M}$

State	CFT	ν	ψ_e	ψ_{qh}
Laughlin	Boson	$\frac{1}{m}$	$e^{i\phi\sqrt{m}}$	$e^{i\phi/\sqrt{m}}$
Moore-Read	Ising	$\frac{1}{m+1}$	$\psi e^{i\phi\sqrt{m+1}}$	$\sigma e^{i\phi/(2\sqrt{m+1})}$
$\mathbb{Z}_3$ RR	$\mathbb{Z}_3$ Paraf.	$\frac{1}{m+2/3}$	$\psi_1 e^{i\phi\sqrt{m+2/3}}$	$\sigma_1 e^{i\phi/(3\sqrt{m+2/3})}$

TABLE I Summary of CFT-wavefunction correspondences discussed here. In all cases $m \geq 0$. Odd (even) m represents a Fermi (Bose) wavefunction.

with boundary $\partial\mathcal{M}$ (Elitzur et al., 1989; Witten, 1989), Eq. 24. The change in the action under a gauge transformation, $a_\mu \to g a_\mu g^{-1} + g\partial_\mu g^{-1}$, is:

$$S_{CS}[a] \to S_{CS}[a] + \frac{k}{4\pi}\int_{\partial\mathcal{M}} \mathrm{tr}(g^{-1}dg \wedge a) \qquad (101)$$

In order for the action to be invariant, we fix the boundary condition so that the second term on the r.h.s. vanishes. For instance, we could take boundary condition $\left(a_0^{\underline{a}}\right)_{|\partial\mathcal{M}} = 0$, where x_0, x_1 are coordinates on the boundary of $\mathcal{M}$ and x_2 is the coordinate perpendicular to the boundary of $\mathcal{M}$. Then the action is invariant under all transformations which respect this boundary condition, i.e. which satisfy $\partial_0 g = 0$ on the boundary. We separate these into gauge and global symmetries. Functions $g : \mathcal{M} \to G$ satisfying $g_{|\partial\mathcal{M}} = 1$ are the gauge symmetries of the theory. (They necessarily satisfy $\partial_0 g = 0$ since x_0 is a coordinate along the boundary.) Meanwhile, functions $f : \mathcal{M} \to G$ which are independent of x_0 are really global symmetries of the theory. The representations of this global symmetry form the spectrum of edge excitations of the theory. (The distinction between gauge and global transformations is that a gauge transformation can leave the $t = 0$ state unchanged while changing the state of the system at a later time t. Since it is, therefore, not possible for a given initial condition to uniquely define the state of the system at a later time, all physically-observable quantities must be invariant under the gauge transformation. By contrast, a global symmetry, even if it acts differently at different spatial points, cannot leave the $t = 0$ state unchanged while changing the state of the system at a later time t. A global symmetry does not prevent the dynamics from uniquely defining the state of the system at a later time for a given initial condition. Therefore, physically-observable quantities need not be invariant under global transformations. Instead, the spectrum of the theory can be divided into representations of the symmetry.)

With this boundary condition, the natural gauge choice for the bulk is $a_0^{\underline{a}} = 0$. We can then transform the Chern-Simons functional integral into the chiral WZW functional integral following the steps in Eqs. 81-83 (Elitzur et al., 1989):

$$S = \frac{k}{4\pi}\int_{\partial\mathcal{M}} \mathrm{tr}\left(\partial_0 U^{-1}\partial_1 U\right) + \frac{k}{12\pi}\int_{\mathcal{M}} \epsilon^{\mu\nu\lambda}\mathrm{tr}\left(\partial_\mu U\, U^{-1}\partial_\nu U\, U^{-1}\,\partial_\lambda U\, U^{-1}\right) \qquad (102)$$

Note the off-diagonal form of the quadratic term (analogous to the $z - \bar{z}$ form in Eq. 83), which follows from our choice of boundary condition. This boundary condition is not unique, however. The topological order of the bulk state does not determine the boundary condition. It is determined by the physical properties of the edge. Consider, for instance, the alternative boundary condition $\left(a_0^{\underline{a}} + v a_1^{\underline{a}}\right)_{|\partial\mathcal{M}} = 0$ for some constant v with dimensions of velocity. With this boundary condition, the quadratic term in the Lagrangian will now be tr $\left((\partial_0 + v\partial_1)\, U^{-1}\partial_1 U\right)$ and the edge theory is the chiral WZW model with non-zero velocity.

It is beyond the scope of this paper to discuss the chiral WZW model in any detail (for more details, see Gepner and Qiu, 1987; Gepner and Witten, 1986; Knizhnik and Zamolodchikov, 1984). However, there are a few key properties which we will list now. The chiral WZW model is a conformal field theory. Therefore, although there is a gap to all excitations in the bulk, there are gapless excitations at the edge of the system. The spectrum of the WZW model is organized into representations of the Virasoro algebra and is further organized into representations of the G_k Kac-Moody algebra. For the sake of concreteness, let us consider the case of SU(2)$_k$. The SU(2)$_k$ WZW model contains primary fields ϕ_j, transforming in the $j = 0, 1/2, 1, \ldots, k/2$ representations. These correspond precisely to the allowed quasiparticle species: when the total topological charge of all of the quasiparticles in the bulk is j, the edge must be in the sector created by acting with the spin j primary field on the vacuum.

The G_k case is a generalization of the U(1)$_m$ case, where $g = e^{i\phi}$ and the WZW model reduces to a free chiral bosonic theory:

$$S = \frac{m}{4\pi}\int d^2x\ (\partial_t + v\partial_x)\,\phi\,\partial_x\phi \qquad (103)$$

(In Sec. III.A, we used k for the coefficient of an Abelian Chern-Simons term; here, we use m to avoid confusion with the corresponding coupling of the SU(2) Chern-Simons term in situations in which both gauge fields are present.) The primary fields are $e^{in\phi}$, with $n = 0, 1, ..., m-1$. (The field $e^{im\phi}$ is either fermionic or bosonic for m odd or even, respecitvely, so it is not a primary field, but is, rather, included as a generator of an extended algebra.) A quantum Hall state will always have such a term in its edge effective field theory; the U(1) is the symmetry responsible for charge conservation and the gapless chiral excitations (103) carry the quantized Hall current.

Therefore, we see that chiral topological phases, such as fractional quantum Hall states, must have gapless chiral edge excitations. Furthermore, the conformal field theory which models the low-energy properties of the edge is *the same* conformal field theory which generates ground state wavefunctions of the corresponding Chern-Simons action. This is clear from the fact that the two derivations (Eqs. 83 and 102) are virtually identical. The underlying reason is that Chern-Simons theory is a topological field theory. When it is solved on a manifold with boundary, it is unimportant whether the manifold is a fixed-time spatial slice or the world-sheet of the edge of the system. In either case, Chern-Simons theory reduces to the same conformal field theory (which is an example of 'holography'). One important difference, however, is that,

in the latter case, a physical boundary condition is imposed and there are real gapless degrees of freedom. (In the former case, the CFT associated with a wavefunction for a fixed-time spatial slice may have apparent gapless degrees of freedom which are an artifact of a gauge choice, as discussed in Section III.D.)

The WZW models do not, in general, have free field representations. One well-known exception is the equivalence between the SU(N)$_1$ × U(1)$_N$ chiral WZW model and N free chiral Dirac fermions. A somewhat less well-known exception is the SU(2)$_2$ chiral WZW model, which has a representation in terms of 3 free chiral Majorana fermions. Before discussing this representation, we first consider the edge excitations of a $p+ip$ superconductor, which supports Ising anyons which, in turn, differ from SU(2)$_2$ only by a U(1) factor.

Let us solve the Bogoliubov-de Gennes Hamiltonian (38) with a spatially-varying chemical potential, just as we did in Section III.B. However, instead of a circular vortex, we consider an edge at $y = 0$:

$$\mu(y) = \Delta\, h(y), \tag{104}$$

with $h(y)$ large and positive for large y, and $h(y) < 0$ for $y < 0$; therefore, the electron density will vanish for y large and positive. Such a potential defines an edge at $y = 0$. There are low-energy eigenstates of the BdG Hamiltonian which are spatially localized near $y = 0$:

$$\phi_E^{edge}(\mathbf{x}) \approx e^{ikx} e^{-\int_0^y h(y')dy'} \phi_0, \tag{105}$$

with $\phi_0 = \binom{1}{1}$ an eigenstate of σ^x. This wavefunction describes a chiral wave propagating in the $x-$direction localized on the edge, with wave vector $k = E/\Delta$. A more complete solution of the superconducting Hamiltonian in this situation would involve self-consistently solving the BdG equations, so that both the density and the gap $\Delta(y)$ would vanish for large positive y. The velocity of the chiral edge mode would then depend on how sharply $h(y)$ varies. However, the solutions given above with fixed constant Δ are sufficient to show the existence of the edge mode.

If we define an edge fermion operator $\psi(\mathbf{x})$:

$$\psi(\mathbf{x}) = e^{-\int_0^y h(y')dy'} \sum_{k>0} [\psi_k e^{ikx}\phi_0 + \psi_{-k} e^{-ikx}\phi_0].$$

The fermion operators, ψ_k, satisfy $\psi_{-k} = \psi_k^\dagger$, so $\psi(x) = \sum_k \psi_k e^{ikx}$ is a real Majorana field, $\psi(x) = \psi^\dagger(x)$. The edge Hamitonian is:

$$\hat{\mathcal{H}}_{edge} = \sum_{k>0} v_n k\, \psi_k^\dagger \psi_k = \int dx\, \psi(x)(-iv_n\partial_x)\psi(x), \tag{106}$$

where the edge velocity $v = \Delta$. The Lagrangian density takes the form:

$$\mathcal{L}_{\text{fermion}} = i\psi(x)(\partial_t + v_n\partial_x)\psi(x) \tag{107}$$

The $2D$ Ising model can be mapped onto the problem of (non-chiral) Majorana fermions on a lattice. At the critical point, the Majorana fermions become massless. Therefore, the edge excitations are the right-moving chiral part of the critical Ising model. (This is why the vortices of a $p+ip$ superconductor are call Ising anyons.) However, the edge excitations have non-trivial topological structure for the same reason that correlation functions of the spin field are non-trivial in the Ising model: while the fermions are free, the Ising spin field is non-local in terms of the fermions, so its correlations are non-trivial. The Ising spin field $\sigma(z)$ inserts a branch cut running from $z = v_n x + it$ to infinity for the fermion ψ. This is precisely what happens when a flux $hc/2e$ vortex is created in a $p+ip$ superconductor.

The primary fields of the free Majorana fermion are $\mathbf{1}$, σ, and ψ with respective scaling dimensions 0, $1/16$, and $1/2$, as discussed in Section III.D. When there is an odd number of flux $hc/2e$ vortices in the bulk, the edge is in the $\sigma(0)|0\rangle$ sector. When there is an even number, the edge is in either the $|0\rangle$ or $\psi(0)|0\rangle$ sectors, depending on whether there is an even or odd number of fermions in the system. So long as quasiparticles don't go from the edge to the bulk or vice versa, however, the system remains in one of these sectors and all excitations are simply free fermion excitations built on top of the ground state in the relevant sector.

However, when a quasiparticle tunnels from the edge to the bulk (or through the bulk), the edge goes from one sector to another – i.e. it is acted on by a primary field. Hence, in the presence of a constriction at which vortices of fermions can tunnel from one edge to another, the edge Lagrangian of a $p+ip$ superconductor is (Fendley et al., 2007a):

$$S = \int d\tau\, dx\, \left(\mathcal{L}_{\text{fermion}}(\psi_a) + \mathcal{L}_{\text{fermion}}(\psi_b)\right) + \int d\tau\, \lambda_\psi\, i\psi_a\psi_b + \int d\tau\, \lambda_\sigma \sigma_a\sigma_b \tag{108}$$

where a, b denote the two edges. (We have dropped all irrelevant terms, e.g descendant fields.) In other words, although the edge theory is a free theory in the absence of coupling to the bulk or to another edge through the bulk, it is perturbed by primary fields when quasiparticles can tunnel to or from the edge through the bulk. The topological structure of the bulk constrains the edge through the spectrum of primary fields.

As in the discussion of Section III.D, the edge of the Moore-Read Pfaffian quantum Hall state is a chiral Majorana fermion together with a free chiral boson ϕ for the charge sector of the theory. As in the case of a $p+ip$ superconductor, the primary fields of this theory determine how the edge is perturbed by the tunneling of quasiparticles between two edges through the bulk (Fendley et al., 2006, 2007a):

$$\begin{aligned} S = \int d\tau\, \Big[\int dx\, \left(\mathcal{L}_{\text{edge}}(\psi_a,\phi_a) + \mathcal{L}_{\text{edge}}(\psi_b,\phi_b)\right) \\ + \lambda_{1/2}\, \cos((\phi_a(0) - \phi_b(0))/\sqrt{2}) + \lambda_{\psi,0}\, i\psi_a\psi_b \\ + \lambda_{1/4}\, \sigma_a(0)\sigma_b(0)\, \cos((\phi_a(0) - \phi_b(0))/2\sqrt{2})\Big] \end{aligned} \tag{109}$$

The most relevant coupling is $\lambda_{1/4}$, so the tunneling of charge $e/4$ quasiparticles dominates the transport of charge from

one edge to the other at the point contact. (The tunneling of charge $e/2$ quasiparticles makes a subleading contribution while the tunneling of neutral fermions contributes only to thermal transport.) At low enough temperatures, this relevant tunneling process causes the point contact to be pinched off (Fendley et al., 2006, 2007a), but at temperatures that are not too low, we can treat the tunneling of $e/4$ quasiparticles perturbatively and neglect other the other tunneling operators. Of course, the structure of the edge may be more complex than the minimal structure dictated by the bulk which we have analyzed here. This depends on the details of the confining potential defining the system boundary, but at low enough temperatures, the picture described here should still apply. Interesting information about the non-Abelian character of the Moore-Read Pfaffian state can be obtained from the temperature dependence of the tunneling conductance (Fendley et al., 2006, 2007a) and from current noise (Bena and Nayak, 2006).

Finally, we return to SU(2)$_2$. The SU(2)$_2$ WZW model is a triplet of chiral Majorana fermions, ψ_1, ψ_2, ψ_3 – i.e. three identical copies of the chiral Ising model. This triplet is the spin-1 primary field (with scaling dimension $1/2$). The spin-$1/2$ primary field is roughly $\sim \sigma_1\sigma_2\sigma_3$ with dimension $3/16$ (a more precise expression involves the sum of products such as $\sigma_1\sigma_2\mu_3$, where μ is the Ising disorder operator dual to σ). This is one of the primary differences between the Ising model and SU(2)$_2$: σ is a dimension $1/16$ field, while the spin-$1/2$ primary field of SU(2)$_2$ has dimension $3/16$. Another way to understand the difference between the two models is that the SU(2)$_2$ WZW model has two extra Majorana fermions. The pair of Majorana fermions can equally well be viewed as a Dirac fermion or, through bosonization, as a free chiral boson, which has U(1) symmetry. Thus, the Ising model is often written as SU(2)$_2$/U(1) to signify that the the U(1) chiral boson has been removed. (This notion can be made precise with the notion of a *coset* conformal field theory (Di Francesco et al., 1997) or by adding a U(1) gauge field to the 2D action and coupling it to a U(1) subgroup of the SU(2) WZW field g (Gawędzki and Kupiainen, 1988; Karabali et al., 1989). The gauge field has no Maxwell term, so it serves only to eliminate some of the degrees of freedom, namely the U(1) piece.) As we discussed in subsection III.C, these differences are also manifested in the bulk, where they lead to some differences in the Abelian phases which result from braiding but do not change the basic non-Abelian structure of the state.

On the other hand, the edge of the Moore-Read Pfaffian quantum Hall state is a chiral Majorana fermion together with a free chiral boson ϕ which carries the charged degrees of freedom. So we restore the chiral boson which we eliminated in passing from SU(2)$_2$ to the Ising model, with one important difference. The compactification radius R (i.e., the theory is invariant under $\phi \to \phi + 2\pi R$) of the charged boson need not be the same as that of the boson which was removed by cosetting. For the special case of bosons at $\nu = 1$, the boson is, in fact, at the right radius. Therefore, the charge boson can be fermionized so that there is a triplet of Majorana fermions. In this case, the edge theory is the SU(2)$_2$ WZW model (Fradkin et al., 1998). In the case of electrons at $\nu = 2 + 1/2$, the chiral boson is not at this radius, so the edge theory is U(1)$_2\times$Ising, which is not quite the SU(2)$_2$ WZW model.

F. Interferometry with Anyons

In Section II of this review we described an interference experiment that is designed to demonstrate the non-Abelian statistics of quasiparticles in the $\nu = 5/2$ state. We start this section by returning to this experiment, and using it as an exercise for the application of the calculational methods reviewed above. We then generalize our analysis to arbitrary SU(2)$_k$ non-Abelian states and also describe other experiments that share the same goal.

In the experiment that we described in Section II, a Fabry-Perot interference device is made of a Hall bar perturbed by two constrictions (see Fig. 2). The back-scattered current is measured as a function of the area of the cell enclosed by the two constrictions and of the magnetic field. We assume that the system is at $\nu = 5/2$ and consider interference experiments which can determine if the electrons are in the Moore-Read Pfaffian quantum Hall state.

Generally speaking, the amplitude for back–scattering is a sum over trajectories that wind the cell ℓ times, with $\ell = 0, 1, 2...$ an integer. The partial wave that winds the cell ℓ times, winds the n quasiparticles localized inside the cell ℓ times. From the analysis in Section III.B, if the electrons are in the Pfaffian state, the unitary transformation that the tunneling quasiparticle applies on the wave function of the zero energy modes is

$$\left(\hat{U}_n\right)^\ell = \left[e^{i\alpha_n}\gamma_a^n \prod_{i=1}^{n}\gamma_i\right]^\ell \tag{110}$$

where the γ_i's are the Majorana modes of the localized bulk quasiparticles, γ_a is the Majorana mode of the quasiparticle that flows around the cell, and α_n is an Abelian phase that will be calculated below.

The difference between the even and odd values of n, that we described in Section II of the review, is evident from Eq. (110) when we we look at the lowest order, $\ell = 1$. For even n, $\hat{U}_n$ is independent of γ_a. Thus, each tunneling quasiparticle applies the same unitary transformation on the ground state. The flowing current then *measures* the operator $\hat{U}_n$ (more precisely, it measures the interference term, which is an hermitian operator. From that term the value of $\hat{U}_n$ may be extracted). In contrast, when n is odd the operator $\hat{U}_n$ depends on γ_a. Thus, a different unitary operation is applied by every incoming quasiparticle. Moreover, the different unitary operators do not commute, and share no eigenvectors. Thus, their expectation values average to zero, and no interference is to be observed. This analysis holds in fact for all odd values of ℓ.

The phase α_n is composed of two parts. First, the quasiparticle accumulates an Aharonov-Bohm phase of $2\pi e^*\Phi/hc$, where $e^* = e/4$ is the quasiparticle charge for $\nu = 5/2$ and Φ is the flux enclosed. And second, the tunneling quasiparticle accumulates a phase as a consequence of its interaction with the n localized quasiparticles. When a charge $e/4$ object goes

around n flux tubes of half a flux quantum each, the phase it accumulates is $n\pi/4$.

Altogether, then, the unitary transformation (110) has two eigenvalues. For even n, they are $(\pm i)^{nl/2}$. For odd n, they are $(\pm i)^{(n-1)l/2}$. The back–scattered current then assumes the following form (Stern and Halperin, 2006),

$$I_{bs} = \sum_{m=0}^{\infty} I_m \cos^2 mn\frac{\pi}{2} \cos m(\phi + \frac{\tilde{n}\pi}{4} + \frac{\pi\alpha}{2}) \qquad (111)$$

where $\tilde{n} = n$ for n even, and $\tilde{n} = n+1$ for n odd. The m^{th} term of this sum is the contribution from a process that loops around m times, which vanishes if n and m are both odd.

We can restate this analysis using the CFT description of the Moore-Read Pfaffian state. Charge $e/4$ quasiparticles are associated with the operator $\sigma\, e^{i\phi/\sqrt{8}}$ operators. The fusion of n such quasiparticles is then to

$$e^{in\phi/\sqrt{8}} \times \begin{cases} 1 \\ \psi \\ \sigma \end{cases} \qquad (112)$$

where either of the first two is possible for even n, and the last is the outcome of the fusion for odd n. In order to determine the effect of braiding an incoming quasiparticle around the n bulk ones, we consider the possible fusion channels of one quasiparticle with (112). The fusion of the bosonic factors (i.e. the electrical charge) is:

$$e^{in\phi(z_1)/\sqrt{8}} \times e^{i\phi(z_2)/\sqrt{8}} \to e^{i(n+1)\phi(z_1)/\sqrt{8}} (z_1 - z_2)^{-n/8} \qquad (113)$$

Thus, when the incoming quasiparticle, at coordinate z_2, encircles the bulk ℓ times, it accumulates a phase of $2\pi \times (n/8) \times \ell = n\ell\pi/4$ purely as a result of the U(1) part of the theory. Now consider the neutral sector. The fusion of the σ operator depends on the state of the bulk. When the bulk is has total topological charge $\mathbf{1}$, the fusion is trivial, and does not involve any accumulation of phases. When the bulk has total topological charge ψ, the fusion is:

$$\sigma(z_2) \times \psi(z_1) \to \sigma(z_1) \times (z_1 - z_2)^{-1/2} \qquad (114)$$

and an extra phase of $\pi\ell$ is accumulated when the incoming quasiparticle winds the bulk quasiparticles ℓ times. When the bulk has total topological charge σ, i.e. when n is odd, the non-Abelian fusion rule applies (see Eq. A3), and

$$\sigma(z_1) \times \sigma(z_2) \to (z_1 - z_2)^{-1/8} \left[1 + (z_1 - z_2)^{1/2} \psi(z_1)\right] \qquad (115)$$

Since the probability for the two fusion outcomes is equal [8], for any odd ℓ we get two interference patterns that are mutually shifted by π, and hence mutually cancel one another,

[8] This follows from $N_{\sigma\sigma}^{\mathbf{1}} = N_{\sigma\sigma}^{\psi} = 1$.

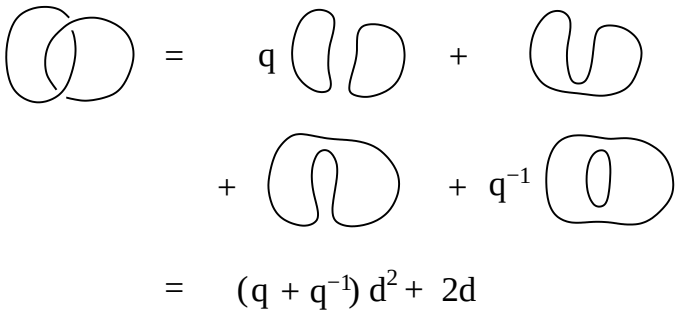

FIG. 10 Using the recursion relation (77), we can evaluate $\langle\chi|\rho(\sigma_2^2)\,|\chi\rangle$.

while for even ℓ we get an extra phase of $\ell\pi/4$. Altogether, this reproduces the expression (111).

Now let us consider the same calculation using the relation between Chern-Simons theory and the Jones polynomial. For simplicity, we will just compute the current due to a single backscattering and neglect multiple tunneling processes, which can be computed in a similar way. The elementary quasiparticles have $j = 1/2$. These are the quasiparticles which will tunnel at the point contacts, either encircling the bulk quasiparticles or not. (Other quasiparticles will give a sub-leading contribution to the current because their tunneling amplitudes are smaller and less relevant in the RG sense.) First, consider the case in which there is a single $j = 1/2$ quasiparticle in the bulk. The back-scattered current is of the form:

$$I_{bs} = I_0 + I_1 \mathrm{Re}\{e^{i\phi}\langle\chi|\rho(\sigma_2^2)|\chi\rangle\} \qquad (116)$$

The matrix element on the right-hand-side is given by the evaluation of the link in Figure 4a (Bonderson et al., 2006a; Fradkin et al., 1998) (up to a normalization of the bra and ket; see Sec. III.C). It is the matrix element between a state $|\chi\rangle$ is the state in which 1 and 2 fuse to the trivial particle as do 3 and 4 and the state $\rho(\sigma_2^2)\,|\chi\rangle$. The former is the state in which the tunneling quasparticle (qp. 3)does not encircle the bulk quasiparticle (qp. 2); the latter is the state in which it does. The matrix element between these two states determines the interference.

Using the recursion relation (77) as shown in Figure 10, we obtain:

$$\begin{aligned} \langle\chi|\rho(\sigma_2^2)\,|\chi\rangle &= \left(q + q^{-1}\right) d^2 + 2d \\ &= -d^3 + 2d \end{aligned} \qquad (117)$$

For $k = 2$, $d = \sqrt{2}$, so this vanishes. Consequently, the interference term in (116) also vanishes, as we found above by other methods. The case of an arbitrary odd number of quasiparticles in the island is similar.

Now consider the case in which there are an even number of quasiparticles in the island. For the sake of simplicity, we consider the case in which there are two quasiparticles in the bulk, i.e. a qubit. The pair can either fuse to $j = 0$ or $j = 1$. In the former case, it is clear that no phase is acquired, see Fig. 11a. In the latter case, the recursion rule (77) gives us a -1,

as depicted in figure 11. This difference allows us to read out the value of a topologically-protected qubit (Das Sarma et al., 2005).

What happens if the qubit is in a superposition of $j = 0$ and $j = 1$? The interference measurement causes the tunneling quasiparticles to become entangled with the bulk quasiparticle (Bonderson et al., 2007; Freedman et al., 2006; Overbosch and Bais, 2001). When the integrated current is large enough that many quasiparticles have tunneled and equilibrated at the current leads, the $j = 0$ and $j = 1$ possibilities will have decohered. The measurement will see one of the two possibilities with corresponding probabilities.

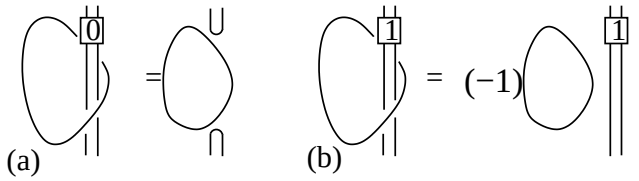

FIG. 11 We can obtain the result of taking a $j = 1/2$ quasiparticle around a qubit from the two diagrams in this figure. In (a) the qubit is in the state 0, while in (b) it is in state 1. These figures are similar to the left-hand-side of Fig. 10, but with the loop on the right replaced by a loop with (a) $j = 0$ or (b) $j = 1$.

The experiment that we analyzed above for $\nu = 5/2$ may be analyzed also for other non-Abelian states. The computation using knot invariants can be immediately adapted to other SU(2)$_k$ states by simply replacing $d = \sqrt{2}$ with $d = 2\cos\pi/(k+2)$. We should calculate the value of the Hopf link as in figures 10 and 11, with one of the loops corresponding to the tunneling quasiparticle and the other loop corresponding to the total topological charge of the bulk quasiparticles. The result can be written in the more general form (Bonderson et al., 2006b):

$$I_{bs}(a) = I_0 + I_1 \, |M_{ab}| \, \cos(\beta + \theta_{ab}) \tag{118}$$

where M_{ab} is defined in terms of the S-matrix:

$$M_{ab} = \frac{S_{ab} S_{\mathbf{11}}}{S_{\mathbf{1}a} S_{\mathbf{1}b}} \tag{119}$$

and $M_{ab} = |M_{ab}| \, e^{i\theta_{ab}}$. The expression (118) gives the current to due to a quasiparticles if the quasiparticles in the bulk fuse to b. If the contribution of $j = 1/2$ quasiparticles dominates, as in the $\nu = 5/2$ case, then we should set $a = \frac{1}{2}$ in this expression. For the level $k = 3$ case, taking $a = \frac{1}{2}$, $|M_{ab}| = 1$ for $b = 0, \frac{3}{2}$ while $|M_{ab}| = \phi^{-2}$ for $b = \frac{1}{2}, 1$, where ϕ is the golden mean, $\phi = (1+\sqrt{5})/2$. (In $\mathbb{Z}_3$ parafermion language, $b = 0, \frac{3}{2}$ correspond to the fields $\mathbf{1}, \psi_{1,2}$ while $b = \frac{1}{2}, 1$ correspond to the fields $\sigma_{1,2}, \varepsilon$.)

Finally, we can analyze the operation of an interferometer using the edge theory (109). The preceding discussion esentially assumed that the current is carried by non-interacting anyonic quasiparticles. However, the edge is gapless and, in general, does not even have well-defined quasiparticles. Therefore, a computation using the edge theory is more complete. The expected results are recovered since they are determined by the topological structure of the state, which is shared by both the bulk and the edge. However, the edge theory also enables one to determine the temperature and voltage dependences of I_0, I_1, ... in (111), (116) (Ardonne and Kim, 2007; Bishara and Nayak, 2007; Fidkowski, 2007). As is discussed in these papers, at finite temperature, interference will not be visible if the two point contacts are further apart than the thermal length scale L_ϕ, where $L_\phi^{-1} = k_B T \left(\frac{1/8}{v_c} + \frac{1/8}{v_n} \right)$, if the charged and neutral mode velocities are v_c, v_n. Another important feature is that the interference term (when it is nonvanishing) is oscillatory in the source-drain voltage while the I_0 term has a simple power law dependence.

The assumption that the edge and the bulk are well separated is crucial to that above calculations of interference, but in practice this may not be the case. When there is bulk-edge tunneling one might imagine that a quasiparticle moving along the edge may tunnel into the bulk for a moment and thereby evade encircling some of the localized quasiparticles thus smearing out any interference pattern. The first theoretical steps to analysing this situation have been taken in (Overbosch and Wen, 2007; Rosenow et al., 2007) where tunnling to a single impurity is considered. Surprisingly it is found that the interfernece pattern is full strength both in the strong tunneling limit as well as in the weak tunneling limit.

While the experiment we described for the $\nu = 5/2$ state does not require a precise determination of n, as it is only its parity that determines the amplitude of the interference pattern, it does require that the number n does not fluctuate within the duration of the experiment. Generally, fluctuations in n would be suppressed by low temperature, large charging energy and diminished tunnel coupling between the bulk and the edge. However, when their suppression is not strong enough, and n fluctuates over a range much larger than 1 within the time of the measurement, two signatures of the non-Abelian statistics of the quasiparticles would still survive, at least as long as the characteristic time scale of these fluctuations is much longer than the time between back–scattering events. First, any change in n would translate to a change in the back–scattered current, or the two-terminal conductance of the device. Hence, fluctuations in n would introduce current noise of the telegraph type, with a unique frequency dependence (Grosfeld et al., 2006). Second, fluctuations in n would suppress all terms in Eq. (111) other than those where $m = 4k$ with k an integer. Thus, the back–scattered current will have a periodicity of one flux quatum Φ_0, and the visibility of the flux oscillations, for weak back–scattering, would be $\frac{I_4}{I_0} \propto I_0^3$.

A similar relation holds also for another type of interference experiment, in which the interferometer is of the Mach-Zehnder type, rather than the Fabry-Perot type. (A Mach-Zehnder interferometer has already been constructed in the integer quantum Hall regime (Ji et al., 2003)). If we are to describe the Mach-Zehnder interferometer in a language close to that we used for the Fabry-Perot one, we would note the following important differences: first, no multiple back–scattering events are allowed. And second, since the area enclosed by the interfering partial waves now encompasses the inner edge, the quantum state of the encircled area *changes with each tunneling quasiparticle*. Thus, it is not surprising

that the outcome of an interference experiment in a Mach-Zehnder geometry will be very close to that of a Fabry-Perot experiment with strong fluctuations in n. The telegraph noise in the Fabry-Perot case(Grosfeld et al., 2006) becomes shot noise in the Mach-Zehnder case. Remarkably(Feldman et al., 2006) the effective charge extracted from that noise carries a signature of the non-Abelian statistics: as the flux is varied, the charge changes from $e/4$ to about $3e$.

Other than interference experiments, there are several proposals for experiments that probe certain aspects of the physics of non-Abelian states. The degeneracy of the ground state in the presence of vortices may be probed(Grosfeld and Stern, 2006) by the consequences of its removal: when the filling factor is $\nu = 5/2 + \epsilon$ with $\epsilon \ll 1$, quasiparticles are introduced into the bulk of the system, with a density proportional to ϵ. For a clean enough sample, and a low enough density, the quasiparticles form a lattice. In that lattice, the Majorana zero modes of the different quasiparticles couple by tunneling, and the degeneracy of the ground states is removed. The subspace of multiply-degenerate ground states is then replaced by a band of excitations. The neutrality of the Majorana modes is removed too, and the excitations carry a charge that is proportional to their energy. This charge makes these modes weakly coupled to an externally applied electric field, and provides a unique mechanism for a dissipation of energy, with a characteristic dependence on the wave vector and frequency of the electric field. Since the tunnel coupling between neighboring quasiparticles depends exponentially on their separation, this mechanism will be exponentially sensitive to the distance of the filling factor from 5/2 (Grosfeld and Stern, 2006).

G. Lattice Models with P, T-Invariant Topological Phases

Our discussion of topological phases has revolved around fractional quantum Hall states because these are the only ones known to occur in nature (although two dimensional ^{3}He-A (Leggett, 1975; Volovik, 1994) and Sr_2RuO_4 may join this list (Kidwingira et al., 2006; Xia et al., 2006)). However, there is nothing inherent in the definition of a topological phase which consigns it to the regime of high magnetic fields and low temperatures. Indeed, highly idealized models of frustrated magnets also show such phases, as we have discussed in section II.D. Of course, it is an open question whether these models have anything to do with any real electronic materials or their analogs with cold atoms in optical lattices, i.e. whether the idealized models can be adiabatically connected to more realistic models. In this section, we do not attempt to answer this question but focus, instead, on understanding how these models of topological phases can be solved. As we will see, their solubility lies in their incorporation of the basic topological structure of the corresponding phases.

One way in which a topological phase can emerge from some microscopic model of interacting electrons, spins, or cold atoms is if the low-lying degrees of freedom of the microscopic model can be mapped to the degrees of freedom of the topological phase in question. As we have seen in section III.C, these degrees of freedom are Wilson loops (59). Loops are the natural degrees of freedom in a topological phase because the topological charge of a particle or collection of particles can only be determined, in general, by taking a test particle around the particle or collection in question. Therefore, the most direct way in which a system can settle into a topological phase is if the microscopic degrees of freedom organize themselves so that the low-energy degrees of freedom are loops or, as we will see below, string nets (in which we allow vertices into which three lines can run). As we will describe more fully below, the Hilbert space of a non-chiral topological phase can be described very roughly as a 'Fock space for loops' (Freedman et al., 2004). Wilson loop operators are essentially creation/annihilation operators for loops. The Hilbert space is spanned by basis states which can be built up by acting with Wilson loop operators on the state with no loops, i.e. $|\gamma_1 \cup \ldots \cup \gamma_n\rangle = W[\gamma_n] \ldots W[\gamma_1]|\emptyset\rangle$ is (vaguely) analgous to $|k_1, \ldots, k_2\rangle \equiv a^\dagger_{k_n} \ldots a^\dagger_{k_1}|0\rangle$. An important difference is that the states in the topological theory must satisfy some extra constraints in order to correctly represent the algebra of the operators $W[\gamma]$. If we write an arbitrary state $|\Psi\rangle$ in the basis given above, $\Psi[\gamma_1 \cup \ldots \cup \gamma_n] = \langle\Psi|\gamma_1 \cup \ldots \cup \gamma_n\rangle$, then the ground state(s) of the theory are linearly independent $\Psi[\gamma_1 \cup \ldots \cup \gamma_n]$ satisfying some constraints.

In fact, we have already seen an example of this in section II.D: Kitaev's toric code model (18). We now represent the solution in a way which makes the emergence of loops clear. We color every link of the lattice on which the spin points up. Then, the first term in (18) requires that there be an even number of colored links emerging from each site on the lattice. In other words, the colored links form loops which never terminate. On the square lattice, loops can cross, but they cannot cross on the honeycomb lattice; for this reason, we will often find it more convenient to work on the honeycomb lattice. The second term in the Hamiltonian requires that the ground state satisfy three further properties: the amplitude for two configurations is the same if one configuration can be transformed into another simply by (1) deforming some loop without cutting it, (2) removing a loop which runs around a single plaquette of the lattice, or (3) cutting open two loops which approach each other within a lattice spacing and rejoining them into a single loop (or vice-versa), which is called *surgery*. A vertex at which the first term in the Hamiltonian is not satisfied is an excitation, as is a plaquette at which the second term is not satisfied. The first type of excitation acquires a -1 when it is taken around the second.

The toric code is associated with the low-energy physics of the deconfined phase of $\mathbb{Z}_2$ gauge theory (Fradkin and Shenker, 1975; Kogut, 1979); see also Senthil and Fisher, 2000 for an application to strongly-correlated electron systems). This low-energy physics can be described by an Abelian BF-theory (Hansson et al., 2004):

$$\begin{aligned} \mathcal{S} &= \frac{1}{\pi}\int e_\mu \epsilon^{\mu\nu\lambda}\partial_\nu a_\lambda \\ &= \mathcal{S}_{CS}\left(a + \tfrac{1}{2}e\right) - \mathcal{S}_{CS}\left(a - \tfrac{1}{2}e\right) \end{aligned} \qquad (120)$$

e_μ is usually denoted b_μ and $\epsilon^{\mu\nu\lambda}\partial_\nu a_\lambda = \frac{1}{2}\epsilon^{\mu\nu\lambda} f_{\nu\lambda}$, hence the name. Note that this theory is non-chiral. Under a combined parity and time-reversal transformation, e_μ must change

sign, and the action is invariant. This is important since it enables the fluctuating loops described above to represent the Wilson loops of the gauge field a_μ. In a chiral theory, it is not clear how to do this since a_1 and a_2 do not commute with each other. They cannot both be diagonalized; we must arbitrarily choose one direction in which Wilson loops are diagonal operators. It is not clear how this will emerge from some microscopic model, where we would expect that loops would not have a preferred direction, as we saw above in the toric code. Therefore, we focus on non-chiral phases, in particular, the SU(2)$_k$ analog of (120) (Cattaneo et al., 1995):

$$\begin{aligned} \mathcal{S} &= \mathcal{S}^k_{CS}(a+e) - \mathcal{S}^k_{CS}(a-e) \\ &= \frac{k}{4\pi}\int \mathrm{tr}\left(e\wedge f + \frac{1}{3}e\wedge e\wedge e\right) \end{aligned} \qquad (121)$$

We will call this theory *doubled* SU(2)$_k$ Chern-Simons theory (Freedman et al., 2004).

We would like a microscopic lattice model whose low-energy Hilbert space is composed of wavefunctions $\Psi[\gamma_1 \cup \ldots \cup \gamma_n]$ which assign a complex amplitude to a given configuration of loops. The model must differ from the toric code in the constraints which it imposes on these wavefunctions. The corresponding constraints for (121) are essentially the rules for Wilson loops which we discussed in subsection III.C (Freedman et al., 2004). For instance, ground state wavefunctions should *not* give the same the amplitude for two configurations if one configuration can be transformed into another simply by removing a loop which runs around a single plaquette of the lattice. Instead, the amplitude for the former configuration should be larger by a factor of $d = 2\cos\pi/(k+2)$, which is the value of a single unknotted Wilson loop. Meanwhile, the appropriate surgery relation is not the joining of two nearby loops into a single one, but instead is the condition that when $k+1$ lines come close together, the amplitudes for configurations in which they are cut open and rejoined in different ways satisfy some linear relation. This relation is essentially the requirement that the $j = (k+1)/2$ Jones-Wenzl projector should vanish within any loop configuration, as we might expect since a Wilson loop carrying the corresponding SU(2) representation should vanish.

The basic operators in the theory are Wilson loops, $W[\gamma]$, of the gauge field a^a_μ in (121) in the fundamental ($j = 1/2$) representation of SU(2). A Wilson loop in a higher j representation can be constructed by simply taking $2j$ copies of a $j = 1/2$ Wilson loop and using the appropriate Jones-Wenzl projector to eliminate the other representations which result in the fusion of $2j$ copies of $j = 1/2$. If the wavefunction satisfies the constraint mentioned above, then it will vanish identically if acted on by a $j > k/2$ Wilson loop.

These conditions are of a topological nature, so they are most natural in the continuum. In constructing a lattice model from which they emerge, we have a certain amount of freedom in deciding how these conditions are realized at the lattice scale. Depending on our choice of short-distance regularization, the model may be more of less easily solved. In some cases, an inconvenient choice of short-distance regularization may actually drive the system out of the desired topological phase. Loops on the lattice prove not to be the most convenient regularization of loops in the continuum, essentially because when d is large, the lattice fills up with loops which then have no freedom to fluctuate (Freedman et al., 2004). Instead, trivalent graphs on the lattice prove to be a better way of proceeding (and, in the case of SU(3)$_k$ and other gauge groups, trivalent graphs are essential (Kuperberg, 1996; Turaev and Viro, 1992)). The most convenient lattice is the honeycomb lattice, since each vertex is trivalent. A trivalent graph is simply a subset of the links of the honeycomb lattice such that no vertex has only a single link from the subset emanating from it. Zero, two, or three links can emanate from a vertex, corresponding to vertices which are not visited by the trivalent graph, vertices through which a curve passes, and vertices at which three curves meet. We will penalize energetically vertices from which a single colored link emanates. The ground state will not contain such vertices, which will be quasiparticle excitations. Therefore, the ground state $\Psi[\Gamma]$ assigns a complex amplitude to a trivalent graph Γ.

Such a structure arises in a manner analogous to the loop structure of the toric code: if we had spins on the links of the honeycomb lattice, then an appropriate choice of interaction at each vertex will require that colored links (on which the spin points up) form a trivalent graph. We note that links can be given a further labeling, although we will not discuss this more complicated situation in any detail. Each colored link can be assigned a j in the set $\frac{1}{2}, 1, \ldots, \frac{k}{2}$. Uncolored links are assigned $j = 0$. Rather than spin-$1/2$ spins on each link, we should take spin-$k/2$ on each link, with $S_z = -k/2$ corresponding to $j = 0$, $S_z = -k/2+1$ corresponding to $j = 1/2$, etc. (or perhaps, we may want to consider models with rather different microscopic degrees of freedom). In this case, we would further require that the links around each vertex should satisfy the branching rules of SU(2)$_k$: $|j_1 - j_2| \geq j_3 \leq \min\left(j_1 + j_2, \frac{k}{2} - j_1 - j_2\right)$. The case which we have described in the previous paragraph, without the additional j label could be applied to the level $k = 1$ case, with colored links carrying $j = 1/2$ or to level $k = 3$, with colored links carrying $j = 1$, as we will discuss further below. A trivalent graph represents a loop configuration in the manner depicted in Figure 12a. One nice feature is that the Jones-Wenzl projections are enforced on every link from the start, so no corresponding surgery constraint is needed.

If we would like a lattice model to be in the doubled SU(2)$_3$ universality class, which has quasiparticle excitations which are Fibonacci anyons, then its Hamiltonian should impose the following: all low-energy states should have vanishing amplitude on configurations which are are not trivalent graphs, as defined above; and the amplitude for a configuration with a contractible loop should be larger than the amplitude for a configuration without this loop by a factor of $d = 2\cos\frac{\pi}{5} = \phi = (1+\sqrt{5})/2$ for a closed, contractible loop. These conditions can be imposed by terms in the Hamiltonian which are more complicated versions of the vertex and plaquette terms of (18). It is furthermore necessary for the ground state wavefunction(s) to assign the same amplitude to any two trivalent graphs which can be continuously deformed into each other. However, as mentioned above, surgery is not necessary. The Hamiltonian takes the form (Levin and Wen, 2005b) (see also

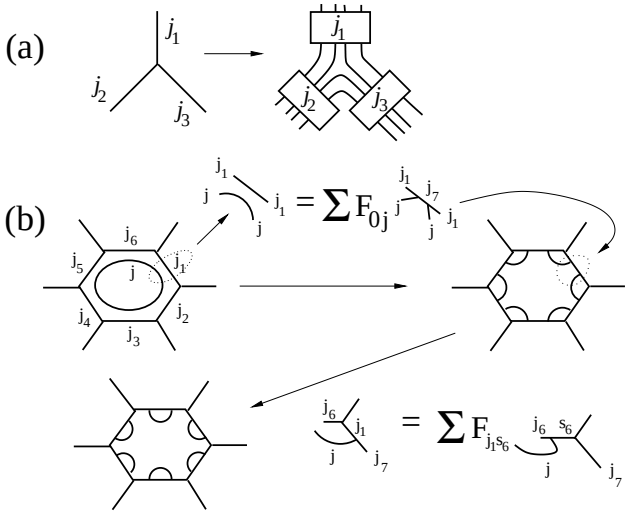

FIG. 12 (a) $j/2$ parallel lines projected onto representation j are represented by the label j on a link. (b) The plaquette terms add a rep.-j loop. This can be transformed back into a trivalent graph on the lattice using the F-matrix as shown.

Turaev and Viro, 1992):

$$H = -J_1 \sum A_i - J_2 \sum_p \sum_{j=0}^{k/2} F_p^{(j)} \qquad (122)$$

Here and below, we specialize to $k = 3$. The degrees of freedom on each link are $s = 1/2$ spins; $s_z = +\frac{1}{2}$ is interpreted as a $j = 1$ colored link, while $s_z = -\frac{1}{2}$ is interpreted as a $j = 0$ uncolored link. The vertex terms impose the triangle inequality, $|j_1 - j_2| \geq j_3 \leq \min\left(j_1 + j_2, \frac{3}{2} - j_1 - j_2\right)$, on the three j's on the links neighboring each vertex. For Fibonacci anyons (see Sec. IV.B), which can only have $j = 0, 1$, this means that if links with $j = 1$ are colored, then the colored links must form a trivalent graph, i.e. no vertex can have only a single up-spin adjacent to it. (There is no further requirement, unlike in the general case, in which there are additional labels on the trivalent graph.)

The plaquette terms in the Hamiltonian are complicated in form but their action can be understood in the following simple way: we imagine adding to a plaquette a loop γ carrying representation j and require that the amplitude for the new configuration $\Psi[\Gamma \cup \gamma]$ be larger than the amplitude for the old configuration by a factor of d_j. For Fibonacci anyons, the only non-trivial representation is $j = 1$; we require that the wavefunction change by a factor of $d = \phi$ when such a loop is added. If the plaquette is empty, then 'adding a loop' is simple. We simply have a new trivalent graph with one extra loop. If the plaquette is not empty, however, then we need to specify how to 'add' the additional loop to the occupied links. We draw the new loop in the interior of the plaquette so that it runs alongside the links of the plaquette, some of which are occupied. Then, we use the F-matrix, as depicted in Figure 12b, to recouple the links of the plaquette (Levin and Wen, 2005b) (see also Turaev and Viro, 1992). This transforms the plaquette so that it is now in a superposition of states with different j's, as depicted in Figure 12b; the coefficients in the superposition are sums of products of elements of the F-matrix. The plaquette term commutes with the vertex terms since adding a loop to a plaquette cannot violate the triangle inequality (see Figure 12a). Clearly vertex terms commute with each other, as do distant plaquette terms. Plaquette terms on adjacent plaquettes also commute because they just add loops to the link which they share. (This is related to the pentagon identity, which expresses the associativity of fusion.) Therefore, the model is exactly soluble since all terms can be simultaneously diagonalized. Vertices with a single adjacent colored (ie. monovalent vertices) are non-Abelian anyonic excitations carrying $j = 1$ under the SU(2) gauge group of a^a_μ in (121). A state at which the plaquette term in (122) is not satisfied is a non-Abelian anyonic excitation carrying $j = 1$ under the SU(2) gauge group of e^a_μ (or, equivalently, a^a_μ flux).

One interesting feature of the ground state wavefunction $\Psi[\Gamma]$ of (122), and of related models with loop representations (Fendley and Fradkin, 2005; Fidkowski et al., 2006; Freedman et al., 2004) is their relation to the Boltzmann weights of statistical mechanical models. For instance, the norm squared of ground state of of (122), satisfies $|\Psi[\Gamma]|^2 = e^{-\beta H}$, where βH is the Hamiltonian of the $q = \phi + 2$ state Potts model. More precisely, it is the low-temperature expansion of the $q = \phi + 2$ state Potts model extrapolated to infinite temperature $\beta = 0$. The square of the ground state of the toric code (18) is the low-temperature expansion of the Boltzmann weight of the $q = 2$ state Potts model extrapolated to infinite temperature $\beta = 0$. On the other hand, the squares of the ground states $|\Psi[\gamma_1 \cup \ldots \cup \gamma_n]|^2$ of loop models (Freedman et al., 2004), are equal to the partition functions of O(n) loop gas models of statistical mechanics, with $n = d^2$. These relations allow one to use known results from statistical mechanics to compute equal-time ground state correlation functions in a topological ground state, although the interesting ones are usually of operators which are non-local in the original quantum-mechanical degrees of freedom of the model.

It is also worth noting that a quasi-one-dimensional analog has been studied in detail (Bonesteel and Yang, 2007; Feiguin et al., 2007a). It is gapless for a single chain and has an interesting phase diagram for ladders.

Finally, we note that the model of Levin and Wen is, admittedly, artificial-looking. However, a model in the same universality class might emerge from simpler models (Fidkowski et al., 2006). Since (122) has a gap, it will be stable against small perturbations. In the case of the toric code, it is known that even fairly large perturbations do not destabilize the state (Trebst et al., 2007).

This brings to a close our survey of the physics of topological phases. In section IV, we will consider their application to quantum computing.

IV. QUANTUM COMPUTING WITH ANYONS

A. $\nu = 5/2$ Qubits and Gates

A topological quantum computer is constructed using a system in a non-Abelian topological phase. A computation is performed by creating quasiparticles, braiding them, and measuring their final state. In section II.C.4, we saw how a qubit could be constructed with the $\nu = 5/2$ state and a NOT gate applied. In this section, we discuss some ideas about how a quantum computer could be built by extending these ideas.

The basic feature of the Ising TQFT and its close relative, SU(2)$_2$, which we exploit for storing quantum information is the existence of two fusion channels for a pair of σ quasiparticles, $\sigma \times \sigma \sim \mathbf{1} + \psi$. When the fusion outcome is $\mathbf{1}$, we say that the qubit is in the state $|0\rangle$; when it is ψ, the state $|1\rangle$. When there are $2n$ quasiparticles, there is a 2^{n-1}-dimensional space of states. (This is how many states there are with total topological charge $\mathbf{1}$; there is an equal number with total topological charge ψ.) We would like to use this 2^{n-1}-dimensional space to store quantum information; the most straightforward way to do so is to view it as $n-1$ qubits.

Generalizing the construction of section II.C.4 to many pairs of anti-dots, we can envision (Freedman et al., 2006) an $(n-1)$-qubit system which is a Hall bar with $2n$ antidots at which quasiholes are pinned, as in Figure 13.

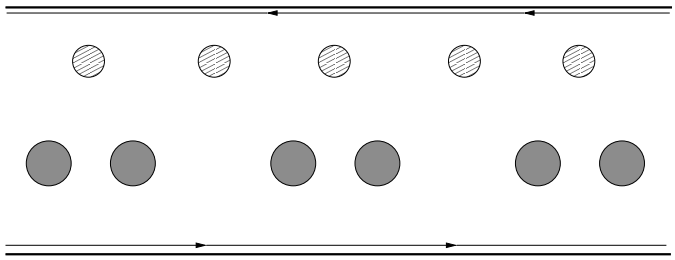

FIG. 13 A system with n quasihole pairs (held at pairs of anti-dots, depicted as shaded circles) supports n qubits. Additional antidots (hatched) can be used to move the quasiparticles.

The NOT gate discussed in section II.C.4 did not require us to move the quasiparticles comprising the qubit, only additional quasiparticles which we brought in from the edge. However, to implement other gates, we will need to move the quasiparticles on the anti-dots. In this figure, we have also depicted additional anti-dots which can be used to move quasiparticles from one anti-dot to another (e.g. as a 'bucket brigade'), see, for instance, Simon, 2000. If we exchange two quasiparticles from the same qubit, then we apply the phase gate $U = e^{\pi i/8}\,\mathrm{diag}(R_1^{\sigma\sigma}, R_\psi^{\sigma\sigma})$ (the phase in front of the matrix comes from the U(1) part of the theory). However, if the two quasiparticles are from different qubits, then we apply the transformation

$$U = \frac{1}{\sqrt{2}} \begin{pmatrix} 1 & 0 & 0 & -i \\ 0 & 1 & -i & 0 \\ 0 & -i & 1 & 0 \\ -i & 0 & 0 & 1 \end{pmatrix}. \qquad (123)$$

to the two-qubit Hilbert space.

By coupling two qubits in this way, a CNOT gate can be constructed. Let us suppose that we have 4 quasiparticles. Then, the first pair can fuse to either $\mathbf{1}$ or ψ, as can the second pair. Naively, this is 4 states but, in fact, it is really two states with total topological charge $\mathbf{1}$ and two states with total topological charge ψ. These two subspaces cannot mix by braiding the four quasiparticles. However, by braiding our qubits with additional quasiparticles, we can mix these four states. (In our single qubit NOT gate, we did this by using quasiparticles from the edge.) Therefore, following Georgiev, 2006, we consider a system with 6 quasiparticles. Quasiparticles 1 and 2 will be qubit 1; when they fuse to 1 or ψ, qubit 1 is in state $|0\rangle$ or $|1\rangle$. Quasiparticles 5 and 6 will be qubit 2; when they fuse to $\mathbf{1}$ or ψ, qubit 2 is in state $|0\rangle$ or $|1\rangle$. Quasiparticles 3 and 4 soak up the extra ψ, if necessary to maintain total topological charge $\mathbf{1}$ for the entire six-quasiparticle system. In the four states $|0,0\rangle$, $|1,0\rangle$, $|0,1\rangle$, and $|1,1\rangle$, the quasiparticle pairs fuse to $\mathbf{1},\mathbf{1},\mathbf{1}$, to $\psi,\psi,\mathbf{1}$, to $\mathbf{1},\psi,\psi$, and to $\psi,\mathbf{1},\psi$, respectively.

In this basis, $\rho(\sigma_1)$, $\rho(\sigma_3)$, $\rho(\sigma_5)$ are diagonal, while $\rho(\sigma_2)$ and $\rho(\sigma_4)$ are off-diagonal (e.g. $\rho(\sigma_2)$ is (123) rewritten in the two qubit/six quasiparticle basis). By direct calculation (e.g. by using $\rho(\sigma_i) = e^{\frac{\pi}{4}\gamma_i\gamma_{i+1}}$), it can be shown (Georgiev, 2006) that:

$$\rho(\sigma_3^{-1}\sigma_4\sigma_3\sigma_1\sigma_5\sigma_4\sigma_3^{-1}) = \begin{pmatrix} 1 & 0 & 0 & 0 \\ 0 & 1 & 0 & 0 \\ 0 & 0 & 0 & 1 \\ 0 & 0 & 1 & 0 \end{pmatrix}. \qquad (124)$$

which is simply a controlled NOT operation.

One can presumably continue in this way, with one extra pair of quasiparticles, which is used to soak up an extra ψ if necessary. However, this is not a particularly convenient way of proceeding since various gates will be different for different numbers of particles: the CNOT gate above exploited the extra quasiparticle pair which is shared equally between the two qubits acted on by the gate, but this will not work in the same way for more than two qubits. Instead, it would be easier to encode each qubit in four quasiparticles. If each quartet of quasiparticles has total topological charge $\mathbf{1}$, then it can be in either of two states since a given pair within a quartet can fuse to either $\mathbf{1}$ or ψ. In other words, each quasiparticle pair comes with its own spare pair of quasiparticles to soak up its ψ if necessary.

Unfortunately, the SU(2)$_2$ phase of matter is not capable of universal quantum computation, i.e. the transformations generated by braiding operations are not sufficient to implement all possible unitary transformations (Freedman et al., 2002a,b). The reason for this shortcoming is that in this theory, braiding of two particles has the effect of a 90 degree rotation (Nayak and Wilczek, 1996) in the multi-quasiparticle Hilbert space. Composing such 90 degree rotations will clearly not allow one to construct arbitrary unitary operations (the set of 90 degree rotations form a finite closed set).

However, we do not need to supplement braiding with much in order to obtain a universal gate set. All that is needed

is a single-qubit $\pi/8$ phase gate and a two-qubit measurement. One way to implement these extra gates is to use some non-topological operations (Bravyi, 2006). First, consider the single-qubit phase gate. Suppose quasiparticles $1, 2, 3, 4$ comprise the qubit. The states $|0\rangle$ and $|1\rangle$ correspond to 1 and 2 fusing to $\mathbf{1}$ or ψ (3 and 4 must fuse to the same as 1 and 2, since the total topological charge is required to be $\mathbf{1}$). If we bring quasiparticles 1 and 2 close together then their splitting will become appreciable. We expect it to depend on the separation r as $\Delta E(r) \sim e^{-r\Delta/c}$, where r is the distance between the quasiparticles and c is some constant with dimensions of velocity. If we wait a time T_p before pulling the quasiparticles apart again, then we will apply the phase gate (Freedman et al., 2006) $U_P = \mathrm{diag}(1, e^{i\Delta E(r)\, T_p})$. If the time T and distance r are chosen so that $\Delta E(r)\, T_p = \pi/4$, then up to an overall phase, we would apply the phase gate:

$$U_{\pi/8} = \begin{pmatrix} e^{-\pi i/8} & 0 \\ 0 & e^{\pi i/8} \end{pmatrix} \tag{125}$$

We note that, in principle, by measuring the energy when the two quasiparticles are brought together, the state of the qubit can be measured.

The other gate which we need for universal quantum computation is the non-destructive measurement of the total topological charge of any four quasiparticles. This can be done with an interference measurement. Suppose we have two qubits which are associated with quasiparticles $1, 2, 3, 4$ and quasiparticles $5, 6, 7, 8$ and we measure the total topological charge of $3, 4, 5, 6$. The interference measurement is of the type described in subsection II.C.3: edge currents tunnel across the bulk at two points on either side of the set of four quasiparticles. Depending on whether the four quasiparticles have total topological charge $\mathbf{1}$ or ψ, the two possible trajectories interfere with a phase ± 1. We can thereby measure the total parity of two qubits. (For more details, see Freedman et al., 2006.)

Neither of these gates can be applied exactly, which means that we are surrendering some of the protection which we have worked so hard to obtain and need some software error correction. However, it is not necessary for the $\pi/8$ phase gate or the two qubit measurement to be extremely accurate in order for error correction to work. The former needs to be accurate to within 14% and the latter to within 38% (Bravyi, 2006). Thus, the requisite quantum error correction protocols are not particularly stringent.

An alternate solution, at least in principle, involves changing the topology of the manifold on which the quasiparticles live (Bravyi and Kitaev, 2001). This can be realized in a device by performing interference measurements in the presence of moving quasiparticles (Freedman et al., 2006).

However, a more elegant approach is to work with a non-Abelian topological state which supports universal topological quantum computation through quasiparticle braiding alone. In the next subsection, we give an example of such a state and how quantum computation can be performed with it. In subsection IV.C, we sketch the proof that a large class of such states is universal.

B. Fibonacci Anyons: a Simple Example which is Universal for Quantum Computation

One of the simplest models of non-Abelian statistics is known as the Fibonacci anyon model, or "Golden theory" (Bonesteel et al., 2005; Freedman et al., 2002a; Hormozi et al., 2007; Preskill, 2004). In this model, there are only two fields, the identity ($\mathbf{1}$) as well as single nontrivial field usually called τ which represents the non-Abelian quasiparticle. (Note there is no field representing the underlying electron in this simplified theory). There is a single nontrivial fusion rule in this model

$$\tau \times \tau = \mathbf{1} + \tau \tag{126}$$

which results in the Bratteli diagram given in Fig. 9b. This model is particularly simple in that any cluster of quasiparticles can fuse only to $\mathbf{1}$ or τ.

The $j = 0$ and $j = 1$ quasiparticles in SU(2)$_3$ satisfy the fusion rules of Fibonacci anyons. Therefore, if we simply omit the $j = 1/2$ and $j = 3/2$ quasiparticles from SU(2)$_3$, we will have FIbonacci anyons. This is perfectly consistent since half-integral j will never arise from the fusions of integral js; the model with only integer spins can be called SO(3)$_2$ or, sometimes, 'the even part of SU(2)$_3$'. As a result of the connection to SU(2)$_3$, sometimes $\mathbf{1}$ is called q-spin "0" and τ is called q-spin "1" (see (Hormozi et al., 2007)). $\mathbb{Z}_3$ parafermions are equivalent to a coset theory SU(2)$_3$/U(1). This can be realized with an SU(2)$_3$ WZW model in which the U(1) subgroup is coupled to a gauge field (Gawędzki and Kupiainen, 1988; Karabali et al., 1989). Consequently, $\mathbb{Z}_3$ parafermions have essentially the same fusion rules as SU(2)$_3$; there are some phase differences between the two theories which show up in the R and F-matrices. In the $\mathbb{Z}_3$ parafermion theory, the field ϵ which results from fusing σ_1 with ψ_1 satisfies the Fibonacci fusion rule Eq. 126, i.e., $\epsilon \times \epsilon = \mathbf{1} + \epsilon$.

As with the $\mathbb{Z}_3$ parafermion model described above, the dimension of the Hilbert space with n quasiparticles (i.e., the number of paths through the Bratteli diagram 9b terminating at $\mathbf{1}$) is given by the Fibonacci number Fib$(n-1)$, hence the name Fibonacci anyons. And similarly the number terminating at τ is Fib(n). Therefore, the quantum dimension of the τ particle is the golden mean, $d_\tau = \phi \equiv (1+\sqrt{5})/2$ (from which the theory receives the name "golden" theory). The Fibonacci model is the simplest known non-Abelian model that is capable of universal quantum computation (Freedman et al., 2002a). (In the next section, the proof will be described for SU(2)$_3$, but the Fibonacci theory, which is its even part, is also universal.) It is thus useful to study this model in some detail. Many of the principles that are described here will generalize to other non-Abelian models. We note that a detailed discussion of computing with the Fibonacci model is also given in Hormozi et al., 2007.

(a) Structure of the Hilbert Space: An important feature of non-Abelian systems is the detailed structure of the Hilbert space. A given state in the space will be described by a "fusion path", or "fusion tree" (See appendix A). For example, using the fusion rule (126), or examining the Bratteli diagram we see that when two τ particles are present, they may fuse into

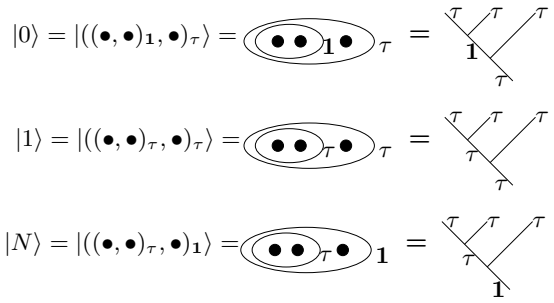

FIG. 14 The three possible states of three Fibonacci particles, shown in several common notations. The "quantum number" of an individual particle is τ. In the parenthesis and ellipse notation (middle), each particle is shown as a black dot, and each pair of parenthesis or ellipse around a group of particles is labeled at the lower right with the total quantum number associated with the fusion of that group. Analogously in the fusion tree notation (right) we group particles as described by the branching of the tree, and each line is labeled with the quantum number corresponding to the fusion of all the particles in the branches above it. For example on the top line the two particles on the left fuse to form $\mathbf{1}$ which then fuses with the remaining particle on the right to form τ. As discussed below in section IV.B.c, three Fibonacci particles can be used to represent a qubit. The three possible states are labeled (far left) as the logical $|0\rangle$, $|1\rangle$ and $|N\rangle$ (noncomputational) of the qubit.

two possible orthogonal degenerate states – one in which they fuse to form $\mathbf{1}$ and one in which they fuse to form τ. A convenient notation (Bonesteel et al., 2005) for these two states is $|(\bullet,\bullet)_{\mathbf{1}}\rangle$ and $|(\bullet,\bullet)_\tau\rangle$. Here, each $\bullet$ represents a particle. From the fusion rule, when a third is added to two particles already in the $\mathbf{1}$ state (i.e., in $|(\bullet,\bullet)_{\mathbf{1}}\rangle$) it must fuse to form τ. We denote the resulting state as $|((\bullet,\bullet)_{\mathbf{1}},\bullet)_\tau\rangle \equiv |0\rangle$. But if the third is added to two in the τ state, it may fuse to form either τ or $\mathbf{1}$, giving the two states $|((\bullet,\bullet)_\tau,\bullet)_\tau\rangle \equiv |1\rangle$ and $|((\bullet,\bullet)_\tau,\bullet)_{\mathbf{1}}\rangle \equiv |N\rangle$ respectively. (The notations $|0\rangle, |1\rangle$ and $|N\rangle$ will be discussed further below). Thus we have a three dimensional Hilbert space for three particles shown using several notations in Fig. 14.

In the previous example, and in Fig. 14 we have always chosen to fuse particles together starting at the left and going to the right. It is, of course, also possible to fuse particles in the opposite order, fusing the two particles on the right first, and then fusing with the particle furthest on the left last. We can correspondingly denote the three resulting states as $|(\bullet,(\bullet,\bullet)_{\mathbf{1}})_\tau\rangle$, $|(\bullet,(\bullet,\bullet)_\tau)_\tau\rangle$, and $|(\bullet,(\bullet,\bullet)_\tau)_{\mathbf{1}}\rangle$. The space of states that is spanned by fusion of non-Abelian particles is independent of the fusion order. However, different fusion orders results in a different basis set for that space. This change of basis is precisely that given by the F-matrix. For Fibonacci anyons it is easy to see that

$$|(\bullet,(\bullet,\bullet)_\tau)_{\mathbf{1}}\rangle = |((\bullet,\bullet)_\tau,\bullet)_{\mathbf{1}}\rangle \qquad (127)$$

since in either fusion order there is only a single state that has total topological charge $\mathbf{1}$ (the overall quantum number of a group of particles is independent of the basis). However, the other two states of the three particle space transform nontrivially under change of fusion order. As described in appendix A, we can write a change of basis using the F-matrix as

$$|(\bullet,(\bullet,\bullet)_i)_k\rangle = \textstyle\sum_j\ [F_k^{\tau\tau\tau}]_{ij}\ \ |((\bullet,\bullet)_j,\bullet)_k\rangle \qquad (128)$$

where i, j, k take the values of the fields $\mathbf{1}$ or τ. (This is just a rewriting of a special case of Fig. 23). Clearly from Eq. 127, $F_{\mathbf{1}}^{\tau\tau\tau}$ is trivially unity. However, the two-by-two matrix $F_\tau^{\tau\tau\tau}$ is nontrivial

$$[F_\tau^{\tau\tau\tau}] = \begin{pmatrix} F_{\mathbf{11}} & F_{\mathbf{1}\tau} \\ F_{\tau\mathbf{1}} & F_{\tau\tau} \end{pmatrix} = \begin{pmatrix} \phi^{-1} & \sqrt{\phi^{-1}} \\ \sqrt{\phi^{-1}} & -\phi^{-1} \end{pmatrix} \qquad (129)$$

Using this F matrix, one can translate between bases that describe arbitrary fusion orders of many particles.

For the Fibonacci theory (Preskill, 2004), it turns out to be easy to calculate the F-matrix using a consistency condition known as the pentagon equation (Fuchs, 1992; Goméz et al., 1996; Moore and Seiberg, 1988, 1989). This condition simply says that one should be able to make changes of basis for four particles in several possible ways and get the same result in the end. As an example, let us consider

$$\begin{aligned} |(\bullet,(\bullet,(\bullet,\bullet)_{\mathbf{1}})_\tau)_{\mathbf{1}}\rangle &= |((\bullet,\bullet)_{\mathbf{1}},(\bullet,\bullet)_{\mathbf{1}})_{\mathbf{1}}\rangle \\ &= |((\bullet,\bullet)_{\mathbf{1}},\bullet)_\tau,\bullet)_{\mathbf{1}}\rangle \end{aligned} \qquad (130)$$

where both equalities, as in Eq. 127 can be deduced from the fusion rules alone. For example, in the first equality, given (on the left hand side) that the overall quantum number is $\mathbf{1}$ and the rightmost two particles are in a state $\mathbf{1}$, then (on the right hand side) when we fuse the leftmost two particles they must fuse to $\mathbf{1}$ such that the overall quantum number remains $\mathbf{1}$. On the other hand, we can also use the F-matrix (Eq. 128) to write

$$\begin{aligned} &|(\bullet,(\bullet,(\bullet,\bullet)_{\mathbf{1}})_\tau)_1\rangle = \qquad (131)\\ &F_{\mathbf{11}}|(\bullet,((\bullet,\bullet)_{\mathbf{1}},\bullet)_\tau)_{\mathbf{1}}\rangle + F_{\mathbf{1}\tau}|(\bullet,((\bullet,\bullet)_\tau,\bullet)_\tau)_{\mathbf{1}}\rangle = \\ &F_{\mathbf{11}}|((\bullet,(\bullet,\bullet)_{\mathbf{1}})_\tau,\bullet)_{\mathbf{1}}\rangle + F_{\mathbf{1}\tau}|((\bullet,(\bullet,\bullet)_\tau)_\tau,\bullet)_{\mathbf{1}}\rangle = \\ &\textstyle\sum_j (F_{\mathbf{11}}F_{\mathbf{1}j} + F_{\mathbf{1}\tau}F_{\tau j})\,|((\bullet,\bullet)_j,\bullet)_\tau,\bullet)_{\mathbf{1}}\rangle \end{aligned}$$

Comparing to Eq. 130, yields $F_{\mathbf{1}\tau}(F_{\mathbf{11}} + F_{\tau\tau}) = 0$ and $F_{\mathbf{11}}F_{\mathbf{11}} + F_{\mathbf{1}\tau}F_{\tau\mathbf{1}} = 1$. This, and other similar consistency identities, along with the requirement that F be unitary, completely fix the Fibonacci F-matrix to be precisely that given in Eq. 129 (up to a gauge freedom in the definition of the phase of the basis states).

(b) Braiding Fibonacci Anyons: As discussed in the introduction, for non-Abelian systems, adiabatically braiding particles around each other results in a unitary operation on the degenerate Hilbert space. Here we attempt to determine which unitary operation results from which braid. We start by considering what happens to two Fibonacci particles when they are braided around each other. It is known (Fuchs, 1992) that the topological spin Θ_τ of a Fibonacci field τ is $\Theta_\tau \equiv e^{2\pi i\Delta_\tau} = e^{4\pi i/5}$. (Note that Δ_τ is also the dimension of the ϵ field of the $\mathbb{Z}_3$ theory, see Appendix A.) With this information, we can use the OPE (see Appendix A)as in section III.D above, to determine the phase accumulated when two

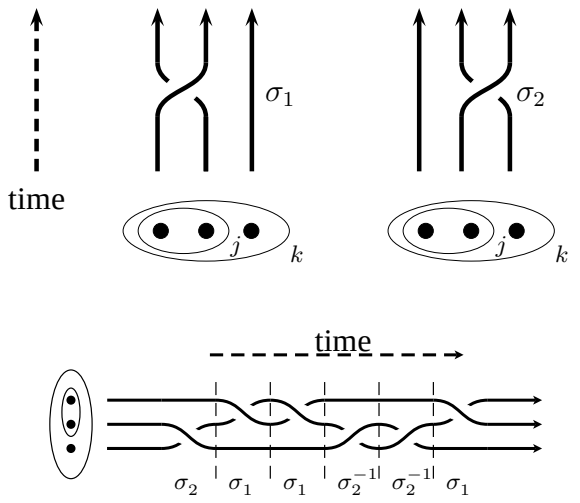

FIG. 15 **Top:** The two elementary braid operations σ_1 and σ_2 on three particles. **Bottom:** Using these two braid operations and their inverses, an arbitrary braid on three strands can be built. The braid shown here is written as $\sigma_2\sigma_1\sigma_1\sigma_2^{-1}\sigma_2^{-1}\sigma_1$.

particles wrap around each other. If the two τ fields fuse together to form $\mathbf{1}$, then taking the two fields around each other clockwise results in a phase $-8\pi/5 = 2\pi(-2\Delta_\tau)$ whereas if the two fields fuse to form τ, taking the two fields around each other results in a phase $-4\pi/5 = 2\pi(-\Delta_\tau)$. Note that a Fibonacci theory with the opposite chirality can exist too (an "antiholomorphic theory"), in which case one accumulates the opposite phase. A particularly interesting non-chiral (or "achiral") theory also exists which is equivalent to a combination of two chiral Fibonacci theories with opposite chiralities. In section III.G, we discussed lattice spin models (Levin and Wen, 2005b) which give rise to a non-chiral (or "achiral") theory which is equivalent to a combination of two chiral Fibonacci theories with opposite chiralities. We will not discuss these theories further here.

Once we have determined the phase accumulated for a full wrapping of two particles, we then know that clockwise exchange of two particles (half of a full wrapping) gives a phase of $\pm 4\pi/5$ if the fields fuse to $\mathbf{1}$ or $\pm 2\pi/5$ if the fields fuse to τ. Once again we must resort to consistency conditions to determine these signs. In this case, we invoke the so-called "hexagon"-identities (Fuchs, 1992; Moore and Seiberg, 1988, 1989) which in essence assure that the rotation operations are consistent with the F-matrix, i.e., that we can rotate before or after changing bases and we get the same result. (Indeed, one way of proving that $\Delta_\tau = 2/5$ is by using this consistency condition). We thus determine that the R-matrix is given by

$$\hat{R}\,|(\bullet,\bullet)_{\mathbf{1}}\rangle = e^{-4\pi i/5}\ |(\bullet,\bullet)_{\mathbf{1}}\rangle \tag{132}$$

$$\hat{R}\,|(\bullet,\bullet)_{\tau}\rangle = -e^{-2\pi i/5}\ |(\bullet,\bullet)_{\tau}\rangle \tag{133}$$

i.e., $R^1_{\tau\tau} = e^{-4\pi i/5}$ and $R^\tau_{\tau\tau} = -e^{2\pi i/5}$. Using the R-matrix, as well as the basis changing F-matrix, we can determine the unitary operation that results from performing any braid on any number of particles. As an example, let us consider three particles. The braid group is generated by σ_1 and σ_2. (See Fig. 15) As discussed above, the Hilbert space of three particles is three-dimensional as shown in Fig. 14. We can use Eqs. 132 and 133 trivially to determine that the unitary operation corresponding to the braid σ_1 is given by

$$\begin{pmatrix} |0\rangle \\ |1\rangle \\ |N\rangle \end{pmatrix} \rightarrow \underbrace{\left(\begin{array}{cc|c} e^{-4\pi i/5} & 0 & 0 \\ 0 & -e^{-2\pi i/5} & 0 \\ \hline 0 & 0 & -e^{-2\pi i/5} \end{array}\right)}_{\rho(\sigma_1)} \begin{pmatrix} |0\rangle \\ |1\rangle \\ |N\rangle \end{pmatrix} \tag{134}$$

where we have used the shorthand notation (See Fig. 14) for the three particle states. Evaluating the effect of σ_2 is less trivial. Here, we must first make a basis change (using F) in order to determine how the two rightmost particles fuse. Then we can make the rotation using $\hat{R}$ and finally undo the basis change. Symbolically, we can write $\rho(\sigma_2) = F^{-1}\hat{R}F$ where $\hat{R}$ rotates the two rightmost particles. To be more explicit, let us consider what happens to the state $|0\rangle$. First, we use Eq. 128 to write $|0\rangle = F_{\mathbf{11}}|(\bullet,(\bullet,\bullet)_{\mathbf{1}})_\tau\rangle + F_{\tau\mathbf{1}}|(\bullet,(\bullet,\bullet)_\tau)_\tau\rangle$. Rotating the two right particles then gives $e^{-4\pi i/5}F_{\mathbf{11}}|(\bullet,(\bullet,\bullet)_{\mathbf{1}})_\tau\rangle - e^{-2\pi i/5}F_{\tau\mathbf{1}}|(\bullet,(\bullet,\bullet)_\tau)_\tau\rangle$, and then we transform back to the original basis using the inverse of Eq. 128 to yield $\rho(\sigma_2)|0\rangle = ([F^{-1}]_{\mathbf{11}}e^{-4\pi i/5}F_{\mathbf{11}} - [F^{-1}]_{\mathbf{1}\tau}e^{-2\pi i/5}F_{\tau\mathbf{1}})|0\rangle + ([F^{-1}]_{\tau\mathbf{1}}e^{-4\pi i/5}F_{\mathbf{11}} - [F^{-1}]_{\tau\tau}e^{-2\pi i/5}F_{\tau\mathbf{1}})|1\rangle = -e^{-\pi i/5}/\phi\,|0\rangle - ie^{-i\pi/10}/\sqrt{\phi}\,|1\rangle$. Similar results can be derived for the other two basis states to give the matrix

$$\rho(\sigma_2) = \left(\begin{array}{cc|c} -e^{-\pi i/5}/\phi & -ie^{-i\pi/10}/\sqrt{\phi} & 0 \\ -ie^{-i\pi/10}/\sqrt{\phi} & -1/\phi & 0 \\ \hline 0 & 0 & -e^{-2\pi i/5} \end{array}\right) \tag{135}$$

Since the braid operations σ_1 and σ_2 (and their inverses) generate all possible braids on three strands (See Fig. 15), we can use Eqs. 134 and 135 to determine the unitary operation resulting from any braid on three strands, with the unitary operations being built up from the elementary matrices $\rho(\sigma_1)$ and $\rho(\sigma_2)$ in the same way that the complicated braids are built from the braid generators σ_1 and σ_2. For example, the braid $\sigma_2\sigma_1\sigma_1\sigma_2^{-1}\sigma_2^{-1}\sigma_1$ shown in Fig. 15 corresponds to the unitary matrix $\rho(\sigma_1)\rho(\sigma_2^{-1})\rho(\sigma_2^{-1})\rho(\sigma_1)\rho(\sigma_1)\rho(\sigma_2)$ (note that the order is reversed since the operations that occur at earlier times are written to the left in conventional braid notation, but on the right when multiplying matrices together).

(c) Computing with Fibonacci Anyons: Now that we know many of the properties of Fibonacci anyons, we would like to show how to compute with them. First, we need to construct our qubits. An obvious choice might be to use two particles for a qubit and declare the two states $|(\bullet,\bullet)_{\mathbf{1}}\rangle$ and $|(\bullet,\bullet)_\tau\rangle$ to be the two orthogonal states of the qubit. While this is a reasonably natural looking qubit, it turns out not to be convenient for computations. The reason for this is that we will want to do single qubit operations (simple rotations) by braiding. However, it is not possible to change the overall quantum number of a group of particles by braiding within that group. Thus, by simply braiding the two particles around

each other, we can never change $|(\bullet,\bullet)_{\mathbf{1}}\rangle$ to $|(\bullet,\bullet)_{\tau}\rangle$. To remedy this problem, it is convenient to use three quasiparticles to represent a qubit as suggested by Freedman et al., 2002a (many other schemes for encoding qubits are also possible (Freedman et al., 2002a; Hormozi et al., 2007)). Thus, we represent the two states of the qubit as the $|0\rangle$ and $|1\rangle$ states shown in Fig. 14. The additional state $|N\rangle$ is a "noncomputational" state. In other words, we arrange so that at the beginning and end of our computations, there is no amplitude in this state. Any amplitude that ends up in this state is known as "leakage error". We note, however, that the braiding matrices $\rho(\sigma_1)$ and $\rho(\sigma_2)$ are block diagonal and therefore never mix the noncomputational state $|N\rangle$ with the computational space $|0\rangle$ and $|1\rangle$ (This is just another way to say that the overall quantum number of the three particles must remain unchanged under any amount of braiding). Therefore, braiding the three particles gives us a way to do single qubit operations with no leakage.

In section IV.C, we will describe a proof that the set of braids has a "dense image" in the set of unitary operations for the Fibonacci theory. This means that there exists a braid that corresponds to a unitary operation arbitrarily close to any desired operation. The closer one wants to approximate the desired unitary operation, the longer the braid typically needs to be, although only logarithmically so (i.e, the necessary braid length grows only as the log of the allowed error distance to the target operation). The problem of actually finding the braids that correspond to desired unitary operations, while apparently complicated, turns out to be straightforward (Bonesteel et al., 2005; Hormozi et al., 2007). One simple approach is to implement a brute force search on a (classical) computer to examine all possible braids (on three strands) up to some certain length, looking for a braid that happen to generate a unitary operation very close to some desired result. While this approach works very well for searching short braids (Bonesteel et al., 2005; Hormozi et al., 2007), the job of searching all braids grows exponentially in the length of the braid, making this scheme unfeasible if one requires high accuracy long braids. Fortunately, there is an iterative algorithm by Solovay and Kitaev (see Nielsen and Chuang, 2000) which allows one to put together many short braids to efficiently construct a long braid arbitrarily close to any desired target unitary operation. While this algorithm does not generally find the shortest braid for performing some operation (within some allowed error), it does find a braid which is only polylogarithmically long in the allowed error distance to the desired operation. Furthermore, the (classical) algorithm for finding such a braid is only algebraically hard in the length of the braid.

Having solved the single qubit problem, let us now imagine we have multiple qubits, each encoded with three particles. To perform universal quantum computation, in addition to being able to perform single qubit operations, we must also be able to perform two-qubit entangling gates (Bremner et al., 2002; Nielsen and Chuang, 2000). Such two-qubit gates will necessarily involve braiding together (physically "entangling"!) the particles from two different qubits. The result of Freedman et al., 2002a generally guarantees that braids exist corresponding to any desired unitary operation on a two-qubit Hilbert space. However, finding such braids is now a much more formidable task. The full Hilbert space for six Fibonacci particles (constituting two qubits) is now 13 dimensional, and searching for a desired result in such a high dimensional space is extremely hard even for a powerful classical computer. Therefore, the problem needs to be tackled by divide-and-conquer approaches, building up two-qubit gates out of simple braids on three particles (Bonesteel et al., 2005; Hormozi et al., 2007). A simple example of such a construction is sketched in Fig. 16. First, in Fig. 16.a, we consider braids on three strands that moves ("weaves" (Simon et al., 2006)) only a single particle (the blue particle in the figure) through two stationary particles (the green particles). We search for such a braid whose action on the Hilbert space is equivalent to exchanging the two green particles twice. Since this is now just a three particle problem, finding such a braid, to arbitrary accuracy, is computationally tractable. Next, for the two qubit problem, we label one qubit the control (blue in Fig. 16.b) and another qubit the target (green). We take a pair of particles from the control qubit (the control pair) and weave them as a group through two of the particles in the target, using the same braid we just found for the three particle problem. Now, if the quantum number of the control pair is **1** (i.e, control qubit is in state $|0\rangle$) then any amount of braiding of this pair will necessarily give just an Abelian phase (since moving **1** around is like moving nothing around). However, if the quantum number of the control pair is τ (i.e, the control qubit is in state $|1\rangle$) then we can think of this pair as being equivalent to a single τ particle, and we will cause the same nontrivial rotation as in Fig.16.a above (Crucially, this is designed to not allow any leakage error!). Thus, we have constructed a "controlled rotation" gate, where the state of the target qubit is changed only if the control qubit is in state $|1\rangle$, where the rotation that occurs is equivalent to exchanging two particles of the target qubit as shown in Fig. 16.b. The resulting two-qubit controlled gate, along with single qubit rotations, makes a universal set for quantum computation (Bremner et al., 2002). More conventional two-qubit gates, such as the controlled NOT gates (CNOT), have also been designed using braids (Bonesteel et al., 2005; Hormozi et al., 2007).

(d) Other theories: The Fibonacci theory is a particularly interesting theory to study, not only because of its simplicity, but also because of its close relationship (see the discussion at the beginning of section IV.B) with the $\mathbb{Z}_3$ parafermion theory — a theory thought to actually describe (Rezayi and Read, 2006) the observed quantum Hall state at $\nu = 12/5$ (Xia et al., 2004). It is not hard to show that a given braid will perform the same quantum computation in either theory (Hormozi et al., 2007) (up to an irrelevant overall Abelian phase). Therefore, the Fibonacci theory and the associated braiding may be physically relevant for fractional quantum Hall topological quantum computation in high-mobility 2D semiconductor structures.

However, there are many other non-Abelian theories, which are not related to Fibonacci anyons. Nonetheless, for arbitrary non-Abelian theories, many of the themes we have discussed in this section continue to apply. In all cases, the Hilbert space can be understood via fusion rules and an F-matrix; rotations

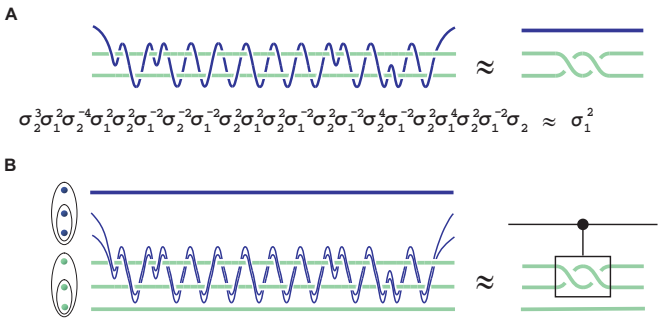

FIG. 16 Construction of a two qubit gate from a certain three particle problem. ime flows from left to right in this picture. In the top we construct a braid on three strands moving only the blue particle which has the same effect as interchanging the two green strands. Using this same braid (bottom), then constructs a controlled rotation gate. If the state of the upper (control) qubit is $|0\rangle$, i.e., the control pair is in state **1** then the braid has no effect on the Hilbert space (up to a phase). if, the upper (control) qubit is in the state $|1\rangle$ then the braid has the same effect as winding two of the particles in the lower qubit. Figure from Bonesteel et al., 2005

of two particles can be understood as a rotation $\hat{R}$ operator that produces a phase dependent on the quantum number of the two particles; and one can always encode qubits in the quantum number of some group of particles. If we want to be able to do single qubit operations by braiding particles within a qubit (in a theory that allows universal quantum computation) we always need to encode a qubit with at least three particles (sometimes more). To perform two-qubit operations we always need to braid particles constituting one qubit with the particles constituting another qubit. It is always the case that for any unitary operation that can be achieved by braiding n particles around each other with an arbitrary braid can also be achieved by weaving a single particle around $n-1$ others that remain stationary (Simon et al., 2006) (Note that we implicitly used this fact in constructing Fig. 15.a). So long as the state is among the ones known to have braid group representations with dense images in the unitary group, as described in Section IV.C below, it will be able to support universal quantum computation. Finally, we note that it seems to always be true that the practical construction of complicated braids for multi-qubit operations needs to be subdivided into more manageable smaller problems for the problem to be tractable.

C. Universal Topological Quantum Computation

As we have seen in subsection IV.A, even if the $\nu = 5/2$ state is non-Abelian, it is not non-Abelian enough to function as a universal quantum computer simply by braiding anyons. However, in subsection IV.B, we described Fibonacci anyons which, we claimed, were capable of supporting universal topological quantum computation. In this subsection, we sketch a proof of this claim within the context of the more general question: which topological states are universal for quantum computation or, in starker terms, for which topological states is the entire gate set required to efficiently simulate an arbitrary quantum circuit to arbitrary accuracy simply that depicted in Figure 17 (see also Kauffman and Lomonaco Jr., 2004, 2007).

The discussion in this section is more mathematical than the rest of the paper and can skipped by less mathematically-inclined readers.

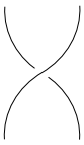

FIG. 17 The entire gate set needed in a state supporting universal quantum computation.

In other words, the general braid is composed of copies of a single operation (depicted in Figure 17) and its inverse. (Actually, as we will see, "positive braids" will prove to be sufficient, so there is no necessity to ever use the inverse operation.) Fibonacci anyons, which we discussed in subsection IV.B, are an example which have this property. In this subsection, we will see why.

For the sake of concreteness, let us assume that we use a single species of quasiparticle, which we will call σ. When there are n σ's at fixed positions $z_1, \ldots, z_n$, there is an exponentially-large ($\sim (d_\sigma)^n$-dimensional) ground state subspace of Hilbert space. Let us call this vector space V_n. Braiding the σ's produces a representation ρ_n characteristic of the topological phase in question, $\rho_n : \mathcal{B}_n \rightarrow \mathrm{U}(V_n)$ from the braid group on n strands into the unitary transformations of V_n. We do not care about the overall phase of the wavefunction, since only the projective reduction in PU(V_n) has physical significance. (PU(V_n) is the set of unitary transformations on V_n with two transformations identified if they differ only by a phase.) We would like to be able to enact an arbitrary unitary transformation, so $\rho(\mathcal{B}_n)$ should be dense in PU(V_n), i.e. dense up to phase. By 'dense' in PU(V_n), we mean that the intersection of all closed sets containing $\rho(\mathcal{B}_n)$ should simply be PU(V_n). Equivalently, it means that an arbitrary unitary transformation can be approximated, up to a phase, by a transformation in $\rho(\mathcal{B}_n)$ to within any desired accuracy. This is the condition which our topological phase must satisfy.

For a modestly large number (≥ 7) of σs, it was shown (Freedman et al., 2002a,b) that the braid group representations associated with $SU(2)$ Chern-Simons theory at level $k \neq 1, 2, 4$ are dense in $SU(V_{n,k})$ (and hence in $PU(V_{n,k})$). With only a small number of low-level and small anyon number exceptions, the same articles show density for almost all SU(N)$_k$.

These Jones-Witten (JW) representations satisfy a key "two eigenvalue property" (TEVP), discussed below, derived in this $SU(N)$ setting from the Hecke relations, and corresponding to the HOMFLY polynomial (see, for instance, Kauffman, 2001 and refs. therein). The analysis was extended with similar conclusions in (Larsen et al., 2005) to the case where the

Lie group G is of type BCD and braid generators have three eigenvalues, corresponding to the BMW algebra and the two variable Kauffman polynomial. For JW-representations of the exceptional group at level k, the number of eigenvalues of braid generators can be composite integers (such as 4 for G_2) and this has so far blocked attempts to prove density for these JW-representations.

In order to perform quantum computation with anyons, there are many details needed to align the topological picture with the usual quantum-circuit model from computer science. First, qubits must be located in the state space V_n. Since V_n has no natural tensor factoring (it can have prime dimension) this alignment (Freedman et al., 2002a) is necessarily a bit inefficient[9]; some directions in V_n are discarded from the computational space and so we must always guard against unintended "leakage" into the discarded directions. A possible research project is how to adapt computation to "Fibonacci" space (see subsection IV.B) rather than attempting to find binary structure within V_n. A somewhat forced binary structure was explained in subsection IV.B in connection with encoding qubits into $SU(2)_3$, as it was done for level 2 in subsection IV.A. (A puzzle for readers: Suppose we write integers out as "Fibonacci numerals": 0 cannot follow 0, but 0 or 1 can follow 1. How do you do addition and multiplication?) However, we will not dwell on these issues but instead go directly to the essential mathematical point: How, in practice, does one tell which braid group representations are dense and which are not, i.e. which ones are sufficient for universal topological quantum computation and which ones need to be augmented by additional non-topological gate operations?

We begin by noting that the fundamental skein relation of Jones' theory is:

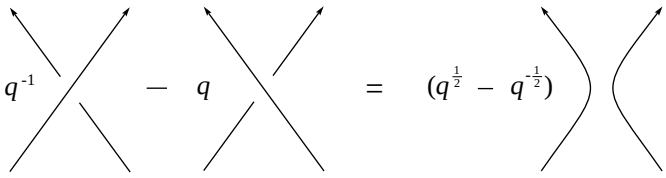

FIG. 18 Jones skein relation. (See (73)

(see (73) and the associated relation for the Kauffman bracket (77)) This is a quadratic relation in each braid generator σ_i and by inspection any representation of σ_i will have only two distinct eigenvalues $q^{\frac{3}{2}}$ and $-q^{\frac{1}{2}}$. It turns out to be exceedingly rare to have a representation of a compact Lie group H where H is densely generated by elements σ_i with this eigenvalue restriction. This facilitates the identification of the compact closure $H = \overline{\text{image}(\rho)}$ among the various compact subgroups of $U(V_n)$.

[9] Actually, current schemes use approximately half the theoretical number of qubits. One finds $\alpha \log_2(\dim V_n)$ computational qubits in V_n, for $\alpha = (\log_2 \tau^3)^{-1} \approx 0.48$, $\phi = \frac{1+\sqrt{5}}{2}$.

Definition IV.1. Let G be a compact Lie group and V a faithful, irreducible, unitary representation. The pair (G, V) has the *two eigenvalue property* (TEVP) if there exists a conjugacy class $[g]$ of G such that:

1. $[g]$ generates a dense set in G
2. For any $g \in [g]$, g acts on V with exactly two distinct eigenvalues whose ratio is not -1.

Let H be the closed image of some Jones representation $\rho : B_n \to U(V_n)$. We would like to use figure 18 to assert that the fundamental representation of $U(V_n)$ restricted to H, call it θ, has the TEVP. All braid generators σ_i are conjugate and, in nontrivial cases, the eigenvalue ratio is $-q \neq -1$. However, we do not yet know if the restriction is irreducible. This problem is solved by a series of technical lemmas in (Freedman et al., 2002a). Using TEVP, it is shown first that the further restriction to the identity component H_0 is isotipic and then irreducible. This implies that H_0 is reductive, so its derived group $[H_0, H_0]$ is semi-simple and, it is argued, still satisfies the TEVP. A final (and harmless) variation on H is to pass to the universal cover $H' := \widetilde{[H_0, H_0]}$. The pulled back representation θ' still has the TEVP and we are finally in a situation, namely irreducible representations of semi-simple Lie groups of bounded dimension, where we can hope to apply the classification of such representations (McKay and Patera, 1981) to show that our mysterious H' is none other than $SU(V_n)$. If this is so, then it will follow that the preceding shenanigans $H \to H_0 \to [H_0, H_0] \to \widetilde{[H_0, H_0]}$ did nothing (beyond the first arrow, which may have eliminated some components of H on which the determinant is a nontrivial root of unity).

In general, milking the answer (to the question of which Jones representations are projectively dense) out of the classification requires some tricky combinatorics and rank-level (Freedman et al., 2002b) duality. Here we will be content with doing the easiest nontrivial case. Consider six Fibonacci anyons τ with total charge $= 1$. The associated $V_6 \cong \mathbb{C}^5 \cong$ 2 qubits $\oplus$ non-computational $\mathbb{C}$ as shown:

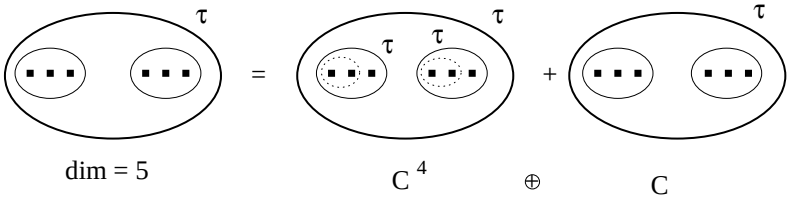

FIG. 19 The charge on the dotted circle can be 1 or τ providing the qubit.

In coordinates, ρ takes the braid generators (projectively) to these operators:

$$\sigma_1 \longmapsto \begin{bmatrix} -1 & & & & \\ & q & & & \\ & & -1 & & \\ & & & q & \\ & & & & q \end{bmatrix}, \qquad q = e^{-\frac{2\pi i}{5}}$$

$$\sigma_2 \longmapsto \begin{bmatrix} \frac{q^2}{q+1} & -\frac{q\sqrt{[3]}}{q+1} & & & \\ -\frac{q\sqrt{[3]}}{q+1} & -\frac{1}{q+1} & & & \\ & & \frac{q^2}{q+1} & -\frac{q\sqrt{[3]}}{q+1} & \\ & & -\frac{q\sqrt{[3]}}{q+1} & -\frac{1}{q+1} & \\ & & & & q \end{bmatrix}$$

where $[3] = q + q^{-1} + 1$, and σ_i, for $i = 3, 4, 5$, are similar. See Funar, 1999 for details.

The closed image of ρ is $H \subset U(5)$, so our irreducible representation θ' of H', coming from $U(5)$'s fundamental, is exactly 5 dimensional (we don't yet know the dimension of H'). From McKay and Patera, 1981, there are four 5-dimensional irreducible representations, which we list by rank:

1. rank = 1: $(SU(2), 4\pi_1)$
2. rank = 2: $(Sp(4), \pi_2)$
3. rank = 4: $(SU(5), \pi_i)$, $i = 1, 4$

Suppose $x \in SU(2)$ has eigenvalues α and β in π_1. Then under $4\pi_1$, it will have $\alpha^i\beta^j$, $i + j = 4$ $(i, j \geq 0)$ as eigenvalues, which are too many (unless $\frac{\alpha}{\beta} = -1$). In case (2), since 5 is odd, every element has at least one real eigenvalue, with the others coming in reciprocal pairs. Again, there is no solution. Thus, the TEVP shows we are in case (3), i.e. that $H' \cong SU(5)$. It follows from degree theory that $[H_0, H_0] \cong SU(5)$ and from this we get the desired conclusion: $SU(5) \subset H \subset U(5)$.

We have not yet explained in what sense the topological implementations of quantum computations are efficient. Suffice it to say that there are (nearly) quadratic time algorithms due to Kitaev and Solvay (Nielsen and Chuang, 2000) for finding the braids that approximate a given quantum circuit. In practice, brute force, load balanced searches for braids representing fundamental gates, should yield accuracies on the order of 10^{-5} (within the "error threshold"). Note that these are systematic, unitary errors resulting from the fact that we are enacting a unitary transformation which is a little different from what an algorithm may ask for. Random errors, due to decoherence, are caused by uncontrolled physical processes, as we discuss in the next subsection.

D. Errors

As we discussed in section II.B.2, small inaccuracies in the trajectories along which we move our quasiparticles are not a source of error. The topological class of the quasiparticles' trajectories (including undesired quasiparicles) must change in order for an error to occur. Therefore, to avoid errors, one must keep careful track of all of the quasiparticles in the system and move them so that the intended braid is performed. As mentioned in the introduction section II.B.2, stray thermally excited quasiparticles could form unintended braids with the quasiparticles of our system and cause errors in the computation. Fortunately, as we mentioned in section II.B.2, there is a large class of such processes that actually do not result in errors. We will discuss the two most important of these.

Perhaps the simplest such process that does not cause errors is when a quasiparticle-quasihole pair is thermally (or virtually) excited from the vacuum, one of the two excited particles wanders around a single quasiparticle in our system then returns to reannihilate its partner. (See Figure 20.a). For the sake of argument, let us imagine that our initial computational system is a pair of quasiparticles in state j. At some time t_1 (marked by an $\times$ in the figure), we imagine that a quasiparticle-quasihole pair becomes excited from the vacuum. Since the pair comes from the vacuum, it necessarily has overall quantum number **1** (i.e., fusing these particles back together gives the vacuum **1**). Thus the overall quantum number of all four particles is j. (In the above notation, we could draw a circle around all four particles and label it j). We then imagine that one of our newly created quasiparticles wanders around one of the quasiparticles of our computational system as shown in the figure. Using F matrices or braiding matrices $\hat{\sigma}$ we could compute the full state of the system after this braiding operation. Importantly, however, the overall quantum number j of all four particles is preserved.

Now at some later time t_2 the two created particles reannihilate each other and are returned to the vacuum as shown by the second $\times$ in Figure 20.a. It is crucial to point out that in order for two particles to annihilate, they must have the identity quantum number **1** (i.e., they must fuse to **1**). The annihilation can therefore be thought of as a measurement of the quantum number of these two particles. The full state of the system, then collapses to a state where the annihilating particles have quantum number **1**. However, the overall quantum number of all four particles must remain in the state j. Further, in order for the overall state of the four particles to be j and the two annihilating particles to be **1** the two other (original) particles must have quantum number j. Thus, as shown in the figure, the two original quasiparticles must end up in their original state j once the created particles are reannihilated. Similarly, if the original particles had started in a superposition of states, that superposition would be preserved after the annihilation of the two excited particles. (Note that an arbitrary phase might occur, although this phase is independent of the quantum number j and therefore is irrelevant in the context of quantum computations).

Another very important process that does not cause errors is shown in Figure 20.b. In this process, one of the members of a thermally excited quasiparticle-quasihole pair annihilate with one of the particles in our computational system, leaving behind its partner as a replacement. Again, since both the created pair and the annihilating particles have the same quantum numbers as the vacuum, it is easy to see (using similar arguments as above) that the final state of the two remaining particles must be the same as that of the original two particles, thus not causing any errors so long as the new particle is used as a replacement for the annihilated quasiparticle.

The fact that the two processes described above do not cause errors is actually essential to the notion of topological

quantum computation. Since the created quasiparticles need not move very far in either process, these processes can occur very frequently, and can even occur virtually since they could have low total action. Thus it is crucial that these likely processes do not cause errors. The simplest processes that can actually cause error would require a thermally (or virtually) created quasiparticle-quasihole pair to braid nontrivially with at least two quasiparticles of our computational system. Since it is assumed that all of the quasiparticles that are part of our system are kept very far from each other, the action for a process that wraps a (virtually) created quasiparticle around two different particles of our system can be arbitrarily large, and hence these virtual processes can be suppressed. Similarly, it can be made unlikely that thermally excited quasiparticles will wrap around two separate particles of our system before re-annihilating. Indeed, since in two dimensions a random walk returns to its origin many times, a wandering quasiparticle may have many chances to re-annihilate before it wraps around two of the particles of our computational system and causes errors. Nonetheless, in principle, this process is a serious consideration and has the potential to cause errors if too many quasiparticle-quasihole pairs are excited.

The probability for these error-causing processes is naively $\sim e^{-\Delta/(2T)}$ (thermally-excited quasiparticles) or $\sim e^{-\Delta L/v}$ (virtual quasiparticles), where T is the temperature, Δ is quasiparticle energy gap, L is the distance between the quasiparticles comprising a qubit, and v is a characteristic velocity. However, transport in real systems is, in fact, more complicated. Since there are different types of quasiparticles, the gap measured from the resistance may not be the smallest gap in the system. For instance, neutral fermionic excitations in the Pfaffian state/SU(2)$_2$ may have a small gap, thereby leading to a splitting between the two states of a qubit if the two quasiparticles are too close together. Secondly, in the presence of disorder, the gap will vary throughout the system. Processes which take advantage of regions with small gaps may dominate the error rate. Furthermore, in a disordered system, variable-range hopping, rather than thermally-activated transport is the most important process. Localized quasiparticles are an additional complication. If they are truly fixed, then they can be corrected by software, but if they drift during the course of a calculation, they are a potential problem. In short, quasiparticle transport, even ordinary electrical transport, is very complicated in semiconductor quantum Hall systems. A complete theory does not exist. Such a theory is essential for an accurate prediction of the error rate for topological quantum computation in non-Abelian quantum Hall states in semiconductor devices and is an important future challenge for solid state theory.

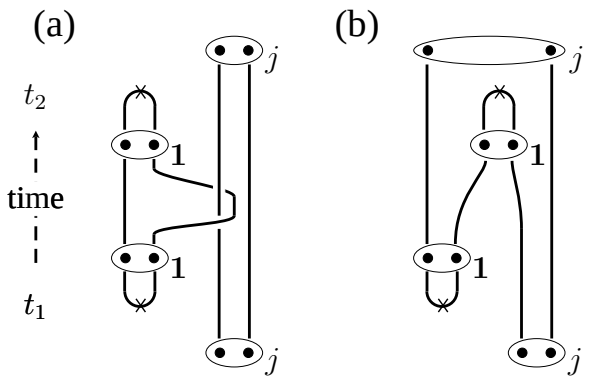

FIG. 20 Two processes involving excited quasiparticle-quasihole pairs that do not cause errors in a topological quantum computation. (a) In the process shown on the left, a quasiparticle-quasihole pair is excited at time t_1 (marked by an $\times$), one of these particles wraps around a quasiparticle of our computational system, and then comes back to its partner and re-annihilates at a later time t_2. When the pair is created it necessarily has the identity quantum number **1** of the vacuum, and when it annihilates, it also necessarily has this vacuum quantum number. As a result (as discussed in the text) the quantum number of the computational system is not changed by this process. (b) In the process shown on the right, a quasiparticle-quasihole pair is excited at time t_1 (marked by an $\times$), one of these particles annihilates an existing quasiparticle of our computational system at a later time t_2, and leaves behind its partner to replace the the annihilated quasiparticle of the computational system. Again, when the pair is created, it necessarily has the identity quantum number **1** of the vacuum. Similarly the annihilating pair has the quantum number of the vacuum. As a result, the two particles remaining in the end have the same quantum numbers as the two initial quantum numbers of the computational system.

V. FUTURE CHALLENGES FOR THEORY AND EXPERIMENT

Quantum mechanics represented a huge revolution in thought. It was such a stretch of the imagination that many great minds and much experimental information were required to put it into place. Now, eighty years later, another collaborative effort is afoot to revolutionize computation by a particularly rich use of quantum mechanics. The preceding information revolution, which was based on the MOSFET, rested on the 1-electron physics of semiconductors. The revolution which we advocate will require the understanding and manipulation of strongly-interacting electron systems. Modern condensed matter physics has powerful tools to analyze such systems: renormalization group (RG), CFT, Bethe Ansatz, dualities, and numerics. Even without the quantum computing connection, many of the most interesting problems in physics lie in this direction. Prominent here is the problem of creating, manipulating, and classifying topological states of matter.

There is a second "richness" in the connection between quantum mechanics and computation. The kind of computation which will emerge is altogether new. While the MOSFET-based silicon revolution facilitated the same arith-

metic as done on the abacus, the quantum computer will compute in superposition. We have some knowledge about what this will allow us to do. Select mathematical problems (factoring, finding units in number fields, searching) have efficient solutions in the quantum model. Many others may succumb to quantum heuristics (e.g. adiabatic computation (Farhi et al., 2000)) but we will not know until we can play with real quantum computers. Some physical problems, such as maximizing T_c within a class of superconductors, should be advanced by quantum computers, even though, viewed as math problems, they lie even outside class NP (i.e. they are *very* hard). A conjectural view of relative computational complexity is shown in Fig. 21.

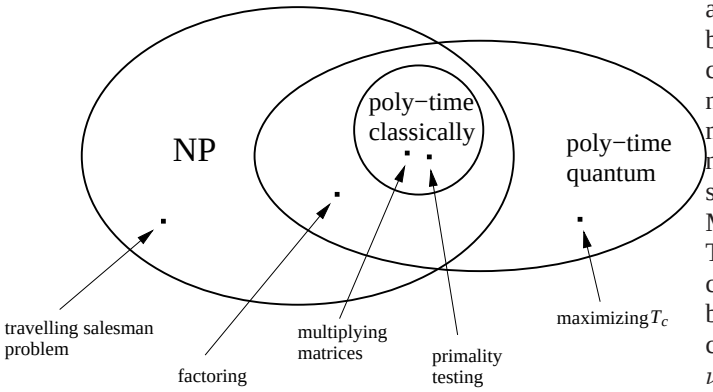

FIG. 21 A conjectural view of relative computational complexity

But, before we can enter this quantum computing paradise, there are fundamental issues of physics to be tackled. The first problem is to find a non-Abelian topological phase in nature. The same resistance to local perturbation that makes topological phases astonishing (and, we hope, useful) also makes them somewhat covert. An optimist might hope that they are abundant and that we are merely untutored and have trouble noticing them. At present, our search is guided primarily by a process of elimination: we have focussed our attention on those systems in which the alternatives don't occur – either quantum Hall states for which there is no presumptive Abelian candidate or frustrated magnets which don't order into a conventional broken-symmetry state. What we need to do is observe some topological property of the system, e.g. create quasiparticle excitations above the ground state, braid them, and observe how the state of the system changes as a result. In order to do this, we need to be able to (1) create a specified number of quasiparticles at known positions, (2) move them in a controlled way, and (3) observe their state. All of these are difficult, but not impossible.

It is instructive to see how these difficulties are manifested in the case of quantum Hall states and other possible topological states. The existence of a topological phase in the quantum Hall regime is signaled by the quantization of the Hall conductance. This is a special feature of those chiral topological phases in which there is a conserved current J_μ (e.g. an electrical charge current or spin current). Topological invariance and P, T-violation permit a non-vanishing correlation function of the form

$$\langle J_\mu(q) J_\nu(-q)\rangle = C\,\epsilon_{\mu\nu\lambda} q_\lambda \tag{136}$$

where C is a topological invariant. If the topological phase does not break P and T or if there is no conserved current in the low-energy effective field theory, then there will not be such a dramatic signature. However, even in the quantum Hall context, in which we have a leg up thanks to the Hall conductance, it is still a subtle matter to determine which topological phase the system is in.

As we have described, we used theoretical input to focus our attention on the $\nu = 5/2$ and $\nu = 12/5$ states. Without such input, the available phase space is simply too large and the signatures of a topological phase are too subtle. One benefit of having a particular theoretical model of a topological phase is that experiments can be done to verify other (i.e. non-topological) aspects of the model. By corroborating the model in this way, we can gain indirect evidence about the nature of the topological phase. In the case of the $\nu = 5/2$ state, the Pfaffian model wavefunction (Greiter et al., 1992; Moore and Read, 1991) for this state is fully spin-polarized. Therefore, measuring the spin polarization at $\nu = 5/2$ would confirm this aspect of the model, thereby strengthening our belief in the the model as a whole – including its topological features (see Tracy et al., 2007 for such a measurement at $\nu = 1/2$). In the case of Sr_2RuO_4, the $p + ip$ BCS model predicts a non-zero Kerr rotation (Xia et al., 2006). This is not a topological invariant, but when it is non-zero and the superconducting order parameter is known to be a spin-triplet, we can infer a non-zero spin quantum Hall effect (which is a topological invariant but is much more difficult to measure). Thus, non-topological measurements can teach us a great deal when we have a particular model in mind.

In frustrated magnets, one often cuts down on the complex many-dimensional parameter space in the following way: one focusses on systems in which there is no conventional long-range order. Although it is possible for a system to be in a topological phase and simultaneously show conventional long-range order (quantum Hall ferromagnets are an example), the absence of conventional long-range order is often used as circumstantial evidence that the ground state is 'exotic' (Coldea et al., 2003; Shimizu et al., 2003). This is a reasonable place to start, but in the absence of a theoretical model predicting a specific topological state, it is unclear whether the ground state is expected to be topological or merely 'exotic' in some other way (see below for a further discussion of this point).

While theoretical models and indirect probes can help to identify strong candidates, only the direct measurement of a topological property can demonstrate that a system is in a topological phase. If, as in the quantum Hall effect, a system has been shown to be in a topological phase through the measurement of one property (e.g. the Hall conductance), then there is still the problem of identifying which topological phase. This requires the complete determination of all of its topological properties (in principle, the quasiparticle species, their topological spins, fusion rules, R- and F-matrices). Finding non-trivial quasiparticles is the first

step. In the quantum Hall regime, quasiparticles carry electrical charge (generally fractional). Through capacitive measurements of quasiparticle electric charges (Goldman and Su, 1995) or from shot noise measurements (De Picciotto et al., 1997; Saminadayar et al., 1997), one can measure the minimal electric charges and infer the allowed quasiparticle electric charges. The observation of charge $e/4$ quasiparticles by either of these methods would be an important step in characterizing the $\nu = 5/2$ state. Detecting charged quasiparticles capacitatively or through noise measurements necessitates gated samples: anti-dots and/or point contacts. In the case of delicate states such as $\nu = 5/2$, this is a challenge; we don't want the gates to reduce the quality of the device and excessively degrade the robustness of the states. Even if this proves not to be surmountable, it only solves the problem of measuring charged quasiparticles; it does not directly help us with non-trivial neutral quasiparticles (such as those which we believe exist at $\nu = 5/2$).

Again, a particular theoretical model of the state can be extremely helpful. In the case of the toric code, an excited plaquette or $\mathbb{Z}_2$ vortex (see Secs. II.D III.G) is a neutral spinless excitation and, therefore, difficult to probe. However, when such a phase arises in models of superconductor-Mott insulator transitions, $\mathbb{Z}_2$ vortices can be isolated by going back and forth through a direct second-order phase transition between a topological phase and a superconducting phase (Senthil and Fisher, 2001a). Consider a superconductor in an annular geometry with a single half-flux quantum vortex through the hole in the annulus. Now suppose that some parameter can be tuned so that the system undergoes a second-order phase transition into an insulating state which is a topological phase of the toric code or $\mathbb{Z}_2$ variety. Then the single vortex ground state of the superconductor will evolve into a state with a $\mathbb{Z}_2$ vortex in the hole of the annulus. The magnetic flux will escape, but the $\mathbb{Z}_2$ vortex will remain. (Eventually, it will either quantum tunnel out of the system or, at finite temperature, be thermally excited out of the system. It is important to perform the experiment on shorter time scales.) If the system is then taken back into the superconducting state, the $\mathbb{Z}_2$ vortex will evolve back into a superconducting vortex; the flux must be regenerated, although its direction is arbitrary. Although Senthil and Fisher considered the case of a $\mathbb{Z}_2$ topological phase, other topological phases with direct second-order phase transitions into superconducting states will have a similar signature. On the other hand, in a non-topological phase, there will be nothing left in the insulating phase after the flux has escaped. Therefore, when the system is taken back into the superconducting phase, a vortex will not reappear. The effect described above is not a feature of the topological phase alone, but depends on the existence of a second-order quantum phase transition between this topological state and a superconducting state. However, in the happy circumstance that such a transition does exist between two such phases of some material, this experiment can definitively identify a topologically non-trivial neutral excitation. In practice, the system is not tuned through a quantum phase transition but instead through a finite-temperature one; however, so long as the temperature is much smaller than the energy gap for a $\mathbb{Z}_2$ vortex, this is an unimportant distinction. This experiment was performed on an underdoped cuprate superconductor by Wynn et al., 2001. The result was negative, implying that there isn't a topological phase in the low-doping part of the phase diagram of that material, but the experimental technique may still prove to be a valuable way to test some other candidate material in the future. It would be interesting and useful to design analogous experiments which could exploit the possible proximity of topological phases to other long-range ordered states besides superconductors.

Even if non-trivial quasiparticles have been found, there is still the problem of determining their braiding properties. In the quantum Hall case, we have described in Secs. II.C.3, III.F how this can be done using quasiparticle tunneling and interferometry experiments. This requires even more intricate gating. However, even these difficult experiments are the most concrete that we have, and they work only because these states are chiral and have gapless edge excitations – and, therefore, have non-trivial DC transport properties – and because charged anyons contribute directly to these transport properties. Neutral quasiparticles are an even bigger challenge. Perhaps they can be probed through thermal transport or even, if they carry spin, through spin transport.

As we have seen in Sec. II.C.3, abelian and non-Abelian interference effects are qualitatively different. Indeed, the latter may actually be easier to observe in practice. It is striking that quasiparticle interferometry, which sounds like an *application* of topological phases, is being studied as a basic probe of the state. The naive logical order is reversed: to see if a system is in a topological phase, we are (ironically) saying "shape the system into a simple computer and if it computes as expected, then it must have been in the suspected phase." This is a charming inversion, but it should not close the door on the subject of probes. It is, however, important to pause and note that we now know the operational principles and methodology for carrying out quasiparticle braiding in a concrete physical system. It is, therefore, possible that non-Abelian anyons will be observed in the quantum Hall regime in the near future. This is truly remarkable. It would not close the book on non-Abelian anyons, but open a new chapter and encourage us to look for non-Abelian anyons elsewhere even while trying to build a quantum computer with a quantum Hall state.

One important feature of non-Abelian anyons is that they generally have multiple fusion channels. These different fusion channels can be distinguished interferometrically, as discussed in Secs. II.C.3, III.F. This is not the only possibility. In ultra-cold neutral atom systems, they can be optically detected (Grosfeld et al., 2007; Tewari et al., 2007b) in the case of states with Ising anyons. Perhaps, in a solid, it will be possible to measure the force between two anyons. Since the two fusion channels will have different energies when the anyons are close together, there will be different forces between them depending on how the anyons fuse. If an atomic force microscope can 'grab' an anyon in order measure this force, perhaps it can also be used to drag one around and perform a braid.

Thus, we see that new ideas would be extremely helpful in the search for non-Abelian topological phases. It may be the case that each physical system, e.g. FQHE, cold atoms,

Sr_2RuO_4 films, etc..., may be suited to its own types of measurements, such as the ones described above and in Secs. II.C.3, III.F, but general considerations, such as topological entropy (Kitaev and Preskill, 2006; Levin and Wen, 2006), may inform and unify these investigations. Another difficulty is that, as mentioned above, we are currently searching for non-Abelian topological phases in those systems in which there is an absence of alternatives. It would be far better to have positive *a priori* reasons to look at particular systems.

This state of affairs points to the dire need for general principles, perhaps of a mathematical nature, which will tell us when a system is likely to have a topological phase. Equivalently, can we define the necessary conditions for the existence of a topological phase with non-Abelian quasiparticle statistics? For contrast, consider the case of magnetism. Although there is a great deal which we don't know about magnetism, we do know that we need solids containing ions with partially filled d or f shells. Depending on the effective Coulomb interaction within these orbitals and their filling fractions, we understand how various mechanisms such as exchange and superexchange can lead to effective spin-spin interactions which, in turn, can lead to ferromagnetism, antiferromagnetism, spin-density-waves, etc.. We need a comparable understanding of topological phases. One direction, which we have described in Sec. III.G, is to analyze models in which the interactions encode some combinatorial relations, such as those associated with string nets or loop gases (Fendley, 2007; Fendley and Fradkin, 2005; Fidkowski et al., 2006; Freedman et al., 2005a; Levin and Wen, 2005b). However, we only have a few examples of microscopic interactions which give rise to these intermediate scale structures. We sorely need more general guidelines which would enable us to look at a given Hamiltonian and determine if it is likely to have a non-Abelian topological phase; a more detailed analysis or experimental study could then be carried out. This is a particularly important direction for future research because, although nature has given us the quantum Hall regime as a promising hunting ground for topological phases, the energy scales are very low. A topological phase in a transition metal oxide might have a much larger gap and, therefore, be much more robust.

An important problem on the mathematical side is a complete classification of topological phases. In this review, we have focussed on a few examples of topological phases: those associated with $SU(2)_k$ Chern-Simons theory, especially the $k = 2, 3$ cases. These are part of a more general class associated with an arbitrary semi-simple Lie group G at level k. Another class is associated with discrete groups, such as phases whose effective field theories are lattice gauge theories with discrete gauge group. New topological phases can be obtained from both of these by coset constructions and/or tensoring together different effective field theories. However, a complete classification is not known. With a complete classification in hand, if we were to observe a topological phase in nature, we could identify it by comparing it against the list of topological phases. Since we have observed relatively few topological phases in nature, we have not needed a complete classification. If, however, many more are lurking, waiting to be observed, then a complete classification could be useful in the way that the closely-related problem of classifying rational conformal field theories has proved useful in understanding classical and quantum critical points.

We refer here, as we have throughout this article, to topological phases as we have defined them in Sec. III (and which we briefly recapitulate below). There are many other possible 'exotic' phases which share some characteristics of topological phases, such as the emergence of gauge fields in their low-energy theories (Wen, 2004), but do not satisfy all of the criteria. These do not appear to be useful for quantum computation.

Finally, the three-dimensional frontier must be mentioned. Most theory (and experiment) pertains to 2D or quasi-2D systems. In 3+1-dimensions, even the underlying mathematical structure of TQFTs is quite open. Little is known beyond finite group gauge theories. For example, we do not know if quantum information can (in the thermodynamic limit) be permanently stored at finite temperature in any 3-dimensional system. (By Dennis et al., 2002, this is possible in 4+1-dimensions, not possible in 2+1-dimensions, and is an open question in 3+1-dimensions.) The case of 2+1-dimensions has been the playground of anyons for 30 years. Will loop-like "particles" in 3+1-dimensions be as rich a story 30 years from now?

Perhaps it is fitting to end this review with a succinct statement of the definition of a topological phase: the ground state in the presence of multiple quasiparticles or in a non-trivial topology has a stable degeneracy which is immune to weak (but finite) local perturbations. Note that the existence of an excitation gap is not needed as a part of this definition although, as should be obvious by this point, the stability of the ground state degeneracy to local perturbations almost always necessitates the existence of an excitation gap. We make three comments about this definition before concluding: (1) incompressible FQH states satisfy our definition and they are, so far, the only experimentally-established topological phases. (2) The existence of a topological phase does not, by itself, enable topological quantum computation – one needs quasiparticles with non-Abelian braiding statistics, and for *universal* topological quantum computation, these quasiparticles' topological properties must belong to a class which includes $SU(2)_k$, with $k = 3, 5, 6, 7, 8, 9, \ldots$, as we have discussed extensively in this article. (3) Possible non-Abelian quantum Hall states, such as $\nu = 5/2$ and $12/5$ are the first among several possible candidates, including Sr_2RuO_4, which has recently been shown to be a chiral p-wave superconductor (Kidwingira et al., 2006; Xia et al., 2006), and p-wave paired cold atom superfluids.

Note added in proof: A measurement of the charge of a quasi-particle in a $\nu = 5/2$ fractional quantum Hall state has been recently reported by Dolev et al. in arXiv:0802.0930 (to appear in Nature). In that measurement, current tunnels across a constriction between two opposite edge states of a Hall bar, and the quasi-particle charge is extracted from the current shot noise. Dolev et al. have found the charge to be consistent with $e/4$, and inconsistent with $e/2$. A quasi-particle charge of $e/4$ is consistent with paired states at $\nu = 5/2$, including both the Moore-Read state, the anti-Pfaffian state, and also

Abelian paired states. Thus, the observation of charge $e/4$ quasiparticles is necessary but not sufficient to show that the $\nu = 5/2$ state is non-Abelian.

Note added in proof:

Dolev *et al.* (arXiv:0802.0930; Nature, in press) have recently measured the low-frequency current noise ('shot noise') at a point contact in the $\nu = 5/2$ state. They find the noise to be consistent with charge-$e/4$ quasiparticles, and inconsistent with $e/2$. A quasi-particle charge of $e/4$ is consistent with paired states at $\nu = 5/2$, including both the Moore-Read (Pfaffian) state, the anti-Pfaffian state, and also Abelian paired states.

In another recent experiment, Radu *et al.* (arXiv:0803.3530) measured the dependence on voltage and temperature of the tunneling current at a point contact in the $\nu = 5/2$ state. They find that the current is well fit by the form $I = T^{\alpha} F(e^* V/k_B T)$ where $e^* = e/4$, and the exponent α and scaling function $F(x)$ are at least consistent with the anti-Pfaffian state, although it is premature to rule out other states.

In a recent preprint (arXiv:0803.0737), Peterson *et al.* have performed finite-system exact diagonalization studies which find the correct ground state degeneracy on the torus at $\nu = 5/2$ and also observe the expected degeneracy between Pfaffian and anti-Pfaffian states. The key new ingredient in their calculation is the inclusion of the effects of the finite-thickness of the 2D layer which also appears to enhance the overlap between the non-Abelian states and the exact numerical finite-system wavefunction at $\nu = 5/2$.

The first two papers provide the first direct experimental evidence in support of the 5/2 state being non-Abelian while the third paper strengthens the case from numerics.

Acknowledgments

The authors are grateful for support from Microsoft Station Q, the National Science Foundation under grant DMR-0411800, the Army Research Office under grant W911NF-04-1-0236, the Israel Science Foundation, the U.S.-Israel Binational Science Foundation, and Alcatel-Lucent Bell Labs.

APPENDIX A: Conformal Field Theory (CFT) for Pedestrians

We consider chiral CFTs in 2 dimensions. "Chiral" means that all of our fields will be functions of $z = x + iy$ only and not functions of $\bar{z}$. (For a good introduction to CFT see (Belavin et al., 1984; Di Francesco et al., 1997)).

(a) OPE: To describe a CFT we give its "conformal data", including a set of primary fields, each with a conformal dimension Δ, a table of fusion rules of these fields and a central charge c (which we will not need here, but is fundamental to defining each CFT). Data for three CFTs are given in Table II.

The operator product expansion (OPE) describes what happens to two fields when their positions approach each other. We write the OPE for two arbitrary fields ϕ_i and ϕ_j as

$$\lim_{z\to w} \phi_i(z)\phi_j(w) = \textstyle\sum_k C_{ij}^k \; (z-w)^{\Delta_k - \Delta_i - \Delta_j} \; \phi_k(w) \quad \text{(A1)}$$

where the structure constants C_{ij}^k are only nonzero as indicated by the fusion table. (For our purposes, we can assume that all fields ϕ_k are primary fields. So called "descendant" fields, which are certain types of "raising operators" applied to the primary fields, can also occur on the right hand side, with the dimension of the descendant being greater than that of its primary by an integer. Since we will be concerned only with leading singularities in the OPE, we will ignore descendants. For all the CFTs that we consider the coefficient of the primary on the right hand side will not vanish, although this can happen.) Note that the OPE works inside a correlator. For example, in the $\mathbb{Z}_3$ parafermion CFT (see Table II), since $\sigma_1 \times \psi_1 = \epsilon$, for arbitrary fields ϕ_i we have

$$\begin{aligned} &\lim_{z\to w} \langle\, \phi_1(z_1) \dots \phi_M(z_M)\, \sigma_1(z)\psi_1(w)\,\rangle \qquad \text{(A2)} \\ \sim\; &(z-w)^{2/5-1/15-2/3} \langle\, \phi_1(z_1) \dots \phi_M(z_M)\epsilon(w)\,\rangle \end{aligned}$$

In addition to the OPE, there is also an important "neutrality" condition: a correlator is zero unless all of the fields can fuse together to form the identity field $\mathbf{1}$. For example, in the $\mathbb{Z}_3$ parafermion field theory $\langle\psi_2\psi_1\rangle \neq 0$ since $\psi_2 \times \psi_1 = \mathbf{1}$, but $\langle\psi_1\psi_1\rangle = 0$ since $\psi_1 \times \psi_1 = \psi_2 \neq \mathbf{1}$.

Chiral Bose Vertex: ($c = 1$)

	Δ
$e^{i\alpha\phi}$	$\alpha^2/2$

$\times$	$e^{i\alpha\phi}$
$e^{i\beta\phi}$	$e^{i(\alpha+\beta)\phi}$

Ising CFT: ($c = 1/2$)

	Δ
ψ	$1/2$
σ	$1/16$

$\times$	ψ	σ
ψ	$\mathbf{1}$	
σ	σ	$\mathbf{1}+\psi$

$\mathbb{Z}_3$ Parafermion CFT: ($c = 4/5$)

	Δ
ψ_1	$2/3$
ψ_2	$2/3$
σ_1	$1/15$
σ_2	$1/15$
ϵ	$2/5$

$\times$	ψ_1	ψ_2	σ_1	σ_2	ϵ
ψ_1	ψ_2				
ψ_2	$\mathbf{1}$	ψ_1			
σ_1	ϵ	σ_2	$\sigma_2+\psi_1$		
σ_2	σ_1	ϵ	$\mathbf{1}+\epsilon$	$\sigma_1+\psi_2$	
ϵ	σ_2	σ_1	$\sigma_1+\psi_2$	$\sigma_2+\psi_1$	$\mathbf{1}+\epsilon$

TABLE II Conformal data for three CFTs. Given is the list of primary fields in the CFT with their conformal dimension Δ, as well as the fusion table. In addition, every CFT has an identity field $\mathbf{1}$ with dimension $\Delta = 0$ which fuses trivially with any field ($\mathbf{1} \times \phi_i = \phi_i$ for any ϕ_i). Note that fusion tables are symmetric so only the lower part is given. In the Ising CFT the field ψ is frequently notated as ϵ. This fusion table indicates the nonzero elements of the fusion matrix N_{ab}^c. For example in the $\mathbb{Z}_3$ CFT, since $\sigma_1 \times \sigma_2 = \mathbf{1} + \epsilon$, $N_{\sigma_1\sigma_2}^1 = N_{\sigma_1\sigma_2}^{\epsilon} = 1$ and $N_{\sigma_1\sigma_2}^c = 0$ for all c not equal to $\mathbf{1}$ or ϵ.

(b) Conformal Blocks: Let us look at what happens when a fusion has more than one possible result. For example, in the Ising CFT, $\sigma \times \sigma = \mathbf{1} + \psi$. Using the OPE, we have

$$\lim_{w_1\to w_2} \sigma(w_1)\sigma(w_2) \sim \frac{\mathbf{1}}{(w_1-w_2)^{1/8}} + (w_1-w_2)^{3/8}\,\psi \quad \text{(A3)}$$

where we have neglected the constants C_{ij}^k. If we consider $\langle\sigma\sigma\rangle$, the neutrality condition picks out only the first term in

Eq. A3 where the two σ's fuse to form $\mathbf{1}$. Similarly, $\langle\sigma\sigma\psi\rangle$ results in the second term of Eq. A3 where the two σ's fuse to form ψ which then fuses with the additional ψ to make $\mathbf{1}$.

Fields may also fuse to form the identity in more than one way. For example, in the correlator $\langle\sigma(w_1)\sigma(w_2)\sigma(w_3)\sigma(w_4)\rangle$ of the Ising CFT, the identity is obtained via two possible fusion paths — resulting in two different so-called "conformal blocks". On the one hand, one can fuse $\sigma(w_1)$ and $\sigma(w_2)$ to form $\mathbf{1}$ and similarly fuse $\sigma(w_3)$ and $\sigma(w_4)$ to form $\mathbf{1}$. Alternately, one can fuse $\sigma(w_1)$ and $\sigma(w_2)$ to form ψ and fuse $\sigma(w_3)$ and $\sigma(w_4)$ to form ψ then fuse the two resulting ψ fields together to form $\mathbf{1}$. The correlator generally gives a linear combination of the possible resulting conformal blocks. We should thus think of such a correlator as living in a vector space rather than having a single value. (If we instead choose to fuse 1 with 3, and 2 with 4, we would obtain two blocks which are linear combinations of the ones found by fusing 1 with 2 and 3 with 4. The resulting vectors space, however, is independent of the order of fusion). Crucially, transporting the coordinates w_i around each other makes a rotation within this vector space.

To be more clear about the notion of conformal blocks, let us look at the explicit form of the Ising CFT correlator

$$\lim_{w\to\infty}\langle\sigma(0)\sigma(z)\sigma(1)\sigma(w)\rangle = a_+ F_+ + a_- F_- \quad \text{(A4)}$$

$$F_\pm(z) \sim (wz(1-z))^{-1/8}\sqrt{1\pm\sqrt{1-z}} \quad \text{(A5)}$$

where a_+ and a_- are arbitrary coefficients. (Eqs. A4-A5 are results of calculations not given here (Di Francesco et al., 1997)). When $z\to 0$ we have $F_+ \sim z^{-1/8}$ whereas $F_- \sim z^{3/8}$. Comparing to Eq. A3 we conclude that F_+ is the result of fusing $\sigma(0)\times\sigma(z)\to\mathbf{1}$ whereas F_- is the result of fusing $\sigma(0)\times\sigma(z)\to\psi$. As z is taken in a clockwise circle around the point $z=1$, the inner square-root changes sign, switching F_+ and F_-. Thus, this "braiding" (or "monodromy") operation transforms

$$\binom{a_+}{a_-} \to e^{2\pi i/8}\begin{pmatrix}0 & 1\\ 1 & 0\end{pmatrix}\binom{a_+}{a_-} \quad \text{(A6)}$$

Having a multiple valued correlator (I.e., multiple conformal blocks) is a result of having such branch cuts. Braiding the coordinates (w's) around each other results in the correlator changing values within its allowable vector space.

A useful technique for counting conformal blocks is the "Bratteli diagram." In Fig. 22 we give the Bratteli diagram for the fusion of multiple σ fields in the Ising CFT. Starting with $\mathbf{1}$ at the lower left, at each step moving from the left to the right, we fuse with one more σ field. At the first step, the arrow points from $\mathbf{1}$ to σ since $\mathbf{1}\times\sigma=\sigma$. At the next step σ fuses with σ to produce either ψ or $\mathbf{1}$ and so forth. Each conformal block is associated with a path through the diagram. Thus to determine the number of blocks in $\langle\sigma\sigma\sigma\sigma\rangle$ we count the number of paths of four steps in the diagram starting at the lower left and ending at $\mathbf{1}$.

(c) Changing Bases: As mentioned above, the space spanned by the conformal blocks resulting from the fusion of fields is independent of the order of fusion (which field is fused with which field first). However, fusing fields together

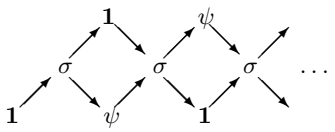

FIG. 22 Bratteli diagram for fusion of multiple σ fields in the Ising CFT.

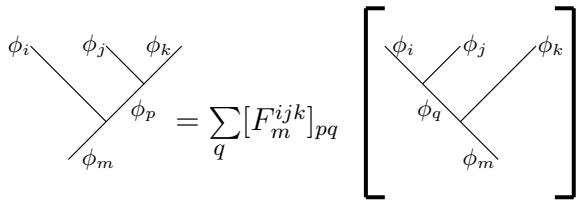

FIG. 23 The basis states obtained by fusing fields together depends on the order of fusion (although the space spanned by these states is independent of the order). The F-matrix converts between the possible bases.

in different orders results in a different basis for that space. A convenient way to notate fusion of fields is a particular order is using fusion tree diagrams as shown in Fig. 23. Both diagrams in this figure show the fusion of three initial fields ϕ_i,ϕ_j,ϕ_k. The diagram on the left shows ϕ_j and ϕ_k fusing together first to form ϕ_p which then fuses with ϕ_i to form ϕ_m. One could equally well have chosen to fuse together ϕ_i and ϕ_j together first before fusing the result with ϕ_k, as shown on the right of Fig. 23. The mathematical relation between these two bases is given in the equation shown in Fig. 23 in terms of the so-called F-matrix (for "fusion"), which is an important property of any given CFT or TQFT. An example of using the F-matrix is given in section IV.B.

(d) The Chiral Boson: A particularly important CFT is obtained from a free Bose field theory in 1+1 dimension by keeping only the left moving modes (Di Francesco et al., 1997). The free chiral Bose field $\phi(z)$, which is a sum of left moving creation and annihilation operators, has a correlator $\langle\phi(z)\phi(z')\rangle = -\log(z-z')$. We then define the normal ordered "chiral vertex operator" : $e^{i\alpha\phi(z)}$: , which is a conformal field. Note that we will typically not write the normal ordering indicators ': :'. Since ϕ is a free field, Wick's theorem can be used to obtain (Di Francesco et al., 1997)

$$\begin{aligned}\left\langle\, e^{i\alpha_1\phi}(z_1)\ldots e^{i\alpha_N\phi}(z_N)\,\right\rangle &= e^{-\sum_{i<j}\alpha_i\alpha_j\langle\phi(z_i)\phi(z_j)\rangle}\\ &= \textstyle\prod_{i<j}\,(z_i-z_j)^{\alpha_i\alpha_j}\end{aligned} \quad \text{(A7)}$$

(Strictly speaking thi identity holds only if the neutrality condition $\sum_i\alpha_i = 0$ is satisfied, otherwise the correlator vanishes).

References

Abo-Shaeer, J. R., C. Raman, J. Vogels, and W. Ketterle, 2001, Observation of vortex lattices in bose-einstein condensate, Science **292**, 476.

Aharonov, D., and M. Ben-Or, 1997, in Proceedings of the twenty-ninth annual ACM symposium on

Theory of computing (ACM Press, New York, NY, USA), pp. 176–188, ISBN 0-89791-888-6.

Anderson, P. W., 1973, Resonating valence bonds: a new kind of insulator?, Mat. Res. Bull. **8**, 153.

Anderson, P. W., 1987, The resonating valence bond state in la_2cuo_4 and superconductivity, Science **235**, 1196.

Aneziris, C., A. P. Balachandran, M. Bourdeau, S. Jo, T. R. Ramadas, and R. D. Sorkin, 1989, Statistics and general relativity, Mod. Phys. Lett. **A4**, 331.

Ardonne, E., 2002, Parafermion statistics and the application to non-Abelian quantum Hall states, J. Phys. A **35**, 447.

Ardonne, E., P. Bouwknegt, and K. Schoutens, 2001, Non-Abelian quantum Hall states - exclusion statistics, k-matrices and duality, J. of Statistical Phys. **102**, 421.

Ardonne, E., and E.-A. Kim, 2007, Hearing non-Abelian statistics from a Moore-Read double point contact interferometer, arXiv:0705.2902.

Ardonne, E., and K. Schoutens, 1999, New class of non-Abelian spin-singlet quantum Hall states, Phys. Rev. Lett. **82**(25), 5096.

Ardonne, E., and K. Schoutens, 2007, Wavefunctions for topological quantum registers, Ann. Phys. (N.Y.) **322**, 221.

Arovas, D., J. R. Schrieffer, and F. Wilczek, 1984, Fractional statistics and the quantum Hall effect, Phys. Rev. Lett. **53**(7), 722.

Bais, F. A., 1980, Flux metamorphosis, Nucl. Phys. **B170**, 32.

Bais, F. A., P. van Driel, and M. de Wild Propitius, 1992, Quantum symmetries in discrete gauge theories, Phys. Lett. **B280**, 63.

Bais, F. A., P. van Driel, and M. de Wild Propitius, 1993a, Anyons in discrete gauge theories with Chern-Simons terms, Nucl. Phys. **B393**, 547.

Bais, F. A., A. Morozov, and M. de Wild Propitius, 1993b, Charge screening in the Higgs phase of Chern-Simons electrodynamics, Phys. Rev. Lett. **71**, 2383.

Bakalov, B., and A. Kirillov, 2001, Lectures on Tensor Categories and Modular Functors, volume 21 of University Lecture Series (American Mathematical Society).

Balatsky, A., and E. Fradkin, 1991, Singlet quantum Hall effect and Chern-Simons theories, Phys. Rev. B **43**(13), 10622.

Balents, L., M. P. A. Fisher, and S. M. Girvin, 2002, Fractionalization in an easy-axis kagome antiferromagnet, Phys. Rev. B **65**(9), 224412.

Balents, L., M. P. A. Fisher, and C. Nayak, 1998, Nodal liquid theory of the pseudo-gap phase of high-T_c superconductors, Int. J. Mod. Phys. B **12**(10), 1033.

Balents, L., M. P. A. Fisher, and C. Nayak, 1999, Dual order parameter for the nodal liquid, Phys. Rev. B **60**, 1654.

Balents, L., M. P. A. Fisher, and C. Nayak, 2000, Dual vortex theory of strongly interacting electrons: A non-fermi liquid with a twist, Phys. Rev. B **61**(9), 6307.

Bantay, P., 1997, The frobenius-schur indicator in conformal field theory, Phys.Lett. B **394**, 87.

Baskaran, G., Z. Zou, and P. W. Anderson, 1987, The resonating valence bond state and high-T_c superconductivity – a mean field theory, Solid State Commun. **63**(11), 973.

Belavin, A. A., A. M. Polyakov, and A. B. Zamolodchikov, 1984, Infinite conformal symmetry in two-dimensional quantum field theory, Nucl. Phys. **B241**, 333.

Bena, C., and C. Nayak, 2006, Effects of non-Abelian statistics on two-terminal shot noise in a quantum Hall liquid in the Pfaffian state, Phys. Rev. B **73**(15), 155335.

Bergholtz, E. J., J. Kailasvuori, E. Wikberg, T. H. Hansson, and A. Karlhede, 2006, Pfaffian quantum Hall state made simple: Multiple vacua and domain walls on a thin torus, Phys. Rev. B **74**(8), 081308.

Berry, M. V., 1984, Quantal phase factors accompanying adiabatic changes, Proc. Roy. Soc. Lond. **A392**, 45.

Bishara, W., and C. Nayak, 2007, Non-Abelian anyon superconductivity, phys. Rev. Lett. (in press); cond-mat/0703097.

Blanchet, C., N. Habegger, G. Masbaum, and P. Vogel, 1995, Topological quantum field theories derived from the kauffman bracket, Topology **34**, 883.

Blok, B., and X. G. Wen, 1990, Effective theories of the fractional quantum Hall effect: Hierarchy construction, Phys. Rev. B **42**(13), 8145.

Blok, B., and X.-G. Wen, 1992, Many-body systems with non-Abelian statistics, Nuc. Phys. B **374**, 615.

Boebinger, G., H. Stomer, D. Tsui, A. Chang, J. Hwang, A. Cho, C. Tu, and G. Weimann, 1987, Activation energies and localization in the fractional quantum Hall effect, Phys. Rev. B **36**, 7919.

Bonderson, P., A. Kitaev, and K. Shtengel, 2006a, Detecting non-Abelian statistics in the $\nu = 5/2$ fractional quantum Hall state, Phys. Rev. Lett. **96**(1), 016803.

Bonderson, P., K. Shtengel, and J. K. Slingerland, 2006b, Probing non-Abelian statistics with quasiparticle interferometry, Phys. Rev. Lett. **97**(1), 016401.

Bonderson, P., K. Shtengel, and J. K. Slingerland, 2007, Decoherence of anyonic charge in interferometry measurements, Phys. Rev. Lett. **98**(7), 070401.

Bonesteel, N. E., 1989, Valence bonds and the Lieb-Schultz-Mattis theorem, Phys. Rev. B **40**(14), 8954.

Bonesteel, N. E., 2000, Chiral spin liquids and quantum error-correcting codes, Phys. Rev. A **62**(6), 062310.

Bonesteel, N. E., L. Hormozi, G. Zikos, and S. H. Simon, 2005, Braid topologies for quantum computation, Phys. Rev. Lett. **95**(14), 140503.

Bonesteel, N. E., I. A. McDonald, and C. Nayak, 1996, Gauge fields and pairing in double-layer composite fermion metals, Phys. Rev. Lett. **77**(14), 3009.

Bonesteel, N. E., and K. Yang, 2007, Infinite-randomness fixed points for chains of non-abelian quasiparticles, Physical Review Letters **99**(14), 140405/1.

Bouwknegt, P., and K. Schoutens, 1999, Exclusion statistics in conformal field theory - generalized fermions and spinons for level-1 wzw theories, Nucl. Phys. B **547**, 501.

Bravyi, S., 2006, Universal quantum computation with the $\nu = 5/2$ fractional quantum Hall state, Phys. Rev. A **73**(4), 042313.

Bravyi, S., and A. Kitaev, 2001, Quantum invariants of 3-manifolds and quantum computation, unpublished.

Bremner, M. J., C. M. Dawson, J. L. Dodd, A. Gilchrist, A. W. Harrow, D. Mortimer, M. A. Nielsen, and T. J. Osborne, 2002, Practical scheme for quantum computation with any two-qubit entangling gate, Phys. Rev. Lett. **89**(24), 247902.

Brennen, G. K., and J. K. Pachos, 2007, Why should anyone care about computing with anyons?, arXiv:0704.2241.

Bretin, V., S. Stock, Y. Seurin, and J. Dalibard, 2004, Fast rotation of a bose-einstein condensate, Phys. Rev. Lett. **92**(5), 050403/1.

de C. Chamon, C., D. E. Freed, S. A. Kivelson, S. L. Sondhi, and X. G. Wen, 1997, Two point-contact interferometer for quantum Hall systems, Phys. Rev. B **55**(4), 2331.

Calderbank, A. R., and P. W. Shor, 1996, Good quantum error-correcting codes exist, Phys. Rev. A **54**, 1098.

Camino, F. E., W. Zhou, and V. J. Goldman, 2005, Realization of a laughlin quasiparticle interferometer: Observation of fractional statistics, Phys. Rev. B **72**(7), 075342.

Cappelli, A., L. S. Georgiev, and I. T. Todorov, 1999, A unified conformal field theory description of paired quantum Hall states, Comm. Math. Phys. **205**, 657.

Cappelli, A., L. S. Georgiev, and I. T. Todorov, 2001, Parafermion Hall states from coset projections of Abelian conformal theories,

Nuc. Phys. B **599**(3), 499.
Cardy, J. L., 1986, Operator content of two-dimensional conformally invariant theories, Nucl. Phys. **B270**, 186.
Cattaneo, A. S., P. Cotta-Ramusino, J. Froehlich, and M. Martellini, 1995, Topological bf theories in 3 and 4 dimensions, J. of Math. Physics **36**, 6137.
Chang, C.-C., and J. K. Jain, 2004, Microscopic origin of the next-generation fractional quantum Hall effect, Phys. Rev. Lett. **92**(19), 196806.
Chayes, J. T., L. Chayes, and S. A. Kivelson, 1989, Valence bond ground states in a frustrated two-dimensional spin-$1/2$ Heisenberg antiferromagnet, Commun. Math. Pys. **123**, 53.
Chen, H.-D., and J. Hu, 2007, Majorana fermions, exact mappings between classical and topological orders, cond-mat/0702366.
Chen, Y., F. Wilczek, E. Witten, and B. Halperin, 1989, On anyon superconductivity, Int. J. Mod. Phys. B **3**, 1001.
Choi, H., W. Kang, S. Das Sarma, L. Pfeiffer, and K. West, 2007, Density matrix renormalization group study of incompressible fractional quantum hall states, arXiv:0706.4469.
Chung, S. B., and M. Stone, 2006, Proposal for reading out anyon qubits in non-Abelian $\nu = 12/5$ quantum Hall state, Phys. Rev. B **73**(24), 245311.
Chung, S. B., and M. Stone, 2007, Explicit monodromy of Moore-Read wavefunctions on a torus, J. of Physics A: Math. and Theor. **40**(19), 4923.
Coldea, R., D. Tennant, and Z. Tylczynski, 2003, Observation of extended scattering continua characteristic of spin fractionalization in the 2d frustrated quantum magnet Cs_2CuCl_4 by neutron scattering, Phys. Rev. B **68**, 134424/1.
Collins, G., 2006, Computing with quantum knots, Sci. American **4**, 57.
Cooper, N. R., and E. H. Rezayi, 2007, Competing compressible and incompressible phases in rotating atomic bose gases at filling factor $\nu = 2$, Phys. Rev. A **75**(1), 013627.
Cooper, N. R., N. K. Wilkin, and J. M. F. Gunn, 2001, Quantum phases of vortices in rotating bose-einstein condensates, Phys. Rev. Lett. **87**, 120405/1.
Das Sarma, S., M. Freedman, and C. Nayak, 2005, Topologically protected qubits from a possible non-Abelian fractional quantum Hall state, Phys. Rev. Lett. **94**(16), 166802.
Das Sarma, S., M. Freedman, and C. Nayak, 2006a, Topological quantum computation, Phys. Today **59**, 32.
Das Sarma, S., C. Nayak, and S. Tewari, 2006b, Proposal to stabilize and detect half-quantum vortices in Strontium Ruthenate thin films: Non-Abelian braiding statistics of vortices in a $p_x + ip_y$ superconductor, Phys. Rev. B **73**(22), 220502.
Das Sarma, S., and A. Pinczuk (eds.), 1997, Perspectives in quantum Hall effects : novel quantum liquids in low-dimensional semiconductor structures (Wiley, New York).
De Picciotto, R., M. Reznikov, M. Heiblum, V. Umansky, G. Bunin, and D. Mahalu, 1997, Direct observation of a fractional charge, Nature **389**, 162.
Dennis, E., A. Kitaev, A. Landahl, and J. Preskill, 2002, Topological quantum memory, J. of Math. Physics **43**, 4452.
Deser, S., R. Jackiw, and S. Templeton, 1982, Three-dimensional massive gauge theories, Phys. Rev. Lett. **48**(15), 975.
Deutsch, D., 1985, Quantum theory, the Church-Turing principle and the universal quantum computer, Proceedings of the Royal Society of London A **400**, 97.
Di Francesco, P., P. Mathieu, and D. Sénéchal, 1997, Conformal Field Theory (Springer, New York).
Dijkgraaf, R., and E. Witten, 1990, Topological gauge theories and group cohomology, Commun. Math. Phys. **129**, 393.
Dimov, I., B. I. Halperin, and C. Nayak, 2007, Spin order in paired quantum hall states, arXiv:0710.1921.
DiVincenzo, D. P., 2000, The physical implementation of quantum computation, fortschritte Der Physik-progress Phys. **48**(9-11), 771.
Doplicher, S., R. Haag, and J. E. Roberts, 1971, Local observables and particle statistics. I, Comm. Math. Phys. **23**, 199.
Doplicher, S., R. Haag, and J. E. Roberts, 1974, Local observables and particle statistics. II, Comm. Math. Phys. **35**, 49.
Doucot, B., M. V. Feigel'man, L. B. Ioffe, and A. S. Ioselevich, 2005, Protected qubits and chern-simons theories in josephson junction arrays, Phys. Rev. B **71**(2), 024505.
Douçot, B., L. B. Ioffe, and J. Vidal, 2004, Discrete non-Abelian gauge theories in Josephson-junction arrays and quantum computation, Phys. Rev. B **69**(21), 214501.
Du, R. R., H. L. Stormer, D. C. Tsui, L. N. Pfeiffer, and K. W. West, 1993, Experimental evidence for new particles in the fractional quantum Hall effect, Phys. Rev. Lett. **70**(19), 2944.
Duan, L.-M., E. Demler, and M. D. Lukin, 2003, Controlling spin exchange interactions of ultracold atoms in optical lattices, Phys. Rev. Lett. **91**(9), 090402.
Dyakonov, M. I., 2006, Is fault-tolerant quantum computation really possible?, arXiv:quant-ph/0610117.
Eisenstein, J. P., K. B. Cooper, L. N. Pfeiffer, and K. W. West, 2002, Insulating and fractional quantum Hall states in the first excited Landau level, Phys. Rev. Lett. **88**(7), 076801/1.
Eisenstein, J. P., R. L. Willett, H. L. Stormer, L. N. Pfeiffer, and K. W. West, 1990, Activation energies for the even-denominator fractional quantum Hall effect, Surface Science **229**, 31.
Elitzur, S., G. Moore, A. Schwimmer, and N. Seiberg, 1989, Remarks on the canonical quantization of the Chern-Simons-Witten theory, Nuc. Phys. B **326**(1), 108.
Farhi, E., J. Goldstone, S. Gutmann, and M. Sipser, 2000, Quantum computation by adiabatic evolution, arXiv.org:quant-ph/0001106.
Fateev, V. A., and A. B. Zamolodchikov, 1985, Parafermionic currents in the two-dimensional conformal quantum field theory and selfdual critical points in $z(n)$ invariant statistical systems, Sov. Phys. JETP **62**, 215.
Feiguin, A., S. Trebst, A. W. W. Ludwig, M. Troyer, A. Kitaev, Z. Wang, and M. H. Freedman, 2007a, Interacting anyons in topological quantum liquids: The golden chain, Phys. Rev. Lett. **98**(16), 160409.
Feiguin, A. E., C. Rezayi, E.and Nayak, and S. Das Sarma, 2007b, Density matrix renormalization group study of incompressible fractional quantum hall states, arXiv:0706.4469.
Feldman, D. E., Y. Gefen, A. Kitaev, K. T. Law, and A. Stern, 2006, Shot noise in anyonic Mach-Zehnder interferometer, arXiv:cond-mat/0612608.
Feldman, D. E., and A. Kitaev, 2006, Detecting non-Abelian statistics with an electronic Mach-Zehnder interferometer, Phys. Rev. Lett. **97**(18), 186803.
Fendley, P., 2007, Quantum loop models and the non-abelian toric code, arXiv:0711.0014.
Fendley, P., M. P. A. Fisher, and C. Nayak, 2006, Dynamical disentanglement across a point contact in a non-Abelian quantum Hall state, Phys. Rev. Lett. **97**(3), 036801.
Fendley, P., M. P. A. Fisher, and C. Nayak, 2007a, Edge states and tunneling of non-Abelian quasiparticles in the $\nu = 5/2$ quantum Hall state and p + ip superconductors, Phys. Rev. B **75**(4), 045317.
Fendley, P., M. P. A. Fisher, and C. Nayak, 2007b, Topological entanglement entropy from the holographic partition function, J. Stat. Phys. **126**, 1111.
Fendley, P., and E. Fradkin, 2005, Realizing non-Abelian statistics in time-reversal-invariant systems, Phys. Rev. B **72**(2), 024412.
Fendley, P., R. Moessner, and S. L. Sondhi, 2002, Classical dimers

on the triangular lattice, Phys. Rev. B **66**, 214513.
Fetter, A., C. Hanna, and R. Laughlin, 1989, Random-phase approximation in the fractional-statistics gas, Phys. Rev. B **39**, 9679.
Feynman, R. P., 1982, Simulating physics with computers, International Journal of Theor. Physics **21**, 467.
Feynman, R. P., 1986, Quantum mechanical computers, Foundations of Physics **16**(6), 507.
Fidkowski, L., 2007, Double point contact in the k=3 read-rezayi state, arXiv:0704.3291.
Fidkowski, L., M. Freedman, C. Nayak, K. Walker, and Z. Wang, 2006, From string nets to nonabelions, cond-mat/0610583.
Fradkin, E., M. Huerta, and G. Zemba, 2001, Effective Chern-Simons theories of Pfaffian and parafermionic quantum Hall states, and orbifold conformal field theories, Nucl. Phys. B **601**, 591.
Fradkin, E., and L. P. Kadanoff, 1980, Disorder variables and parafermions in two-dimensional statistical mechanics, Nucl. Phys. B **170**(1), 1.
Fradkin, E., C. Nayak, and K. Schoutens, 1999, Landau-Ginzburg theories for non-Abelian quantum Hall states, Nucl. Phys. B **546**, 711.
Fradkin, E., C. Nayak, A. Tsvelik, and F. Wilczek, 1998, A Chern-Simons effective field theory for the Pfaffian quantum Hall state, Nucl. Phys. B **516**(3), 704.
Fradkin, E., and S. H. Shenker, 1975, Phase diagrams of lattice gauge theories with Higgs fields, Phys. Rev. D **19**(12), 3682.
Fredenhagen, K., K. H. Rehren, and B. Schroer, 1989, Superselection sectors with braid group statistics and exchange algebras, Commun. Math. Phys. **125**, 201.
Freedman, M., A. Kitaev, M. Larsen, and Z. Wang, 2003a, Topological quantum computation, Bull. Amer. Math. Soc. **40**, 31.
Freedman, M., C. Nayak, and K. Shtengel, 2003b, Non-Abelian topological phases in an extended Hubbard model.
Freedman, M., C. Nayak, and K. Shtengel, 2005a, Extended Hubbard model with ring exchange: A route to a non-Abelian topological phase, Phys. Rev. Lett. **94**(6), 066401.
Freedman, M., C. Nayak, and K. Shtengel, 2005b, Line of critical points in 2 + 1 dimensions: Quantum critical loop gases and non-Abelian gauge theory, Phys. Rev. Lett. **94**(14), 147205.
Freedman, M., C. Nayak, K. Shtengel, K. Walker, and Z. Wang, 2004, A class of P, T-invariant topological phases of interacting electrons, Ann. Phys. (N.Y.) **310**, 428.
Freedman, M., C. Nayak, and K. Walker, 2006, Towards universal topological quantum computation in the $\nu = 5/2$ fractional quantum Hall state, Phys. Rev. B **73**(24), 245307.
Freedman, M. H., 2001, Quantum computation and the localization of modular functors, Found. Comput. Math. **1**, 183.
Freedman, M. H., 2003, A magnetic model with a possible Chern-Simons phase, Commun. Math. Phys. **234**, 129.
Freedman, M. H., M. J. Larsen, and Z. Wang, 2002a, A modular functor which is universal for quantum computation, Commun. Math. Phys. **227**, 605.
Freedman, M. H., M. J. Larsen, and Z. Wang, 2002b, The two-eigenvalue problem and density of Jones representation of braid groups, Commun. Math. Phys. **228**, 177.
Fröhlich, J., and F. Gabbiani, 1990, Braid statistics in local quantum theory, Rev. Math. Phys. **2**, 251.
Fröhlich, J., and P. A. Marchetti, 1988, Quantum field theory of anyons, Lett. Math. Phys. **16**, 347.
Fröhlich, J., and P. A. Marchetti, 1989, Quantum field theories of vortices and anyons, Commun. Math. Phys. **121**, 177.
Frohlich, J., and P. A. Marchetti, 1991, Spin-statistics theorem and scattering in planar quantum field theories with braid statistics, Nucl. Phys. **B356**, 533.
Fubini, S., 1991, Vertex operators and quantum hall effect, Mod. Phys. Lett. **A6**, 347.
Fubini, S., and C. A. Lutken, 1991, Vertex operators in the fractional quantum Hall effect, Mod. Phys. Lett. **A6**, 487.
Fuchs, J., 1992, Affine Lie Algebras and Quantum Groups (Cambridge University Press).
Funar, L., 1999, On TQFT representations, Pac. J. Math. **188**, 251.
Gaebler, J. P., J. T. Stewart, J. L. Bohn, and D. S. Jin, 2007, p-wave feshbach molecules, Phys. Rev. Lett. **98**(20), 200403/1.
Gawędzki, K., and A. Kupiainen, 1988, G/H conformal field theory from gauged WZW model, Phys. Lett. B **215**, 119.
Georgiev, L. S., 2006, Topologically protected gates for quantum computation with non-Abelian anyons in the Pfaffian quantum Hall state, Phys. Rev. B **74**(23), 235112.
Georgiev, L. S., and M. R. Geller, 2006, Aharonov-bohm effect in the non-Abelian quantum Hall fluid, Phys. Rev. B **73**(20), 205310.
Gepner, D., and Z.-a. Qiu, 1987, Modular invariant partition functions for parafermionic field theories, Nucl. Phys. **B285**, 423.
Gepner, D., and E. Witten, 1986, String theory on group manifolds, Nucl. Phys. **B278**, 493.
Girvin, S. M., and A. H. MacDonald, 1987, Off-diagonal long-range order, oblique confinement and the fractional quantum Hall effect, Phys. Rev. Lett. **58**(12), 1252.
Godfrey, M. D., P. Jiang, W. Kang, S. H. Simon, K. W. Baldwin, L. N. Pfeiffer, and K. W. West, 2007, Aharonov-bohm-like oscillations in quantum Hall corrals, arXiv:0708.2448.
Goerbig, M. O., P. Lederer, and C. M. Smith, 2004, Second generation of composite fermions and the self-similarity of the fractional quantum Hall effect, Int J. Mod. Phys. B **18**, 3549.
Goldin, G. A., R. Menikoff, and D. H. Sharp, 1981, Representations of a local current algebra in nonsimply connected space and the aharonovbohm effect, J. Math. Phys. **22**(8), 1664.
Goldman, V. J., and B. Su, 1995, Resonant Tunneling in the Quantum Hall Regime: Measurement of Fractional Charge, Science **267**(5200), 1010.
Goldstone, J., and F. Wilczek, 1981, Fractional quantum numbers of solitons, Phys. Rev. Lett. **47**, 986.
Goméz, C., M. Ruiz-Altaba, and G. Sierra, 1996, Quantum Groups in Two-Dimensional Physics (Cambridge Monographs on Mathematical Physics, Cambridge University Press).
Gottesman, D., 1998, Theory of fault-tolerant quantum computation, Phys. Rev. A **57**(1), 127.
Greiter, M., X.-G. Wen, and F. Wilczek, 1991, Paired Hall state at half filling, Phys. Rev. Lett. **66**(24), 3205.
Greiter, M., X. G. Wen, and F. Wilczek, 1992, Paired Hall states, Nucl. Phys. B **374**(3), 567.
Grosfeld, E., N. R. Cooper, A. Stern, and R. Ilan, 2007, Predicted signatures of p-wave superfluid phases and Majorana zero modes of fermionic atoms in rf absorption, Phys. Rev. B **76**(10), 104516/1.
Grosfeld, E., S. H. Simon, and A. Stern, 2006, Switching noise as a probe of statistics in the fractional quantum Hall effect, Phys. Rev. Lett. **96**(22), 226803.
Grosfeld, E., and A. Stern, 2006, Electronic transport in an array of quasiparticles in the $\nu = 5/2$ non-Abelian quantum Hall state, Phys. Rev. B **73**(20), 201303.
Gurarie, V., and C. Nayak, 1997, A plasma analogy and Berry matrices for non-Abelian quantum Hall states, Nucl. Phys. B **506**(3), 685.
Gurarie, V., L. Radzihovsky, and A. V. Andreev, 2005, Quantum phase transitions across a p-wave feshbach resonance, Phys. Rev. Lett. **94**(23), 230403.
Haldane, F. D. M., 1983, Fractional quantization of the Hall effect: A hierarchy of incompressible quantum fluid states, Phys. Rev. Lett.

51(7), 605.
Halperin, B. I., 1982, Quantized Hall conductance, current-carrying edge states, and the existence of extended states in a two-dimensional disordered potential, Phys. Rev. B **25**(4), 2185.
Halperin, B. I., 1983, Theory of the quantized Hall conductance, Helv. Phys. Acta **56**, 75.
Halperin, B. I., 1984, Statistics of quasiparticles and the hierarchy of fractional quantized Hall states, Phys. Rev. Lett. **52**(18), 1583.
Halperin, B. I., P. A. Lee, and N. Read, 1993, Theory of the half-filled Landau level, Phys. Rev. B **47**(12), 7312.
Hansson, T. H., V. Oganesyan, and S. L. Sondhi, 2004, Superconductors are topologically ordered, Ann. Phys. (N.Y.) **313**, 497.
Harrow, A., 2001, Quantum compiling, Ph.D. Thesis. Available online at http://www.media.mit.edu/physics/publications/theses/01.05.aram.pdf.
He, S., S. Das Sarma, and X. C. Xie, 1993, Quantized Hall effect and quantum phase transitions in coupled two-layer electron systems, Phys.. Rev. B **47**(8), 4394.
He, S., X. C. Xie, S. Das Sarma, and F. C. Zhang, 1991, Quantum Hall effect in double-quantum-well systems, Phys. Rev. B **43**(11), 9339.
Heinonen, O., 1998, Composite Fermions (World Scientific).
Henley, C. L., 1997, Relaxation time for a dimer covering with height representation, J. of Statistical Phys. **89**, 483.
Hormozi, L., G. Zikos, N. E. Bonesteel, and S. H. Simon, 2007, Topological quantum compiling, Phys. Rev. B **75**(16), 165310.
Hou, C.-Y., and C. Chamon, 2006, "wormhole" geometry for entrapping topologically protected qubits in non-Abelian quantum Hall states and probing them with voltage and noise measurements, Phys. Rev. Lett. **97**(14), 146802.
Ilan, R., E. Grosfeld, and A. Stern, 2007, Coulomb blockade as a probe for non-Abelian statistics in Read-Rezayi states, arXiv:0705.2187.
Imbo, T. D., C. S. Imbo, and E. C. G. Sudarshan, 1990, Identical particles, exotic statistics and braid groups, Phys. Lett. **B234**, 103.
Imbo, T. D., and J. March-Russell, 1990, Exotic statistics on surfaces, Phys. Lett. B **252**, 84.
Ioffe, L. B., M. Feigel'man, V. A. Ioselevich, D. Ivanov, M. Troyer, and G. Blatter, 2002, Topologically protected quantum bits using Josephson junction arrays, Nature **415**, 503 .
Ivanov, D. A., 2001, Non-Abelian statistics of half-quantum vortices in p-wave superconductors, Phys. Rev. Lett. **86**(2), 268.
Jackiw, R., and C. Rebbi, 1976, Solitons with fermion number 1/2, Phys. Rev. D **13**, 3398.
Jackiw, R., and J. R. Schrieffer, 1981, Solitons with fermion number 1/2 in condensed matter and relativistic field theories, Nucl. Phys. B **190**, 253.
Jacob, P., and P. Mathieu, 2000, Parafermionic character formulae, Nucl. Phys. B **587**, 514.
Jacob, P., and P. Mathieu, 2002, Parafermionic quasi-particle basis and fermionic-type characters, Nucl. Phys. B **620**, 351.
Jain, J. K., 1989, Composite-fermion approach for the fractional quantum Hall effect, Phys. Rev. Lett. **63**(2), 199.
Jaksch, D., and P. Zoller, 2005, The cold atom hubbard toolbox, Ann. Phys. (N.Y.) **351**, 52.
Ji, Y., Y. Chung, D. Sprinzak, M. Heiblum, D. Mahalu, and H. Shtrikman, 2003, An electronic MachZehnder interferometer, Nature **422**, 415.
Jolicoeur, T., 2007, Non-abelian states with negative flux: A new series of quantum Hall states, Physical Review Letters **99**(3), 036805.
Jones, V. F. R., 1985, A polynomial invariant for knots via von Neumann algebras, Bull. Amer. Math. Soc. **12**, 103.
Kalmeyer, V., and R. B. Laughlin, 1987, Equivalence of the resonating-valence-bond and fractional quantum Hall states, Phys. Rev. Lett. **59**, 2095.
Karabali, D., Q.-H. Park, H. J. Schnitzer, and Z. Yang, 1989, A GKO construction based on a path integral formulation of gauged Wess-Zumino-Witten actions, Phys. Lett. B **216**, 307.
Kassel, C., 1995, Quantum Groups (Springer-Verlag, New York, Berlin, Heidelberg).
Kauffman, L., 1987, State models and the Jones polynomial, Topology **26**, 395.
Kauffman, L., and S. Lins, 1994, Temperley-Lieb Recoupling theory and invariants of 3-manifolds., volume 134 of Ann. Math. Stud. (Princeton Univ. Press).
Kauffman, L. H., 2001, Knots and Physics, 3ed (World Scientific).
Kauffman, L. H., and S. J. Lomonaco Jr., 2004, Braiding operators are universal quantum gates, New J. Phys **6**, 134.
Kauffman, L. H., and S. J. Lomonaco Jr., 2007, q-deformed spin networks, knot polynomials and anyonic topological quantum computation, J. Knot Theory Ramifications **16**, 267.
Kawamura, T., and S. Das Sarma, 1992, Phonon-scattering-limited electron mobilities in $Al_xGa_{1-x}As/GaAs$ heterojunctions, Phys. Rev. B **45**(7), 3612.
Kidwingira, F., J. D. Strand, D. J. Van Harlingen, and Y. Maeno, 2006, Dynamical Superconducting Order Parameter Domains in Sr_2RuO_4, Science **314**, 1267.
Kirtley, J. R., C. Kallin, C. W. Hicks, E. A. Kim, Y. Liu, K. A. Moler, Y. Maeno, and K. D. Nelson, 2007, Upper limit on spontaneous supercurrents in sr_2ruo_4, arXiv.org:0704.3364.
Kitaev, A. Y., 2003, Fault-tolerant quantum computation by anyons, Ann. Phys. (N.Y.) **303**, 2.
Kitaev, A. Y., 2006, Anyons in an exactly solved model and beyond, Ann. Phys. (N.Y.) **321**, 2.
Kitaev, A. Y., and J. Preskill, 2006, Topological entanglement entropy, Phys. Rev. Lett. **96**, 110404.
Kitaev, A. Y., A. Shen, and M. Vyalyi, 1999, Classical and Quantum Computation (American Mathmetatical Society, Providence).
Kivelson, S. A., 1989, Statistics of holons in the quantum hard-core dimer gas, Phys. Rev. B **39**(1), 259.
Kivelson, S. A., and D. S. Rokhsar, 1990, Bogoliubov quasiparticles, spinons, and spin-charge decoupling in superconductors, Phys. Rev. B **41**(16), 11693.
Kivelson, S. A., D. S. Rokhsar, and J. P. Sethna, 1987, Topology of the resonating valence-bond state: solitons and high-T_c superconductivity, Phys. Rev. B **35**(16), 8865.
Klein, D. J., 1982, Exact ground states for a class of antiferromagnetic Heisenberg models with short-range interactions, J. Phys. A. Math. Gen. **15**(2), 661.
Knill, E., R. Laflamme, and Z. W. H., 1998, Resilient quantum computation: error models and thresholds, Proc. Roy. Soc. Lond.A **454**, 365.
Knizhnik, V. G., and A. B. Zamolodchikov, 1984, Current algebra and wess-zumino model in two dimensions, Nucl. Phys. **B247**, 83.
Kogut, J. B., 1979, An introduction to lattice gauge theory and spin systems, Rev. Mod. Phys. **51**, 659.
Koulakov, A. A., M. M. Fogler, and B. I. Shklovskii, 1996, Charge density wave in two-dimensional electron liquid in weak magnetic field, Phys. Rev. Lett. **76**(3), 499.
Kuperberg, G., 1996, Spiders for rank 2 lie algebras, Comm. Math. Phys. **180**, 109.
Larsen, M. J., E. C. Rowell, and Z. Wang, 2005, The n-eigenvalue problem and two applications, Intl. Math. Res. Not. **64**, 3987.
Laughlin, R. B., 1981, Quantized Hall conductivity in two dimensions, Phys. Rev. B **23**(10), 5632.
Laughlin, R. B., 1983, Anomalous quantum Hall effect: an in-

compressible quantum fluid with fractionally charged excitations, Phys. Rev. Lett. **50**(18), 1395.

Laughlin, R. B., 1988a, The relationship between high-temperature superconductivity and the fractional quantum Hall effect, Science **242**, 525.

Laughlin, R. B., 1988b, Superconducting ground state of noninteracting particles obeying fractional statistics, Phys. Rev. Lett. **60**(25), 2677.

Lee, D.-H., G.-M. Zhang, and T. Xiang, 2007a, Edge solitons of topological insulators and fractionalized quasiparticles in two dimensions, arXiv:0705.3499.

Lee, S.-S., S. Ryu, C. Nayak, and M. P. Fisher, 2007b, Particle-hole symmetry and the $\nu = 5/2$ quantum Hall state, arXiv:0707.0478, to appear in Phys. Rev. Lett.

Lee, T., and P. Oh, 1994, Non-Abelian Chern-Simons quantum mechanics, Phys. Rev. Lett. **72**(8), 1141.

Leggett, A. J., 1975, A theoretical description of the new phases of liquid ^{3}He, Rev. Mod. Phys. **47**(2), 331.

Leinaas, J. M., and J. Myrheim, 1977, On the theory of identical particles, Nuovo Cimento **37B**, 1.

Levin, M., B. I. Halperin, and B. Rosenow, 2007, Particle-hole symmetry and the Pfaffian state, arXiv:0707.0483, to appear in Phys. Rev. Lett.

Levin, M. A., and X.-G. Wen, 2005a, Colloquium: Photons and electrons as emergent phenomena, Rev. of Mod. Phys. **77**(3), 871.

Levin, M. A., and X.-G. Wen, 2005b, String-net condensation: A physical mechanism for topological phases, Phys. Rev. B **71**(4), 045110.

Levin, M. A., and X.-G. Wen, 2006, Detecting topological order in a ground state wave function, Phys. Rev. Lett. **96**(11), 110405.

Levinsen, J., N. Cooper, and V. Gurarie, 2007, Strongly-resonant p-wave superfluids, arXiv:0705.4460.

Lilly, M. P., K. B. Cooper, J. P. Eisenstein, L. N. Pfeiffer, and K. W. West, 1999a, Anisotropic states of two-dimensional electron systems in high Landau levels: Effect of an in-plane magnetic field, Phys. Rev. Lett. **83**(4), 824.

Lilly, M. P., K. B. Cooper, J. P. Eisenstein, L. N. Pfeiffer, and K. W. West, 1999b, Evidence for an anisotropic state of two-dimensional electrons in high Landau levels, Phys. Rev. Lett. **82**(2), 394.

Lo, H.-K., and J. Preskill, 1993, Non-abelian vortices and non-abelian statistics, Phys. Rev. D **48**(10), 4821.

López, A., and E. Fradkin, 1991, Fractional quantum Hall effect and Chern-Simons gauge theories, Phys. Rev. B **44**(10), 5246.

López, A., and E. Fradkin, 2004, Fermion Chern-Simons theory of hierarchical fractional quantum Hall states, Phys. Rev. B **69**(15), 155322/1.

Mackenzie, A. P., and Y. Maeno, 2003, The superconductivity of sr_2ruo_4 and the physics of spin-triplet pairing, Rev. Mod. Phys. **75**(2), 657.

Manfra, M. J., R. de Picciotto, Z. Jiang, S. H. Simon, L. N. Pfeiffer, K. W. West, and A. M. Sergent, 2007, Impact of spin-orbit coupling on quantum Hall nematic phases, Phys. Rev. Lett. **98**(20), 206804.

Manin, Y. I., 1980, Computable and Uncomputable, volume 21 (Sovetskoye Radio).

Marzuoli, A., and M. Rasetti, 2005, Spin network setting of topological quantum computation, Int. J. of Quant. Info. **3**, 65.

McKay, W., and J. Patera, 1981, Tables of dimensions, indices, and branching rules for representations of simple Lie algebras,, volume 69 of Lecture Notes in Pure and Applied Mathematics (M. Dekker, New York).

Miller, J. B., I. P. Radu, D. M. Zumbuhl, E. M. Levenson-Falk, M. A. Kastner, C. M. Marcus, L. N. Pfeiffer, and K. W. West, 2007, Fractional quantum Hall effect in a quantum point contact at filling fraction 5/2, Nature Phys. **3**, 561.

Milovanović, M., and N. Read, 1996, Edge excitations of paired fractional quantum Hall states, Phys. Rev. B **53**(20), 13559.

Misguich, G., C. Lhuillier, B. Bernu, and C. Waldtmann, 1999, Spin-liquid phase of the multiple-spin exchange hamiltonian on the triangular lattice, Phys. Rev. B **60**(2), 1064.

Mochon, C., 2003, Anyons from nonsolvable finite groups are sufficient for universal quantum computation, Phys. Rev. A **67**(2), 022315.

Mochon, C., 2004, Anyon computers with smaller groups, Phys. Rev. A **69**(3), 032306.

Moessner, R., and S. L. Sondhi, 2001, An RVB phase in the triangular lattice quantum dimer model, Phys. Rev. Lett. **86**, 1881.

Moessner, R., S. L. Sondhi, and P. Chandra, 1999, Two-dimensional periodic frustrated ising models in a transverse field, Phys. Rev. Lett. **84**(19), 4457.

Moller, G., and S. H. Simon, 2007, Paired composite fermion wavefunctions, arXiv:0708.2680.

Moore, G., and N. Read, 1991, Nonabelions in the fractional quantum Hall effect, Nucl. Phys. B **360**(2-3), 362.

Moore, G., and N. Seiberg, 1988, Polynomial equations for rational conformal field theories, Phys. Lett.. B **212**, 451.

Moore, G., and N. Seiberg, 1989, Classical and quantum conformal field theory, Commun. Math. Phys. **123**, 177.

Morf, R., and N. d'Ambrumenil, 2003, Disorder in fractional quantum Hall states and the gap at $\nu = 5/2$, Phys. Rev. B **68**, 113309/1.

Morf, R. H., 1998, Transition from quantum Hall to compressible states in the second Landau level: new light on the $\nu = 5/2$ enigma, Phys. Rev. Lett. **80**(7), 1505.

Morf, R. H., and N. d'Ambrumenil, 1995, Stability and effective masses of composite fermions in the first and second Landau level, Phys. Rev. Lett. **74**(25), 5116.

Morf, R. H., N. d'Ambrumenil, and S. Das Sarma, 2002, Excitation gaps in fractional quantum Hall states: An exact diagonalization study, Phys. Rev. B **66**(7), 075408.

Motrunich, O. I., 2003, Bosonic model with z_3 fractionalization, Phys. Rev. B **67**, 115108.

Motrunich, O. I., and T. Senthil, 2002, Exotic order in simple models of bosonic systems, Phys. Rev. Lett. **89**, 277004.

Mudry, C., and E. Fradkin, 1994a, Mechanism of spin and charge separation in one-dimensional quantum antiferromagnets, Phys. Rev. B **50**, 11409.

Mudry, C., and E. Fradkin, 1994b, Separation of spin and charge quantum numbers in strongly correlated systems, Phys. Rev. B **49**, 5200.

Mueller, E. J., 2004, Artificial electromagnetism for neutral atoms: Escher staircase and laughlin liquids, Phys. Rev. A **70**(4), 041603.

Murthy, G., and R. Shankar, 2003, Hamiltonian theories of the fractional quantum hall effect, Rev. Mod. Phys. **75**(4), 1101.

Nayak, C., and K. Shtengel, 2001, Microscopic models of two-dimensional magnets with fractionalized excitations, Phys. Rev. B **64**, 064422.

Nayak, C., and F. Wilczek, 1996, $2n$-quasihole states realize 2^{n-1}-dimensional spinor braiding statistics in paired quantum Hall states, Nucl. Phys. B **479**(3), 529.

Nielsen, M. A., and I. L. Chuang, 2000, Quantum Computation and Quantum Information (Cambridge University Press, Cambridge).

Niu, Q., D. J. Thouless, and Y.-S. Wu, 1985, Quantized Hall conductance as a topological invariant, Phys. Rev. B **31**(6), 3372.

Ortalano, M. W., S. He, and S. Das Sarma, 1997, Realistic calculations of correlated incompressible electronic states in GaAs-$Al_xGa_{1-x}As$ heterostructures and quantum wells, Phys. Rev. B **55**(12), 7702.

Oshikawa, M., Y. B. Kim, K. Shtengel, C. Nayak, and S. Tewari, 2007, Topological degeneracy of non-Abelian states for dummies, Ann. Phys. (N.Y.) **322**, 1477.

Overbosch, B. J., and F. A. Bais, 2001, Inequivalent classes of interference experiments with non-Abelian anyons, Phys. Rev. A **64**(6), 062107.

Overbosch, B. J., and X.-G. Wen, 2007, Dynamical and scaling properties of $\nu = 5/2$ interferometer.

Pachos, J. K., 2005, Quantum computation with Abelian anyons on the honeycomb lattice, cond-mat/0511273.

Pachos, J. K., 2006, The wavefunction of an anyon, cond-mat/0605068.

Pan, W., R. R. Du, H. L. Stormer, D. C. Tsui, L. N. Pfeiffer, K. W. Baldwin, and K. W. West, 1999a, Strongly anisotropic electronic transport at Landau level filling factor $\nu = 9/2$ and $\nu = 5/2$ under a tilted magnetic field, Phys. Rev. Lett. **83**(4), 820.

Pan, W., H. L. Stormer, D. C. Tsui, L. N. Pfeiffer, K. W. Baldwin, and K. W. West, 2001, Experimental evidence for a spin-polarized ground state in the $\nu = 5/2$ fractional quantum Hall effect, Sol. State Comm. **119**, 641.

Pan, W., J.-S. Xia, V. Shvarts, D. E. Adams, H. L. Stormer, D. C. Tsui, L. N. Pfieffer, K. W. Baldwin, and K. W. West, 1999b, Exact quantization of the even-denominator fractional quantum Hall state at $\nu = 5/2$ Landau level filling factor, Phys. Rev. Lett. **83**(17), 3530.

Peterson, M. R., and S. Das Sarma, 2007, unpublished.

Popp, M., B. Paredes, and J. I. Cirac, 2004, Adiabatic path to fractional quantum hall states of a few bosonic atoms, Phys. Rev. A **70**(5), 053612.

Prange, R., and S. M. Girvin (eds.), 1990, The Quantum Hall effect (Springer-Verlag, New York).

Preskill, J., 2004, Lecture notes for physics 219:quantum computation, available at http://www.theory.caltech.edu/∼preskill/ph219/ph219_2004.html.

Read, N., 1989, Order parameter and Ginzburg-Landau theory for the fractional quantum Hall effect, Phys. Rev. Lett. **62**(1), 86.

Read, N., 1990, Excitation structure of the hierarchy scheme in the fractional quantum Hall effect, Phys. Rev. Lett. **65**(12), 1502.

Read, N., 2003, Non-Abelian braid statistics versus projective permutation statistics, J. Math Phys **44**, 558.

Read, N., 2006, Wavefunctions and counting formulas for quasiholes of clustered quantum Hall states on a sphere, Phys. Rev. B **73**(24), 245334.

Read, N., and B. Chakraborty, 1989, Statistics of the excitations of the resonating-valence-bond state, Phys. Rev. B **40**(10), 7133.

Read, N., and D. Green, 2000, Paired states of fermions in two dimensions with breaking of parity and time-reversal symmetries and the fractional quantum Hall effect, Phys. Rev. B **61**(15), 10267.

Read, N., and E. Rezayi, 1996, Quasiholes and fermionic zero modes of paired fractional quantum Hall states: the mechanism for non-Abelian statistics, Phys. Rev. B **54**(23), 16864.

Read, N., and E. Rezayi, 1999, Beyond paired quantum Hall states: Parafermions and incompressible states in the first excited Landau level, Phys. Rev. B **59**(12), 8084.

Rezayi, E. H., 2007, unpublished.

Rezayi, E. H., and F. D. M. Haldane, 2000, Incompressible paired Hall state, stripe order, and the composite fermion liquid phase in half-filled Landau levels, Phys. Rev. Lett. **84**(20), 4685.

Rezayi, E. H., and N. Read, 2006, Non-Abelian quantized Hall states of electrons at filling factors 12/5 and 13/5 in the first excited Landau level, cond-mat/0608346.

Rezayi, E. H., N. Read, and N. R. Cooper, 2005, Incompressible liquid state of rapidly rotating bosons at filling factor 3/2, Phys. Rev. Lett. **95**(16), 160404.

Rokhsar, D. S., 1990, Solitons in chiral-spin liquids, Phys. Rev. Lett. **65**(12), 1506.

Rokhsar, D. S., and S. A. Kivelson, 1988, Superconductivity and the quantum hard-core dimer gas, Phys. Rev. Lett. **61**(20), 2376.

Rosenow, B., B. Halperin, S. Simon, and A. Stern, 2007, Bulk-edge coupling in the non-abelian $\nu = 5/2$ quantum Hall interferometer.

Rosenow, B., and B. I. Halperin, 2007, Influence of interactions on flux and back-gate period of quantum Hall interferometers, Phys. Rev. Lett. **98**(10), 106801.

Saminadayar, L., D. C. Glattli, Y. Jin, and B. Etienne, 1997, Observation of the e/3 fractionally charged laughlin quasiparticle, Phys. Rev. Lett. **79**, 2526.

Scarola, V. W., J. K. Jain, and E. H. Rezayi, 2002, Possible pairing-induced even-denominator fractional quantum Hall effect in the lowest Landau level, Phys. Rev. Lett. **88**(21), 216804.

Schwarz, A. S., 1978, The partition function of degenerate quadratic functional and ray-singer invariants, Lett. Math. Phys. **2**, 247.

Schweikhard, V., I. Coddington, P. Engels, V. P. Mogendorff, and E. A. Cornell, 2004, Rapidly rotating bose-einstein condensates in and near the lowest landau level, Physical Review Letters **92**(4), 040404.

Seidel, A., and D.-H. Lee, 2006, Abelian and non-Abelian Hall liquids and charge-density wave: Quantum number fractionalization in one and two dimensions, Phys. Rev. Lett. **97**(5), 056804.

Semenoff, G. W., and P. Sodano, 2006a, Stretching the electron as far as it will go, Electron. J. Theor. Phys. **10**, 157.

Semenoff, G. W., and P. Sodano, 2006b, Teleportation by a majorana medium, cond-mat/0601261.

Senthil, T., and M. P. A. Fisher, 2000, z_2 gauge theory of electron fractionalization in strongly correlated systems, Phys. Rev. B **62**, 7850.

Senthil, T., and M. P. A. Fisher, 2001a, Fractionalization in the cuprates: Detecting the topological order, Phys. Rev. Lett. **86**, 292.

Senthil, T., and M. P. A. Fisher, 2001b, Fractionalization, topological order, and cuprate superconductivity, Phys. Rev. B **63**, 134521.

Senthil, T., and O. Motrunich, 2002, Microscopic models for fractionalized phases in strongly correlated systems, Phys. Rev. B **66**, 205104.

Shimizu, Y., K. Miyagawa, K. Kanoda, M. Maesato, and G. Saito, 2003, Spin liquid state in an organic Mott insulator with a triangular lattice, Phys. Rev. Lett. **91**(10), 107001.

Shor, P. W., 1994, in Proc. 35nd Annual Symposium on Foundations of Computer Science (IEEE Computer Society Press, Los Alamitos, CA), pp. 124–134, shafi Goldwasser, ed.

Shor, P. W., 1995, Scheme for reducing decoherence in quantum computer memory, Phys. Rev. A **52**(4), R2493.

Simon, S. H., 2000, Proposal for a quantum hall pump, Phys. Rev. B **61**(24), R16327.

Simon, S. H., 2007, Effect of landau level mixing on braiding statistics, arXiv:0710.1088.

Simon, S. H., N. E. Bonesteel, M. H. Freedman, N. Petrovic, and L. Hormozi, 2006, Topological quantum computing with only one mobile quasiparticle, Phys. Rev. Lett. **96**(7), 070503.

Simon, S. H., E. H. Rezayi, and N. R. Cooper, 2007a, Generalized quantum Hall projection hamiltonians, Phys. Rev. B **75**(7), 075318.

Simon, S. H., E. H. Rezayi, and N. R. Cooper, 2007b, Pseudopotentials for multiparticle interactions in the quantum Hall regime, Phys. Rev. B **75**(19), 195306.

Simon, S. H., E. H. Rezayi, N. R. Cooper, and I. Berdnikov, 2007c, Construction of a paired wave function for spinless electrons at filling fraction $\nu = 2/5$, Phys. Rev. B **75**(7), 075317/1.

Slingerland, J. K., and F. A. Bais, 2001, Quantum groups and non-

Abelian braiding in quantum Hall systems, Nuc. Phys. B **612**, 229.
Sørensen, A. S., E. Demler, and M. D. Lukin, 2005, Fractional quantum hall states of atoms in optical lattices, Physical Review Letters **94**(8), 086803.
Steane, A., 1996a, Multiple particle interference and quantum error correction, Proc. Roy. Soc. Lond.A **452**, 2551.
Steane, A. M., 1996b, Error correcting codes in quantum theory, Phys. Rev. Lett. **77**(5), 793.
Steane, A. M., 1996c, Simple quantum error-correcting codes, Phys. Rev. A **54**(6), 4741.
Stern, A., and B. I. Halperin, 2006, Proposed experiments to probe the non-Abelian $\nu = 5/2$ quantum Hall state, Phys. Rev. Lett. **96**(1), 016802.
Stern, A., F. von Oppen, and E. Mariani, 2004, Geometric phases and quantum entanglement as building blocks for non-Abelian quasiparticle statistics, Phys. Rev. B **70**(20), 205338.
Stone, M., and S.-B. Chung, 2006, Fusion rules and vortices in $p_x + ip_y$ superconductors, Phys. Rev. B **73**(1), 014505.
Stormer, H. L., L. N. Pfeiffer, K. W. Baldwin, and K. W. West, 1990, Observation of a Bloch-Grüneisen regime in two-dimensional electron transport, Phys. Rev. B **41**(2), 1278.
Su, W. P., and J. R. Schrieffer, 1981, Fractionally charged excitations in charge-density-wave systems with commensurability 3, Phys. Rev. Lett. **46**(11), 738.
Su, W. P., J. R. Schrieffer, and A. J. Heeger, 1980, Soliton excitations in polyacetylene, Phys. Rev. B **22**(4), 2099.
Sutherland, B., 1988, Systems with resonating-valence-bond ground states: Correlations and excitations, Phys. Rev. B **37**, 3786.
Tao, R., and Y.-S. Wu, 1984, Gauge invariance and fractional quantum Hall effect, Phys. Rev. B **30**(2), 1097.
Tewari, S., S. Das Sarma, and D. H. Lee, 2007a, An index theorem for the majorana zero modes in chiral p-wave superconductors, Phys. Rev. Lett. (in press); arXiv:cond-mat/0609556.
Tewari, S., S. Das Sarma, C. Nayak, C. Zhang, and P. Zoller, 2007b, Quantum computation using vortices and Majorana zero modes of a $p_x + ip_y$ superfluid of fermionic cold atoms, Phys. Rev. Lett. **98**(1), 010506.
Tewari, S., C. Zhang, S. Das Sarma, C. Nayak, and D.-H. Lee, 2007c, Non-local quantum phenomena associated with the majorana fermion bound states in a $p_x + ip_y$ superconductor, arXiv:cond-mat/0703717.
Thouless, D. J., and Y. Gefen, 1991, Fractional quantum Hall effect and multiple Aharonov-Bohm periods, Phys. Rev. Lett. **66**(6), 806.
Toke, C., and J. K. Jain, 2006, Understanding the 5/2 fractional quantum Hall effect without the Pfaffian wave function, Phys. Rev. Lett. **96**, 246805/14.
Toke, C., N. Regnault, and J. K. Jain, 2007, Nature of excitations of the 5/2 fractional quantum Hall effect, Phys. Rev. Lett. **98**, 036806/1.
Tracy, L. A., J. P. Eisenstein, L. N. Pfeiffer, and K. W. West, 2007, Spin transition in the half-filled Landau level, Phys. Rev. Lett. **98**(8), 086801.
Trebst, S., P. Werner, M. Troyer, K. Shtengel, and C. Nayak, 2007, Breakdown of a topological phase: Quantum phase transition in a loop gas model with tension, Phys. Rev. Lett. **98**(7), 070602.
Tserkovnyak, Y., and S. H. Simon, 2003, Monte carlo evaluation of non-Abelian statistics, Phys. Rev. Lett. **90**(1), 016802.
Tsui, D. C., H. L. Stormer, and A. C. Gossard, 1982, Two-dimensional magnetotransport in the extreme quantum limit, Phys. Rev. Lett. **48**(22), 1559.
Turaev, V. G., 1994, Quantum Invariants of Knots and 3-Manifolds (Walter de Gruyter, Berlin, New York).
Turaev, V. G., and O. Y. Viro, 1992, State sum invariants of 3-manifolds and quantum 6j-symbols, Topology **31**(4), 865902.
Verlinde, E., 1988, Fusion rules and modular transformations in 2d conformal field theory, Nuc. Phys. B **300**, 360.
Verlinde, E., 1990, in Proceedings of the International Colloquium on Modern Quantum Field Theory (World Scientific, Singapore).
Volovik, G. E., 1994, The Universe in a Helium Droplet (Oxford University Press).
Walker, K., 1991, On witten's 3-manifold invariants, available at http://canyon23.net/math/1991TQFTNotes.pdf.
Wan, X., K. Yang, and E. H. Rezayi, 2006, Edge excitations and non-Abelian statistics in the Moore-Read state: A numerical study in the presence of coulomb interaction and edge confinement, Phys. Rev. Lett. **97**(25), 256804.
Wen, X. G., 1990, Topological orders in rigid states, Int. J. Mod. Phys. B **4**(2), 239.
Wen, X. G., 1991a, Mean-field theory of spin-liquid states with finite energy gap and topological orders, Phys. Rev. B **44**(6), 2664.
Wen, X. G., 1991b, Non-Abelian statistics in the fractional quantum Hall states, Phys. Rev. Lett. **66**(6), 802.
Wen, X. G., 1992, Theory of the edge states in fractional quantum Hall effects, Intl. J. Mod. Phys. B **6**(10), 1711.
Wen, X.-G., 1999, Projective construction of non-Abelian quantum Hall liquids, Phys. Rev. B **60**(12), 8827.
Wen, X.-G., 2004, Quantum Field Theory of Many-body Systems (Oxford University Press).
Wen, X. G., and Q. Niu, 1990, Ground-state degeneracy of the fractional quantum Hall states in the presence of a random potential and on high-genus riemann surfaces, Phys. Rev. B **41**(13), 9377.
Wen, X.-G., and Y.-S. Wu, 1994, Chiral operator product algebra hidden in certain fractional quantum Hall wave functions, Nucl. Phys. B **419**, 455.
Wen, X. G., and A. Zee, 1992, Classification of Abelian quantum Hall states and matrix formulation of topological fluids, Phys. Rev. B **46**(4), 2290.
Wen, X.-G., and A. Zee, 1998, Topological degeneracy of quantum Hall fluids, Phys. Rev. B **58**(23), 15717.
Wess, J., and B. Zumino, 1971, Consequences of anomalous ward identities, Phys. Lett. B **37**, 95.
Wilczek, F., 1982a, Magnetic flux, angular momentum, and statistics, Phys. Rev. Lett. **48**(17), 1144.
Wilczek, F., 1982b, Quantum mechanics of fractional-spin particles, Phys. Rev. Lett. **49**(14), 957.
Wilczek, F., 1990, Fractional Statistics and Anyon Superconductivity (World Scientific, Singapore).
Wilkin, N. K., J. M. F. Gunn, and R. A. Smith, 1998, Do attractive bosons condense?, Phys. Rev. Lett. **80**(11), 2265.
Willett, R., J. P. Eisenstein, H. L. Stormer, D. C. Tsui, A. C. Gossard, and J. H. English, 1987, Observation of an even-denominator quantum number in the fractional quantum Hall effect, Phys. Rev. Lett. **59**(15), 1776.
Willett, R., H. Stormer, D. Tsui, A. Gossard, and J. English, 1988, Quantitative experimental test for the theoretical gap energies in the fractional quantum Hall effect, Phys. Rev. B **37**, 8476.
Willett, R. L., M. J. Manfra, L. N. Pfeiffer, and K. W. West, 2007, Confinement of fractional quantum Hall states in narrow conducting channels, Appl. Phys. Lett. **91**.
Witten, E., 1983, Global aspects of current algebra, Nucl. Phys. **B223**, 422.
Witten, E., 1989, Quantum field theory and the Jones polynomial, Comm. Math. Phys. **121**, 351.
Witzel, W. M., and S. Das Sarma, 2006, Quantum theory for electron spin decoherence induced by nuclear spin dynamics in semiconductor quantum computer architectures: Spectral diffusion of localized electron spins in the nuclear solid-state environment, Phys.

Rev. B **74**(3), 035322.

Wójs, A., 2001, Electron correlations in partially filled lowest and excited Landau levels, Phys. Rev. B **63**(12), 125312.

Wojs, A., and J. J. Quinn, 2002, Electron correlations in a partially filled first excited Landau level, Physica E **12**, 63.

Wojs, A., and J. J. Quinn, 2006, Landau level mixing in the $\nu = 5/2$ fractional quantum Hall state, Phys. Rev. B **74**(23), 235319.

Wojs, A., D. Wodzinski, and J. J. Quinn, 2006, Second generation of Moore-Read quasiholes in a composite-fermion liquid, Phys. Rev. B **74**(3), 035315.

Wojs, A., K.-S. Yi, and J. J. Quinn, 2004, Fractional quantum Hall states of clustered composite fermions, Phys. Rev. B **69**(20), 205322.

Wu, Y.-S., 1984, General theory for quantum statistics in two dimensions, Phys. Rev. Lett. **52**(24), 2103.

Wynn, J. C., D. A. Bonn, B. W. Gardner, Y.-J. Lin, R. Liang, W. N. Hardy, J. R. Kirtley, and K. A. Moler, 2001, Limits on spin-charge separation from $h/2e$ fluxoids in very underdoped $YBa_2Cu_3O_{6+x}$, Phys. Rev. Lett. **87**, 197002/1.

Xia, J., Y. Maeno, P. T. Beyersdorf, M. M. Fejer, and A. Kapitulnik, 2006, High resolution polar kerr effect measurements of Sr_2RuO_4: Evidence for broken time-reversal symmetry in the superconducting state, Phys. Rev. Lett. **97**(16), 167002.

Xia, J. S., W. Pan, C. L. Vicente, E. D. Adams, N. S. Sullivan, H. L. Stormer, D. C. Tsui, L. N. Pfeiffer, K. W. Baldwin, and K. W. West, 2004, Electron correlation in the second Landau level: A competition between many nearly degenerate quantum phases, Phys. Rev. Lett. **93**(17), 176809.

Zhang, C., V. Scarola, S. Tewari, and S. Das Sarma, 2006, Anyonic braiding in optical lattices, quant-ph/0609101.

Zhang, C., S. Tewari, and S. Das Sarma, 2007, Bell's inequality and universal quantum gates in a cold atom chiral fermionic p-wave superfluid, arXiv:0705.4647.

Zhang, F., and S. Das Sarma, 1986, Excitation gap in the fractional quantum Hall effect: Finite layer thickness corrections, Phys.Rev. B **33**, 2903.

Zhang, S. C., T. H. Hansson, and S. Kivelson, 1989, Effective-field-theory model for the fractional quantum Hall effect, Phys. Rev. Lett. **62**(1), 82.